CHARLES UNIVERSITY

Faculty of Medicine in Pilsen

Department of Pathology

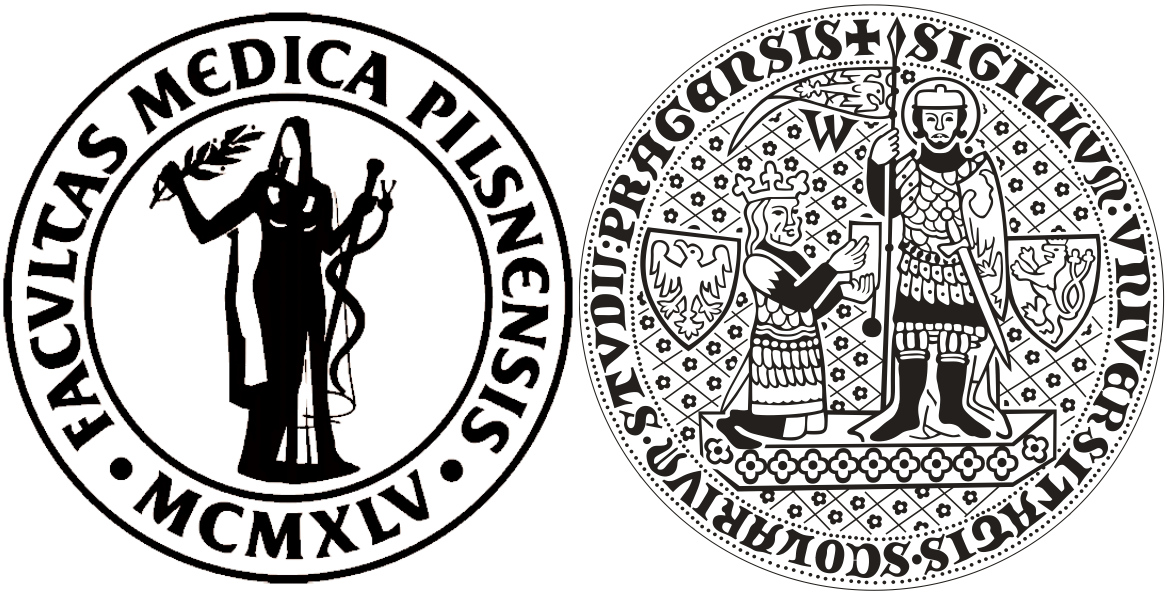

Clinicopathological, morphological, immunohistochemical and molecular biological features of tumours of genitourinary tract

Joanna Rogala, M.D.
Doctoral dissertation

Pilsen 2023
Department: Pathology
Supervisor: Doc. MUDr. Kristýna Pivovarčíková, Ph.D. and Prof. MUDr. Ondřej Hes, Ph.D.

Abstract

The thesis “Clinicopathological, morphological, immunohistochemical and molecular biological features of tumours of genitourinary tract” includes seven commented articles from the area of genitourinary (GU) tract neoplasms. Due to the wide spectrum of tumours of the GU tract, the presented dissertation is limited only to morphologic, immunohistochemical and molecular aspects of renal tumours – in the field of pathology, we have observed fundamental changes in recent years and where molecular techniques have begun to play an integral role in pathological examination.

The introduction comments current 5th edition of WHO classification of kidney tumours, it emphasizes changes and new entities defined by distinctive morphology and molecular signature as well as comments on new insights in well-established entities.

In the results, there are presented recently published original publications describing variant morphologies of common tumours with their immunohistochemical and molecular profile, as well as newly describe entity with its immunohistochemical and molecular characteristics.

In the conclusion, dynamics of changes in renal tumours classification is discussed together with the importance of molecular testing, its therapeutic implications and limitations.

Foreword

Doctoral dissertation is a collection of author´s original publications dedicated to morphological variants and molecular background of tumours of genitourinary system. The author participated as a member of author collectives. The dissertation is written from a point of view of a practicing pathologist – discipline that the author is specialised in. The work is focused on recent 5th edition of WHO classification of kidney tumours and new insight to the renal neoplasms. Seven original articles were included, preceded by introduction. In the conclusion, the limitations and perspectives in diagnostic approach to kidney tumours are commented in the light of presented studies.

Declaration

I declare that I have prepared the final work independently and that I have properly listed and cited all the sources and literature used. I agree to the permanent storage of the electronic version of my work in a database of Faculty of Medicine in Pilsen, Charles University.

Pilsen 2023

Joanna Rogala

Acknowledgment

Prof. MUDr. Ondřej Hes, Ph.D. – my supervisor for the opportunity offered, professional leadership, mentorship, proven patience,

Doc. MUDr. Kristýna Pivovarčíková, Ph.D. – my supervisor for leadership, willingness and friendly approach.

Prof. MUDr. Michal Michal – for support and provided background.

Content

List of abbreviations used

2SC	S-(2-sukcino)-cysteine
aCGH	Array Comparative Genomic Hybridization
AE1/AE3	A mixture/cocktail of immunohistochemical antibodies detecting cytokeratins
ALK	Immunohistochemical antibody detecting anaplastic lymphoma kinase protein
AMACR	Immunohistochemical antibody detecting enzyme α-methylacyl-CoA racemase
CA-IX	Immunohistochemical antibody detecting carbonic anhydrase (CA) IX
CAM5.2	Immunohistochemical antibody detecting cytokeratin *KRT8*
CCPRCT	Clear Cell Papillary Renal Cell Tumour
CCRCC	Clear Cell Renal Cell Carcinoma
CDC	Collecting Duct Carcinoma
CD10	Immunohistochemical antibody detecting membrane metalloendopeptidase
CD117	Immunohistochemical antibody detecting transmembrane tyrosine kinase receptor CD117/c-kit
CK7	Immunohistochemical antibody detecting cytokeratin *KRT7*
CK20	Immunohistochemical antibody detecting cytokeratin *KRT20*
CNA	Copy Number Alteration
CNV	Copy Number Variation
EMA	Immunohistochemical antibody detecting epithelial membrane antigen
ESC RCC	Eosinophilic Solid and Cystic Renal Cell Carcinoma
ESKD	End Stage Kidney Disease
EVT	Eosinophilic Vacuolated Tumour
FH	Fumarate hydratase
FISH	Fluorescence In Situ Hybridization
GATA3	Immunohistochemical antibody detecting one of members of the GATA family of transcription factor
GUPS	Genitourinary Pathology Society
HLRCC	Hereditary Leiomyomatosis and Renal Cell Carcinoma-Associated Renal Cell Carcinoma
HMB45	Immunohistochemical antibody detecting antigen PMEL/Melanoma gp100
HMWCK	High molecular weight keratin - Immunohistochemical antibody detecting protein Cytokeratin 34 beta E12
HPF	High Power Field
INI1 (SMARCB1)	Immunohistochemical antibody detecting Integrase interactor 1 protein
ISUP	International Society of Urological Pathology
LOH	Loss of Heterozygosity
LOT	Low-grade Oncocytic Tumour
MCRNLMP	Multilocular Cystic Renal Neoplasm of Low Malignant Potential
MESTK	Mixed epithelial and stromal tumor of the kidney
Melan A	Immunohistochemical antibody detecting product of the MART-1 gene
MIA	Immunohistochemical antibody detecting antimitochondrial antigen
MTSCC	Mucinous Tubular and Spindle Cell Carcinoma
NOS	Not Otherwise Specified
OCT3/4	Immunohistochemical antibody detecting Octamer binding transcription factor
OPRCC	Oncocytic Papillary Renal Cell Carcinoma
PAX8	Immunohistochemical antibody detecting protein PAX8
PRCC	Papillary Renal Cell Carcinoma
RCC	Renal Cell Carcinoma

RO	Renal Oncocytoma
SDH	Succinate dehydrogenase
TCRCC	Tubulocystic Renal Cell Carcinoma
TNM	Classification of Malignant Tumours
TFEB	Transcription factor TFEB
TFE3	Transcription Factor TFE3
TTF-1	Immunohistochemical antibody detecting of thyroid transcription factor-1
VHL	von Hippel-Lindau
WHO	World Health Organization
WT-1	Immunohistochemical antibody detecting protein WT1

1 Introduction

1.1 New WHO classification of renal neoplasms

Classification of kidney tumours represents a dynamic field of constant changes that can be noted by shortening of time between each "blue book" edition, as well as high number of entities included in most recent ones. First published classification of kidney tumours (dated 1997 - so called The Heidelberg classification of renal cell tumours) described 7 renal epithelial entities (1). The most recent classification (published in 2022 - 5th edition of WHO classification of tumours of the kidneys) lists 21 renal cell neoplasms, including benign ones (2). Interestingly, both editions concluded that using strict criteria would make it possible to categorize 95% of renal tumours. It shows that after almost 30 years of extensive effort and new developments, there still remains a group of renal neoplasms that cannot be classified.

Shortly before the release of current 2022 WHO "blue book", updates and "guidelines" on kidney tumours were published by the Genitourinary Pathology Society (GUPS) (3, 4) and the International Society of Urological Pathology (ISUP) (5) – two international pathologists societies dedicated to the field of GU pathology. All works summarized most recent insight in kidney tumour pathology and served as a "basis" and recommendations for WHO contributors (many WHO authors also contributed to these publications).

Much knowledge was brought to this field by widely applied molecular studies, which were also dictated by the search for possible options for targeted therapy. It became apparent that we have arrived in the "histo-molecular" era of renal tumour pathology, where certain entities are clearly defined by their molecular alterations. However, we cannot forget that the great majority of tumours can still be diagnosed using defined morphological criteria.

In introduction, the main changes in the 2022 WHO classification will be discussed. The changes will be divided into minor/small (changes in subclassification) and major (introduction of molecularly defined RCC into the classification, introduction of new entities and changes of nomenclature).

1.2 Unchanged entities, minor changes

1.2.1 Clear cell renal cell carcinoma

Clear cell renal cell carcinoma (CCRCC) represents most frequent type of RCC in adults, accounting for 60-75% of RCCs (2). It is classically composed of cells with abundant pale cytoplasm arranged in nests or tubules surrounded by a rich and delicate vascular network. However, variable patterns may be seen within the same tumour as CCRCCs are

notorious for its intratumoral heterogeneity. Rare morphologies, including CCRCC with Paneth-like cells (6), CCRCC with a syncytial-type multinucleated giant tumour cell component (7) or CCRCC with a papillary architecture (8) have been recently reported.

Immunohistochemistry reveals positive staining for wide spectrum cytokeratin (AE1/AE3 or CAM5.2) vimentin and CAIX with diffuse, membranous "box-like "pattern. CK7 is usually referred as negative; however it may be positive to some extent in low grade tumours in cystic and papillary areas (9, 10).

Inactivation of *VHL* gene located on chromosome 3p (by *VHL* gene mutation or methylation, LOH 3p) stands for molecular signature of CCRCC.

1.2.2 Multilocular cystic renal neoplasm of low malignant potential

Multilocular cystic renal neoplasm of low malignant potential (MCRNLMP) is indolent tumour composed exclusively of cysts lined by low grade (WHO/ISUP grade 1/2), pale cells. Intraseptal collections of tumour cells exceeding 1 mm in the diameter (causing expansion of the cystic septum), as well as presence of necrosis, atypical mitoses, lymphangiovascular invasion or high grade transformation are not compatible with MCRNLMP diagnosis. Moreover, the diagnosis should not be made on limited samples due to overlapping features with low grade CCRCC with cystic degeneration.

The immunoprofile corresponds to that of CCRCC with more frequently pronounced CK7 positivity (9). Again, alterations of *VHL* gene are commonly detected.

1.2.3 Renal papillary adenoma

Renal papillary adenoma is benign, unencapsulated, sharply demarcated tumour composed of low grade cells arranged in papillary to tubulopapillary formations (morphology typically described as type 1 PRCC in historical classification). By the definition, the adenoma must measure up to 15 mm in the greatest dimension (2). Adenomas frequently arise in the background of chronic kidney disease.

By immunohistochemistry tumours show positivity to AMACR, CK7 CD10, and vimentin. Adenomas often exhibit trisomy 7 and 17 together with loss of chromosome Y in molecular-genetic testing (similar to the papillary carcinoma traditionally called as type 1).

1.2.4 Papillary renal cell carcinoma

Papillary renal cell carcinoma (PRCC) is second most common type of renal carcinoma accounting for 13-20% of kidney epithelial tumours (2). It represents well demarcated, frequently encapsulated tumour with papillary to tubulopapillary architecture. Neoplastic cells show a broad spectrum of morphology, ranging from bland-looking cells with scant cytoplasm, trough cells with abundant clear cytoplasm to cells with voluminous eosinophilic and/or vacuolated cytoplasm with variability of nuclear grades. Foamy macrophages, haemorrhages, psammoma bodies, or extensive necrosis may be frequently present. Traditional subdivision into type 1 and type 2 is no longer recommended. According to the new approach (coming with a new "blue book" 2022), morphologic patterns of PRCC should be distinguished, as it seems to better predict biological behaviour (11). Well established morphologic variants of PRCC include for example: solid/pseudosolid PRCC (with collapsed, densely packed papillae/tubules with pseudosolid appearance of the tumorous mass) (12), Warthin-like PRCC (with extensive inflammatory infiltrates within papillary cores) (13), biphasic squamoid alveolar PRCC (with two populations of cells and empheripolesis) (14), or PRCC with clear cells.

Recently described entity of PRCC with reverse polarity/papillary renal cell neoplasm with reverse polarity is composed of oncocytic/eosinophilic cells with regular round to oval nuclei arranged in a linear fashion away (elevated) from basement membrane (15). This tumour has characteristic immunoprofile, including positive staining for GATA3, AMACR and negative staining for vimentin, CAIX. *KRAS* mutation is frequent event in PRCC with reverse polarity /papillary renal neoplasm with reverse polarity (16). Designation/subtype of "oncocytic PRCC" is no longer applied (2).

Immunohistochemistry of PRCCs shows constant positivity for racemase (AMACR), regardless of morphologic pattern, frequent positivity for vimentin and CD10. CK7 positivity depends on tumour cell type - it is less frequently expressed in tumours composed of eosinophilic cells.

Molecular-genetic background of PRCC varies. However, gains of chromosomes 7 and 17, and loss of the Y chromosome (in male patients) together with *MET* gene mutations are described as the most common alterations.

1.2.5 Oncocytoma of the kidney

Renal oncocytoma (RO) represents a benign neoplasm. It accounts for 6–9% of renal neoplasms (2). Tumour is typically well demarcated, encapsulated, composed of solid nests of cells. Neoplastic cells exhibit characteristic cytoplasmic eosinophilic granularity, reflecting high condensation of mitochondria. Nuclei are uniform, round with visible nucleolus. Nests of cells are frequently embedded in loose stroma, macroscopically creating the central scar.

Other architectural patterns include microcystic, macrocystic, and small cell composed of oncoblasts-like cells with scant cytoplasm arranged in rosette-like formations (10, 11). Areas of cells with hyperchromatic, smudged nuclei, and so-called ancient like atypias may by focally present. Perinuclear halos, mitoses, nuclear irregularities, necrosis or true papillary formation are not consistent with the diagnosis of RO (12, 13).

Immunohistochemical profile consists of CD 117, and cytokeratin (AE1/AE3 positivity. CK7 and vimentin are typically negative or limited to scattered cells (usually to areas of scarring, where both markers tend to be more accentuated) (17).

Molecularly RO exhibits either normal karyotype or alterations including loss of chromosome 1 (whole chromosome or deletion 1p36), 14, or gonosomes (X/Y) or 11q13 rearrangement (affecting *CCND1*gene) (18).

1.2.6 Chromophobe renal cell carcinoma

Chromophobe renal cell carcinoma (ChRCC) represents third most common RCC, accounting for 5 - 7% renal epithelial tumours (2). Tumours are usually well demarcated, unencapsulated with solid-alveolar growth pattern. Chromophobe RCCs are typically composed of two populations of cells: large, “plant like” cells with pale, voluminous cytoplasm and smaller cells, with eosinophilic cytoplasm. Characteristic cytology of the neoplastic cells shows wrinkled ”rasinoid” nuclei with perinuclear halos and often binucleation. Variable architectural patterns have been described, including cystic, adenomatoid, pigmented or papillary (19-21). True neuroendocrine differentiation with positive neuroendocrine markers as well as ChRCC with neuroendocrine-like features or ChRCC with small cells (22, 23) were also reported. Eosinophilic ChRCC is defined by predominance (according to some authors pure presence) of the smaller eosinophilic cells.

Immunohistochemistry shows positivity for CD 117 and CK 7 in majority of cases. However expression of CK 7 varies from diffuse to completely negative (with negative CK7 staining frequently in eosinophilic subtype ChRCC). Staining for vimentin typically shows negative results.

Chromophobe RCC is characterised by multiple chromosomal loses, most commonly involving chromosomes 1, 2, 17, 6, 10, 13, 21 as well as multiple gains (heterogeneous numerical chromosomal aberration profile). Moreover, ChRCC may exhibit mutations in different genes - the most frequently affected genes include *TP53*, *PTEN*, *TERT*, and *FOXI1*.

1.2.7 Collecting duct carcinoma

Collecting duct carcinoma (CDC) is diagnosis per exclusion. It is typically high grade, high stage carcinoma accounting less than 1% of renal cancers. Collecting duct carcinoma is typically medullary based, and characterised by tubulary to tubulopapillary architecture with infiltrating growth pattern and extensive desmoplastic stromal reaction. Coexistence of any component of "classic" RCC or urothelial carcinoma excludes the diagnosis of CDC.

Immunohistochemistry shows positivity for HMWCK, CK7, and PAX8. Expression of FH and SMARCB1 (INI1) are retained. There are no known specific molecular alterations.

1.2.8 Mucinous tubular and spindle cell carcinoma

Mucinous tubular and spindle cell renal cell carcinoma (MTSCRCC) is rare neoplasm accounting for less than 1% renal tumours (2). It represents morphologically biphasic tumour composed of anastomosing, elongated tubules lined by bland cells admixed with low grade spindle cells areas, both often set in myxoid stroma with extracellular mucin. Extent of each component varies. Collections of foamy macrophages may occur. The presence of frequent collections of foamy macrophages and areas with papillary architecture represent overlapping morphology with PRCC and favour the diagnosis PRCC.

By immunohistochemistry, MTSCRCC shows positivity in CK7, AMACR, and PAX8. Positivity to CD10 is infrequent.

Molecular findings reveal multiple chromosomal losses involving chromosomes 1, 4, 6, 8, 9, 13, 14, 15, 22 and VSTM2A RNA expression.

1.2.9 Tubulocystic renal cell carcinoma

Tubulocystic renal cell carcinoma (TCRCC) is rare tumour again, it accounts for less than 1% of kidney neoplasms (2). Tubulocystic RCC is well demarcated, typically with sponge-like appearance on the cross section reflecting exclusive tubulocystic architecture with variably sized cysts. Cells type range from flat to hobnail, with intermediate to large nuclei and striking nucleoli.

Immunohistochemistry shows reactivity for AMACR, CK7, CD10 and vimentin. Tumour has retained expression of FH stain.

Results of molecular studies vary. It most commonly exhibits gain of chromosome 17 and losses of chromosomes 9 and Y as well as mutations affecting genes *ABL1*, *PDGFRA*, *KMT2C*, *KDM5C*.

1.2.10 Acquired cystic disease-associated renal cell carcinoma

Acquired cystic disease-associated RCC is neoplasm occurring only in a setting of acquired cystic disease, in patients with the history of long-term hemodialysis. Tumours show varied architectural patterns, with sieve-like appearance as the most characteristic together with oxalate crystal depositions. Cells show voluminous, eosinophilic cytoplasm.

Immunohistochemical profile and molecular features are not specific.

1.2.11 Renal cell carcinoma NOS

Group of high grade renal cancers, including sarcomatoid carcinoma, with no morphologic features of any of well-established entities. It is more a tumour management category rather than proper entity. Logically, category has no specific immunoprofile or molecular findings.

1.2.12 *TFE3*-rearranged renal cell carcinomas

TFE3-rearranged renal cell carcinomas (TFE3 RCC) is molecularly defined RCC characterised by gene fusions involving *TFE3* gene (located on chromosome Xp11.23) with the wide spectrum of different fusion partners. A various fusion partners of *TFE3* gene result in a broad morphology spectrum ranging from low grade to high grade tumours. The classic description includes papillary architecture with voluminous cells and deposits of psammoma bodies.

TFE3 RCCs show diffuse, strong, nuclear positivity for TFE3 immunohistochemistry (however, TFE3 immunostaining is not reliable, the reactivity is significantly affected by fixation of the material). Expression of melanocytic markers may be occasionally present. Epithelioid markers are underexpressed, PAX 8 reactivity is retained.

The most common fusion partners of *TFE3* gene are *PRCC*, *ASPSCR1* and *SFPQ*. Other partners include *NONO* (*P54NRB*), *RBM10*, *MED15*, *CLTC*, *DVL2*, *PARP14*, *KAT6A*, *NEAT1*, *MATR3*, *FUBP1*, and *EWSR1*. Of note, TFE3 break-apart FISH may show negative

results in cases of intrachromosomal translocations (*RBM10*::*TFE3*, *GRIPAP1*::*TFE3*, *RBMX*::*TFE3*, and *NONO*::*TFE3*).

1.2.13 *TFEB*-rearranged renal cell carcinomas

TFEB-rearranged renal cell carcinomas are part of the molecularly defined group of RCCs. Tumours harbour fusions or amplifications involving the gene encoding TFEB transcription factor on the 6p21 locus - two different entities are recognised in *TFEB*-rearranged category. *TFEB*-translocation RCC (in its "classic"/typically described morphology) shows a biphasic pattern with nests of large cells and second population of small cells surrounding basement membrane-like material (rosette formation). *TFEB*-amplified RCCs show a broad spectrum of morphology, frequently with papillary architecture and high grade oncocytic cells. However, the morphology of both subtypes *TFEB*-rearranged renal cell carcinomas vary significantly.

TFEB rearranged RCCs underexpress epithelial markers, typically with retained positivity for PAX8. Tumours consistently show reactivity for melanocytic markers and Cathepsin K, as well as TFEB immunohistochemistry. All above mentioned stains are less consistent in *TFEB* amplified RCC.

TFEB translocation and amplification may be identified by break-apart FISH. Assessment of variable fusion partners requires RNA sequencing.

1.2.14 Succinate dehydrogenase-deficient renal cell carcinoma (SDH-deficient RCC)

Succinate dehydrogenase-deficient RCC is group of neoplasm defined by loss of SDHB staining by immunohistochemistry and presence of the *SDH* gene mutation (most commonly *SDHB*, followed by *SDHC*, *SDHA*, and *SDHD)*. Tumours are usually well circumscribed and composed of solid nests of bland looking eosinophilic cells containing characteristic cytoplasmatic inclusions. Entrapment of non-neoplastic renal tubules is often seen on the periphery of the tumour. High grade transformation may occur.

True negative SDHB staining is defined as a loss of mitochondrial type positivity (normally strong granular, cytoplasmic stain), the staining should be assessed in comparison with the positive internal control in non-neoplastic kidney parenchyma. CD117 and CK 7 frequently show negative results.

Germline mutation in the SDH genes is defining molecular alteration.

1.3 Major changes, new entities, emerging entities

1.3.1 Other oncocytic tumours

This new diagnostic category/group is reserved for indolent, eosinophilic/oncocytic tumours that cannot be further classified either as RO or CHRCC or other well established renal neoplasms. It was clarified that multiple bilateral tumours occurring in syndromic setting (Birt–Hogg–Dubé syndrome) with intermediate features between ChRCC and RO are classified as "hybrid oncocytic tumour". Solitary, non-syndromic counterparts without necrosis, severe atypia and mitosis should be categorised as "oncocytic renal neoplasms of low malignant potential NOS" according to the GUPS recommendation (3).

Two recently described entities with distinctive morphologic, immunohistochemical and molecular features were included by WHO in "other oncocytic tumours" group (as an emerging entities): low-grade oncocytic tumour (LOT) and eosinophilic vacuolated tumour (EVT) (2). LOT is composed of compact nests of monotonous cells with eosinophilic cytoplasm, regular round to oval nuclei, frequently accompanied by perinuclear halo. Areas of abrupt transition to edematous stroma with elongated cells (with sometimes described myoid shape) are frequently seen. Defining feature is CK7 diffuse positivity and CD117 negativity (24-26). EVT features nest of cells showing voluminous, vacuolated eosinophilic cytoplasm and high grade nuclei with prominent nucleoli. Focally, tubulocystic pattern may be seen. Immunohistochemical profile varies, usually with positivity for CD117, CD10, Cathepsin K reported as the most common. CK7 is negative or may show positivity limited to scattered cells. Both tumours harbour mutations in the mTOR pathway genes (*TSC1*, *TSC2*, *MTOR*)(27-30).

1.3.2 Clear cell papillary renal cell tumour (CCPRCT)

Entity was previously known as clear cell papillary renal cell carcinoma. This tumour was "downgraded" and "renamed" to clear cell papillary renal cell tumour in current WHO classification (2) as evidence proved its indolent behaviour. Lesion may demonstrate variable architectural patterns from papillary, tubulopapillary and nested formations up to almost entirely cystic lesion. It is characterised by low grade morphology and cells with clear cytoplasm and nuclei arranged in linear fashion away from basement membrane (forming so-called "shark smiles" and "piano keys"- typically described in literature (31, 32)). Tumours may be associated with fibromyomatous stroma. Presence of high grade areas, necrosis, regression, local invasion are excluding features for CCPRCT diagnosis. Due to overlapping features with CCRCC, diagnosis should not be made on limited samples.

Tumour shows typical, diffuse positivity for CK 7 and "cup shaped" positivity for CAIX. HMWCK and GATA3 may be also positive. Racemase (AMACR), CD10 exhibit negative staining.

No specific molecular alterations were described in this entity. However, due to slightly overlapping features with CCRCC and other tumour with fibromyomatous stroma it is important to mention, that CCPRCT lacks chromosome 3p loss and alterations of *VHL*, and no mutations were reported in *TSC1*, *TSC2*, *MTOR*, or *ELOC* (*TCBE1*) genes.

1.3.3 Eosinophilic solid and cystic renal cell carcinoma

Eosinophilic solid and cystic renal cell carcinoma (ESC RCC) was in the previous WHO edition listed as an emerging entity (33). Thanks to growing evidence it gained a formal position in current WHO "blue book" as a separate entity (2). Tumour most often exhibits solid-cystic to solid architecture. It is composed of large, polygonal, eosinophilic cells with basophilic cytoplasmatic stripping sometimes likened to "leishmania-like" bodies. Cysts are covered by a single layer of hobnail to multinucleated cells. Foamy macrophages, psammomatous calcifications may be found.

Tumour usually express characteristic CK20 positivity with variable extent (diffuse, focally, single dispersed cells), however, negative staining may be seen in significant proportion of cases. Cathepsin K shows similar results. Vimentin is positive. CK7, CD117 are generally negative. Occasionally, melanocytic markers may exhibit positive reaction.

Mutations in the *TSC1* or *TSC2* genes are commonly demonstrated molecular alteration.

1.3.4 *ELOC* (formerly *TCEB1*)-mutated renal cell carcinoma

ELOC-mutated RCC is molecularly defined RCCs, harbouring mutations in the *ELOC* (*TCEB1*) gene at 8q21.11 (2). Tumour is composed of clear, voluminous cells arranged in branching tubules and/or true papillary formations, set in the background of striking fibromuscular stroma.

Tumour reveals constant, patchy to diffuse reactivity with CK7 along with "box-like" CAIX and CD10. HMWCK appears to be negative. Prove of *ELOC* mutation is required for diagnosis this neoplasm.

1.3.5 Fumarate hydratase-deficient renal cell carcinoma (FH-deficient RCC)

Fumarate hydratase-deficient RCC is molecularly defined entity with germline/somatic mutation of *FH* and exhibiting loss of staining for FH by

immunohistochemistry. In 4th WHO edition (from year 2016), it was designated as hereditary leiomyomatosis and renal cell carcinoma (HLRCC) syndrome–associated renal cell carcinoma (33). Due to frequently unknown clinical context/unknown germline mutation status, the renaming for FH–deficient RCC appears to be more reasonable. The tumour is well-known for multiple architectural patterns within one tumour mass (intratumoral heterogeneity). Cells with prominent inclusion-like nucleoli are usually found at least focally. The high grade morphology is most frequently seen, however low grade spectrum was also described in this tumour.

Besides negative immunohistochemical reactivity for FH, positive staining for 2SC is also typical.

Inactivating mutation of *FH* gene (germline or somatic) is defining molecular alteration in this entity.

1.3.6 ALK-rearranged renal cell carcinomas

ALK-rearranged RCC is included in molecularly defined category of renal tumours, harbouring fusions involving the gene encoding anaplastic lymphoma kinase (*ALK*) at chromosome 2p23 (2). Tumour is composed of voluminous eosinophilic cells with intracytoplasmatic vacuolization. Architecture and morphology of the tumour partially depends on the fusion partners. Solid sheets of large, eosinophilic cells with cytoplasmatic vacuolization surrounded by inflammatory rim characterises RCC with *VCL::ALK* gene fusion (seen in patients with sickle cell trait). More heterogeneous morphology with papillary, cribriform formations are seen in fusion partners like *TPM3*, *EML4*, *STRN*, *HOOK1*. Mucinous background is a commonly described feature. Morphologic variants mimicking metanephic adenoma or mucinous tubular and spindle cell RCC have also been described (34).

Immunohistochemistry reveals typical ALK positivity with concurrently retained SMARCB1 (INI1) expression.

1.3.7 SMARCB1-deficient renal medullary carcinoma

SMARCB1-deficient renal medullary carcinoma is a part of molecularly defined group of RCC, entity featuring loss of SMARCB1 (INI1) staining by immunohistochemistry and occurring in patients with sickle cell trait. Morphology reveals highly infiltrative nests/tubules/microcysts/cords of pleomorphic cells set in desmoplastic, myxomatous, frequently inflamed stroma.

Immunohistochemical examination demonstrates reactivity for epithelial markers (broad spectrum cytokeratins, EMA) and vimentin. Around 50% of cases show strong positivity to OCT3/4.

Translocations or deletions leading to inactivation of the *SMARCB1* gene (at 22q11.23) are most common molecular alterations in this tumour.

2 Objectives of the work

1. To describe unusual and not so frequent morphologic pattern of PRCC – precisely specified so called MESTK-like PRCC with its immunohistochemical, molecular features and discuss differential diagnosis and impact on prognosis.
2. To describe the morphologic spectrum of ChRCCs, its immunohistochemical, molecular features, discuss differential diagnoses, and impact on prognosis.
3. To describe new entities within recent WHO chapter “other oncocytic tumours”.

3 Results

The results of the dissertation are presented by the seven original papers listed below.

3.1 Papillary renal cell carcinoma with prominent spindle cell stroma - tumor mimicking mixed epithelial and stromal tumor of the kidney: Clinicopathologic, morphologic, immunohistochemical and molecular genetic analysis of 6 cases.

Extensive studies on papillary renal cell carcinoma have resulted in report of multiple morphologic variants of PRCC. We described a series of 6 PRCCs featuring prominent spindle cell stroma, resembling stroma in mixed epithelial and stromal tumor of the kidney (MESTK) or sarcomatoid RCC. Clinicopathologic, morphologic, immunohistochemical and molecular features were analysed.

Clinical data, including follow up, were available for 4 patients. All patients were male with age range 44 to 98 years. Follow up ranged from 3 to 96 months. Tumour size ranged from 2.4–11.4 cm. Pathologic stage ranged from pT1 to pT3 and with one patient presented initially with regional lymph node metastasis but no further information about the clinical course of this patient provided. All tumours were well demarcated, with one surrounded by a thick fibrous capsule. Cytologic features of the epithelial compartment exhibited cuboidal to cylindrical cells with variable amount of pale to eosinophilic cytoplasm and nuclei with low to high grade. Mitotic count was low, up to 5 mitoses/10 HPF. Necrosis was present only focally. Most striking feature was an extensive stromal component with variable cellular density, reminiscent of Müllerian type stroma. There was no atypia, necrosis or mitotic figures. No mesenchymal heterogeneous elements were found. Immunohistochemistry of epithelial component revealed positivity for CK7, AMACR, vimentin and negative results for HMB45, TFE3. FH expression was retained. Stromal component was positive for vimentin and actin S. CD34 positivity was limited to vessels wall. Estrogen and progesterone receptors were negative in both components. In five analysable cases, numerical chromosomal aberration pattern was either variable (with multiple chromosomal gains and losses) or with no aberrations detectable. Polysomy of chromosomes 7 and 17 was detected, however not in a pattern considered typical for PRCC (i.e. trisomy or polysomy of both chromosome 7 and 17). No other alterations described in PRCCs (*CDKN2A*, *BAP1*, or *MET* gene abnormalities) were found. Differential diagnosis includes mixed epithelial and stromal tumor of the kidney (MESTK), sarcomatoid RCC, group of RCCs featuring fibroleiomyomatous stroma (*ELOC* (formerly *TCEB1*)-mutated RCC and subset of RCCs associated with mutations in genes in the mTOR pathway) and clear cell papillary RCT (formerly clear cell papillary RCC).

Based on this study, we concluded that PRCC with MESTK-like stroma is a rare, distinctive variant of PRCC. Further investigations of morphology and underlying molecular

alterations will help us properly categorize subgroups within PRCC and, hence, may result in adequate clinical management and the development of more effective forms of the therapy.

Annals of Diagnostic Pathology 44 (2020) 151441

Contents lists available at ScienceDirect

Annals of Diagnostic Pathology

journal homepage: www.elsevier.com/locate/anndiagpath

Original Contribution

Papillary renal cell carcinoma with prominent spindle cell stroma - tumor mimicking mixed epithelial and stromal tumor of the kidney: Clinicopathologic, morphologic, immunohistochemical and molecular genetic analysis of 6 cases

Joanna Rogala[a,b], Fumiyoshi Kojima[c], Reza Alaghehbandan[d], Abbas Agaimy[e], Petr Martinek[a], Ondrej Ondic[a], Monika Ulamec[f], Maris Sperga[g], Kvetoslava Michalova[a], Kristyna Pivovarcikova[a], Tomáš Pitra[h], Milan Hora[h], Ivan Ferak[i], Jana Marečková[a], Michal Michal[a], Ondrej Hes[a,*]

[a] Department of Pathology, Charles University, Medical Faculty and Charles University Hospital Plzen, Czech Republic
[b] Department of Pathology, Regional Specialist Hospital Wroclaw, Poland
[c] Department of Human Pathology, Wakayama Medical University, Wakayama, Japan
[d] Department of Pathology, Faculty of Medicine, University of British Columbia, Royal Columbian Hospital, Vancouver, BC, Canada
[e] Department of Pathology, University of Erlangen, Erlangen, Germany
[f] "Ljudevit Jurak" Pathology Department, Clinical Hospital Center "Sestre milosrdnice", Pathology Department, Medical University, Medical Faculty Zagreb, Croatia
[g] Department of Pathology, Riga Stradin's University, Riga, Latvia
[h] Department of Urology, Charles University, Medical Faculty and Charles University Hospital Plzen, Czech Republic
[i] Department of Pathology, Agel Laboratory, Novy Jicin, Czech Republic

ARTICLE INFO

Keywords:
Kidney
Papillary renal cell carcinoma
MESTK-like
Sarcomatoid-like

ABSTRACT

Papillary renal cell carcinoma (PRCC) is currently a well-studied type of RCC. In addition to PRCC type 1, there are a number of other subtypes and variants of PRCCs which have been reported. We describe a series of 6 PRCCs with papillary, micropapillary and/or tubulopapillary architecture and prominent spindle cell stroma, resembling stroma in mixed epithelial and stromal tumor of the kidney (MESTK) or sarcomatoid RCC.

Clinicopathologic, morphologic, immunohistochemical and molecular features were analyzed.

All patients were males with an age range of 44–98 years (mean 65.3, median 65.5 years). Tumor size ranged from 2.4–11.4 cm (mean 5.8, median 4.5 cm). Follow-up data were available for 4 patients, ranging from 3 to 96 months (mean 42.75, median 36 months). Epithelial cells were mostly cylindrical with eosinophilic cytoplasm, showing nuclear grade 2 and 3 (ISUP/WHO).

In all cases, loose to compact prominent stroma composed of spindle cells, without malignant mesenchymal heterologous elements was detected. No atypical mitoses were found, while typical mitoses were rare in both epithelial and stromal components.

Epithelial cells were positive for CK7, AMACR, and vimentin in all cases, while negative for TFE3, HMB45, desmin, CD34, and actin. The stroma was positive for vimentin, actin and focally for CD34, while negative for CK7, AMACR, TFE3, HMB45, and desmin. Estrogen and progesterone receptors were completely negative. FH and SDHB expression was retained in all analyzable cases. Proliferative index was barely detectable in stromal component and low in epithelial component, ranging 0 to 5% positive stained cells/high power field.

Copy number variation was variable with no distinct pattern. No mutations in *CDKN2A*, *BAP1*, *MET* were detected.

PRCC with MESTK-like features is a distinct variant of PRCC mimicking MESTK. Our findings add to the body of literature on ever expanding variants of PRCCs. Both epithelial and stromal components lacked true Müllerian features, which was also proven by immunohistochemistry.

* Corresponding author at: Department of Pathology, Medical Faculty and Charles University Hospital Plzen, Alej Svobody 80, 304 60 Pilsen, Czech Republic.
E-mail address: hes@medima.cz (O. Hes).

https://doi.org/10.1016/j.anndiagpath.2019.151441

1. Introduction

Papillary renal cell carcinoma (PRCC) is the second most common type of renal cell carcinoma. PRCC is traditionally classified according to the 2016 World Health Organization (WHO) Classification of Genitourinary Tumors into type 1 and type 2 [1]. However, studies published recently have shown more evidence emphasizing heterogeneity within this group of tumors, particularly the so-called type 2.

A number of PRCC variants were described recently in the literature such as oncocytic, solid, mucin secreting, biphasic squamoid, Warthin–like, and PRCC with reverse polarity [2-8]. All these variants are mostly defined by using morphologic and immunohistochemical features and they are more close to (at least in part variant of) type 1 PRCC. However even at the molecular genetic level, there are substantial differences among tumors classified generally as PRCC. The so-called type 2 PRCC seems to be rather composed of a group of tumors sharing papillary architecture than a uniform and distinct entity.

In this study, we analyzed clinicopathologic, morphologic, immunohistochemical, and molecular features of 6 unusual PRCC with papillary and/or tubulopapillary architecture and with prominent spindle cell stroma resembling mixed epithelial and stromal tumor of the kidney (MESTK).

2. Material and methods

2.1. Case selection and routine microscopy

Index case was sent to one of the authors (OH) for second opinion. Later we searched several institutional archives for cases, using the key words: renal cell, papillary, stroma-rich, sarcomatoid-like, MESTK-like, and spindle cell. The final review and case selection for the study was carried out by 2 pathologists (JR and OH) resulting in inclusion of 6 cases meeting the study criteria. Clinicopathologic and follow-up data were collected using the available medical records from the participating institutions. The tissue was fixed in 4% formalin, embedded in paraffin using routine procedures. 2 um thin sections were cut and stained with hematoxylin and eosin.

2.2. Immunohistochemistry

All immunohistochemistry (IHC) stains except for PBRM1 were performed in one laboratory (University Hospital Plzen), using a Ventana Benchmark XT automated stainer (Ventana Medical System, Inc., Tucson, AZ, USA). The following primary antibodies were used: CK7 (OV-TL12/30, monoclonal, DakoCytomation, 1:200), CK20 (M7019, monoclonal, DakoCytomation, 1:100), alpha-methylacyl-CoA-racemase (AMACR) (P504S, monoclonal, Zeta, Sierra Madre, CA, 1:50), vimentin (D9, monoclonal, NeoMarkers, Westinghouse, CA, 1:1000), Ki67 (MIB1, monoclonal, Dako, Glostrup, Denmark, 1:1000), anti-melanosome (HMB45, monoclonal, DakoCytomation, 1:200), TFE3 (polyclonal, Abcam, Cambridge, UK, 1:100), desmin (D33, monoclonal, DakoCytomation, 1:2500), actin S (1A4, Cell Marque, Rocklin, CA, RTU), CD34 (QBEnd-10, monoclonal, Dako, 1:100) and fumarate hydratase (J13, monoclonal, Santa Cruz, Dallas, TX, 1:3000). PBRM1 was stained in the Pathology Department, University Hospital Erlangen, Germany using a fully automated system ("Benchmark XT System", Ventana Medical Systems Inc., 1910 Innovation Park Drive, Tucson, Arizona, USA) and a primary anti-PBRM1 monoclonal antibody retrieved from Atlas Antibodies AB, SE-168 69 Bromma, Sweden (clone CLO331, dilution, 1: 50). The primary antibodies were visualized using a supersensitive streptavidin-biotin-peroxidase complex (BioGenex). Internal biotin was blocked by standard protocol used by Ventana Benchmark XT automated stainer (hydrogen peroxide based). Appropriate positive and negative controls were also used. The immunohistochemical evaluation was based on the staining percentage of cells: focal positive < 50%, diffuse positive > 50%, negative (−) 0%.

2.3. DNA extraction

Tumor areas of the formalin-fixed paraffin-embedded (FFPE) samples were determined using hematoxylin-eosin stained slides and macro dissected. DNA from FFPE tumor tissue was extracted using QIAsymphony DNA Mini Kit (Qiagen, Hilden, Germany) on an automated extraction system (QIAsymphony SP; Qiagen) according to manufacturer's supplementary protocol for FFPE samples. Concentration and purity of isolated DNA were measured using NanoDrop ND-1000 and DNA integrity was examined by amplification of control genes in a multiplex polymerase chain reaction (PCR). Only samples that were able to produce at least 400 bp long amplicons were used for low pass whole genome sequencing.

2.4. Low pass whole genome sequencing

SurePlex DNA amplification system (Illumina, San Diego, CA) was used to generate DNA template from tumor samples. Amplification is highly representative, which makes the resulting product suitable for copy number variation detection. The library of all samples was prepared using Nextera DNA Sample Prep Kit (Illumina, San Diego, CA) and was sequenced on MiSeq sequencer, copy-number variant analysis was performed using BlueFuse Multi software with the Veriseq plugin (Illumina, San Diego, CA). Following quality control filters for valid samples were set: minimum 1 million reads per sample, average quality score and average alignment score > 30, and overall noise < 0,3. Thresholds for CNV calling were set based on a group of samples with known CNVs, that were validated using array CGH and fluorescence in-situ hybridization. The percentage of tumor in the DNA sample was considered, when calling the lower frequency CNVs and thresholds for CNVs were set individually for each case typically the copy number was 1.5 for loss and 2.5 for gain. CNVs spanning less than the whole length of a chromosome arm were not called. Selected CNVs were confirmed by FISH as described previously [9]. The more complex changes are written out in the table description. Gonosomes were excluded from the analysis. CNV detection using low pass whole genome sequencing was proven to produce similar results as in fresh frozen tissue [10].

2.5. Targeted sequencing

The DNA part of TruSight Tumor 170 kit (Illumina) was used to analyze DNA mutations in CDKN2A, BAP1, and MET genes. The quality control (QC) of the input DNA was performed using Infinium HD FFPE QC Kit (Illumina), only samples with a Ct value < 5 were used for analysis. Library preparation was performed according to manufacturer's instructions and the libraries were sequenced on NextSeq 500. The quality of resulting data was controlled for median insert size (larger than 79 base pairs) and the percentage of bases, covered > 100× had to be at least 95%. Additionally, regions of interest were checked for minimal coverage of 100×. The variants were called using dedicated app for TruSight Tumor 170 kit, and then annotated and filtered using Variant Interpreter both on Illumina's cloud portal Basespace. The filters kept only non-synonymous variants that passed variant QC, had allelic frequency > 0.05, and had population frequency from ExAC database < 0.01. The remaining subset of variants was checked visually, and suspected artefactual variants were excluded.

3. Results

Six patients were included in this study. Detailed clinical data with follow up were available for 4 patients (Table 1). All patients were male with age range 44 to 98 years (mean 65.3, median 65.5 years). Tumor size ranged from 2.4–11.4 cm (mean 5.8 median 4.5 cm). Pathologic stage was pT1 in 3 cases (case 1, 5, and 6), pT2 in 1 (case 4), and pT3 in 2 cases (case 2 and 3). One patient initially presented with regional lymph node metastasis (case 4). Unfortunately, no further information

Table 1
Clinicopathological data.

Case no.	Sex	Age (years)	Tumor size-diameter (cm)	Stage	Grade	F/U time (months)	F/U
1	M	72	2.9	pT1a	2	12	AD[a]
2	M	44	6	pT3, No	2	96	AWD
3	M	98	9	pT3	3	LE	LE
4	M	47	11.4	pT2, N1	3	LE	LE
5	M	59	2.4	pT1a	2	60	AWD
6	M	72	3	pT1a	2	3	AWD

M, Male; Grade, according to the WHO/ISUP grading system; F/U, follow up; LE, Lost of evidence; AWD, Alive without evidence of disease; AD, Alive with disease; p TNM according to the 8th Edition, AJCC Staging Manual 2017.
[a] Uncertain findings by ultrasonography-suspect recurrence.

about clinical course was available for this particular patient.

Follow up data were available (for 4 patients), ranging from 3 to 96 months (mean 42.75, median 36 months). No records concerning aggressive behavior were found in 3 patients (case 2, 5 and 6). In one patient (case 1) ultrasonographic examination revealed suspicious residual lesion in the area of previous surgery. However, no biopsy was performed to further verify this finding.

Main morphologic characteristics are summarized in Table 2. All tumors were well demarcated, with one tumor demonstrating thick fibrous pseudocapsule (case 5). In two cases (case 2 and 3) renal sinus fat involvement by the tumor was documented. In 1 case (Case 3) lymphovascular invasion was also noted. The architecture was papillary and tubulopapillary (Fig. 1A + B). Micropapillation was detected in 5/6 cases (at least focally) (Fig. 2). However, true prominent micropapillae were not recognized. Papillae were lined by cuboidal to cylindrical neoplastic cells, with variable amount of eosinophilic cytoplasm (Fig. 3). Case 4 showed mostly pale cytoplasm, however no typical clear cell areas were identified. Nuclear grade was 2 in four cases (cases 1, 2, 5 and 6), while the remaining two cases showed grade 3 (case 3 and 4), according to Fuhrman (ISUP/WHO modification).

Necrosis in epithelial component was present in 2 cases (case 4 and 5). Mitotic activity was relatively low: no mitoses were found in 2 cases (case 2 and 5), 1 mitosis/10 HPF in 1 case (case 1) and up to 5 mitoses/10 HPF in 2 cases (case 3 and 4). No atypical mitotic figures were noted. Stroma was composed of uniform spindle cells resembling those of the Müllerian type stroma. The density of the spindle cell elements was variable, ranging from weak to dense (Fig. 4A + B). No smooth muscle differentiation was found. Foamy macrophages and psammoma bodies were present in all but one case (case 2). No necrosis or mesenchymal heterologous elements were found. Mitotic activity was absent.

Results of immunohistochemical examination are summarized in Tables 3A and 3B, separately for epithelial and stromal component. All tumors showed uniform strong and diffuse positivity for CK7, AMACR, and vimentin in the epithelial component (Fig. 5A + B). HMB45, TFE3, desmin, CD34, and actin were negative in the epithelial cells. Fumarate hydratase (FH) staining was retained in all cases. PBRM1 was positive (retained) in 5/6 cases (Fig. 6). In one case, both epithelial and stromal components were negative, as well as adjacent non-neoplastic tissues. This case was interpreted as non-analyzable. Stromal component was invariably positive for actin and vimentin. CD34 was positive in vessel wall within the stromal component, while stromal cells were negative. Estrogen and progesterone receptors were negative in both epithelial and stromal components. The Ki67 proliferation index was low in epithelial component and nearly absent in stromal component.

Numerical chromosomal aberration pattern of the analyzed cases is summarized in Table 4. Five cases were analyzable, copy number variation pattern was variable (multiple gains and losses of whole chromosomes or chromosomal arms were detected). In one case (case 4) multiple losses and gains were detected. Gain of chromosome 12 and loss of chromosome 18 were documented in 1 case (case 2). Multiple losses were documented in 1 case (case 5). One case had no detectable chromosomal numerical aberrations (case 1). No *CDKN2A*, *BAP1*, or *MET* gene abnormalities were found (Table 4).

4. Discussion

PRCC is a group of kidney tumors characterized mostly by papillary and/or tubulopapillary architecture. Type 1 PRCC is considered to represent a distinct entity with uniform characteristic morphologic, immunohistochemical, and molecular genetic features. The so-called type 2 is defined according to the WHO 2016 by presence of epithelial cells with abundant eosinophilic cytoplasm, high nuclear grade and nuclear pseudostratification [1]. However, immunohistochemical profile of so-called type 2 is rather variable as well as the molecular genetic profile. In fact, recent studies have shown that the so-called type 2 PRCC represents several distinct variants or subtypes of RCC sharing predominantly a papillary pattern [11,12].

Several studies describing unusual morphologic forms of PRCC, together with immunohistochemical and genetic profiles have been recently published in the literature. Such tumors significantly differ from type 1 and type 2 PRCC. The most frequently discussed variant is oncocytic PRCC (OPRCC), which is one of the provisional entities in the latest WHO classification [1]. OPRCC is relatively poorly understood entity without a precise or reproducible definition. In addition to OPRCC, a number of other PRCC variants have been documented, including Warthin-like PRCC, solid PRCC, biphasic squamoid PRCC, "mucin" secreting PRCC, PRCCs with clear cells, and papillary renal neoplasm with reverse polarity [3,5-8,13,14]. Immunohistochemical profile and molecular genetic features of above-mentioned variants of PRCC are variable and mostly are not consistent with type 1 or type 2 PRCC. Such variants represent a highly heterogeneous group of tumors, which share papillary or tubulopapillary architecture. Cytological features are different as well as immunohistochemical profile. Further, it is now evident that previous known historic "landmark" of chromosomal

Table 2
Morphological data.

Case	ISUP grade	Architectural pattern (a)	Foamy macrophages (b)	Psammoma bodies (c)	Necrosis (d)	Capsule	Stromal cellularity (e)	Type of epithelial cells (f)	Mitoses stroma	Mitoses epithelium
1	2	P	+	+	−	−	+	Cb	1/10HPF	1/10 HPF
2	2	P	+	−	−	−	+ +	Cb	−	−
3	3	T-P	+ + +	+ +	−	−	+ + +	Cl	−	5/10 HPF
4	3	T-P	+ +	+ +	+F	−	+ +	Cl	−	5/10HPF
5	2	P	+ +	+	+	+	+	Cl	−	−
6	2	P	+	−	+F	+	+	Cl	−	1/10HPF

a) architectural pattern: P-papillary, T-P -tubulo-papillary; b) foamy macrophages were assessed as absent (−), sparse (+), moderate (+ +), prominent (+ + +), c) psammoma bodies were assessed as absent (−), sparse (+), moderate (+ +), prominent (+ + +); d) necrosis was assessed as + (present), − (absent) F- focal; e) stromal cellularity was assessed as: sparse (+), moderate (+ +), prominent (+ + +); f) type of epithelial cells lining papillae were assessed as Cl- columnar, Cb-cuboidal; HPF high power field, absent mitoses (−).

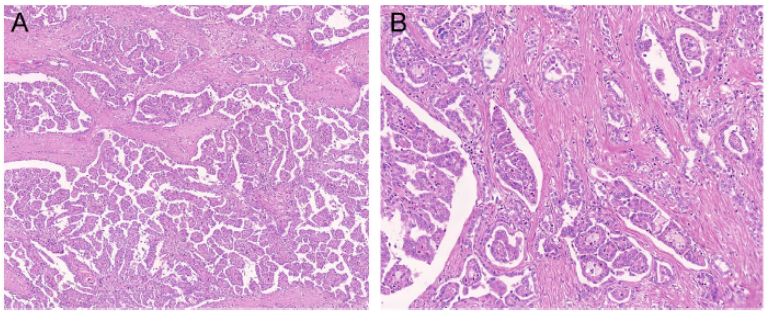

Fig. 1. The architecture was papillary (A) and tubulopapillary (B) in all cases.

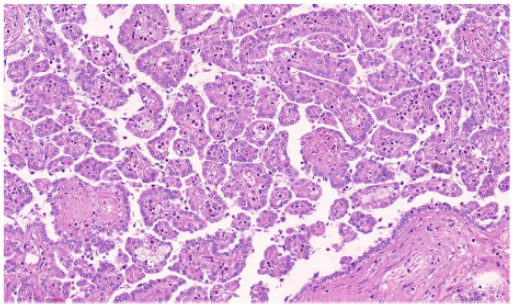

Fig. 2. Micropapillation was at least focally detected in majority of cases. No true prominent micropapillary areas were found.

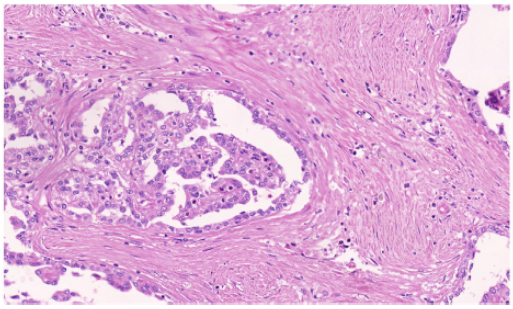

Fig. 3. Papillae or tubules were lined by cuboidal to cylindrical cells with variable amount of eosinophilic cytoplasm.

copy number variation pattern for PRCC - trisomy/polysomy of chromosomes 7 and 17 - is not a consistent finding in the ever expanding heterogeneous "PRCC" group [15]. In fact, it is not surprising that within such a heterogeneous group of tumors, all being lumped under the PRCC diagnostic umbrella, new variants/subtypes are still emerging.

Müllerian type stroma is a feature typically found in mixed epithelial and stromal tumor of the kidney (MESTK) [1,16-18]. Less prominent Müllerian type stroma is seen in subepithelial zones of cysts within so-called angiomyolipoma with epithelial cyst (AMLEC) [19]. Müllerian stroma is characterized by a loose to dense population of bland spindle cells, which immunohistochemically express estrogen and/or progesterone receptors. Similar type of stroma can also be found in other extra-renal tumors such as mucinous cystic neoplasm of the pancreas and mucinous cystadenoma of the liver [20]. Focal luteinization and corpus albicans-like changes may be seen, regardless of the tumor location, as a reactive change secondary to damaged stroma [21].

Tumors in our series are distinct owing to the architecture and the presence of prominent stroma resembling Müllerian type stroma. However, in a closer look, stroma in our cases differs in many aspects from stroma known as Müllerian type stroma. The stromal component in our cases was rather cellular despite the fact that it was slightly variable between the cases (dense to loose cellularity), but overall showed low grade morphologic features and was relatively uniform. No conspicuous mitotic activity, necrosis, or sarcomatous differentiation was documented. Also, epithelial component lacked features typically seen in MESTK. The neoplastic cells were relatively uniform, cuboidal to cylindrical. No intracytoplasmic vacuoles or ciliated epithelium were identified within our series. There were no true Müllerian structures (within stromal and epithelial component), which was further supported by immunohistochemistry.

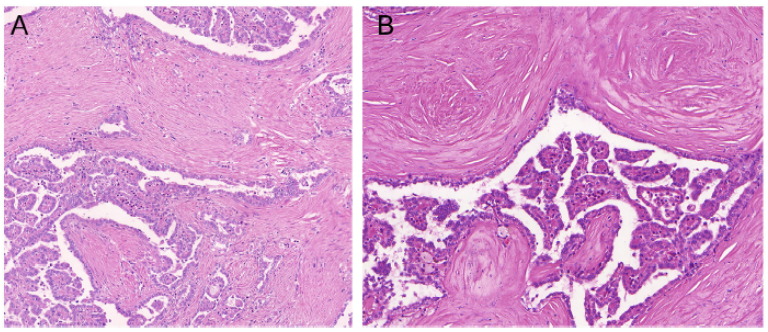

Fig. 4. Stroma was composed of uniform spindle cells resembling those in Müllerian type of stroma (panel A). Density of spindle cell elements was variable, ranged from weak to dense. Panel B shows weakly cellular parts of stroma.

Table 3A
Results of immunohistochemical examination-epithelial component.

Case	CK7	AMACR	vim	TFE3	HMB45	Desmin	CD34	Ki67	Actin	FH	ER	PR	PBMR1
1	+ + +	+ + + +	+ + +	–	–	–	–	2–4/HPF	–	ret	–	–	ret
2	+ + +	+ + +	+ + +	–	–	–	–	0–2/HPF	–	ret	–	–	ret
3	+ + /foc + + +	+ + +	+ + +	–	–	–	–	4–8/HPF	–	ret	–	–	ret
4	+ +	+ + +	+ +	–	–	–	–	0–1/HPF	–	ret	–	–	ret
5	+ + +	+ + +	+ + +	–	–	–	–	4–7/HPF	–	ret	–	–	NA
6	+ + +	+ + +	+ + +	–	–	–	–	0–4/HPF	–	ret	–	–	ret

Abbreviations: foc, focally positive; ret, expression retained; + weakly positive, + + moderately positive, + + + strongly positive; vim, vimentin; FH, fumarate hydratase; ER, estrogen receptor; PR, progesterone receptor; NA, not analyzable; HPF, High Power Field.

Table 3B
Results of immunohistochemical examination-stromal component.

Case	CK7	AMACR	vim	TFE3	HMB45	desmin	CD34	Ki67	Actin	FH	ER	PR	PBMR1
1	–	–	foc + + +[a]	–	–	–	foc + + +[a]	0–1/HPF	+ +	ret	–	–	ret
2	–	–	foc + + +[a]	–	–	–	foc + + +[a]	0–1/HPF	+ +	ret	–	–	ret
3			+ + +	–	–	–	foc + + +[a]	0–2/HPF	+ + +	ret	–	–	ret
4	–	–	+ + /foc + + +[a]	–	–	–	foc + + +[a]	0–1/HPF	+ + +	ret	–	–	ret
5	–	–	foc + + +[a]	–	–	–	foc + + +[a]	0–1/HPF	+ + +	ret	–	–	NA
6	–	–	foc + +	–	–	–	foc + + +[a]	0	+ + +	ret	–	–	ret

Abbreviations: foc, focally positive; ret., + weakly positive, + + moderately positive, + + + strongly positive, ret expression retained, vim vimentin, FH fumarate hydratase, ER estrogen receptor, PR progesterone receptor, NA not analyzable, HPF, High Power Field.
[a] Vessels.

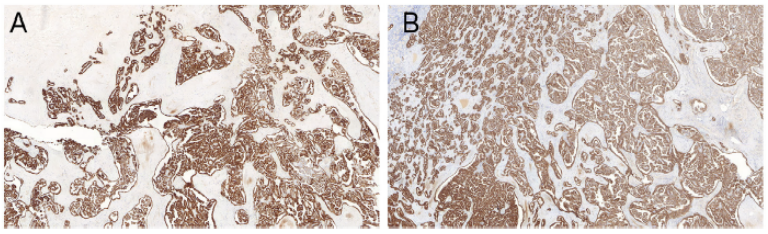

Fig. 5. Epithelial component was positive diffusely for CK7 (A) and AMACR (B).

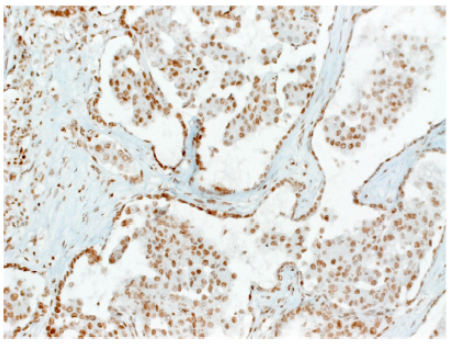

Fig. 6. Immunoreactivity for PBMR1 was retained in all analyzable cases.

Immunohistochemical profile of tumors in current series did not substantially differ (despite heterogeneity of PRCC as a group) from majority of PRCC variants. Co-expression of AMACR, CK7, and vimentin is considered as a relatively characteristic immunoprofile for PRCC. Immunohistochemical examination failed to confirm estrogen or progesterone receptor positivity both within stromal and epithelial components.

Morphologic features along with immunohistochemical profile strongly suggest the diagnosis of an unusual variant of PRCC.

At molecular genetic level, we were able to successfully analyze

Table 4
Summary of genetic analyses.

Case	Gains (chromosome)	Losses (chromosome)	*CDKN2A, BAP1, MET* mutations
1	None	None	Negative
2	12	18	Negative
3	16	None	Negative
4	1q,3q,12,17	1p,2q,3p, 9, 11q,13,21,22	Negative
5	None	6,9p,15q,22	Negative
6	NP	NP	Negative

Abbreviation: NP, not performed.

CNV pattern in 5/6 cases. CNV pattern was rather variable with multiple losses and gains. Polysomy of chromosomes 7 and 17 was detected, however not in a "characteristic" combination (i.e. trisomy or polysomy of both chromosome 7 and 17) seen in type 1 PRCC. This further supports the fact that trisomy/polysomy of chromosomes 7 and 17 is not a constant genetic feature in majority of PRCC subtypes [12,15].

Recent molecular studies confirmed that type 1 PRCC is a distinct entity, while type 2 PRCC is rather a heterogeneous group of renal tumors with predominantly papillary architecture. Type 1 PRCC is characterized by altered *MET* gene or increased chromosome 7 and 17 copy number. The Cancer Genomic Atlas Network study on the so-called type 2, and a group of unclassified PRCCs showed a heterogeneous genetic profile in 3 clusters: 1) *CDKN2A* altered PRCCs, 2)

Table 5
Differential diagnosis.

	Architecture	Epithelial component	Stroma	Immunohistochemistry	Molecular genetic features	Biological behavior
PRCC with MESTK-like stroma	P/T-P	Low to high grade, clear to eosinophilic cytoplasm	Fibroleiomyomatous	CK7, AMACR, vim (+) ER, PR (−)	Variable	Malignant
MESTK	T-C/S	Flat, hobnailed, cuboidal, columnar, urothelial-like, clear cell	Fibroleiomyomatous and true Müllerian stroma	ER, PR (+)	No specific alteration	Indolent
Sarcomatoid RCC	Variable	High-grade epithelial cells with clear to eosinophilic cytoplasm (if any epithelial elements present)	Malignant, high grade spindle cells, possible heterogeneous mesenchymal differentiation	Variable cytokeratin positivity	Variable	Malignant
Clear cell papillary RCC	P/T-P	Low-grade epithelial cells with clear cytoplasm	Fibroleiomyomatous	CK 7, CANH 9 (cup shaped pattern) (+); CD10, AMACR (−)	Lack of *VHL* gene abnormalities	Indolent
RCC with prominent leiomyomatous stroma	N/T	Low-grade epithelial cells with clear cytoplasm	Leiomyomatous	CANH 9, vim (+); CK 7, AMACR, CD10 variable(+)	Lack of *VHL* gene abnormalities Chr.7, 17 gain-variable	Indolent
AMLEC	TC/S	Benign/entrapped epithelium	Leiomyomatous and true Müllerian stroma	ER, PR,CD10, HMB-45, Melan-A(+)	Possible mutation in *TSC 1/TSC 2*	Indolent
FH deficient RCC	P/TP, variable	Eosinophilic cytoplasm, high grade CMV inclusion-like deep red nucleoli	Fibrous, hyalinized	FH (−), 2SC (−) CK7 (−)	Mutation/LOH of *FH* gene	Malignant, aggressive
TCEB1 mutated renal cell carcinoma	S/T	Low-grade epithelial cells with clear cytoplasm	Fibromuscular	CANH 9(+), CK7 freq(+)	Mutations in *TCEB1* gene, lack of *VHL* gene abnormalities	Indolent

Abbreviations: RCC, renal cell carcinoma; PRCC, papillary renal cell carcinoma; MESTK, mixed epithelial and stromal tumor; AMLEC, angiomyolipoma with epithelioid cyst; FH, fumarate hydratase; P-papillary; T-P, Tubulo-papillary; T-C, Tubulo-cystic; N, Nested; S, Solid; T, Tubular; ER estrogen receptor, PR progesterone receptor, CANH9, carbonic anhydrase 9; +, positive; −, negative; freq, frequently.

SETD2, *BAP1* and *PBRM1* mutated PRCCs, and 3) CpG Island Methylator Phenotype associated tumors [11,22].

We analyzed *CDKN2A*, *BAP1*, *MET* genes in this study, and no mutations were found in our cases. It should be noted that the above-listed molecular classification has not been fully validated, and as such it seems that our tumors were not entirely compatible with at least 2 proposed groups. *PBRM1* was analyzed using immunohistochemistry. All analyzable cases (5/6) showed retained expression which is a strong surrogate for absence of inactivating or truncating *PBRM1* mutations. This suggests that it is unlikely that MESTK-like PRCC belongs to *BAP1* and *PBRM1* mutated PRCC subgroup proposed by Saleeb et al. [11].

From differential diagnostic point of view (Table 5), sarcomatoid differentiation within RCC should be taken into consideration.

"Sarcomatoid RCC" could be a diagnostic pitfall particularly on limited material, however clinical presentation and imaging studies may assist in resolving the matter. Patients with sarcomatoid RCC often present at an advanced stage with large tumor with infiltrative borders and necrosis. Morphologically, growth pattern is usually mosaic of original epithelial RCC component and solid sarcomatoid areas. Mitotic activity is usually brisk with atypical mitotic figures, as well as prominent necrotic foci. Heterologous mesenchymal neoplastic elements such as differentiation toward osteosarcoma, chondrosarcoma or other types of sarcomas can also be found [26]. Immunohistochemically, positivity of sarcomatoid spindle cell component for keratin cocktail AE1/AE3 or OSCAR, Cam5.2 or EMA can vary from focal to diffuse. Adequate sampling and basic immunohistochemical examination usually help to resolve the problematic differential diagnosis. The so-called RCC with prominent leiomyomatous stroma and/or RCC with *TFEB1* mutation should also be considered in the differential diagnosis, given prominent voluminous stroma an essential part of morphologic picture of such tumors [23-25]. However, the stromal component is less cellular in these tumors, compared to our cases. Moreover, stroma in RCC with prominent leiomyomatous stroma and/or RCC with *TFEB1* mutation is voluminous and rather fibroleiomyomatous, frequently with conspicuous leiomyomatous component. The architectural pattern in our cases is much complex. Further, the epithelial component of both RCC with prominent leiomyomatous stroma and *TFEB1*mutated RCC is nearly identical to low-grade clear cell RCC (arranged in nested/tubular pattern with clear voluminous cytoplasm) [23-25]. Papillary pattern is not documented in these RCCs. Low-grade spindle cell elements were described within clear cell RCC. However these cells were obviously epithelial origin and they did not represent stromal component [26]. Clear cell papillary RCC is another RCC with more or less prominent fibroleiomyomatous stroma that can enter into the differential diagnosis. Clear cell papillary RCC was first described as renal angioleiomyomatous tumor (RAT), owing to the presence of prominent leiomyomatous stroma, bland epithelial component and benign clinical course [27-28]. Subsequently, discussion about the relation of RAT and clear cell papillary renal cell carcinoma were held, which led to reserve the term RAT for cases with significant amount of stroma, while clear cell papillary RCC for cases with less prominent stroma [29]. Finally, both subtypes (stroma rich and cases with less prominent stroma) were proposed to be unified under –the term clear cell papillary RCC [1,30]. Stroma in clear cell papillary RCC is different in many aspects from the cases described herein. In clear cell papillary RCC, the stroma is mostly leiomyomatous, less cellular, and mostly without conspicuous spindle cell population. Further, the epithelial component of clear cell papillary RCC is different from our cases. Clear cell papillary RCC is composed of clear cell elements, different from pale eosinophilic cells in our tumors. Moreover, epithelial cells are arranged mostly in tubulopapillary pattern, wrapped in a delicate capillary network [30,31]. No capillary network around tubulary or tubulopapillary structures was noted, no elongated tubulary spaces (so-called "shark" smiles) or epithelial lining with nuclei orientated away from the basement membrane (so-called" piano keys") were noticed in any case in the current series. All such features are typical but not specific for clear cell papillary RCC.

In summary, we described a series of 6 distinct and uniform PRCCs with MESTK-like stroma. Further investigations of morphology and underlying molecular alterations will help us properly categorize subgroups within PRCC and, hence, may result in adequate clinical management and the development of more effective forms of therapy.

Funding

The study was supported by the Charles University Research Fund (project number Q39) and by the project Institutional Research Fund of University Hospital Plzen (Faculty Hospital in Plzen- FNPl 00669806).

Declaration of competing interest

All authors declare no conflict of interest.

References

[1] Moch H, Humphrey PA, Ulbright TM, R VE. WHO classification of tumours of the urinary system and male genital organs. IARC Lyon; 2016.
[2] Hes O, Brunelli M, Michal M, Cossu Rocca P, Hora M, Chilosi M, et al. Oncocytic papillary renal cell carcinoma: a clinicopathologic, immunohistochemical, ultrastructural, and interphase cytogenetic study of 12 cases. Ann Diagn Pathol 2006 Jun;10(3):133–9. (PubMed PMID: 16730306).
[3] Hes O, Condom Mundo E, Peckova K, Lopez JI, Martinek P, Vanecek T, et al. Biphasic squamoid alveolar renal cell carcinoma: a distinctive subtype of papillary renal cell carcinoma? Am J Surg Pathol 2016 May;40(5):664–75. (PubMed PMID: 26999503).
[4] Mantoan Padilha M, Billis A, Allende D, Zhou M, Magi-Galluzzi C. Metanephric adenoma and solid variant of papillary renal cell carcinoma: common and distinctive features. Histopathology 2013 Feb 4;62(6):941–53.
[5] Ulamec M, Skenderi F, Trpkov K, Kruslin B, Vranic S, Bulimbasic S, et al. Solid papillary renal cell carcinoma: clinicopathologic, morphologic, and immunohistochemical analysis of 10 cases and review of the literature. Ann Diagn Pathol 2016 Aug;23:51–7. (PubMed PMID: 27209513).
[6] Pivovarcikova K, Peckova K, Martinek P, Montiel DP, Kalusova K, Pitra T, et al. "Mucin"-secreting papillary renal cell carcinoma: clinicopathological, immunohistochemical, and molecular genetic analysis of seven cases. Virchows Arch 2016 Jul;469(1):71–80. (PubMed PMID: 27072821).
[7] Skenderi F, Ulamec M, Vanecek T, Martinek P, Alaghehbandan R, Foix MP, et al. Warthin-like papillary renal cell carcinoma: clinicopathologic, morphologic, immunohistochemical and molecular genetic analysis of 11 cases. Ann Diagn Pathol 2017 Apr;27:48–56. (PubMed PMID: 28325361).
[8] Al-Obaidy KI, Eble JN, Cheng L, Williamson SR, Sakr WA, Gupta N, et al. Papillary renal neoplasm with reverse polarity: a morphologic, immunohistochemical, and molecular study. Am J Surg Pathol 2019 Aug;43(8):1099–111. (PubMed PMID: 31135486).
[9] Sperga M, Martinek P, Vanecek T, Grossmann P, Bauleth K, Perez-Montiel D, et al. Chromophobe renal cell carcinoma—chromosomal aberration variability and its relation to Paner grading system: an array CGH and FISH analysis of 37 cases. Virchows Arch 2013 Oct;463(4):563–73. (PubMed PMID: 23913167).
[10] Munchel S, Hoang Y, Zhao Y, Cottrell J, Klotzle B, Godwin AK, et al. Targeted or whole genome sequencing of formalin fixed tissue samples: potential applications in cancer genomics. Oncotarget 2015 Sep 22;6(28):25943–61. (PubMed PMID: 26305677. Pubmed Central PMCID: 4694877).
[11] Saleeb RM, Brimo F, Farag M, Rompre-Brodeur A, Rotondo F, Beharry V, et al. Toward biological subtyping of papillary renal cell carcinoma with clinical implications through histologic, immunohistochemical, and molecular analysis. Am J Surg Pathol 2017 Dec;41(12):1618–29. (PubMed PMID: 28984673).
[12] Akhtar M, Al-Bozom IA, Al HT. Papillary renal cell carcinoma (PRCC): an update. Adv Anat Pathol 2019 Mar;26(2):124–32. (PubMed PMID: 30507616).
[13] Trpkov K, Athanazio D, Magi-Galluzzi C, Yilmaz H, Clouston D, Agaimy A, et al. Biphasic papillary renal cell carcinoma is a rare morphological variant with frequent multifocality: a study of 28 cases. Histopathology 2018 Apr;72(5):777–85. (PubMed PMID: 29119638).
[14] Petersson F, Sperga M, Bulimbasic S, Martinek P, Svajdler M, Kuroda N, et al. Foamy cell (hibernoma-like) change is a rare histopathological feature in renal cell carcinoma. Virchows Arch 2014 Aug;465(2):215–24. (PubMed PMID: 24903672).
[15] Pitra T, Pivovarcikova K, Alaghehbandan R, Hes O. Chromosomal numerical aberration pattern in papillary renal cell carcinoma: review article. Ann Diagn Pathol 2019 Jun;40:189–99. (PubMed PMID: 29454759).
[16] Michal M, Syrucek M. Benign mixed epithelial and stromal tumor of the kidney. Pathol Res Pract 1998;194(6):445–8. (PubMed PMID: 9689654).
[17] Michal M. Benign mixed epithelial and stromal tumor of the kidney. Pathol Res Pract 2000;196(4):275–6. (PubMed PMID: 10782473).
[18] Michal M, Hes O, Bisceglia M, Simpson RH, Spagnolo DV, Parma A, et al. Mixed epithelial and stromal tumors of the kidney. A report of 22 cases. Virchows Arch 2004 Oct;445(4):359–67. (PubMed PMID: 15322873).
[19] Fine SW, Reuter VE, Epstein JI, Argani P. Angiomyolipoma with epithelial cysts (AMLEC): a distinct cystic variant of angiomyolipoma. Am J Surg Pathol 2006 May;30(5):593–9. (PubMed PMID: 16699313).
[20] Quigley B, Reid MD, Pehlivanoglu B, Squires 3rd MH, Maithel S, Xue Y, et al. Hepatobiliary mucinous cystic neoplasms with ovarian type stroma (so-called "hepatobiliary cystadenoma/cystadenocarcinoma"): clinicopathologic analysis of 36 cases illustrates rarity of carcinomatous change. Am J Surg Pathol 2018 Jan;42(1):95–102. (PubMed PMID: 29016404).
[21] Michal M, Hes O. Corpora albicantia-like bodies in extraovarian lesions. Int J Surg Pathol 2004 Jul;12(3):298. (PubMed PMID: 15306946).
[22] Cancer Genome Atlas Research N, Linehan WM, Spellman PT, Ricketts CJ, Creighton CJ, Fei SS, et al. Comprehensive molecular characterization of papillary renal-cell carcinoma. N Engl J Med 2016 Jan 14;374(2):135–45. (PubMed PMID: 26536169. Pubmed Central PMCID: 4775252).
[23] Peckova K, Grossmann P, Bulimbasic S, Sperga M, Perez Montiel D, Daum O, et al. Renal cell carcinoma with leiomyomatous stroma—further immunohistochemical and molecular genetic characteristics of unusual entity. Ann Diagn Pathol 2014 Oct;18(5):291–6. (PubMed PMID: 25175809).
[24] Petersson F, Martinek P, Vanecek T, Pivovarcikova K, Peckova K, Ondic O, et al. Renal cell carcinoma with leiomyomatous stroma: a group of tumors with indistinguishable histopathologic features, but 2 distinct genetic profiles: next-generation sequencing analysis of 6 cases negative for aberrations related to the VHL gene. Appl Immunohistochem Mol Morphol 2018 Mar;26(3):192–7. (PubMed PMID: 29084058).
[25] Hakimi AA, Tickoo SK, Jacobsen A, Sarungbam J, Sfakianos JP, Sato Y, et al. TCEB1-mutated renal cell carcinoma: a distinct genomic and morphological subtype. Mod Pathol 2015 Jun;28(6):845–53. (PubMed PMID: 25676555. Pubmed Central PMCID: 4449825).
[26] Tanas Isikci O, He H, Grossmann P, Alaghehbandan R, Ulamec M, Michalova K, et al. Low-grade spindle cell proliferation in clear cell renal cell carcinoma is unlikely to be an initial step in sarcomatoid differentiation. Histopathology 2018 Apr;72(5):804–13. (PubMed PMID: 29194709).
[27] Michal M, Hes O, Havlicek F. Benign renal angiomyoadenomatous tumor: a previously unreported renal tumor. Ann Diagn Pathol 2000 Oct;4(5):311–5. (PubMed PMID: 11073338).
[28] Tickoo SK, dePeralta-Venturina MN, Harik LR, Worcester HD, Salama ME, Young AN, et al. Spectrum of epithelial neoplasms in end-stage renal disease: an experience from 66 tumor-bearing kidneys with emphasis on histologic patterns distinct from those in sporadic adult renal neoplasia. Am J Surg Pathol 2006 Feb;30(2):141–53. (PubMed PMID: 16434887).
[29] Srigley JR, Delahunt B, Eble JN, Egevad L, Epstein JI, Grignon D, et al. The International Society of Urological Pathology (ISUP) Vancouver classification of renal neoplasia. Am J Surg Pathol 2013 Oct;37(10):1469–89. (PubMed PMID: 24025519).
[30] Hes O, Comperat EM, Rioux-Leclercq N. Clear cell papillary renal cell carcinoma, renal angiomyoadenomatous tumor, and renal cell carcinoma with leiomyomatous stroma relationship of 3 types of renal tumors: a review. Ann Diagn Pathol 2016 Apr;21:59–64. (PubMed PMID: 26897641).
[31] Michal M, Hes O, Nemcova J, Sima R, Kuroda N, Bulimbasic S, et al. Renal angiomyoadenomatous tumor: morphologic, immunohistochemical, and molecular genetic study of a distinct entity. Virchows Arch 2009 Jan;454(1):89–99. (PubMed PMID: 19020896).

3.2 Renal cell carcinomas with tubulopapillary architecture and oncocytic cells: Molecular analysis of 39 difficult tumors to classify.

"Oncocytic" papillary renal cell carcinomas are a poorly defined group of neoplasms. Variable published studies about "oncocytic" PRCCs revealed conflicting results. Previous, 4th edition of WHO classification, mentioned oncocytic papillary renal cell carcinoma (OPRCC) as a "third type" of PRCC. However, it became apparent that some of defining morphologic and immunohistochemical properties described in WHO 2016 follow description of recently published PRCC with reverse polarity. Even on the basis of our work, it is evident that defining criteria of OPRCC are missing. Probably because of poor characterisation of OPRCC with poor reproducibility of morphologic, immunohistochemical and genetic criteria, likewise for contradictory biological potential documented in many OPRCCs the most recent 5th edition of WHO classification withdrew OPRCC as a distinct subtype of PRCC.

In this study, we analysed morphological, immunohistochemical, and molecular genetic features of renal tumours exhibiting papillary/tubulopapillary to solid/compressed architecture and oncocytic cells in order to better understand the relationship between morphology and genetic background of these heterogeneous group of RCCs. Group of 39 tumours with aforementioned morphologic features, confirmed oncocytic nature by immunohistochemical stain with antimitochondrial antigen antibody (MIA) and with well-preserved DNA was selected for the study. The tumours were divided in three distinct molecular subgroups based on chromosomal copy number variation (CNV) pattern:1) PRCC with oncocytic cells and CNV identical to RO (enumeration of chromosome 1 - loss of whole chromosome 1 or its deletion, typically 1p36; and/or loss of chromosome 14; and/or loss of gonosomes; and/or 11q13 rearrangement - gene CCND1, or normal karyotype. 2) PRCC with oncocytic cells and gains of chromosomes 7 and 17, and 3) PRCC with oncocytic cells and variable CNV not matching the two previously mentioned subgroups. In first group (renal oncocytoma-like CNV subgroup), 23 cases were included. Patients were 15 males and 8 females, with age range 52 to 81 years. Tumour size (available in 22/23 cases) ranged from 0.8 to 9 cm in greatest dimension. Tumour stage was available for 7 cases, it ranged from pT1 to pT3. Follow up was available for 14 patients, ranging from 0,5 to 8 years. All but one patient showed no evidence of disease, the one patient developed metastases. By morphology, papillary architecture was a dominant pattern, followed by compressed papillary architecture. Two cases fulfilled criteria for PRCC with reverse polarity. Pseudostratification, macrophages, necrosis, bloody lakes, calcification were variably seen. Immunoprofile varied with most frequent positivity for CK7 (single cell /focal positivity), AMACR, Cyclin D1. All tumours were negative for CD117, Melan A, and HMB45. GATA3 was positive only in cases meeting criteria for PRCC with reverse positivity. *KRAS* gene mutation was also documented in those cases. Cases with positive TFE3 staining showed no rearrangement of TFE3 by FISH. To second subgroup (PRCC with oncocytic cells and gains of chromosomes 7and 17), seven cases were included, 6 males and 1 female. One case represented a recurrence from a patient initially included in a previous group (group one). The age of six remaining patients ranged from 40 to 69 years. Tumour size ranged from 1.2 to 5 cm in greatest dimension.

Pathologic stage (available in 5 cases) was no higher than pT1b. Follow-up was available in 5/6 patients, ranging from 0.5 to 9 years. One patient died of disease 6 years following surgery. Remaining patients showed no evidence of disease. Morphology revealed more heterogeneous architecture with papillary as the most frequent, admixed with tubular, cystic up to solid and compressed papillary patterns. Pseudostratification, macrophages, psammoma bodies were rarely seen. All cases stained for AMACR, vimentin, cyclin D1. CD117, Melan A, HMB45, TFE3 were negative. CK7 was positive in the majority of cases. Two cases were positive for CK20. One case not meeting criteria for PRCC with reverse polarity was positive for GATA3. Nine cases were included to the third group (PRCC with oncocytic cells and with variable CNV). Group included 7 males and 2 females. Age ranged between 55 and 81 years. Size of tumours ranged between 1.3 and 7 cm in the largest dimension. Pathologic stage was available in 6 cases and ranged from pT1 to pT3a. Follow-up data was available for 6 patients ranging from 4 to 14.5 years. One patient developed lymph node metastases, one patient died of disease. No recurrence was reported in four patients. By morphology, all cases exhibited predominant papillary pattern or compressed papillary pattern. Pseudostratification, macrophages, psammoma bodies were unfrequently seen. All cases exhibited vimentin and Cyclin D1 positivity with variable extent. CK20, CD117, TFE3, Melan A, HMB45, and GATA3 were negative in all cases. Six cases were positive for CK7.

OPRCC was first described in 2005 by Lefèvre. True oncocytic character was confirmed by immunohistochemical positivity for MIA and by electron microscopy verifying presence of abundant mitochondria. Since then much literature with ambiguous results was published. In our study we conclude that the term “OPRCC” clusters a heterogeneous group of tumours sharing papillary/tubulopapillary architecture with oncocytic cells but varying in immunoprofile and spectrum of cytogenetic changes ranging from RO to former PRCC type 1 (classic pattern according to WHO 2022). From this point of view, for daily practice, it is more reasonable to apply generous sampling rather than expensive molecular techniques, which may erroneously lead to underestimating malignant tumours. Concluding, based on available data, we would not recommend using ambiguous term “OPRCC” as a distinct category.

Annals of Diagnostic Pathology 52 (2021) 151734

Contents lists available at ScienceDirect

Annals of Diagnostic Pathology

journal homepage: www.elsevier.com/locate/anndiagpath

Original Contributions

Renal cell carcinomas with tubulopapillary architecture and oncocytic cells: Molecular analysis of 39 difficult tumors to classify☆

Kristyna Pivovarcikova [a], Petr Grossmann [a], Veronika Hajkova [a], Reza Alaghehbandan [b], Tomas Pitra [c], Delia Perez Montiel [d], Maris Sperga [e], Joanna Rogala [a], Maryna Slisarenko [a], Adriena Bartos Vesela [c], Peter Svajdler [a], Kvetoslava Michalova [a], Pavla Rotterova [a], Milan Hora [c], Michal Michal [a], Ondrej Hes [a,*]

[a] Department of Pathology, Charles University in Prague, Faculty of Medicine in Plzeň, Pilsen, Czech Republic
[b] Department of Pathology, Faculty of Medicine, University of British Columbia, Royal Columbian Hospital, Vancouver, BC, Canada
[c] Department of Urology, Charles University in Prague, Faculty of Medicine in Plzeň, Pilsen, Czech Republic
[d] Department of Pathology, Institute Nacional de Cancerologia, Mexico City, Mexico
[e] Department of Pathology, Stradin's University, Riga, Latvia

ARTICLE INFO

Keywords:
Kidney
Oncocytic renal cell carcinoma
Papillary
Unclassified
Copy number variation pattern
Oncocytoma
Overlapping

ABSTRACT

So-called oncocytic papillary renal cell carcinoma (OPRCC) is a poorly defined variant of papillary renal cell carcinoma. Since its first description, several studies were published with conflicting results, and thus precise definition is lacking.

A cohort of 39 PRCCs composed of oncocytic cells were analyzed. Cases were divided into 3 groups based on copy number variation (CNV) pattern. The first group consisted of 23 cases with CNV equal to renal oncocytoma. The second group consisted of 7 cases with polysomy of chromosomes 7 and 17 and the last group of 9 cases included those with variable CNV.

Epidemiologic, morphologic and immunohistochemical features varied among the groups. There were not any particular histomorphologic features correlating with any of the genetic subgroups. Further, a combination of morphologic, immunohistochemical, and molecular-genetic features did not allow to precisely predict biologic behavior.

Owing to variable CNV pattern in OPRCC, strict adherence to morphology and immunohistochemical profile is recommended, particularly in limited samples (i.e., core biopsy). Applying CNV pattern as a part of a diagnostic algorithm can be potentially misleading.

OPRCC is a highly variable group of tumors, which might be misdiagnosed as renal oncocytoma. Using the term OPRCC as a distinct diagnostic entity is, thanks to its high heterogeneity, questionable.

1. Introduction

Renal cell carcinomas (RCC) composed of oncocytic cells represents a heterogeneous group of renal neoplasms, which can pose diagnostic challenge in routine practice. Despite the existence of well-established renal tumor entities such as renal oncocytoma (RO) and chromophobe RCC, there are several morphologic variants of "oncocytic" tumors, for which rendering exact diagnosis may be very challenging. Among others, group of papillary RCC with oncocytic cells represents example of such challenging tumors. Papillary renal cell carcinoma (PRCC) has traditionally been divided into two morphologic subgroups – PRCC type 1 and PRCC type 2 [1]. However, in the "histo-molecular" classification era, this does not hold true and remains unsatisfactory as many PRCC cannot be classified as per existing criteria [2].

The WHO classification defines oncocytic PRCC (OPRCC) as a PRCC with voluminous, finely granular, evenly distributed eosinophilic

☆ The study was supported by the Charles University Research Fund (project number Q39), by Institutional Research Fund FN 00669806, and by Biobank Research on Telemedical Approaches for Human Biobanks in a European Region, Bavarian-Czech University Agency (BTHA), and by SVV-2020 No. 260 539 provided by the Ministry of Education, Youth, and Sports of the Czech Republic.

* Corresponding author at: Department of Pathology, Medical Faculty, Charles University Hospital Plzen, Alej Svobody 80, 304 60 Pilsen, Czech Republic.
E-mail address: hes@biopticka.cz (O. Hes).

https://doi.org/10.1016/j.anndiagpath.2021.151734

Available online 31 March 2021

cytoplasm and oncocytoma-like nuclei (usually with low nuclear grade), which are single-layered and linearly aligned [3]. Apparently, "OPRCC" fulfilling these WHO criteria fits well in a subgroup of PRCC recently described as "PRCC with reverse polarity" [4]. However from the reverse perspective, PRCCs composed of oncocytic cells are a part of much broader spectrum, where PRCC with reverse polarity is one of the existing variants/subtypes. The whole group of PRCCs composed of oncocytic cells is so far poorly understood and histologic diagnostic criteria have not yet been determined.

In this study, we analyzed morphological, immunohistochemical, and molecular genetic features of renal tumors showing combined papillary/tubullopapillary/papillary, compressed to solid architecture and oncocytic cells (some of them overlapping with OPRCC as defined by WHO classification/PRCC with reverse polarity) in order to better understand the relationship between morphology and genetic background of these heterogeneous group of RCCs.

2. Material and methods

2.1. Case identification

A total of 287 cases of RCC with oncocytic/eosinophilic cells and tubulopapillary/papillary architecture were retrieved from the Pilsen Tumor Registry. A search algorithm including the keywords "oncocytic, papillary, tubular, tubulopapillary, unusual, renal cell carcinoma" was used to identify appropriate renal tumors. All cases were reviewed by 2 pathologists (K.P., O.H.). Basic inclusion criteria were papillary/tubulopapillary/papillary compressed architecture and oncocytic cells. All cases with poorly fixed quality tissue or fixation artifacts were excluded from the study. Further, we excluded high grade clear cell RCCs, unusual chromophobe RCCs, tubulocystic RCCs, as well as cases with limited available material (i.e., core biopsy). Upon completion of initial review of 246 cases, 53 tumors were selected to be tested for DNA quality, of which seven cases with low DNA quality were further excluded. In total, 46 tumors with papillary, tubulopapillary, and/or papillary-solid (compressed papillae) architecture were analyzed and a representative block from each case was stained with antimitochondrial antigen antibody (MIA) to confirm the oncocytic nature of neoplastic cells (for details see below). Only tumors with diffuse and strong cytoplasmic positivity were accepted, leading to the exclusion of seven more cases from the study.

Finally, 39 tumors were enrolled in the study, with 1–20 tissue blocks (median 4) available for each case. One to two representative blocks were selected for immunohistochemical and molecular–genetic studies. It should be noted that 10 cases were previously published in the study of Michalova et al. (cases 1–10) [5].

2.2. Light microscopy

Tissues for light microscopy were fixed in 4% formaldehyde and embedded in paraffin using routine procedure. Sections 2 μm thick were cut from tissue blocks and stained with hematoxylin and eosin (H&E).

2.3. Immunohistochemistry

The immunohistochemical analysis was performed using a Ventana BenchMark ULTRA (Ventana Medical System, Inc., Tucson, Arizona). The following primary antibodies were used: cytokeratin 7 (OV-TL12/30, monoclonal; Dako, Glostrup, Denmark; 1:200), cytokeratin 20 (M7019, monoclonal; Dako; 1:100), racemase/AMACR (P504S, monoclonal; Zeta, Sierra Madre, CA; 1:50), vimentin (V9, monoclonal; Cell Marque, Rocklin, CA; RTU), carbonic anhydrase IX (EP161, monoclonal; Cell Marque; RTU), antimelanosome (HMB45, monoclonal; Dako; 1:200), TFE3 (MRQ-37, monoclonal; Cell Marque; RTU), Melan A (A103, monoclonal; Cell Marque; RTU), mitochondrial antigen antibody/MIA (113-1, Biogenex, San Ramon, CA; 1:100), GATA3 (monoclonal, Biocare Medical, Concord, CA, 1:100), cyclin D1 (SP4-R; monoclonal, Cell Marque, RTU). Appropriate positive controls were used.

2.4. Fluorescent in-situ hybridization (FISH)

Four μm thick FFPE sections were placed onto positively charged slides. The unstained slides were routinely deparaffinized and incubated in the 1× Target Retrieval Solution Citrate pH 6 (Dako, Glostrup, Denmark) at 95 °C for 40 min and subsequently cooled for 20 min at room temperature in the same solution. Slides were washed in deionized water for 5 min and digested in protease solution with Pepsin (0.5 mg/ml, Sigma Aldrich, St. Louis, MO, USA) in 0.01 M HCl at 37 °C for 35 to 60 min, according the sample conditions. Slides were then placed into deionized water for 5 min, dehydrated in a series of ethanol solution (70%, 85%, and 96% for 2 min each) and air-dried. Vysis probes (Vysis/Abbott Molecular, IL, USA) were mixed with water and CEP or LSI/WCP Hybridization buffer (Vysis/Abbott Molecular) in a 1:2:7 ratio respectively. ZytoLight probe (ZytoVision GmbH, Bremerhaven, Germany) was factory premixed. Overview of all used probes is summarized in Supplemental Table 1.

An appropriate amount of probe was applied on specimen, covered with a glass coverslip and sealed with rubber cement. Slides were incubated in the ThermoBrite instrument (StatSpin/Iris Sample Processing, Westwood, MA, USA) with co-denaturation at 85 °C for 8 min and hybridization at 37 °C for 16 h. Rubber cemented coverslip was then removed and the slide was placed in post-hybridization wash solution (2xSSC + 0.3% NP-40) at 72 °C for 2 min. The slides were air-dried in the dark, counterstained with 4′, 6′-diamidino-2-phenylindole DAPI (Vysis/Abbott Molecular), coverslipped and immediately examined.

The sections were examined with an Olympus BX51 fluorescence microscope (Olympus Corporation, Tokyo, Japan) using a 100× objective and filter sets Triple Band Pass (DAPI/SpectrumGreen/SpectrumOrange), Dual Band Pass (SpectrumGreen/SpectrumOrange) and Single Band Pass (SpectrumGreen, SpectrumOrange, SpectrumGold, SpectrumRed and SpectrumAqua). For each probe, one hundred randomly selected nonoverlapping tumor cell nuclei were examined for presence of fluorescent signals.

Scoring of loss 1p was performed by counting the ratio of the number of 1p36 to 1q25. Cut-off value was used 0.7 according to the classification of Mohapatra et al. [6]. Loss and gain for studied centromeres and loci *CCND1* and *IGH* were defined as the presence of one specific signal per nucleus in >45% and three and more signals in >10% (mean value in normal non-neoplastic control tissues +3 standard deviations), respectively [7]. Regarding break-apart probes, yellow signals were considered negative, separate orange and green signals were considered as positive. Cut off value was set to more than 10% of breakpoint signals (mean value in normal non-neoplastic control tissues +3 standard deviations).

2.5. NGS method

DNA from FFPE samples was extracted using QIAsymphony DSP DNA mini kit (Qiagen, Hilden, Germany). Purified DNAs were quantified using the Qubit Broad Range DNA Assays (Thermo Fisher Scientific, Waltham, Massachusetts, USA).

Hotspot mutations in *KRAS* gene were analyzed using the Accel-Amplicon Plus EGFR PAthway Panel (Swift Biosciences, USA). The libraries were prepared following the Accel-Amplicon protocol for Illumina sequencing. Final libraries were multiplexed, spiked with 20% PhiX control and sequenced on a NextSeq 550 (Illumina, San Diego, CA) to achieve at least 150,000 reads per sample. The analysis of the sequencing results (fastq files) was performed using the Varsome Clinical software (Saphetor SA, CH). Parameters for variant reporting were set to a minimum coverage per amplicon 300 and allelic frequency over 5%.

2.6. Evaluation of the cases, study groups

The tumors were divided into three distinct molecular subgroups according to their chromosomal copy number variation (CNV) pattern as follows: 1) PRCC with oncocytic cells and CNV identical to RO (enumeration of chromosome 1 - loss of whole chromosome 1 or its deletion, typically 1p36; and/or loss of chromosome 14; and/or loss of gonosomes; and/or 11q13 rearrangement - gene *CCND1*, or normal karyotype – see in Supplemental Table 2), 2) PRCC with oncocytic cells and gains of chromosomes 7 and 17, and 3) PRCC with oncocytic cells and variable CNV not matching the two previously mentioned subgroups. All neoplasms were analyzed by morphology and immunohistochemistry, and clinical data were compared.

2.7. Statistical analysis

The values of continuous parameters were calculated as means ± standard deviation (SD). Pearson's χ^2 test was used for categorical variables and Student's *t*-test for comparing the means. All tests were two-tailed, and $p < 0.05$ was considered statistically significant. All descriptive and inferential statistical analyses were carried out using the Statistical Package for the Social Sciences (SPSS), version 19.0 (Chicago, IL, USA).

3. Results

All 39 cases of PRCC composed of oncocytic cells were divided into three distinct subgroups according to their chromosomal CNV of selected chromosomes:

3.1. GROUP 1: PRCC with oncocytic cells and renal oncocytoma-like CNV

Basic clinicopathologic data are listed in Table 1. This study subgroup included 23 cases. Patients were 15 males and 8 females, with age range 52 to 81 years (median 68 years, mean 67.9 years). Tumor size (available in 22/23 cases) ranged from 0.8 to 9 cm in greatest dimension (median 3.8 cm, mean 4.4 cm). Pathologic stage included pT1 in 13 cases (pT1a in 11 cases, pT1b in 2 cases), pT2 in 1, and pT3a in 2 cases. No information on pathologic stage was available in 7 cases. Follow-up data were available for 14 patients (range 0.5 to 8 years, mean 4.5 years, median 7.5 years). One patient developed recurrence and metastatic disease (case 15a, for further recurrence details see case 15b in subgroup "PRCC with oncocytic cells and gains of chromosomes 7 and 17"), thirteen patients are alive with no evidence of disease.

Morphologic features are summarized in Table 2. Papillary component was documented, at least focally, in all 23 tumors (Fig. 1A+B). Papillary architecture was the predominant growth pattern in 18/23 cases, with 6/18 cases exhibiting secondary compressed papillary structures, and 5/18 with other minor components (tubulopapillary in 3 cases, tubular in 1 case, and cystic and tubular in 1 case). In the remaining 5/23 cases, the papillary areas were only focally present, of which 3/5 cases showed predominant tubulopapillary areas (in two cases with more tubulopapillary compressed architecture), and 2/5 cases combined papillary areas with tubular structures (even tubular compressed mimicking "solid" areas) (Fig. 2). Two cases (case 3 and case 16) with papillary architecture, uniform eosinophilic cells and round nuclei met criteria for diagnosis of PRCC with reverse polarity (see below) (Fig. 3A+B). 10/23 cases showed WHO/ISUP nuclear grade 2, while the remaining 13/23 cases were nuclear grade 3. Pseudostratification was noted in 8/23 cases (in 5 cases only focally). Macrophages were present in 11 cases. Further, we found necrosis in 2 cases, hemorrhage in 6 cases, so-called bloody lakes in 2 cases, calcifications in 5 cases, and hemosiderin pigmentation in 3 cases (Fig. 4).

Results of immunohistochemical analysis are summarized in Table 3. All cases showed positivity for anti-mitochondrial antigen antibody (MIA) and vimentin (in 2 cases only focally), while all tumors were negative for CD117, Melan A, and HMB45. Twelve cases were positive for CK7 (focally in 5/12 and single cells in 1/12). Racemase (AMACR) showed positive result in 20/21 cases and cyclin D1 in 21/22 cases (focal in 2/22 and single cells in 6/21 cases). Carbonic anhydrase IX was positive in 7/21 cases (focally in all seven cases), GATA3 in 2/21 cases, and CK20 in 1/22 cases. GATA3 positivity corresponded with cases fulfilling morphologic criteria for PRCC with reverse polarity (case 3 and

Table 1
GROUP 1: PRCC with oncocytic cells and renal oncocytoma-like CNV - clinical data.

CASE	SEX	AGE	SIDE	SIZE – in the greatest dimension (cm)	STAGE	FU	
CASE 1*	M	69	L	10	pT3a	6y	ANED
CASE 2*	F	61	L	7	NA	6y	ANED
CASE 3*	F	56	NA	2	pT1a	LFU	LFU
CASE 4*	F	75	L	3.5	pT1a	6y	ANED
CASE 5*	F	68	NA	4	pT1a	1.5y	ANED
CASE 6*	F	58	R	5	NA	13y	ANED
CASE 7*	M	79	R	9	pT2	3y	ANED
CASE 8*	M	73	R	3	pT1a	2y	ANED
CASE 9*	M	76	R	NA	NA	LFU	LFU
CASE 10*	M	63	NA	5.5	pT1b	LFU	LFU
CASE 11	M	76	R	7.9	pT3a	10y	ANED
CASE 12	F	66	R	4	pT1a	2.6y	ANED
CASE 13	M	67	R	2	pT1a	1.5	ANED
CASE 14	F	67	R	3	pT1a	0.5y	ANED
CASE 15a	M	60	R	5	pT1b	8	AWD (see case 15b in subgroup "PRCC with oncocytic cells and gains of chromosomes 7 and 17")
CASE 16	F	71	L	2.1	pT1a	1.4y	ANED
CASE 17	M	73	L	6.5	NA	LFU	LFU
CASE 18	M	66	R	3.5	NA	LFU	LFU
CASE 19	M	68	R	1.5	pT1a	LFU	LFU
CASE 20	M	52	L	4	NA	LFU	LFU
CASE 21	M	65	R	1.8	pT1a	1.6 y	ANED
CASE 22	M	81	NA	5.5	NA	LFU	LFU
CASE 23	M	72	R	0.8	pT1a	LFU	LFU

M male, *F* female, *L* left, *R* right, *NA* not available, *ANED* alive with no evidence of disease, *AWD* alive with the disease, *LFU* lost for follow up, * cases previously included in study by Michalova et al. [5].

Table 2
GROUP 1: PRCC with oncocytic cells and renal oncocytoma-like CNV – morphologic study.

CASE	Pattern of growth		Cytoplasm	Grade ISUP/WHO	Pseudostratification	Calcification (C), necrosis (N), hemosiderin (HEM), hemorrhage (HEMOR)	Macrophages
	Papillary structures	Other growth pattern					
CASE 1[a]	Compressed papillary	Compressed tubular	Granular and eosinophilic, cuboidal cells	2	No	N+	Not present
CASE 2[a]	Only		Granular, abundant, eosinophilic	2, nuclei elevated from BM	No	HEM +, C +	+++
CASE 3[a]	Only		Granular, eosinophilic, cuboidal cells	2	No	Not present	Not present
CASE 4[a]	Only		Granular, abundant, eosinophilic	2	Present focally	Not present	++
CASE 5[a]	Focally	Tubulopapillary	Granular, abundant, eosinophilic	3, nuclei elevated from BM	No	HEMOR +	Not present
CASE 6[a]	Only		Granular, abundant, eosinophilic	3	Present focally	Not present	Not present
CASE 7[a]	Focally, compressed	Tubular, "solid"	Granular, abundant, eosinophilic	2, granular chromatin	no	HEMOR +	++
CASE 8[a]	Predominantly	Tubulopapillary	Granular, abundant, eosinophilic	3	Present focally	Not present	Not present
CASE 9[a]	Only		Granular, abundant, eosinophilic	3	Present	Not present	Not present
CASE 10[a]	Papillary and papillary compressed		Granular, abundant, eosinophilic	2, granular chromatin	No	Not present	Not present
CASE 11	Predominantly	Tubulopapillary	Granular, abundant eosinophilic	2, optically empty, grooves, nuclei luminally located	present focally	C + (discrete), HEMOR + (discrete)	Not present
CASE 12	Papillary compressed to "solid"		Granular, eosinophilic cytoplasm	3, granular chromatin, nuclei centrally located	No	Occasional siderophages	+
CASE 13	Papillary compressed		Granular, abundant eosinophilic	3, elevated from BM	No	C +, HEMOR +	+
CASE 14	Predominantly	Tubular	Granular, abundant eosinophilic	3, granular chromatin	No	Bloody lakes	++
CASE 15a	Focally papillary compressed	Cystic, tubular	Granular, abundant eosinophilic, giant multinucleated cells	3	present focally	C +, bloody lakes, N +, HEMOR +	+ (collections of foamy macrophages)
CASE 16	Only		Granular, abundant eosinophilic, intracytoplasmatic vacuoles	2	No	Not present	Not present
CASE 17	Papillary compressed		Granular, abundant eosinophilic	2, granular chromatin, luminal localization of nuclei	No	Not present	+ (collections of foamy macrophages)
CASE 18	Papillary compressed		Granular, abundant eosinophilic	3	Present	Bloody lakes	+
CASE 19	Only		Granular, abundant eosinophilic	2, granular chromatin, nuclei centrally located	Present	C + cholesterol clefts, bloody lakes	+ (collections of foamy macrophages)
CASE 20	Focally	Tubulopapillary compressed	Granular, abundant eosinophilic	3, granular chromatin, nuclei centrally located	No	Not present	++
CASE 21	Only		Granular, abundant eosinophilic	3	No	Not present	Not present
CASE 22	Focally	Tubulopapillary compressed	Granular, abundant eosinophilic	3	No	HEMOR+	Not present
CASE 23	Predominantly	Tubulopapillary compressed	Granular, abundant eosinophilic	3	Present focally	HEM+	Not present

[a] Cases previously included in study by Michalova et al. [5], *BM* basal membrane, + present.

16). TFE3 staining was positive in two cases (clear nuclear staining in more than 50% of neoplastic cells), while FISH for detection of break in *TFE3* gene was negative in both cases.

Cytogenetic study showed spectrum of changes typically described in RO. Eight cases (8/23) had normal karyotype in tracked characters. Loss of gonosomes was identified in 5/23 cases, including 4/5 cases with loss of Y and 1/5 case with loss of X. Deletion 1p36 (2/23 cases) and combined deletion of 1p36 with loss Y (2/23 cases) were detected. Rearrangement of gene *CCND1* localized on 11q13 was noted in 2/23 cases. The remaining of 6/23 cases each showed combined different cytogenetic changes compatible with RO as follows, one case with deletion 1p36 concurrently with loss 14 and Y, one case with deletion 1p36 concurrently with loss 14, one case with loss 14 concurrently with loss Y, and one case with loss 14. Cases fulfilling the morphologic criteria of PRCC with reverse polarity had rearrangement of gene *CCND1* in one case (case 3) and normal karyotype in the second case (case 16). Mutation of *KRAS* gene was documented in both cases. Overview of all detected changes are presented in Table 4.

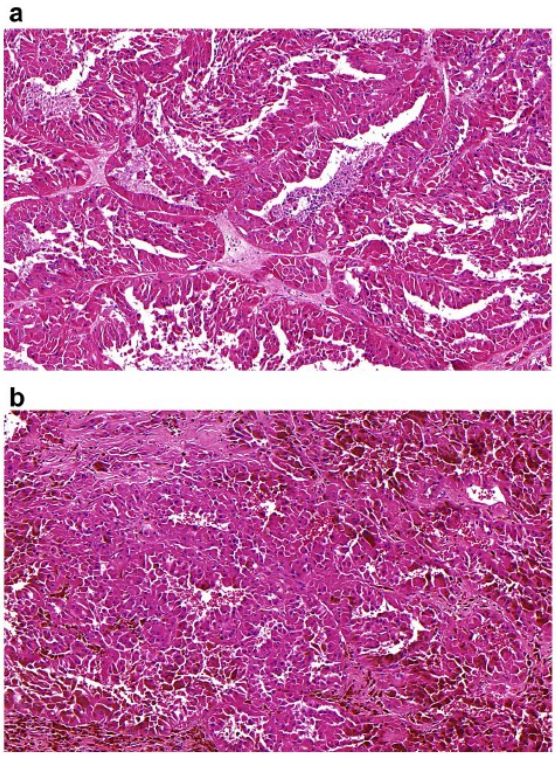

Fig. 1. A: Papillary renal cell carcinoma composed of oncocytic cells. Mild to moderate pseudostratification is present, however, nuclei are round and small with low nucleo-cytoplasmatic ratio.
B: In some tumors from "PRCC with oncocytic cells and renal oncocytoma-like CNV" group, voluminous deposits of hemosiderin were present.

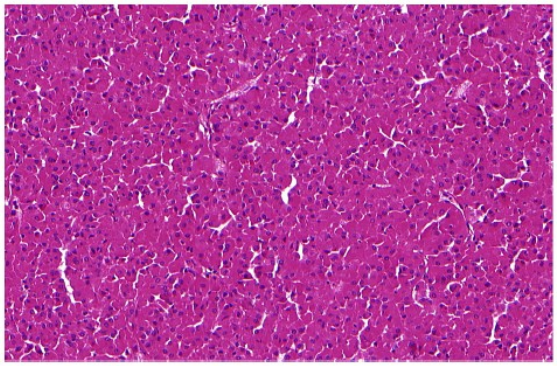

Fig. 2. In some tumors, compressed tubulopapillary structures imparted pseudosolid appearance.

3.2. GROUP 2: PRCC with oncocytic cells and gains of chromosomes 7 and 17

Clinicopathologic data are showed in Table 5. This subgroup contained seven tumors, with 6 males and 1 female. One case (15b) represented a recurrence from a patient initially included in a previous group as case 15a. Clinicopathologic data regarding case 15b are described

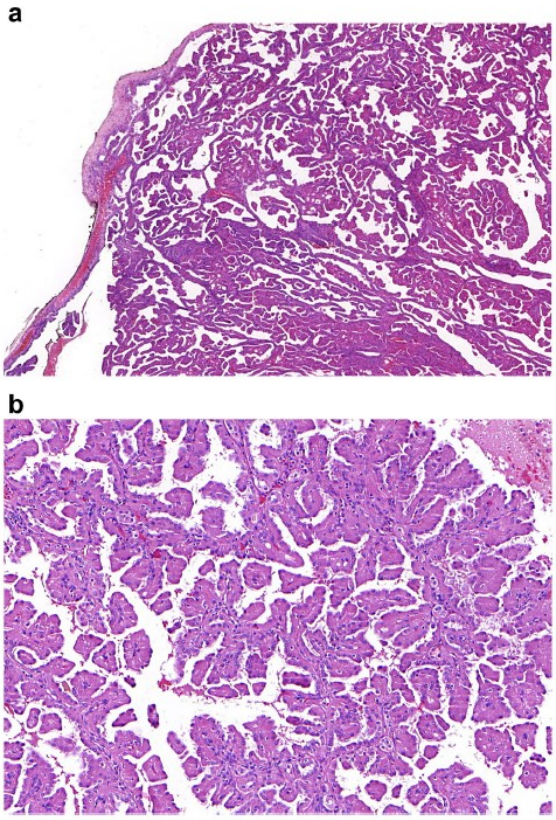

Fig. 3. A: Two cases from "PRCC with oncocytic cells and renal oncocytoma-like CNV group" fulfilled diagnostic criteria for "PRCC with reverse polarity".
B: Neoplastic cells were arranged in single row on papillary cores.

above. The age of six remaining patients ranged from 40 to 69 years (mean 59.9 years, median 61 years). Tumor size ranged from 1.2 to 5 cm in greatest dimension (median 3 cm, mean 3.3 cm). Pathologic staging was available in 5 cases (pT1a in 3 and pT1b in 2 cases). Follow-up was available in 5/6 patients, ranging 0.5 to 9 years (mean 6.7 years, median 6 years). No records concerning aggressive behavior were found in 4 patients, while one patient died of the disease 6 years post-surgery.

Morphologic data are summarized in Table 6. Morphologically, three cases had only or predominantly papillary architecture (in 1 case with focal tubulopapillary areas, and in 1 case with compressed papillae). In two cases, there were papillary areas admixed with tubular and cystic areas (in 1 case), and with more solid and tubular compressed areas (in 1 case) (Fig. 4A+B). Two cases were composed of compressed tubulopapillary/tubular structures. Nuclear grade was 2 in 3/7 cases, and grade 3 in 4/7 tumors (WHO/ISUP). Pseudostratification was focally present in 1 case, in the remaining 6/7 cases was not documented. Three tumors contained macrophages. Psammoma bodies were found in one case. Hemosiderin deposition was found in one case and large hemorrhage in another case.

The immunohistochemical results are summarized in Table 7. All cases were positive for MIA, racemase (AMACR), and vimentin (in 4/7 cases focally). CD117, Melan A, HMB45, TFE3 were negative. CK7 positivity was found in 4/7 cases (in one case focally), while two cases showed reactivity for CK20. Carbonic anhydrase IX was focally positive in 2/7 tumors and GATA3 in one tumor (case 29, this case did not meet the morphologic criteria of PRCC with reverse polarity). Cyclin D1 was

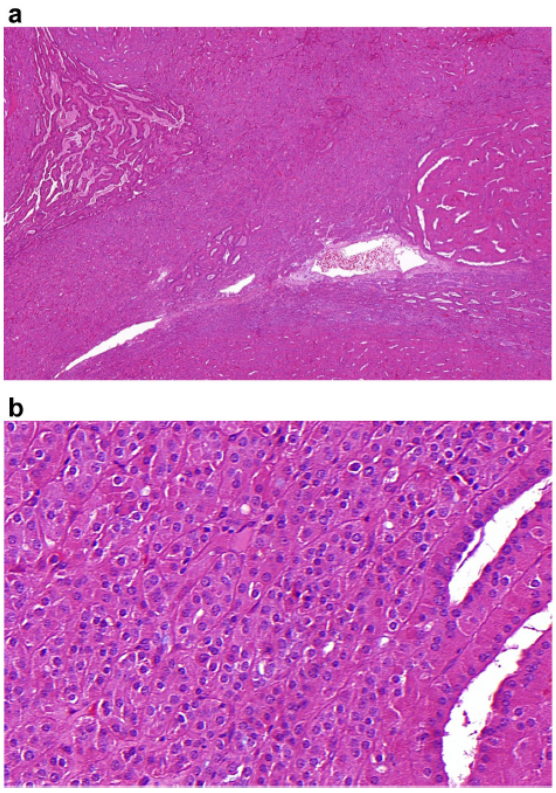

Fig. 4. A: Some cases from group 2 (PRCC with oncocytic cells and gains of chromosomes 7 and 17) showed papillary areas only focally, admixed with more solid and tubular compressed areas.
B: Oncocytic neoplastic cells formed solid component reaching grade 3 (ISUP/WHO).

positive in 7/7 cases (in 3 cases focally).

Cytogenetic study detected gain of chromosomes 7 and 17 in all these cases (Table 8). Loss of chromosome Y was noted in 4/6 male patients and loss of chromosome X in 1/1 female. In four cases, there were additional cytogenetic changes characteristic for RO (1× rearrangement of *CCND1*, 1× deletion 1p36 together with loss 14, 1× loss 14, 1× deletion 1p36). In 2 cases, in addition to the polysomies 7 and 17 and loss Y, we noted gain in locus 11q13.

3.3. GROUP 3: PRCC with oncocytic cells and with variable CNV

Basic clinicopathologic data are summarized in Table 9. In this subgroup, nine cases were collected based on the results of cytogenetic study - PRCCs with oncocytic cells and variable CNV not matching the former subgroups. This group included 7 males and 2 females, with age ranged between 55 and 81 years (median 71 years, mean 71.7 years). Size of tumors ranged between 1.3 and 7 cm in the largest dimension (mean 3.9 cm; median 3 cm). Pathologic stage was pT1 in 3 cases (pT1a in 2 cases, pT1b in 1 case), and pT3a in 3 cases. Information about stage was not available in 3 cases. Follow-up data were available for 6 patients (range 4 to 14.5 years, mean 7.5, median 6.2 years). One patient had metastatic disease (lymph nodes metastasis), and one patient died of the disease 4 years post-surgery. Four patients showed no aggressive behavior.

Morphologic features are shown in Table 10. All 9 cases had predominantly/solely papillary architecture (in 1 case there were focal tubular and cystic areas, and in 1 case focally tubulopapillary areas). In 2/9 cases papillary structures were predominantly compressed. Four tumors had nuclear grade 2, and four tumors had nuclear grade 3 (WHO/ISUP). Nuclear pseudostratification was present in 3 cases (in 2/3 cases focally). Two tumors contained macrophages (Fig. 5), and hemosiderin deposition was found in four cases. One tumor contained psammoma bodies and necrosis was documented in 1 case.

Immunohistochemical findings are summarized in Table 11. All cases were positive for MIA, vimentin (focal positivity in 3 cases), and Cyclin D1 (6 cases with focal positivity, positive single cells in 1 case). CK20, CD117, TFE3, Melan A, HMB45, and GATA3 were negative in all cases. Six cases were positive for CK7 (2/6 cases focally, single cells reactivity in 1/6). Carbonic anhydrase IX showed focal positivity in 3/8 cases.

Cytogenetic study in this subgroup showed variable results (Table 12). Cases frequently showed cytogenetic changes partially overlapping with both PRCC and RO. However, in contrast with the former two subgroups, the full cytogenetic overlap with either of PRCC or RO was not recorded in any of these cases. Namely, 2/9 cases had polysomy of chromosome 17 and loss of chromosome Y; 2/9 cases showed loss of chromosome 17; 1/9 case showed loss of chromosome 7 and loss of chromosome 17. In 1/9 case loss of chromosome 17, together with loss of chromosome Y and deletion 1p36 was found. In 1/9 case loss of chromosome 17 together with loss of chromosome Y was found. In 1/9 case gain of chromosome 7 together with loss of chromosome 17 was documented. Finally, in 1/9 case gain of chromosome 7 together with loss of chromosome Y was encountered.

3.4. Inferential analysis findings

This analysis was carried out to examine statistical significant differences between the above-mentioned three cohorts. No significant statistical differences were found between mean age of patients in group one (PRCC with oncocytic cells and RO-like CNV) and the other two groups. Similar findings were also observed for following variables: sex, tumor size, pathologic staging, and clinical follow-up data. Data on age, sex, and pathologic staging were statistically different between the second group (PRCC with oncocytic cells and gains of chromosomes 7 and 17) and the third group (PRCC with oncocytic cells and with variable CNV).

4. Discussion

The so-called "OPRRC" was first time described in 2005 by Lefevre et al. [8]. The authors published 10 tumors with combined extensive papillary architecture and oncocytic neoplastic cells (packed by mitochondrias, which imparts a finely granular appearance of the cytoplasm) in a single layer. The presence of mitochondrias was further verified by electron-microscopy and supported by specific immunolabeling with anti-mitochondria antigen antibody (MIA). The tumors showed immunohistochemical profile similar to PRCC (AMACR and vimentin positivity). However, the cytogenetic features were similar to RO. None of the cases showed trisomy of chromosome 7 and/or 17. The authors used a descriptive term "adult papillary tumor with oncocytic cells". A few months later, a study of other 12 cases was subsequently published [9]. Similarly to the initial study, the tumors were mostly composed of papillary structures lined by single (occasionally pseudostratified) layers of cells with granular eosinophilic cytoplasm, electron-microscopically filled by numerous mitochondria, and with an immunoprofile "typical" of PRCC. However, few cases showed pseudostratification. Interestingly, in 11/12 cases solid areas with morphological features overlapping with typical RO were documented. Nine cases presented with higher nuclear grade. Cytogenetic study of these tumors detected changes usually described in PRCC (polysomy of chromososome 7 and/or 17) in majority of cases. The authors for the first time used the term

Table 3
GROUP 1: PRCC with oncocytic cells and renal oncocytoma-like CNV – immunohistochemistry.

CASE	MIA	CK7	CK20	CD117	TFE3	Melan A	HMB45	AMACR	VIM	Cyclin D1	GATA3	CANH
CASE 1*	+++	Foc. ++	–	–	–	–	–	+++	Foc. +++	SC +	–	Foc. +++
CASE 2*	+++	–	–	–	–	–	–	+++	+++	SC +++	–	Foc. +++
CASE 3*	+++	+++	–	–	–	–	–	+	Foc. +	+++	+++	–
CASE 4*	+++	+++	–	–	–	–	–	+++	++	+++	–	Foc. +++
CASE 5*	+++	–	–	–	–	–	–	Foc. +++	+++	SC +	–	Foc. +++
CASE 6*	+++	–	–	–	–	–	–	+	+++	++	–	–
CASE 7*	+++	Foc. ++	–	–	–	–	–	+++	+++	+ SC	–	–
CASE 8*	+++	Foc. +++	–	–	–	–	–	NA	+++	Foc. +++	–	–
CASE 9*	++	–	–	–	–	–	–	+++	+++	+ SC	NA	NA
CASE 10*	+++	–	–	–	–	–	–	+++	+++	Foc. +++	–	Foc. +++
CASE 11	+++	++	–	–	–	–	–	+++	+++	++	–	–
CASE 12	+++	–	–	–	–	–	–	+++	+++	++	–	–
CASE 13	++	–	–	–	–	–	–	+++	+++	++	–	–
CASE 14	+++	–	–	–	–	–	–	+++	+++	++	–	–
CASE 15[a]	+++	++ SC	+++	–	–	–	–	+++	+++	–	–	Foc. +++
CASE 16	+++	+++	–	–	–	–	–	–	+++	++	+++	–
CASE 17	+++	–	–	–	–	–	–	+++	+++	+	–	–
CASE 18	+++	+++	–	–	–	–	–	+++	+++	+++	–	–
CASE 19	+++	–	–	–	–	–	–	+++	+++	++	–	–
CASE 20	+++	Foc. +	–	–	–	–	–	++	+++	+ SC	–	–
CASE 21	+++	+++	–	–	–	–	–	+++	+++	++	–	Foc. +++
CASE 22	+++	Foc. +	–	–	++ [a]	–	–	+++	+++	–	–	–
CASE 23	+++	–	–	–	+++ [a]	–	–	+++	+++	++	–	–

– negative, + weak positivity, ++ moderate positivity, +++ strong positivity, *Foc.* focally (up to 50%), *SC* single cells.
[a] FISH (break *TFE3*) negative.
* Cases previously included in study by Michalova et al. [5].

Table 4
GROUP 1: PRCC with oncocytic cells and renal oncocytoma-like CNV - cytogenetic study.

CASE	Del 1p36	Enumeration 1	BA BCL1 (CCND1)	Enumeration BCL1 (CCND1)	Enumeration 7	Enumeration 14	Enumeration 17	X/Y	SWIFT KRAS
CASE 1[a]	Negative	Negative	Negative	Negative	Negative	Negative	Negative	Loss Y	NP
CASE 2[a]	Present	Negative	Negative	Negative	Negative	Loss	Negative	Negative	NP
CASE 3[a]	Negative	Negative	Present	NA	Negative	Negative	Negative	Negative	Mutation KRAS c.35G>A, p.(Gly12Asp), AF:30%
CASE 4[a]	Negative	Negative	Negative	NA	Negative	Negative	Negative	Negative	NP
CASE 5[a]	Negative	Negative	Negative	Negative	Negative	Negative	Negative	Negative	NP
CASE 6[a]	Present	Negative	Negative	Negative	Negative	Negative	Negative	Negative	NP
CASE 7[a]	Negative	Negative	Negative	Negative	Negative	Negative	Negative	Loss Y	NP
CASE8[a]	Negative	Negative	Negative	Negative	Negative	Negative	Negative	Negative	NP
CASE 9[a]	Present	Negative	Negative	Negative	Negative	Negative	Negative	Negative	NP
CASE 10[a]	Present	Negative	Negative	NA	Negative	loss	Negative	Loss Y	NP
CASE 11	Negative	Negative	Present	Negative	Negative	Negative	Negative	NA	NP
CASE 12	Negative	Negative	Negative	Negative	Negative	Negative	Negative	Loss X	NP
CASE 13	Present	Negative	Negative	Negative	Negative	Negative	Negative	Loss Y	NP
CASE 14	Negative	Negative	Negative	Negative	Negative	Negative	Negative	Negative	NP
CASE 15a	NA	NA	Negative	Negative	Negative	Negative	Negative	Negative	NP
CASE 16	Negative	Negative	Negative	Negative	Negative	Negative	Negative	Negative	Mutation KRAS c.181C>A, p.(Gln61Lys), AF:19%
CASE 17	Negative	Negative	Negative	Negative	Negative	Negative	Negative	Loss Y	NP
CASE 18	Negative	Negative	Negative	Negative	Negative	loss	Negative	Negative	NP
CASE 19	Negative	Negative	Negative	Negative	Negative	Negative	Negative	Negative	NP
CASE 20	Negative	Negative	Negative	Negative	Negative	Negative	Negative	Negative	Negative
CASE 21	Negative	Negative	Negative	Negative	Negative	Negative	Negative	Loss Y	Negative
CASE 22	Present	Negative	Negative	Negative	Negative	Negative	Negative	Loss Y	Negative
CASE 23	Negative	Negative	Negative	Negative	Negative	loss	Negative	Loss Y	NA

NA not available, *NP* not performed.
[a] Cases previously included in study by Michalova et al. [5].

oncocytic PRCC, and since then, a number of different studies have been published, mostly with conflicting results [10-12].

The so-called "OPRCC" is not yet fully characterized. The basic morphologic criteria (papillary and/or tubulopapillary architecture and cells with abundant granular/oncocytic cytoplasm) are non-specific and a number of different renal tumors meets these characteristics. Particularly, the term "oncocytic" is frequently erroneously applied to all cells with voluminous eosinophilic cytoplasm, without confirming their true "oncocytic" nature by immunohistochemical or electron microscopic examination. Another problematic point is the definition of OPRCC by WHO 2016. When applying the 2016 WHO criteria, majority of the tumors from the initial studies [8,9] would not fulfill the proposed morphologic characteristics for the diagnosis of OPRCC [3]. However, the majority of these initial cases would mostly be compatible with another recently described PRCC subtype – "PRCC with reverse polarity" [4].

Table 5
GROUP 2: PRCC with oncocytic cells and gains of chromosomes 7 and 17 - clinical data.

CASE	SEX	AGE	SIDE	SIZE – in the greatest dimension (cm)	STAGE	FU	
CASE 24	M	69	R	5	pT1b	6y	DOD
CASE 25	M	63	NA	3	pT1a	9y	DNED
CASE 26	M	59	L	3	pT1a	10y	ANED
CASE 27	F	59	R	1.2	pT1a	8y	ANED
CASE 28	M	40	NA	NA	NA	LFU	LFU
CASE 29	M	67	R	4.5	pT1b	0.5y	ANED
CASE 15b	M	64	R	2.4	pT1a	8y	AWD

M male, *F* female, *L* left, *R* right, *NA* not available, *DNED* death with no evidence of disease, *ANED* alive with no evidence of disease, *AWD* alive with the disease, *DOD* death of the disease, *LFU* lost for follow up.

In this study, we presented a cohort of tumors fulfilling the basic criteria for the diagnosis of so-called "OPRCC" as it has been used in previously published studies (papillary and/or tubulopapillary architecture and cells with abundant oncocytic cytoplasm packed with mitochondria) [8-12]. Following strict criteria accepted by the WHO 2016, substantial part of our cohort cannot be classified as OPRCC. According to WHO 2016, the combination of morphology and immunoprofile of the tumors discussed herein would classify them either as OPRCC or PRCC, NOS. Therefore, we decided to split our cases into 3 distinct categories using CNV and other molecular features as a divider line: RO-like group, 7 and 17 polysomy group, and mixture of patterns.

Our cytogenetic findings showed interesting results and occasional overlapping diagnostic features. Only seven cases (17.9%) showed polysomy of chromosome 7 and 17, which is consistent with traditional cytogenetic changes of PRCC, particularly the so-called type 1 [13]. Interestingly, four cases with chromosome 7 and 17 polysomy concurrently had some RO-like cytogenetic features as well. Molecular genetic changes consistent with the diagnosis of RO were documented in 28/39 cases (71.8%). Five cases showed variable cytogenetic profile, with changes partly consistent with RO or with those of PRCC. Four cases in this study showed changes, which not typically belong to either RO or PRCC (loss of chromosomes 7 and/or 17).

Patients were mostly older, only 7/39 were in age under 60 years (only one patient was 40 years). There was a strong male predominance (27:11). Four patients with documented aggressive behavior showed variable cytogenetic profile, thus we were not able to identify any CNV characteristic features associated with aggressive behavior.

Analysis of architectural growth patterns showed overlapping features across all 3 groups. However, the number of cases in each group is relatively small and does not allow to predict any particular subgroup-specific architecture. In all 3 groups, tumors were mainly arranged in papillary and tubulopapillary patterns, while rarely with "pseudosolid" (compressed) areas. Across the study groups 1–3, nuclear pseudostratification was detected in 8/23, 1/7 and 3/9 cases, respectively (in majority of cases only focally). Further, we evaluated the presence of

Table 6
GROUP 2: PRCC with oncocytic cells and gains of chromosomes 7 and 17 - morphologic study.

CASE	Pattern of growth		Cytoplasm	Grade ISUP/ WHO	Pseudostratification	Calcification (C), necrosis (N), hemosiderin (HEM), hemorrhage (HEMOR)	Macrophages
	Presence of papillary structures						
CASE 24	Predominantly	Tubulopapillary (focally compressed)	Granular, abundant, eosinophilic, areas of cells with clear cytoplasm	3, nuclei elevated from BM	No	HEM +	++
CASE 25	Papillary and papillary compressed		Granular, abundant, eosinophilic, cuboidal to cylindrical cells	3	No	HEM +, C + (psammoma)	++
CASE 26	Only		Granular, eosinophilic, cylindrical cells	3	Present focally	Not present	+
CASE 27	Not present	Compressed tubulopapillary, alveolar	Granular, abundant, eosinophilic	2, granular chromatin	No	Not present	Not present
CASE 28	Not present	Compressed tubular	Granular, abundant	2, granular chromatin	No	Not present	Not present
CASE 29	Focally	Predominantly solid, tubullary compressed	Granular, eosinophilic, cuboidal cells	2, granular chromatin	No	Not present	Not present
CASE 15b	Papillae sporadically	Tubular, cystic	Granular, abundant, eosinophilic, intracytoplasmic vacuoles ("empty")	3	No	HEMOR +	Not present

BM basal membrane, + present.

Table 7
GROUP 2: PRCC with oncocytic cells and gains of chromosomes 7 and 17 – immunohistochemistry.

CASE	MIA	CK7	CK20	CD117	TFE3	Melan A	HMB45	AMACR	VIM	Cyclin D1	GATA3	CANH
CASE 24	+++	–	+++	–	–	–	–	+++	Foc. ++	Foc. ++	–	–
CASE 25	++	+++	–	–	–	–	–	+++	++	Foc. +++	–	Foc. +++
CASE 26	++	+++	–	–	–	–	–	+++	+++	Foc. ++	–	Foc. +++
CASE 27	+++	–	–	–	–	–	–	++	+++	+++	–	–
CASE 28	++	Foc. +++	–	–	–	–	–	+	Foc. +++	++	–	–
CASE 29	+++	+++	–	–	–	–	–	+++	Foc. ++	+++	+++	–
CASE 15b	++	–	+++	–	–	–	–	+++	Foc. ++	++	–	–

– negative, + weak positivity, ++ moderate positivity, +++ strong positivity, *Foc.* focally (up to 50%), *SC* single cells.

Table 8
GROUP 2: PRCC with oncocytic cells and gains of chromosomes 7 and 17 - cytogenetic study.

CASE	Del 1p36	Enumeration 1	BA BCL1 (CCND1)	Enumeration BCL1 (CCND1)	Enumeration 7	Enumeration 14	Enumeration 17	X/Y	SWIFT KRAS
CASE 24	Negative	Negative	Present	NA	Gain	Negative	Gain	Negative	NP
CASE 25	Negative	Negative	NA	NA	Gain	Negative	Gain	Negative	NP
CASE 26	Negative	Negative	Negative	Gain	Gain	Negative	Gain	Loss Y	NP
CASE 27	Present	Negative	Negative	Negative	Gain	Loss	Gain	Loss X	NP
CASE 28	NA	NA	Negative	Gain	Gain	NA	Gain	Loss Y	NP
CASE 29	Negative	Loss	Negative	Negative	Gain	Loss	Gain	Loss Y	NP
CASE 15b	Present	Negative	Negative	Negative	Gain	Negative	Gain	Loss Y	NP

NA not available, *NP* not performed.

Table 9
GROUP 3: PRCC with oncocytic cells and with variable CNV – clinical data.

CASE	SEX	AGE	SIDE	SIZE – in the greatest dimension (cm)	STAGE	FU
CASE 30	M	73	R	3	pT1a	4.3y ANED
CASE 31	M	71	R	3	NA	LFU
CASE 32	M	55	NA	7	pT3a	4y DOD
CASE 33	M	70	R	4	pT3a	10y AWD (Lymph nodes metastasis)
CASE 34	F	81	R	2	NA	LFU
CASE 35	M	69	L	6.5	pT1b	14.5y DNED
CASE 36	F	70	L	6	pT3a	8y ANED
CASE 37	M	75	R	2	pT1a	4.3y ANED
CASE 38	M	81	R	1.3	NA	LFU

M male, *F* female, *L* left, *R* right, *NA* not available, *DNED* death with no evidence of disease, *ANED* alive with no evidence of disease, *AWD* alive with the disease, *DOD* death of the disease, *LFU* lost for follow up.

foam cells, calcifications, hemorrhagia, hemosiderin and necrosis, which yielded no differences between the study groups. There were no significant differences in immunohistochemical profile among the study groups, with all cases positive for MIA, AMACR and vimentin. Immunoreactivity for CK7, CK20, AMACR, cyclin D1, GATA3, and carbonic anhydrase IX was variable across the three groups. All tumors were negative for CD117, HMB45, and Melan A. No correlation between immunoprofile and CNV status was found.

An interesting finding in this study were 2 cases fulfilling the diagnostic criteria (both morphologically and immunohistochemically) for so-called PRCC with reverse polarity. Both cases were listed in the group of PRCC with oncocytic cells and RO-like CNV. Moreover, we showed *KRAS* mutation in both tumors, believed to be another characteristic feature of PRCC with reverse polarity.

Case 15 provided another interesting and study design complicating results. The primary tumor (case 15a) showed molecular genetic pattern similar to RO, while its recurrence (case 15b) presented with polysomy of chromosomes 7 and 17. Primary lesion exhibited mostly tubular architectural pattern with cystic changes, the recurrent tumor was predominantly tubular. However in recurrent lesion, intracytoplasmic vacuoles were focally present. Both primary and recurrent tumor expressed CK20. Such findings demonstrated that renal cell carcinomas with papillary/tubulopapillary patterns and oncocytic cells are heterogeneous and that CNV analysis can potentially be confusing and need to be interpreted with caution.

The differential diagnosis of "oncocytic" renal tumors is rather challenging and includes RO, OPRCC, chromophobe renal cell carcinoma, and less frequently encountered neoplasms such as so-called hybrid oncocytic-chromophobe tumor/low grade oncocytic neoplasia of uncertain malignant potential (according to the WHO 2016 classified as chromophobe RCC), so-called low-grade oncocytic tumor (LOT), and so-called eosinophilic vacuolated tumor [3,14].

Because of oncocytic features of the neoplastic cells and the presence of more "solid" areas in our tumors, RO is a morphological leading differential diagnosis. It should be noted that sometimes, focal papillary foci can even be seen in RO [15]. Alveolar growth pattern, occasionally with island-like structures in a rich fibrotic or edematous background is characteristic for RO. Membranous positivity of CD117 is also typical for RO [16]. AMACR positivity was described in RO [17], and central scar-like areas in RO can show focal positivity for vimentin at the periphery or in small clusters scattered throughout the tumor [18]. The cytogenetic alterations in RO encompass enumeration of chromosome 1 (loss of whole chromosome 1or its deletion – typically 1p36), and/or loss of chromosome 14, and/or loss of gonosomes (X/Y), and/or 11q13 rearrangement (gene *CCND1*) or normal karyotype. Recent study of 130 RO identified three classes of mutually exclusive cytogenetic categories in RO: Rearrangement 11q13 – *CCND1* gene, loss of chromosome 1 and/or losses of Y in males and X in females and divergent types of chromosome abnormalities. The authors raised hypothesis that cytogenetic categories may have different roles in initiation and/or progression of the disease [19]. Cytogenetic study in our cases also showed features overlapping with RO (similar to Lefevre's study [8]). Based on our findings, it seems that extensive sampling of the tumor, aiming to identify papillae with foam cells, is more effective than utilizing expensive genetic testing [9].

Papillary architecture can rarely be seen in chromophobe RCC, but characteristic cytologic features such as so-called raisinoid nuclei and perinuclear clearing, as well as combination of large leaf-like cells and smaller eosinophilic cells can help to establish correct diagnosis [20]. So-called low-grade oncocytic tumor (LOT), and so-called eosinophilic vacuolated tumor are solid tumors, without papillation or well-formed papillae. Both tumors can be easily ruled out using basic morphologic features [14,21].

As previously mentioned, both the primary tumor and the recurrence of one of the cases (case 15) was diffusely reactive for CK20 (with variable intensity). Similar pattern was also documented in another primary tumor in our study. The former case was grouped as "PRCC with oncocytic cells and RO-like CNV" group, while the recurrence and the latter case were listed in group of "PRCC with oncocytic cells and gains of chromosomes 7 and 17". It is important to note that CK20 positivity can be seen in up to 85% of eosinophilic solid and cystic RCC (ESC) RCCs. In our study, CK20 positive cases did show neither solid and cystic architectures, nor voluminous eosinophilic cytoplasm with cytoplasmic stippling, which is typical in ESC RCCs. CNV pattern for ESC is also different, with no polysomy of chromosomes 7 and 17 being reported [22].

Our findings clearly showed that tumors grouped under umbrella term "OPRCC" forms a heterogeneous group of renal tumors. Although they all share papillary/tubulopapillary architecture with oncocytic

Table 10
GROUP 3: PRCC with oncocytic cells and with variable CNV - morphologic study.

CASE	Pattern of growth		Cytoplasm	Grade ISUP/WHO	Pseudostratification	Calcification (C), necrosis (N), hemosiderin (HEM), hemorrhage (HEMOR)	Macrophages
	Presence of papillary structures	Presence of other structures					
CASE 30	Predominantly	Tubular, cystic	Granular, abundant, eosinophilic	3, granular chromatin	No	HEM +	+
CASE 31	Only		granular, abundant, eosinophilic, cylindrical cells	3	Present	Not present	Not present
CASE 32	Papillary compressed, focally to "solid"		Granular, eosinophilic, cuboidal to cylindrical cells	2, granular chromatin	Present focally	Not present	Not present
CASE 33	Only		Granular, eosinophilic, cuboidal cells	2, granular chromatin	No	HEM + (occasionally fine pigmentation in the stalks)	Not present
CASE 34	Only, focally compressed		Abundant, granular, eosinophilic, cuboidal to cylindrical cells	2, nuclei centrally located	No	Not present	Not present
CASE 35	Only		Granular, abundant, eosinophilic, apically slightly granular and eosinophilic "globules", cylindrical cells	3, granular chromatin, luminal localization of nuclei	Present focally	C + (psammomatous), HEM + (prominent granular disperse)	Not present
CASE 36	Predominantly	Tubulopapillary	Granular, eosinophilic, focally clear cell changes, cuboidal cells	3, optically empty, nuclei centrally located	No	HEM + (prominent granular disperse), N +, HEMOR +	Not present
CASE 37	Only		Granular, eosinophilic, cuboidal cells	2, granular chromatin, nuclei centrally located	No	N +, HEM + (fine), bloody lakes	+ (collections of foamy macrophages)
CASE 38	Only		Granular, abundant, eosinophilic	2, nuclei centrally located	No	Not present	+ (collections of foamy macrophages)

BM basal membrane, + present.

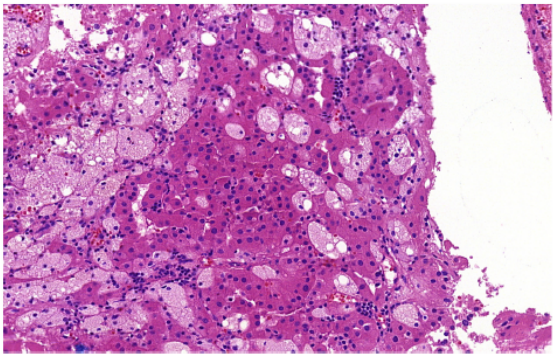

Fig. 5. Some tumors contained voluminous foam cell deposits (e.g. case from group 3: PRCC with oncocytic cells and with variable CNV).

cells, immunohistochemical and molecular genetic profiles are variable. Cytogenetic changes may be similar to RO at one end of the spectrum or identical to typical PRCC "type 1" at the other end. Unfortunately, as broad is the genetic profile, as variable biologic behavior and prognosis would be. In this study, 4/26 cases (15.4%) showed aggressive clinical course. Two cases with stage pT1b (first case was part of PRCC with oncocytic cells and CNV equal to renal oncocytoma and second case was part of PRCC with oncocytic cells and gains of chromosomes 7 and 17) developed aggressive clinical course. The two other cases with stage pT3a also developed metastatic aggressive disease; both were in group 3 "PRCC with oncocytic cells and variable CNV". Abnormalities in *CCND1* gene did not have impact on biologic behavior either.

Our findings suggest that using molecular testing in diagnosing PRCC with oncocytic cells can be potentially misleading, as the majority of such cases show cytogenetic features consistent with the diagnosis of RO. We would also not recommend using cytogenetic analysis in limited material (i.e., core biopsy) to establish the diagnosis as this can be misleading. However, in tumors composed of oncocytic cells but with debatable architecture (i.e., papillary, tubulopapillary and compressed/solid), all available diagnostic modalities should be appropriately utilized. Nonetheless, we recommend generous sampling of surgical

Table 11
GROUP 3: PRCC with oncocytic cells and with variable CNV – immunohistochemistry.

CASE	MIA	CK7	CK20	CD117	TFE3	Melan A	HMB45	AMACR	VIM	Cyclin D1	GATA3	CANH
CASE 30	+++	+++	–	–	–	–	–	+++	+++	SC +	NA	NA
CASE 31	+++	Foc. ++	–	–	–	–	–	+++	++	Foc. +	–	–
CASE 32	+++	–	–	–	–	–	–	+++	++	Foc. +	–	–
CASE 33	+++	–	–	–	–	–	–	NA	Foc. +	Foc. ++	–	–
CASE 34	++	–	–	–	–	–	–	+++	+++	Foc. ++	–	–
CASE 35	+++	+++	–	–	–	–	–	+++	Foc. +++	Foc. ++	–	Foc. +++
CASE 36	+++	+ SC	–	–	–	–	–	+++	+++	Foc. +++	–	–
CASE 37	+++	+++	–	–	–	–	–	+++	Foc. ++	+++	–	Foc. +++
CASE 38	+++	Foc. ++	–	–	–	–	–	+++	+++	+	–	Foc. ++

– negative, + weak positivity, ++ moderate positivity, +++ strong positivity, *Foc.* focally (up to 50%), *SC* single cells.

Table 12
GROUP 3: PRCC with oncocytic cells and with variable CNV – cytogenetic study.

CASE	Del 1p36	Enumeration 1	BA BCL1 (CCND1)	Enumeration BCL1 (CCND1)	Enumeration 7	Enumeration 14	Enumeration 17	X/Y	SWIFT KRAS
CASE 30	Negative	Negative	Negative	Negative	Loss	Negative	Loss	Negative	NP
CASE 31	Negative	Negative	Negative	Negative	Negative	Negative	Gain	Loss Y	NP
CASE 32	Present	Negative	Negative	Negative	Negative	Negative	Loss	Loss Y	NP
CASE 33	Negative	Negative	Negative	Negative	Negative	Negative	Loss	Negative	NP
CASE 34	Negative	Negative	Negative	Negative	Negative	Negative	Loss	Loss Y	Negative
CASE 35	Negative	Negative	Negative	Negative	Negative	Negative	Loss	Negative	NP
CASE 36	Negative	Negative	Negative	Negative	Gain	Negative	Loss	Negative	NP
CASE 37	Negative	Negative	Negative	Negative	Negative	Negative	Gain	Loss Y	NP
CASE 38	Negative	Negative	Negative	Negative	Gain	Negative	Negative	Loss Y	Negative

NA not available, *NP* not performed.

specimen since it seems to be the most reliable method in rendering an accurate diagnosis. For clinical practice and patient management, it is reasonable to potentially "overcall" RO as PRCC than the opposite.

5. Conclusions

Nearly 16 years after the initial description of so-called "OPRCC" and many published and unpublished discussions, "OPRCC" still remains a controversial group of renal carcinomas. With the exception of so-called PRCC with reverse polarity, which seems to be a relatively uniform, compact and well-defined tumor, the vast majority of RCC with papillary/tubulopapillary architecture and oncocytic cells are highly variable in aspects of biologic behavior, morphology, and molecular-genetic features. However, within genitourinary tumors classification this is not an exception. For example, testicular Sertoli cell tumors, NOS share even broader morphologic, immunohistochemical and genetic heterogeneity [3]. Based on our results and existing published data, we would not recommend using the term "OPRCC" as a distinct diagnostic category.

Supplementary data to this article can be found online at https://doi.org/10.1016/j.anndiagpath.2021.151734.

Declaration of competing interest

All authors declare no conflict of interest.

References

[1] Delahunt B, Eble JN. Papillary renal cell carcinoma: a clinicopathologic and immunohistochemical study of 105 tumors. Mod Pathol 1997;10(6):537–44.
[2] Trpkov K, Hes O, Williamson SR, Adeniran AJ, Agaimy A, Alaghehbandan R, et al. New developments in existing WHO entities and evolving molecular concepts: the Genitourinary Pathology Society (GUPS) update on renal neoplasia. Mod Pathol 2021. https://doi.org/10.1038/s41379-021-00779-w [Epub ahead of print].
[3] Moch H, Humphrey PA, Ulbright TM, Reuter VE. WHO classification of tumours of the urinary system and male genital organs. Lyon: IARC; 2016.
[4] Al-Obaidy KI, Eble JN, Cheng L, Williamson SR, Sakr WA, Gupta N, et al. Papillary renal neoplasm with reverse polarity: a morphologic, immunohistochemical, and molecular study. Am J Surg Pathol 2019;43(8):1099–111. https://doi.org/10.1097/PAS.0000000000001288.
[5] Michalova K, Steiner P, Alaghehbandan R, Trpkov K, Martinek P, Grossmann P, et al. Papillary renal cell carcinoma with cytologic and molecular genetic features overlapping with renal oncocytoma: analysis of 10 cases. Ann Diagn Pathol 2018;35:1–6. doi:https://doi.org/10.1016/j.anndiagpath.2018.01.010.
[6] Mohapatra G, Betensky RA, Miller ER, Carey B, Gaumont LD, Engler DA, et al. Glioma test array for use with formalin-fixed, paraffin-embedded tissue: array comparative genomic hybridization correlates with loss of heterozygosity and fluorescence in situ hybridization. The Mol Diagn 2006;8(2):268–76. doi:https://doi.org/10.2353/jmoldx.2006.050109.
[7] Petersson F, Gatalica Z, Grossmann P, Perez Montiel MD, Alvarado Cabrero I, Bulimbasic S, et al. Sporadic hybrid oncocytic/chromophobe tumor of the kidney: a clinicopathologic, histomorphologic, immunohistochemical, ultrastructural, and molecular cytogenetic study of 14 cases. Virchows Arch 2010;456(4):355–65. https://doi.org/10.1007/s00428-010-0898-4.
[8] Lefevre M, Couturier J, Sibony M, Bazille C, Boyer K, Callard P, et al. Adult papillary renal tumor with oncocytic cells: clinicopathologic, immunohistochemical, and cytogenetic features of 10 cases. Am J Surg Pathol 2005;29(12):1576–81. https://doi.org/10.1097/01.pas.0000184821.09871.ec.
[9] Hes O, Brunelli M, Michal M, Cossu Rocca P, Hora M, Chilosi M, et al. Oncocytic papillary renal cell carcinoma: a clinicopathologic, immunohistochemical, ultrastructural, and interphase cytogenetic study of 12 cases. Ann Diagn Pathol 2006;10(3):133–9. doi:https://doi.org/10.1016/j.anndiagpath.2005.12.002.
[10] Kunju LP, Wojno K, Wolf Jr JS, Cheng L, Shah RB. Papillary renal cell carcinoma with oncocytic cells and nonoverlapping low grade nuclei: expanding the morphologic spectrum with emphasis on clinicopathologic, immunohistochemical and molecular features. Hum Pathol 2008;39(1):96–101. https://doi.org/10.1016/j.humpath.2007.05.016.
[11] Xia QY, Rao Q, Shen Q, Shi SS, Li L, Liu B, et al. Oncocytic papillary renal cell carcinoma: a clinicopathological study emphasizing distinct morphology, extended immunohistochemical profile and cytogenetic features. Int J Clin Exp Pathol 2013;6(7):1392–9.
[12] Han G, Yu W, Chu J, Liu Y, Jiang Y, Li Y, et al. Oncocytic papillary renal cell carcinoma: a clinicopathological and genetic analysis and indolent clinical course in 14 cases. Pathol Res Pract 2017;213(1):1–6. https://doi.org/10.1016/j.prp.2016.04.009.
[13] Pitra T, Pivovarcikova K, Alaghehbandan R, Hes O. Chromosomal numerical aberration pattern in papillary renal cell carcinoma: review article. Ann Diagn Pathol 2019;40:189–99. doi:https://doi.org/10.1016/j.anndiagpath.2017.11.004.
[14] Trpkov K, Williamson SR, Gill AJ, Adeniran AJ, Agaimy A, Alaghehbandan R, et al. Novel, emerging and provisional renal entities: the Genitourinary Pathology Society (GUPS) update on renal neoplasia. Mod Pathol 2021. https://doi.org/10.1038/s41379-021-00737-6.
[15] Amin MB, Crotty TB, Tickoo SK, Farrow GM. Renal oncocytoma: a reappraisal of morphologic features with clinicopathologic findings in 80 cases. Am J Surg Pathol 1997;21(1):1–12. https://doi.org/10.1097/00000478-199701000-00001.
[16] Reuter VE, Argani P, Zhou M, Delahunt B, Members of the IIiDUPG. Best practices recommendations in the application of immunohistochemistry in the kidney tumors: report from the International Society of Urologic Pathology consensus conference. Am J Surg Pathol 2014;38(8):e35–49. doi:https://doi.org/10.1097/PAS.0000000000000258.
[17] Tretiakova MS, Sahoo S, Takahashi M, Turkyilmaz M, Vogelzang NJ, Lin F, et al. Expression of alpha-methylacyl-CoA racemase in papillary renal cell carcinoma. Am J Surg Pathol 2004;28(1):69–76. https://doi.org/10.1097/00000478-200401000-00007.
[18] Hes O, Michal M, Kuroda N, Martignoni G, Brunelli M, Lu Y, et al. Vimentin reactivity in renal oncocytoma: immunohistochemical study of 234 cases. Arch Pathol Lab Med 2007;131(12):1782–8. https://doi.org/10.1043/1543-2165(2007)131[1782:VRIROI]2.0.CO;2.
[19] Anderson CB, Lipsky M, Nandula SV, Freeman CE, Matthews T, Walsh CE, et al. Cytogenetic analysis of 130 renal oncocytomas identify three distinct and mutually exclusive diagnostic classes of chromosome aberrations. Genes Chromosomes Cancer 2019. doi:https://doi.org/10.1002/gcc.22766.
[20] Michalova K, Tretiakova M, Pivovarcikova K, Alaghehbandan R, Perez Montiel D, Ulamec M, et al. Expanding the morphologic spectrum of chromophobe renal cell

carcinoma: a study of 8 cases with papillary architecture. Ann Diagn Pathol 2020; 44:151448. doi:https://doi.org/10.1016/j.anndiagpath.2019.151448.
[21] Trpkov K, Hes O. New and emerging renal entities: a perspective post-WHO 2016 classification. Histopathology. 2019;74(1):31–59. doi:https://doi.org/10.1111/his.13727.
[22] Trpkov K, Hes O, Bonert M, Lopez JI, Bonsib SM, Nesi G, et al. Eosinophilic, solid, and cystic renal cell carcinoma: clinicopathologic study of 16 unique, sporadic neoplasms occurring in women. Am J Surg Pathol 2016;40(1):60–71. https://doi.org/10.1097/PAS.0000000000000508.

3.3 Expanding the morphologic spectrum of chromophobe renal cell carcinoma: A study of 8 cases with papillary architecture.

Papillary architecture is unfrequently seen in chromophobe renal cell carcinoma (ChRCC). In the presented study, we collected series of 8 RCC with prominent papillary growth pattern to describe clinicopathological, immunohistochemical and molecular features of this rare variant, as well as broad differential diagnosis.

Patients were 3 males and 5 females, with age ranging from 30 to 84 years. Tumor size ranged from 2 to 14 cm. Follow-up was available for 7 of 8 patients (from 1 to 61 months in duration). Six patients were alive with no recurrent disease, one died of the disease. By morphology, extent of papillary architecture ranged from 15 to 100%. All tumours showed classic ChRCC features with dual population of cells: leaf-like cells with abundant pale cytoplasm and smaller, eosinophilic cells. Typical wrinkled, rasinoid nuclei and perinuclear halos were readily seen. Sarcomatoid transformation was present only in the case with fatal outcome. Immunohistochemically, all tumours were positive for CK7, CD117 and Hale's Colloidal Iron. Staining for PAX8, TFE3 and Cathepsin K showed variable results. All cases were negative for vimentin, AMACR and HMB45. Fumarate hydratase staining was retained in all tested cases. The proliferative activity was low. Three tumours were suitable for array Comparative Genomic Hybridisation (aCGH), which in an all cases showed a variable copy number variation profile, with multiple chromosomal gains and losses.

ChRCC has a favourable prognosis when compared to CCRCC or PRCC. Even though limited number of cases included in our study, it appears that the presence of papillary architecture rather does not influence indolent clinical course of ChRCC. Awareness of this particular pattern is important as differential diagnosis includes a broad spectrum of RCCs with papillary architecture and adverse prognosis (i.e., TFE3-rearranged RCC, FH-deficient RCC). Careful tumour sampling to find classic morphology of ChRCC as well as low threshold to apply immunohistochemistry (i.e. FH) are critical to arrive at the correct conclusions/diagnosis.

Annals of Diagnostic Pathology 44 (2020) 151448

Contents lists available at ScienceDirect

Annals of Diagnostic Pathology

journal homepage: www.elsevier.com/locate/anndiagpath

Original Contribution

Expanding the morphologic spectrum of chromophobe renal cell carcinoma: A study of 8 cases with papillary architecture

Kvetoslava Michalova[a], Maria Tretiakova[b], Kristyna Pivovarcikova[a], Reza Alaghehbandan[c], Delia Perez Montiel[d], Monika Ulamec[e], Adeboye Osunkoya[f], Kiril Trpkov[g], Gao Yuan[g], Petr Grossmann[a], Maris Sperga[h], Ivan Ferak[i], Joanna Rogala[a], Jana Mareckova[a], Tomas Pitra[j], Jiri Kolar[j], Michal Michal[a], Ondrej Hes[a,*]

[a] Department of Pathology, Charles University, Medical Faculty and Charles University Hospital Plzen, Czech Republic
[b] Department of Pathology, University of Washington, Seattle, WA, USA
[c] Department of Pathology, Faculty of Medicine, University of British Columbia, Royal Columbian Hospital, Vancouver, BC, Canada
[d] Department of Pathology, Institute Nacional de Cancerologia, Mexico City, Mexico
[e] Ljudevit Jurak Pathology Department, University Clinical Hospital "Sestre milosrdnice", Pathology Department, School of Dental Medicine, University of Zagreb, Croatia
[f] Department of Pathology, Emory Hospital, Atlanta, USA
[g] Department of Pathology and Laboratory Medicine, Calgary Laboratory Services and University of Calgary, Calgary, AB, Canada
[h] Department of Pathology, University of Split, Croatia
[i] Department of Pathology, AGEL, Novy Jicin, Czech Republic
[j] Department of Urology, Charles University, Medical Faculty and Charles University Hospital Plzen, Czech Republic

ARTICLE INFO

Keywords:
Chromophobe renal cell carcinoma
Papillary
Immunohistochemistry
Copy number variation
CNV

ABSTRACT

Although typically arranged in solid alveolar fashion, chromophobe renal cell carcinoma (RCC) may also show several other architectural growth patterns. We include in this series 8 chromophobe RCC cases with prominent papillary growth, a pattern very rarely reported or only mentioned as a feature of chromophobe RCC, which is lacking wider recognition The differential diagnosis of such cases significantly varies from the typical chromophobe RCC with its usual morphology, particularly its distinction from papillary RCC and other relevant and clinically important entities.

Of 972 chromophobe RCCs in our files, we identified 8 chromophobe RCCs with papillary growth. We performed immunohistochemistry and array Comparative Genomic Hybridisation (aCGH) to investigate for possible chromosomal aberrations.

Patients were 3 males and 5 females with age ranging from 30 to 84 years (mean 57.5, median 60 years). Tumor size was variable and ranged from 2 to 14 cm (mean 7.5, median 6.6 cm). Follow-up was available for 7 of 8 patients, ranging from 1 to 61 months (mean 20.1, median 12 months). Six patients were alive with no signs of aggressive behavior, and one died of the disease. Histologically, all cases were composed of dual cell population consisting of variable proportions of leaf-like cells with pale cytoplasm and eosinophilic cells. The extent of papillary component ranged from 15 to 100% of the tumor volume (mean 51%, median 50%). Sarcomatoid differentiation was identified only in the case with fatal outcome. Immunohistochemically, all tumors were positive for CK7, CD117 and Hale's Colloidal Iron. PAX8 was positive in 5 of 8 cases, TFE3 was focally positive 3 of 8 tumors, and Cathepsin K was focally positive in 2 of 8 tumors. All cases were negative for vimentin, AMACR and HMB45. Fumarate hydratase staining was retained in all tested cases. The proliferative activity was low (up to 1% in 7, up to 5% in one case). Three cases were successfully analyzed by aCGH and all showed a variable copy number variation profile with multiple chromosomal gains and losses. *Conclusions:* Chromophobe RCC demonstrating papillary architecture is an exceptionally rare carcinoma. The diagnosis can be challenging, although the cytologic features are consistent with the classic chromophobe RCC. Given the prognostic and therapeutic implications of accurately diagnosis other RCCs with papillary architecture (i.e., Xp11.2 translocation RCC, *FH*-deficient RCC), it is crucial to differentiate these cases from chromophobe RCC with papillary architecture. Based on this limited series, the presence of papillary architecture does not appear to have negative prognostic impact. However, its wider recognition may allow in depth studies on additional examples of this rare morphologic variant.

* Corresponding author.
E-mail address: hes@medima.cz (O. Hes).

https://doi.org/10.1016/j.anndiagpath.2019.151448

1. Introduction

Chromophobe RCC is an indolent renal neoplasm with specific morphologic features demonstrated by dual population of pale leaf-like and eosinophilic cells encountered in various proportions. The cells have accentuated cellular borders, hyperchromatic wrinkled nuclei and perinuclear halos. In most cases, chromophobe RCC demonstrates solid-alveolar growth. Several architectural morphologic patterns (or variants) have also been described, including chromophobe RCC with pigmented microcystic adenomatoid/multicystic growth [1-4], chromophobe RCC with neuroendocrine differentiation [5-9] and renal oncocytoma-like variant [10]. In this report, we expand the morphologic spectrum of chromophobe RCC by presenting a cohort of 8 cases with distinct and prominent papillary architecture. Differential diagnosis in such cases encompasses a wide spectrum of neoplasms and is different than in cases showing typical architectural growth of chromophobe RCC or from other described patterns.

The aim of this study was to improve our understanding of this rare architectural variant and to discuss its differential diagnosis in the relevant context, incorporating the entities where incorrect diagnosis would have prognostic and therapeutic implications.

2. Materials and methods

The 8 cases of chromophobe RCC with papillary architecture were identified and selected out of 972 chromophobe RCC documented in the Plzen tumor registry. The clinical information and follow-up data were obtained when available. Generally, the cases were collected over a period of two years (2017–2019). None of the cases included in the study has been previously reported. Tissues for light microscopy were formalin fixed and embedded in paraffin using the routine procedure. In general four to five-μm-thick sections were cut from the tissue blocks and stained with hematoxylin and eosin (H&E) and Hale's colloidal iron. When possible, the same tissue block from each case was used for the immunohistochemical (IHC) study and for the genetic analysis.

2.1. Immunohistochemistry

The IHC analysis was performed using a Ventana BenchMark ULTRA (Ventana Medical System, Inc., Tucson, Arizona). The following primary antibodies were used: CK7 (monoclonal, OV-TL12/30, 1:200, Dako, Glostrup, Denmark), CD117 (polyclonal, 1:800, Dako), vimentin (monoclonal, V9, RTU, Ventana Medical System, Inc., Tucson, Arizona), PAX8 (monoclonal, MRQ-50, RTU, Ventana Medical System, Inc.), AMACR (monoclonal, 13H4, RTU, Dako), Ki-67 (monoclonal, MIB-1, 1:400, Dako), TFE3 (monoclonal, MRQ-37, RTU, Ventana Medical System, Inc.), HMB45 (monoclonal, HMB45, 1:400, Ventana Medical System, Inc.), Cathepsin K (monoclonal, 3F9, 1:100, Abcam, Cambridge, UK), Fumarate hydratase (FH) (monoclonal, J-13, 1:3000, Santa Cruz, Wien, Austria). The primary antibodies were visualized using either alkaline phosphatase or peroxidase-based detecting systems (both from Ventana Medical System, Inc.).

2.2. DNA extraction

Representative tumor areas from the formalin-fixed paraffin-embedded (FFPE) samples were marked using H&E slides and were macro dissected. DNA from FFPE tumor tissue was extracted using QIAsymphony DNA Mini Kit (Qiagen, Hilden, Germany) on an automated extraction system (QIAsymphony SP; Qiagen) according to the manufacturer's supplementary protocol for FFPE samples. The concentration and the purity of the isolated DNA were measured using NanoDrop ND-1000 and DNA integrity was examined by amplification of control genes in a multiplex polymerase chain reaction (PCR).

2.3. Low pass whole genome sequencing

SurePlex DNA amplification system (Illumina, San Diego, CA) was used to generate DNA templates of tumor samples. DNA amplification in this setting is highly representative, which allows the resulting product to be suitable for copy number variation (CNV) detection. The library of all samples was prepared using Nextera DNA Sample Prep Kit (Illumina, San Diego, CA) using MiSeq sequencer. CNV analysis was performed using BlueFuse Multi software with the Veriseq plugin (Illumina, San Diego, CA). Following quality control filters for valid samples were set at a minimum 1 million reads per sample, with average quality score and average alignment score > 30, and overall noise < 0.3. Thresholds for CNV calling were set based on the group of samples with known CNV that were validated using array comparative genomic hybridisation (aCGH) and fluorescence in-situ hybridization (FISH). The percentage of tumor in the DNA sample was considered when calling the lower frequency CNVs. Thresholds for CNVs were set individually for each case, typically with the copy number of 1.5 for loss and 2.5 for gain. CNVs spanning less than the whole length of a chromosomal arm were not called. FISH was also used for confirmation of the three analyzable cases, as previously described [11] (results not shown). Aberrations on gonosomes were excluded from the results. CNV detection using low pass whole genome sequencing was shown to produce similar and comparable results as in the fresh frozen tissue [12].

3. Results

3.1. Clinicopathologic features

The clinicopathologic characteristics are summarized in Table 1. There were 3 males and 5 females with the age range (at the time of diagnosis) from 30 to 84 years (mean 57.5, median 60 years). Follow-up

Table 1
Clinical features and morphology.

Case	Age (years)	Sex	Size (cm)[a]	TNM, AJCC 2017	Follow-up (months)	Morphology					
						Papillary (%)	Adenomatous (%)	Solid (%)	Microcalcif	Pigment	Necrosis
1	55	M	12	pT3a, pNx	AND 12	100	0	0	Yes	No	Yes
2	39	M	3	pT1a, pNx	AND 48	15	85	0	No	Yes	No
3	75	F	2	pT1a, pNx	AND 2	15	70	15	No	Yes	No
4	84	F	13	pT3a, pN1	DOD 3	20	0	30[b]	No	No	No
5	67	M	9.6	pT3a, pNx	NA	80	20	0	No	No	Yes
6	65	F	3.5	pT1a, pNx	AND 14	40	60	0	No	No	No
7	30	F	14	pT2b, pNx	AND 61	80	20	0	No	Yes	No
8	45	F	2.9	pT1a, pNx	AND 1	50	10	10	Yes	Yes	No

M: male; F: female; AND: alive no evidence of disease; NA: not available; DOD: death of disease; Microcalcif: microcalcification
[a] Greatest dimension
[b] Sarcomatoid dedifferentiation.

was available for 7 patients and ranged from 1 to 61 months (mean 20.1, median 12 months). Six patients were alive with no evidence of disease progression, while 1 died of the disease 3 months after the surgery. There was no association with Birt-Hogg-Dubé syndrome in any patient. Three patients presented with pT3a stage, 1 with pT2b and 4 with pT1a.

Tumor size showed a broad range from 2 to 14 cm (mean 7.5, median 6.6). Tumors were described as solid, solid-cystic with focal hemorrhages on gross examination (Fig. 1). Histologically, the tumors were arranged in papillary, adenomatoid and solid structures. The extent of papillary component ranged from 15% to 100% of the tumor volume (mean 51%, median 50%) (Fig. 2). The papillae contained delicate fibrovascular cores without foamy histiocytes (Fig. 3). All cases consisted of two cell populations of pale leaf-like and eosinophilic cells that were represented in variable proportions. Typical raisinoid nuclei were present in all cases (Fig. 4).

Cytologically, the cells in the papillary structures did not differ from those found in the other areas showing a typical chromophobe RCC morphology. Case 2 was predominantly composed of eosinophilic oncocytic cells with mostly centrally located, round nuclei. In this case, raisinoid nuclei (without halos) as well as rounded nuclei with perinuclear halos were identified only at the periphery of the tumor. Amorphous rough microcalcifications and/or psammoma bodies and extracellular dark brown pigment (lipofuscin and/or hemosiderin) were also occasionally found (for details see Table 1) (Fig. 5). Sarcomatoid differentiation involving about 50% of the tumor was present in Case 4.

3.2. Immunohistochemical and histochemical features

The results are summarized in Table 2. All tumors were positive for CK7 (Fig. 6), CD117 (Fig. 7), and Hale's colloidal iron. PAX8 was positive in 7 of 8 cases. TFE3 was focally positive in 3 of 8 tumors. All cases were negative for vimentin, AMACR, Cathepsin K and HMB45. FH staining was retained in all evalauted cases. The proliferative activity was low with Ki-67 proliferative index of 1% in 7 tumors and 5% in the remaining case.

3.3. Chromosomal aneuploidy study

The results are summarized in Table 2. Three cases included in the current study were analyzable. Case 3 revealed loss of chromosome 1p36.33–p36.22, −9q21.11–q34.3, Case 4 showed gains of chromosomes 4, 5, 7, 12, 14, 15q11.2 - q25.3, 18, 19, 20 and 22 and Case 7 showed losses of chromosomes 1, 2, 6, 10 and 17.

4. Discussion

Papillary architecture can occur in a broad spectrum of renal tumors and is by no means specific for papillary RCC. In fact, the papillary morphology represents one of the most common architectural configurations encountered in renal neoplasms. Prominent papillary pattern is however not widely recognized as a morphological feature of chromophobe RCC [13,14]. Papillary arrangement as a focal feature in these tumors has been only rarely mentioned in the literature [13,15-17]. To our best knowledge, only 1 chromophobe RCC with predominant papillary morphology has been documented [17]. This case was reported in one of the largest series of chromophobe RCC published to date, comprising 145 cases [17], and was therefore not discussed in detail. The 8 cases included in this study exhibited a prominent papillary architecture, representing 15% to 100% of the tumor volume. The other architectural patterns observed in these cases were tubulary to cribriform, and solid. The diagnosis of chromophobe RCC was based on the typical cytological features, i.e. on a combination of enlarged pale and leaf-like cells and smaller population of eosinophilic cells. In all cases, raisinoid nuclei and perinuclear clearing were identified. Case 2 exhibited similar features to oncocytic chromophobe RCC, another rare variant [10]. Nuclear features typical for chromophobe RCC were identified only at the periphery of this case. Immunophenotype, showing positivity with CK7, CD117, Hale, low Ki-67 index and negativity with vimentin, was also consistent with chromophobe RCC. Uniformly negative staining with AMACR also argued against the diagnosis of papillary RCC. The cytogenetic features further supported our diagnosis, as multiple chromosomal losses and gains pathognomonic for chromophobe RCC [18-23] were detected in all 3 analyzable cases.

It has been hypothesized that certain morphological features of chromophobe RCC may influence its otherwise indolent clinical course. Neuroendocrine differentiation may occur as the result of dedifferentiation with a potentially negative impact on prognosis [5-7,9]. In our series, Case 4 behaved aggressively and the patient succumbed to the disease 3 months after the surgery. In addition to papillary arrangement, this case also showed sarcomatoid differentiation. Its presence in chromophobe RCC worsens its prognosis by reducing 10-year cancer specific survival rate from 90% to 27% [24,25]. According to one of the largest series on sarcomatoid chromophobe RCC, the mean percentage of tumor showing sarcomatoid differentiation was 67% [26]. Therefore, it is most likely that the aggressive clinical behavior in Case 4 was owing to the presence of sarcomatoid transformation, which comprised about 50% of the tumor, rather than by the papillary component. The remaining 7 cases lacked sarcomatoid areas and all 6 with available clinical information had an indolent clinical course.

The differential diagnostic work-up should be primarily based on the careful cytomorphologic evaluation. Tumors composed mainly of pale cells may be misdiagnosed as papillary RCC with clear cell change, clear cell RCC, or as Xp11.2 translocation RCC. The presence of characteristic cytomorphologic features of chromophobe RCC is however sufficient to make or to strongly suggest the correct diagnosis in most cases.

Papillary RCC can occasionally demonstrate clear cell change [27-30], which is probably caused by the phagocytic activity of the carcinoma cells or by the local microenviroment [29]. This phenomenon is illustrated by the tendency of clear cells to cluster in the vicinity of areas of necrosis and hemorrhage. However, no such zonal distribution was observed in any of the cases in the current series. Psammoma bodies can be also seen in both tumor types, but other structures typical of papillary RCC, such as aggregates of foamy macrophages and cholesterol clefts were not observed in this case series. In contrary to chromophobe RCC, papillary RCC typically stains with AMACR and vimentin. As multiple chromosomal imbalances including chromosomal losses and gains may be found in both papillary [22,31-33] and

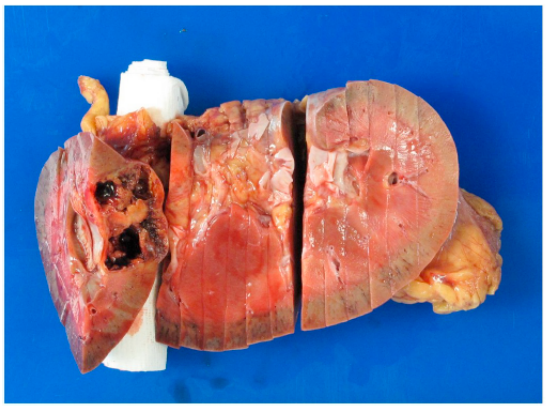

Fig. 1. The tumors were solid or solid-cystic with focal hemorrhages on gross section.

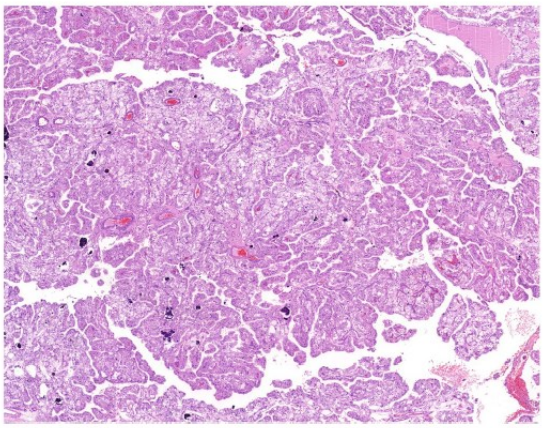

Fig. 2. The tumors were arranged in papillary, adenomatoid and solid structures.

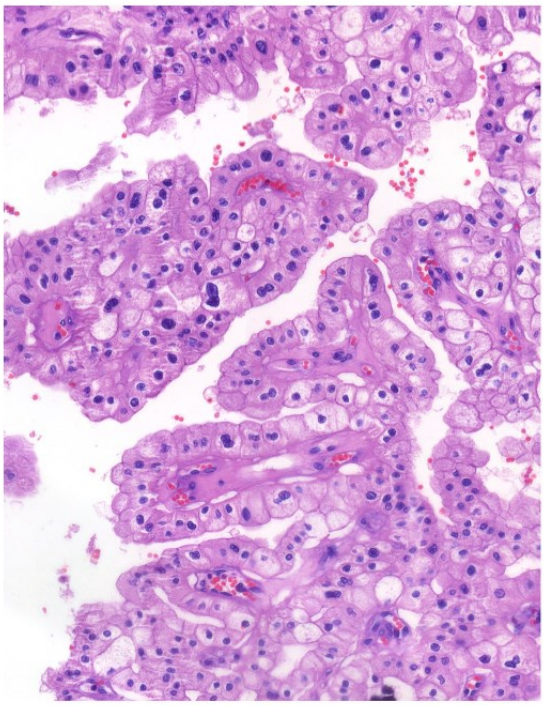

Fig. 3. The papillae contained delicate fibrovascular cores lined by large pale epithelial cells and smaller eosinophilic epithelial cells.

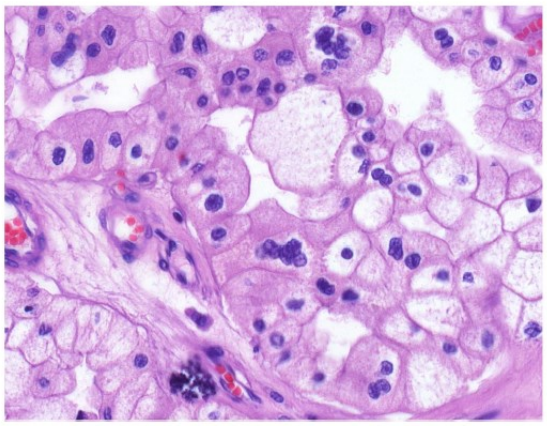

Fig. 4. Typical raisinoid nuclei were prominent and present in all cases.

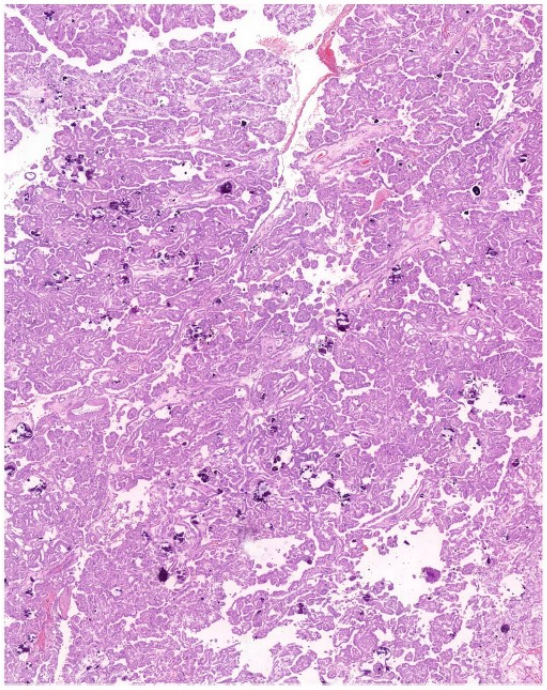

Fig. 5. Amorphous rough microcalcifications, psammoma bodies, and lipochrome were found in several cases.

chromophobe RCC, the results of the cytogenetic analyses should always be correlated with the morphologic and immunohistochemical features.

Papillary structures can also rarely occur in low-grade clear cell RCC [27-29,34-36]. Apart from the differences in the cytomorphology, the vascular pattern in clear cell RCC may offer a helpful diagnostic clue. Pseudoacinar and fascicular patterns are more common in clear cell RCC, whereas reticular pattern is more often present in chromophobe RCC [37]. Likewise, vimentin reactivity and an absence of reactivity for CD117 are uniformly present in clear cell RCC, but are typically not found in chromophobe RCC. In contrast to the traditional view that clear cell RCC are CK7 negative, CK 7 positivity can be often found in the low-grade clear cell RCC [38]. Although CK7 can be strongly positive in such cases, it is invariably focal, in contrast to the strong and diffuse positivity found in chromophobe RCC. In addition, cytogenetic methods for detection of *VHL* mutation, *VHL* hypermethylation or LOH 3p may also help to establish the diagnosis of clear cell RCC in equivocal cases.

It has become evident that Xp11.2 translocation RCC represents a morphologically heterogeneous group of tumors [39]. Histological

Table 2
Results of immunohistochemical and molecular genetic analysis.

Case	CK 7	CD117	vim	PAX8	AMACR	Ki-67	TFE3	HMB45	Hale's	cath K	FH	aCGH
1	+ + +	+ + +	–	+ + +	–	1%	–	–	+ + +	–	+ + +	NA
2	+ + +	+	–	+ + +	–	1%	foc + +	–	+ + +	–	+ + +	NA
3	+ + +	+ +	–	+ + +	–	1%	–	–	+ + +	–	+ + +	−1p36.33–p36.22, −9q21.11–q34.3.
4	+ + +	+ +	–	–	–	5%	foc + +	–	+ + +	–	+ + +	+4, +5, +7, +12, +14, +15q11.2–q25.3, +18, +19, +20, +22.
5	+ + +	+	–	foc+	–	1%	–	–	+ + +	–	NP	NP
6	+ + +	+	–	+	–	1%	–	–	+ + +	–	+ + +	NA
7	+ + +	+ +	–	+	–	1%	–	–	+ + +	–	+ + +	−1, −2, −6, −10, −17
8	+ + +	+ + +	–	+ + +	–	1%	foc +	–	+ +	–	+ + +	NA

vim: vimentin; cath K: cathepsin K; FH: fumarat hydratase; foc:focal aCGH: array Comparative Genomic Hybridization; NP: not performed; NA: not analyzable.

features similar to the cases described in this series may theoretically observed only in a subset of Xp11.2 translocation RCCs demonstrating an *ASPL-TFE3* fusion. These tumors are characterized by papillary and nested structures, lined by epithelioid clear and eosinophilic cells, often intermingled with psammoma bodies. Although the positive immune reaction for TFE3 is considered relatively specific for Xp11.2 translocation RCC, frequent false positive (or negative) results are well documented [40]. TFE3 was focally positive in 3 of the cases in this series, while the remaining 5 were negative. The fraction of positive neoplastic cells was however typically below 20% and can be considered as non-specific. FISH analysis for further confirmation was not performed. Cathepsin K is another widely used marker in the diagnosis of the translocation RCC, but its expression depends on the type of *TFE3* fusion partner. *ASPL-TFE3* RCC is typically negative for Cathepsin K, which has no discriminatory value in this situation [41,42]. In our series, Cathepsin K was negative in all cases. The key diagnostic test in this setting relies on the use of break-apart FISH or RT-PCR, which are necessary for diagnostic confirmation of Xp11.2 translocation RCC.

Case 2 was predominantly eosinophilic, resembling an oncocytic papillary RCC, which is a malignant renal tumor characterized by papillary structures lined by eosinophilic (oncocytic) cells with rounded, low-grade nuclei, lacking perinuclear clearing [43,44]. The nuclei in Case 2 closely resembled those found in oncocytic papillary RCC. However, after closer evaluation, cells with raisinoid nuclei (without halo) and rounded nuclei encircled by halos were identified at the periphery of the neoplasm. Scattered foci of foamy macrophages, typical of oncocytic papillary RCC, can serve as another useful discriminatory feature and no such features were documented in this case. Comparison of immunoprofile of papillary and chromophobe RCC was already discussed. The cytogenetic data available on the oncocytic papillary RCC are somewhat inconsistent, and some indicate cytogenetic similarities to type 1 papillary RCC (demonstrating polysomy of chromosomes 7, 17 and loss of Y), whereas other cases were documented with diploid status of 7, 17 and Y or even diploid status of all chromosomes [45]. In the current study, Case 2 was cytogenetically not analyzable.

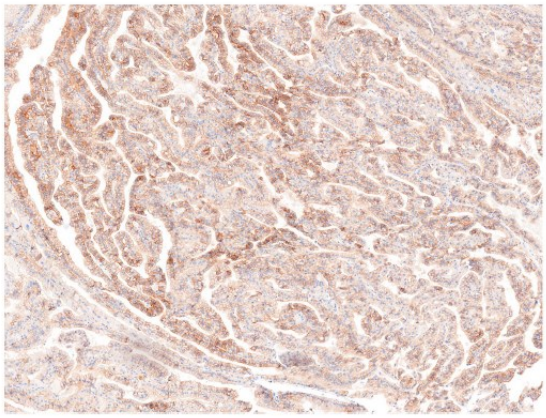

Fig. 7. All cases were positive for CD117; staining pattern was predominantly membranous.

Fumarate hydratase (*FH*)-deficient RCC often demonstrates papillary architecture with large cells containing abundant eosinophilic

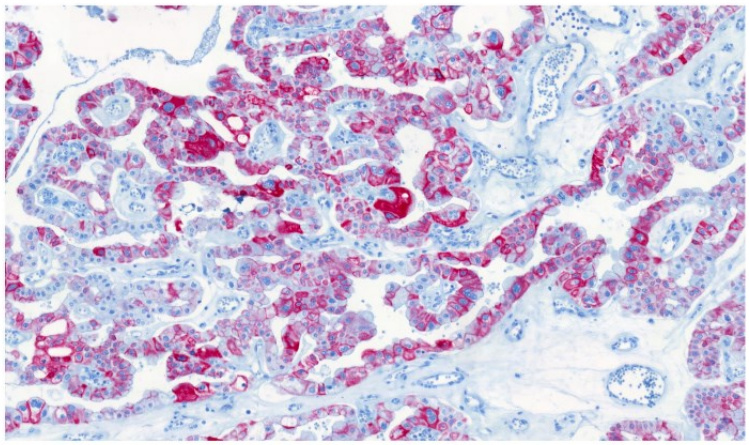

Fig. 6. Strong diffuse positivity was found for CK7 in all cases.

cytoplasm. The typical finding includes large viral-like nucleoli [46], which were not seen in our cases. Another helpful morphologic feature can be the detection of multiple architectural patterns in *FH*-deficient RCC [47]. The overall high-grade morphology and an advanced pathologic stage at the time of diagnosis underscore the aggressiveness of *FH*-deficient RCC and with the IHC loss of FH and the overexpression of S-(2-succino)-cysteine can help in this differential scenario. In all evaluated cases in this study, the FH staining was retained. The detection of the *FH* gene mutation on chromosome 1q42.3-q43 can also confirm the diagnosis.

In summary, we expand the morphologic spectrum of chromophobe RCC by presenting 8 cases demonstrating a prominent papillary architecture, which is a feature exceptionally rarely documented in these neoplasms. Although our study is limited, it seems that the presence of papillary architecture does not affect the indolent clinical course of chromophobe RCC. In contrast to chromophobe RCC demonstrating classic architecture, the presence of prominent papillary structures in this tumor alters the list of entities that should be considered in the differential diagnosis. It is therefore important to distinguish chromophobe RCC with papillary features in particular from the biologically aggressive entities, such as *FH*-deficient RCC or Xp11.2 translocation RCC. The correct diagnosis in this setting can usually be rendered or strongly suggested by identifying the typical cytomorphology of chromophobe RCC.

Compliance with ethical standards

Neither ethics approval nor informed consent was required for our study.

Funding

The study was supported by the Charles University Research Fund (project number Q39) and by the project Institutional Research Fund of University Hospital Plzen (FNPl 00669806).

Declaration of competing interest

All authors declare no conflict of interest.

References

[1] Hes O, Vanecek T, Perez-Montiel DM, Alvarado Cabrero I, Hora M, Suster S, et al. Chromophobe renal cell carcinoma with microcystic and adenomatous arrangement and pigmentation–a diagnostic pitfall. Morphological, immunohistochemical, ultrastructural and molecular genetic report of 20 cases. Virchows Archiv : An International Journal of Pathology 2005;446:383–93.
[2] Michal M, Hes O, Svec A, Ludvikova M. Pigmented microcystic chromophobe cell carcinoma: a unique variant of renal cell carcinoma. Ann Diagn Pathol 1998;2:149–53.
[3] Dundr P, Pesl M, Povysil C, Tvrdik D, Pavlik I, Soukup V, et al. Pigmented microcystic chromophobe renal cell carcinoma. Pathol Res Pract 2007;203:593–7.
[4] Foix MP, Dunatov A, Martinek P, Mundo EC, Suster S, Sperga M, et al. Morphological, immunohistochemical, and chromosomal analysis of multicystic chromophobe renal cell carcinoma, an architecturally unusual challenging variant. Virchows Archiv : An International Journal of Pathology. 2016;469:669–78.
[5] Peckova K, Martinek P, Ohe C, Kuroda N, Bulimbasic S, Condom Mundo E, et al. Chromophobe renal cell carcinoma with neuroendocrine and neuroendocrine-like features. Morphologic, immunohistochemical, ultrastructural, and array comparative genomic hybridization analysis of 18 cases and review of the literature. Ann Diagn Pathol 2015;19:261–8.
[6] Parada DD, Pena KB. Chromophobe renal cell carcinoma with neuroendocrine differentiation. APMIS : Acta Pathologica, Microbiologica, et Immunologica Scandinavica 2008;116:859–65.
[7] Kuroda N, Tamura M, Hes O, Michal M, Gatalica Z. Chromophobe renal cell carcinoma with neuroendocrine differentiation and sarcomatoid change. Pathol Int 2011;61:552–4.
[8] Mokhtar GA, Al-Zahrani R. Chromophobe renal cell carcinoma of the kidney with neuroendocrine differentiation: a case report with review of literature. Urology Annals 2015;7:383–6.
[9] Ohe C, Matsuura K, Kai T, Moriyama M, Sugiguchi S, Terahata S, et al. Chromophobe renal cell carcinoma with neuroendocrine differentiation/morphology: a clinicopathological and genetic study of three cases. Human Pathology: Case Reports 2014;1:31–9.
[10] Kuroda N, Tanaka A, Yamaguchi T, Kasahara K, Naruse K, Yamada Y, et al. Chromophobe renal cell carcinoma, oncocytic variant: a proposal of a new variant giving a critical diagnostic pitfall in diagnosing renal oncocytic tumors. Med Mol Morphol 2013;46:49–55.
[11] Sperga M, Martinek P, Vanecek T, Grossmann P, Bauleth K, Perez-Montiel D, et al. Chromophobe renal cell carcinoma–chromosomal aberration variability and its relation to Paner grading system: an array CGH and FISH analysis of 37 cases. Virchows Archiv : An International Journal of Pathology. 2013;463:563–73.
[12] Munchel S, Hoang Y, Zhao Y, Cottrell J, Klotzle B, Godwin AK, et al. Targeted or whole genome sequencing of formalin fixed tissue samples: potential applications in cancer genomics. Oncotarget. 2015;6:25943–61.
[13] Przybycin CG, Cronin AM, Darvishian F, Gopalan A, Al-Ahmadie HA, Fine SW, et al. Chromophobe renal cell carcinoma: a clinicopathologic study of 203 tumors in 200 patients with primary resection at a single institution. Am J Surg Pathol 2011;35:962–70.
[14] Din NU, Fatima S, Ahmad Z. Chromophobe renal cell carcinoma: a morphologic and immunohistochemical study of 45 cases. Ann Diagn Pathol 2013;17:508–13.
[15] Kuroda N, Iiyama T, Moriki T, Shuin T, Enzan H. Chromophobe renal cell carcinoma with focal papillary configuration, nuclear basaloid arrangement and stromal osseous metaplasia containing fatty bone marrow element. Histopathology. 2005;46:712–3.
[16] Karashima T, Kuroda N, Taguchi T, Matsumoto M, Hiroi M, Nao T, et al. Chromophobe renal cell carcinoma, eosinophilic variant with papillary growth: a case report. Int J Clin Exp Pathol 2015;8:13590–5.
[17] Amin MB, Paner GP, Alvarado-Cabrero I, Young AN, Stricker HJ, Lyles RH, et al. Chromophobe renal cell carcinoma: histomorphologic characteristics and evaluation of conventional pathologic prognostic parameters in 145 cases. Am J Surg Pathol 2008;32:1822–34.
[18] Moch H, Cubilla AL, Humphrey PA, Reuter VE, Ulbright TM. The 2016 WHO classification of tumours of the urinary system and male genital organs-part a: renal, penile, and testicular tumours. Eur Urol 2016;70:93–105.
[19] Brunelli M, Eble JN, Zhang S, Martignoni G, Delahunt B, Cheng L. Eosinophilic and classic chromophobe renal cell carcinomas have similar frequent losses of multiple chromosomes from among chromosomes 1, 2, 6, 10, and 17, and this pattern of genetic abnormality is not present in renal oncocytoma. Modern Pathology : An Official Journal of the United States and Canadian Academy of Pathology, Inc. 2005;18:161–9.
[20] Speicher MR, Schoell B, du Manoir S, Schrock E, Ried T, Cremer T, et al. Specific loss of chromosomes 1, 2, 6, 10, 13, 17, and 21 in chromophobe renal cell carcinomas revealed by comparative genomic hybridization. Am J Pathol 1994;145:356–64.
[21] Hagenkord JM, Gatalica Z, Jonasch E, Monzon FA. Clinical genomics of renal epithelial tumors. Cancer Genet 2011;204:285–97.
[22] Kim HJ, Shen SS, Ayala AG, Ro JY, Truong LD, Alvarez K, et al. Virtual-karyotyping with SNP microarrays in morphologically challenging renal cell neoplasms: a practical and useful diagnostic modality. Am J Surg Pathol 2009;33:1276–86.
[23] Yokomizo A, Yamamoto K, Furuno K, Shiota M, Tatsugami K, Kuroiwa K, et al. Histopathologic subtype-specific genomic profiles of renal cell carcinomas identified by high-resolution whole-genome single nucleotide polymorphism array analysis. Oncol Lett 2010;1:1073–8.
[24] Volpe A, Novara G, Antonelli A, Bertini R, Billia M, Carmignani G, et al. Chromophobe renal cell carcinoma (RCC): oncological outcomes and prognostic factors in a large multicentre series. BJU Int 2012;110:76–83.
[25] de Peralta-Venturina M, Moch H, Amin M, Tamboli P, Hailemariam S, Mihatsch M, et al. Sarcomatoid differentiation in renal cell carcinoma: a study of 101 cases. Am J Surg Pathol 2001;25:275–84.
[26] Lauer SR ZM, Master VA, Osunkoya AO. Chromophobe renal cell carcinoma with sarcomatoid differentiation. A clinicopathologic study of 14 cases. Anal Quant Cytol Histol35:77–84.
[27] Ross H, Martignoni G, Argani P. Renal cell carcinoma with clear cell and papillary features. Arch Pathol Lab Med 2012;136:391–9.
[28] Klatte T, Said JW, Seligson DB, Rao PN, de Martino M, Shuch B, et al. Pathological, immunohistochemical and cytogenetic features of papillary renal cell carcinoma with clear cell features. J Urol 2011;185:30–5.
[29] Gobbo S, Eble JN, Maclennan GT, Grignon DJ, Shah RB, Zhang S, et al. Renal cell carcinomas with papillary architecture and clear cell components: the utility of immunohistochemical and cytogenetical analyses in differential diagnosis. Am J Surg Pathol 2008;32:1780–6.
[30] Petersson F, Sperga M, Bulimbasic S, Martinek P, Svajdler M, Kuroda N, et al. Foamy cell (hibernoma-like) change is a rare histopathological feature in renal cell carcinoma. Virchows Archiv : An International Journal of Pathology. 2014;465:215–24.
[31] Saleeb RM, Brimo F, Farag M, Rompre-Brodeur A, Rotondo F, Beharry V, et al. Toward biological subtyping of papillary renal cell carcinoma with clinical implications through histologic, immunohistochemical and molecular analysis. Am J Surg Pathol 2017;41:1618–29.
[32] Antonelli A, Tardanico R, Balzarini P, Arrighi N, Perucchini L, Zanotelli T, et al. Cytogenetic features, clinical significance and prognostic impact of type 1 and type 2 papillary renal cell carcinoma. Cancer Genet Cytogenet 2010;199:128–33.
[33] Vieira J, Henrique R, Ribeiro FR, Barros-Silva JD, Peixoto A, Santos C, et al. Feasibility of differential diagnosis of kidney tumors by comparative genomic hybridization of fine needle aspiration biopsies. Genes Chromosomes Cancer 2010;49:935–47.
[34] Salama ME, Worsham MJ, DePeralta-Venturina M. Malignant papillary renal tumors with extensive clear cell change: a molecular analysis by microsatellite

analysis and fluorescence in situ hybridization. Arch Pathol Lab Med 2003;127:1176–81.
[35] Haudebourg J, Hoch B, Fabas T, Cardot-Leccia N, Burel-Vandenbos F, Vieillefond A, et al. Strength of molecular cytogenetic analyses for adjusting the diagnosis of renal cell carcinomas with both clear cells and papillary features: a study of three cases. Virchows Archiv : An International Journal of Pathology. 2010;457:397–404.
[36] Alaghehbandan R, Ulamec M, Martinek P, Pivovarcikova K, Michalova K, Skenderi F, et al. Papillary pattern in clear cell renal cell carcinoma: Clinicopathologic, morphologic, immunohistochemical and molecular genetic analysis of 23 cases. Ann Diagn Pathol 2019;38:80–6.
[37] Ruiz-Sauri A, Garcia-Bustos V, Granero E, Cuesta S, Sales MA, Marcos V, et al. Distribution of vascular patterns in different subtypes of renal cell carcinoma. A morphometric study in two distinct types of blood vessels. Pathology Oncology Research : POR 2018;24:515–24.
[38] Gonzalez ML, Alaghehbandan R, Pivovarcikova K, Michalova K, Rogala J, Martinek P, et al. Reactivity of CK7 across the spectrum of renal cell carcinomas with clear cells. Histopathology. 2019;74:608–17.
[39] Inamura K. Translocation renal cell carcinoma: an update on clinicopathological and molecular features. Cancers. 2017;9.
[40] Hayes M, Peckova K, Martinek P, Hora M, Kalusova K, Straka L, et al. Molecular-genetic analysis is essential for accurate classification of renal carcinoma resembling Xp112 translocation carcinoma. Virchows Archiv : an international journal of pathology 2015;466:313–322.
[41] Martignoni G, Gobbo S, Camparo P, Brunelli M, Munari E, Segala D, et al. Differential expression of cathepsin K in neoplasms harboring TFE3 gene fusions. Modern Pathology : An Official Journal of the United States and Canadian Academy of Pathology, Inc 2011;24:1313–9.
[42] Argani P, Zhong M, Reuter VE, Fallon JT, Epstein JI, Netto GJ, et al. TFE3-fusion variant analysis defines specific clinicopathologic associations among Xp11 translocation cancers. Am J Surg Pathol 2016;40:723–37.
[43] Lefevre M, Couturier J, Sibony M, Bazille C, Boyer K, Callard P, et al. Adult papillary renal tumor with oncocytic cells: clinicopathologic, immunohistochemical, and cytogenetic features of 10 cases. Am J Surg Pathol 2005;29:1576–81.
[44] Hes O, Brunelli M, Michal M, Cossu Rocca P, Hora M, Chilosi M, et al. Oncocytic papillary renal cell carcinoma: a clinicopathologic, immunohistochemical, ultrastructural, and interphase cytogenetic study of 12 cases. Ann Diagn Pathol 2006;10:133–9.
[45] Michalova K, Steiner P, Alaghehbandan R, Trpkov K, Martinek P, Grossmann P, et al. Papillary renal cell carcinoma with cytologic and molecular genetic features overlapping with renal oncocytoma: analysis of 10 cases. Ann Diagn Pathol 2018;35:1–6.
[46] Chen YB, Brannon AR, Toubaji A, Dudas ME, Won HH, Al-Ahmadie HA, et al. Hereditary leiomyomatosis and renal cell carcinoma syndrome-associated renal cancer: recognition of the syndrome by pathologic features and the utility of detecting aberrant succination by immunohistochemistry. Am J Surg Pathol 2014;38:627–37.
[47] Muller M, Guillaud-Bataille M, Salleron J, Genestie C, Deveaux S, Slama A, et al. Pattern multiplicity and fumarate hydratase (FH)/S-(2-succino)-cysteine (2SC) staining but not eosinophilic nucleoli with perinucleolar halos differentiate hereditary leiomyomatosis and renal cell carcinoma-associated renal cell carcinomas from kidney tumors without FH gene alteration. Modern Pathology : An Official Journal of the United States and Canadian Academy of Pathology, Inc. 2018;31:974–83.

3.4 Small cell variant of chromophobe renal cell carcinoma: Clinicopathologic and molecular-genetic analysis of 10 cases.

Solid-alveolar architecture is most typically present in classic or eosinophilic ChRCC. Less common morphologic variants include: adenomatoid-pigmented ChRCC, ChRCC with neuroendocrine differentiation (or with neuroendocrine-like differentiation), oncocytic ChRCC, multicystic ChRCC, and ChRCC with papillary architecture. In this study we assessed clinicopathologic, morphologic, immunohistochemical, and molecular features of ChRCC containing considerable amount of small cells.

Tumour including criteria were 10% cut-off for the small-cell component and absence of true neuroendocrine differentiation (which was confirmed by the negative immunohistochemical staining for synaptophysin, chromogranin, and CD56). The patients' age ranged from 40 to 78 years, with five males and five females. Stage of disease ranged from pT1a to pT3a. Follow up was available in nine cases, ranging from 24 to 73 months. Eight patients were reported with no disease progression. One patient was diagnosed with concurrent pancreatic carcinoma at stage pT3a and died due to widespread metastatic disease following surgery and treatment. Tumour size ranged from 2.2 cm to 11 cm in the greatest dimension. All tumours were well demarcated and non-encapsulated. By microscopy, extent of small-cell component ranged from 10% to 80% of the tumour volume and it was characterised by cells with scant cytoplasm, round to oval, frequently overlapping nuclei with non-conspicuous nucleoli. Small cell component was arranged in nested, tubular, or palisaded pattern. In most cases, the distribution of small cell component was multifocal with a gradual transition from classic ChRCC to the small cell area, with an exception to one case, where the transition was abrupt. None of the cases showed sarcomatoid transformation or necrosis. Immunohistochemically, CK7 showed similar staining pattern in both - classic and small cell component, however in one case it was more extensive in classic comparing to small cell component. CD117 showed analogous results with an exception to aforementioned case where staining was limited to classic ChRCC component only. Five cases were suitable for NGS. Mutations of 13 genes were found (*DICER1, FGFR3, JAK3, SUFO, FAM46C, FANCG, MET, PLCG2, APC, POLE, EPICAM, MUTYH,* and *AR)*. However, only the *PLCG2* mutation was listed as pathogenic. No mutations of *FLCN, VHL, SDH, TSC1, TSC2*, and *MTOR* were documented. Seven cases were suitable for *TERT* hot spot analysis. Two tumours carried *TERT* mutation in position 228 (chr5:1295228 C>T).

Awareness of this rare variant of ChRCC is important, particularly when assessing limited material where small cell morphology rise possibility of highly aggressive cancers. Generous sampling to find classic morphology of ChRCC, as well as excluding neuroendocrine nature by immunohistochemistry, may help resolve difficult cases.

Small cell variant of chromophobe renal cell carcinoma: Clinicopathologic and molecular-genetic analysis of 10 cases

Joanna Rogala[1,2], Fumiyoshi Kojima[3], Reza Alaghehbandan[4], Nikola Ptakova[5], Ana Bravc[6], Stela Bulimbasic[7], Delia M. Perez Montiel[8], Maryna Slisarenko[1,9], Leila Ali[10], Levente Kuthi[11], Kristýna Pivovarčíková[1], Květoslava Michalová[1], Boris Bartovic[12], Adriena Bartos Vesela[13], Olga Dolejsova[13], Michal Michal[1], Ondrej Hes[1*]

ABSTRACT

The morphologic diversity of chromophobe renal cell carcinoma (ChRCC) is well-known. Aside from typical morphology, pigmented adenomatoid, multicystic, and papillary patterns have been described. Ten cases of CHRCC composed of small-cell population in various percentages were analyzed, using morphologic parameters, immunohistochemistry, and next-generation sequencing testing. Patients were five males and five females, with age ranging from 40 to 78 years. The size of tumors ranged from 2.2 cm to 11 cm (mean 5.17 cm). Small-cell component comprised 10 to 80% of the tumor volume, while the remaining was formed by cells with classic ChRCC morphology. The immunohistochemical profile of the small-cell component was consistent with typical ChRCC immunophenotype, with CD117 and CK7 positivity. Neuroendocrine markers were negative. Mutations of 13 genes were found: *DCIER1, FGFR3, JAK3, SUFO, FAM46C, FANCG, MET, PLCG2, APC, POLE, EPICAM, MUTYH*, and *AR*. However, only the *PLCG2* mutation is considered pathogenic. The small-cell variant of ChRCC further highlights and expands on existing morphologic heterogeneity spectrum. Recognition of small-cell variant of CHRCC is not problematic in tumors, where the "classic" CHRCC component is present. However, in limited material (i.e., core biopsy), this may present a diagnostic challenge. Based on the limited follow-up data available, it appears that the small-cell tumor component had no impact on prognosis, since there was no aggressive behavior documented. Awareness of this unusual pattern and applying additional sections to find classic morphology of ChRCC, as well as excluding neuroendocrine nature by immunohistochemistry, may help resolve difficult cases.

KEYWORDS: Kidney; chromophobe renal cell carcinoma; small-cell variant

[1]Department of Pathology, Charles University in Prague, Faculty of Medicine in Plzeň, Pilsen, Czech Republic, [2]Department of Pathology "Hist-Med," Regional Specialized Hospital, Wroclaw, Poland, [3]Department of Human Pathology, Wakayama Medical University, Wakayama, Japan, [4]Department of Pathology, Faculty of Medicine, University of British Columbia, Royal Columbian Hospital, Vancouver, Canada, [5]Department of Biology and Medical Genetics, 2nd Faculty of Medicine, Charles University in Prague and Motol University Hospital, Prague, Czech Republic, [6]Department of Pathology, General Hospital, Slovenj Gradec, Slovenia, [7]Department of Pathology, University Hospital Centre Zagreb, Zagreb, Croatia, [8]Department of Pathology, Institute Nacional de Cancerologia, Mexico City, Mexico, [9]Department of Pathology, CSD Laboratory, Kiev, Ukraine, [10]Department of Pathology, "Carol Davila" University of Medicine and Pharmacy, Bucharest, Romania, [11]Department of Pathology, University of Szeged, Szeged, Hungary, [12]Departmnet of Pathology, Cytopathos, Bratislava, Slovakia, [13]Department of Urology, Charles University in Prague, Faculty of Medicine in Plzeň, Pilsen, Czech Republic

*Corresponding author: Ondrej Hes, Department of Pathology, Charles University, Medical Faculty and Charles University Hospital Plzen, Alej Svobody 80, 304 60 Pilsen, Czech Republic. E-mail: hes@biopticka.cz;

DOI: https://doi.org/10.17305/bjbms.2021.6935

Submitted: 11 January 2022/Accepted: 31 January 2021/ Published online: 10 March 2022

Conflicts of interest: The authors declare no conflicts of interest.

Funding: This study was supported by the Charles University Research Fund (project number Q39), by the grant of Ministry of Health of the Czech republic-Conceptual Development of Research Organization (Faculty Hospital in Plzen-FNPl 00669806), Czech Republic.

INTRODUCTION

Several morphologic variations of chromophobe renal cell carcinoma (ChRCC) have been reported since Thoenes and Storkel [1,2] first described it. Cases with morphology that differs from the typical solid-alveolar architecture seen in classic or eosinophilic ChRCC have been well-documented in the literature, including adenomatoid pigmented ChRCC, ChRCC with neuroendocrine differentiation (or with neuroendocrine-like differentiation), oncocytic ChRCC, multicystic ChRCC, and ChRCC with papillary architecture [3-9].

The small-cell variant of renal oncocytoma (RO) is a well-defined morphologic subtype of a common renal tumor [10-12]. In addition, ChRCC and RO are thought to be closely related tumors derived from the intercalated cells. However, small-cell variant of ChRCC has not been described. We selected a group of ChRCCs with a small-cell component forming from 10 to 80% of the tumor volume. Clinicopathologic, morphologic, immunohistochemical, and molecular genetic analysis of 10 cases were performed.

MATERIALS AND METHODS

The database of Tumor Registry in Plzen was searched for keywords: Kidney; oncocytoma; and chromophobe. A total number of 2067 tumors were retrieved. All ChRCCs with

"classic" morphology, as well as the eosinophilic variants, were excluded. Since no case from the RO cohort was reclassified as a small-cell variant of ChRCC, all ROs were excluded. All ChRCC with so-called variant histology were re-evaluated. We particularly focused on cases with true neuroendocrine differentiation, which were excluded after the initial immunohistochemical staining for synaptophysin, chromogranin, and CD56 (see later for details). Three cases with strong focal CD56 positivity in the small-cell tumor component were also eliminated from the study. Out of 1092 ChRCC and 975 RO cases from the Plzen Tumor Registry, 13 cases were found to be suitable. For the final selection, a 10% cutoff for the small-cell component was applied. Ultimately, 10 cases were enrolled in the study. Each participating institution provided clinical data and follow-up information. None of the cases included in the study had ever been reported before. Tissues for microscopic examination were formalin fixed and paraffin embedded using standard procedure. Two to 4 μm thick sections were cut and stained for hematoxylin and eosin. For each case, 1-13 paraffin blocks were available. All of the tumors were independently reviewed by three pathologists (JR, FK, and OH).

Immunohistochemistry

The immunohistochemical study was performed using a Ventana Benchmark XT automated immunostainer (Ventana Medical System, Inc., Tucson, AZ, USA) on formalin-fixed paraffin-embedded (FFPE) tissue. The primary antibodies used were as follows: CK7 (OV-TL12/30, monoclonal, DakoCytomation, Glostrup, Denmark, 1:200), cytokeratin 20 (M7019, monoclonal; Dako; 1:100), vimentin (D9, monoclonal, NeoMarkers, Westinghouse, CA, 1:1000), CD56 (1B6, monoclonal, Leica Biosystems, Newcastle, UK, 1:100), synaptophysin (polyclonal, LabVision, Fremont, CA, 1:350), chromogranin A (monoclonal, DAK-A3, DakoCytomation, 1:600), c-kit (CD117, polyclonal, DakoCytomation, 1:300), TTF1 (monoclonal, SPT24, Ventana, 1:400), GATA3 (monoclonal, L50-823, Biocare Medical, Concord, CA, 1:100), NKX3.1 (polyclonal, Biocare Medical, 1:50), FLI 1 (monoclonal, MRQ-1, Cell Marque, Rocklin, CA, 1:50), CD99 (monoclonal, HO36-1.1, Neo Markers, Rockford, IL, 1:200), WT1 (monoclonal, 6F-H2, DAKO, 1:50), and napsin (polyclonal, Ventana, RTU), Ki-67 (monoclonal, MIB-1, DAKO, 1:400). The primary antibodies were visualized using a supersensitive streptavidin-biotin-peroxidase complex (BioGenex). Internal biotin was blocked by the standard protocol used by Ventana Benchmark XT Automated Stainer (hydrogen peroxide based).

Appropriate positive and negative controls were employed. The slides were evaluated as follows: (–) Negative; (±) <10% positive cells; (+) 10-25% positive cells; (++) >25-50% positive cells; (+++) >50-75% positive cells; and (++++) >75% of positive cells.

Molecular genetic methods

Mutation analysis was performed using the TruSight Oncology 500 assay (Illumina, San Diego, CA). Total nucleic acid was extracted using the FFPE DNA kit (automated on RSC 48 Instrument, Promega, Madison, Wisconsin, USA). Purified DNA was quantified using the Qubit Broad Range DNA. The quality of DNA was assessed using the FFPE QC kit (Illumina), and DNA samples having Cq<5 were used for further analysis. After the DNA enzymatic fragmentation with KAPA Frag Kit (KAPA Biosystems, Washington, MA), DNA libraries were generated using the TruSight Oncology 500 assay (Illumina), according to the manufacturer's protocol.

Sequencing was performed using the NextSeq 550 sequencer (Illumina) following the manufacturer's guidelines. Data analysis (DNA variant filtering and annotation) was performed using the Omnomics Next-generation sequencing (NGS) analysis software (Euformatics, Finland). The custom variant filter was set up including only non-synonymous variants with coding consequences, read depth greater than 50. Benign variants according to the ClinVar database were excluded as well [13]. The remaining subset of variants was examined visually, and any apparent artefactual variants were excluded.

Ethical statement

The study was performed in accordance with the Declaration of Helsinki. Ethics committee approval was not required by Charles University and University Hospital Plzen.

RESULTS

Table 1 summarizes the basic clinicopathologic data. The patients ranged in age from 40 to 78 years old (median 58.5 years; mean 58.5 years), with five males and five females. According to UICC 2017, four patients presented with pT1a stage, one with pT1b, one with pT2a, one with pT2b, and three with pT3a. Follow-up was provided in nine cases, ranging from 24 to 73 months (mean 50.75 months; median 48 months). Eight of the patients were alive with no evidence of disease progression. One patient was diagnosed with concurrent pancreatic carcinoma at stage pT3a and died due to widespread metastatic disease following surgery and treatment.

Tumor size spanned from 2.2 cm to 11 cm in the greatest dimension (mean 5.17 cm). Macroscopically, all lesions were well-demarcated and non-capsulated. On cut section, the tumorous parenchyma was orange-yellow to brownish in color, homogeneous, with no grossly visible necrosis. Morphologic features of the tumors are summarized in Table 2.

Microscopically, all cases had "classic chromophobe" morphology, at least focally. The extent of small-cell component ranged from 10% to 80% of the tumor volume. The distribution

of the small-cell component was multifocal with a gradual transition from classic ChRCC to the small cell area (Figures 1 and 2). In one case (case 2), both components were sharply demarcated (Figure 3). The architecture in a majority of the cases was predominantly solid (Figure 4), with small foci, nested, tubular, or palisaded arrangement in small-cell component and solid alveolar in a classic component.

The cells of the classic component were typical, large, with voluminous cytoplasm and raisinoid nuclei, accompanied by smaller, eosinophilic cells with perinuclear clearing and occasional nuclei with irregular contours (Figure 5). Cells in the small-cell component showed scant cytoplasm, round to oval, and frequently overlapping nuclei with non-conspicuous nucleoli (Figure 6). No nuclear grooves or coffee bean patterns were documented. There were no nuclear grooves or coffee bean patterns. In both large and small-cell components, no mitotic figures were found.

In three cases, foci of bizarre cells with large, hyperchromatic nuclei similar to those frequently observed in oncocytoma (so-called polyploid cells) were present. None of the cases showed sarcomatoid transformation or necrosis. Results of immunohistochemical examination are summarized in Table 3A, 3B. Immunohistochemically, CK 7 staining pattern in small cell areas was almost identical to the staining pattern in classic ChRCC areas (Figure 7). In one case (case 9), the classic component of ChRCC showed diffuse, mosaic positivity, whereas the small-cell component showed a focal, oncocytoma-like pattern of staining (Figure 8). On cell membranes, CD117 was mostly diffusely positive, with weak to moderate intensity in both components (Figure 9). In one case (case 9), CD117 showed positive staining in the classic ChRCC component only. In both

TABLE 1. Basic clinicopathologic data of ChRCC with small-cell morphology

Case no.	Sex	Age	Tumor size (cm)	Stage	Follow-up (months)
1	M	65	7.5×5.4×4	pT3a	DUD*
2	M	78	diam. 3.2	pT1a	24 AW
3	M	61	2.1×2.2×1.5	pT2b	70 AW
4	F	52	diam. 4.3	pT1a	36 AW
5	F	71	diam. 2.6	pT1a	36 AW
6	F	45	9×8 × 5	pT2a	73 AW
7	F	56	3.1×2.2×1.9	pT3a	48 AW
8	M	58	2.8×2.8×2.1	pT1a	48 AW
9	F	59	10×11×8	pT3a	NA
10	M	40	6×4.8×4.5	pT1b	71 AW

M: Male, F: Female, AW: Alive without evidence of disease, diam: Diameter, NA: Not available, DUD: Death of unrelated disease. *Simultaneously diagnosed with pancreatic adenocarcinoma pT3a, after surgery, and treatment patient died of metastatic pancreatic adenocarcinoma

TABLE 2. Morphologic parameters

Case no.	% of small-cell area	Architecture of small-cell component	Bizarre cells<5%	Transition between classic and small cell	Necrosis	MI
1	80	Alveolar	+	Gradual	–	0/HPF
2	80	Solid*/**	–	Abrupt	–	0/HPF
3	40	Solid*/**	–	Gradual	–	0/HPF
4	25	Solid**	–	Gradual	–	0/HPF
5	30	Solid	+	Gradual	–	0/HPF
6	20	Solid**	–	Gradual	–	0/HPF
7	20	Solid*	–	Gradual	–	0/HPF
8	30	Solid*	–	Gradual	–	0/HPF
9	20	Solid*	–	Gradual	–	0/HPF
10	10	Solid**	+	Gradual	–	0/HPF

(–) Absent; (+) present; *focal palisading<5% of the tumor, **Focal tubular pattern<5% of the tumor, MI: Mitotic index

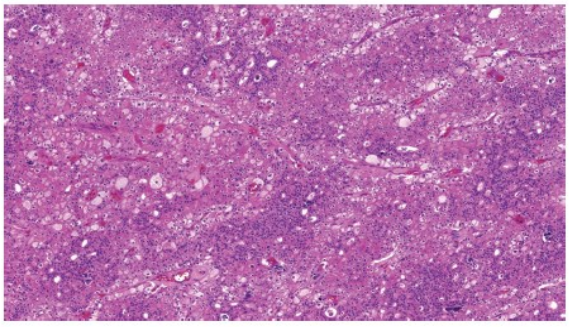

FIGURE 1. The distribution of the small-cell component was multifocal, with a gradual transition from classic ChRCC to the small-cell area in the majority of cases.

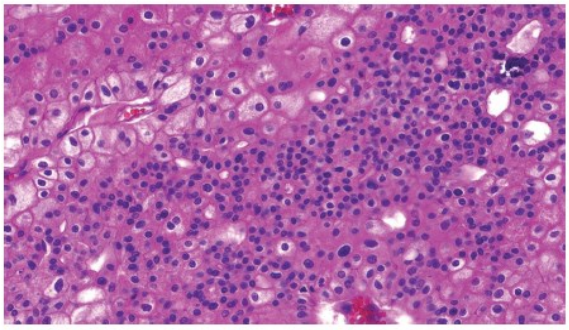

FIGURE 2. Classic chromophobe cells were intermingled among a dense population of small-cell component.

FIGURE 3. Case where the both components were sharply demarcated without transitional zone between both cell types.

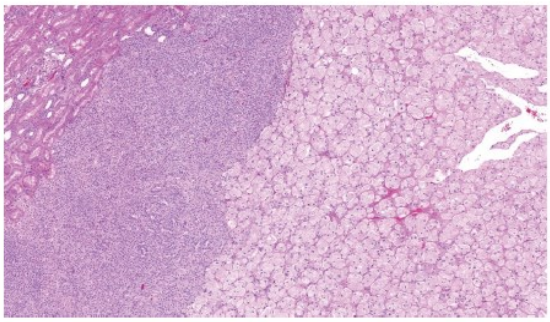

FIGURE 4. The architecture was solid in some cases.

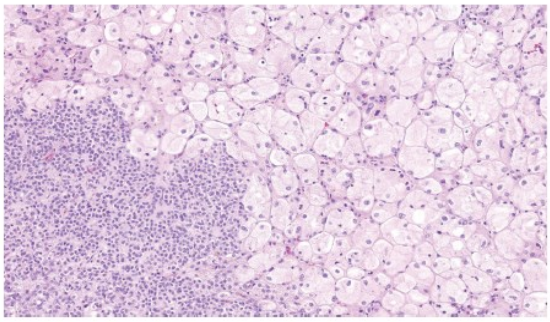

FIGURE 5. Effect of TDF and TDF-AgNPs on the prefrontal cortex pyramidal cell. The cells of classic component were typical with voluminous cytoplasm and raisinoid nuclei.

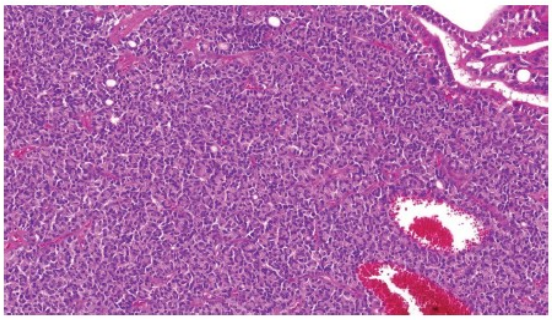

FIGURE 6. The cells in the small-cell component showed scant cytoplasm and round to oval nuclei. Mitotic activity was absent.

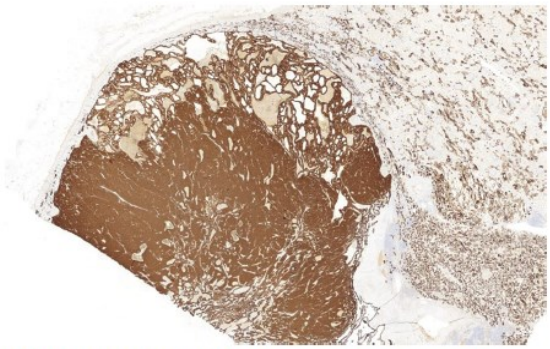

FIGURE 7. Tumors were CK7 positive in both components.

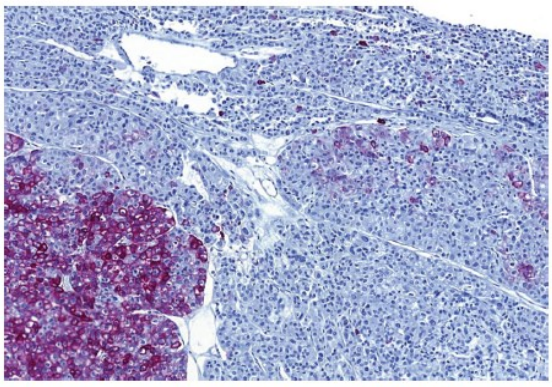

FIGURE 8. In case 9, small-cell component displayed a patchy pattern of reactivity with CK 7, superficially resembled reactivity of renal oncocytoma.

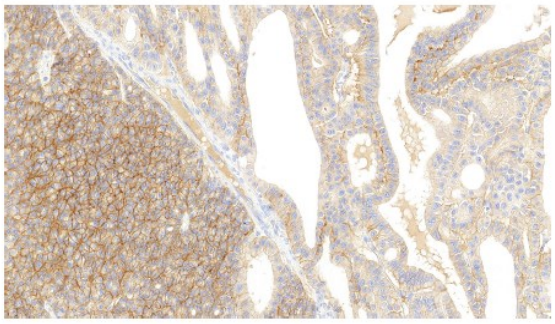

FIGURE 9. CD117 was positive in the vast majority of cases in diffuse membranous pattern.

the classic and small-cell components, all cases were negative for synaptophysin and chromogranin. CD56 expressed focal to patchy, very weak positivity in large cells of the classic component in four cases, which was considered non-specific. FLI 1 was positive in one case (case 1) in both the classic and small-cell component. CK 20, GATA3, NKX 3.1, TTF1, napsin A, WT 1, and CD99 were negative in all cases. Ki-67 positivity ranged from 2 to 20 cells per HPF in both components. NGS analysis was successful in five cases. Results are summarized in Table 4.

Mutations of 13 genes were found, namely, *DCIER1, FGFR3, JAK3, SUFO, FAM46C, FANCG, MET, PLCG2, APC, POLE, EPICAM, MUTYH,* and *AR*. However, only the *PLCG2* mutation is listed as pathogenic. No mutations of *FLCN, VHL, SDH, TSC1, TSC2*, and *MTOR* were documented. Seven cases were suitable for *TERT* hot spot analysis. Two tumors carried *TERT* mutation in position 228 (chr5:1295228 C>T).

DISCUSSION

ChRCC and RO are considered tumors derived from so-called intercalated cells of collecting ducts [14,15]. In addition to a common cell of origin, they share several morphologic

TABLE 3A. Results of immunohistochemical examination of small cell ChRCC component

Case No	Syn.	Chrom.	CD56	TTF1	Napsin A	CK7	CD117	CK20	GATA3	NKX3.1	FLI1	CD99	Vim	WT1	Ki67
1	–	–	–	–	–	+++	++++	–	–	–	++++	–#	±	–	2-10/hpf
2	–	–	–	–	–	++++	++++	–	–	–	–	–#	±	–	15-20/hpf
3	–	–	–	–	–	++++	+	–	–	–	–	–#	±	–	8-15/hpf
4	–	–	–	–	–	+++	++++	–	–	–	–	–	±	–	4-8/hpf
5	–	–	–	–	–	+++	++++	–	–	–	–	–	±	–	5-10/hpf
6	–	–	–	–	–	+/-	++++	–	–	–	–	–	±	–	1-8/hpf
7	–	–	–	–	–	++++	++++	–	–	–		–	±	–	1-4/hpf
8	–	–	–	–	–	++++	+++	–	–	–	–	–	±	–	5-10/hpf
9	–	–	–	–	–	+/-	–	–	–	–	–	–	±	–	1-10/hpf
10	–	–	–	–	–	++++	++++	–	–	–	–	–	+	–	10-15/hpf

(–) Negative, (±) less than 10% positive cells, (+) 10-25% POSITIVE cells, (++) >25-50% positive cells, (+++) >50-75% positive cells, (++++) >75% positive cells, #cytoplasmic positivity, *high background staining, difficult to interpret, hpf: High-power field, Syn: Synaptophysin, Chrom: Chromogranin, Vim: Vimentin

TABLE 3B. Results of immunohistochemical examination of classic ChRCC component

Case no.	Syn	Chrom	CD56	TTF1	Napsin A	CK7	CD117	CK20	GATA3	NKX3.1	FLI1	CD99	Vim	WT1	Ki67
1	–	–	–	–	–	+++	++++	–	–	–	++++	–#	±	–	2-10/hpf
2	–	–	–	–	–	++++	++++	–	–	–	–	–#	–	–	5-15/hpf
3	–		–*	–	–	++++	++++	–	–	–	–	–#	–	–	8-15/hpf
4	–	–	–*	–	–	++++	++++	–	–	–	–	–	–	–	2-8/hpf
5	–	–	–	–	–	++++	++++	–	–	–	–	–	±	–	5-10/hpf
6	–	–	–	–	–	+/-	++++	–	–	–	–	–	–	–	1-5/hpf
7	–	–	–*	–	–	+++	++++	–	–	–		–	±	–	1-4/hpf
8	–	–	–*	–	–	+++	+++	–	–	–	–	–	–	–	5-10/hpf
9	–	–	–	–	–	+++	+++	–	–	–	–	–	–	–	5-10/hpf
10	–	–	–*	–	–	++++	++++	–	–	–	–	–	±	–	10-15/hpf

(–) Negative, (±) less than 10% positive cells; (+) 10-25% positive cells; (++) >25-50% positive cells; (+++) >50-75% positive cells (++++) >75% positive cells; #cytoplasmic positivity, *high background staining, difficult to interpret, hpf: High-power field, Syn: Synaptophysin, Chrom: Chromogranin, Vim: Vimentin

TABLE 4. Results of next-generation sequencing

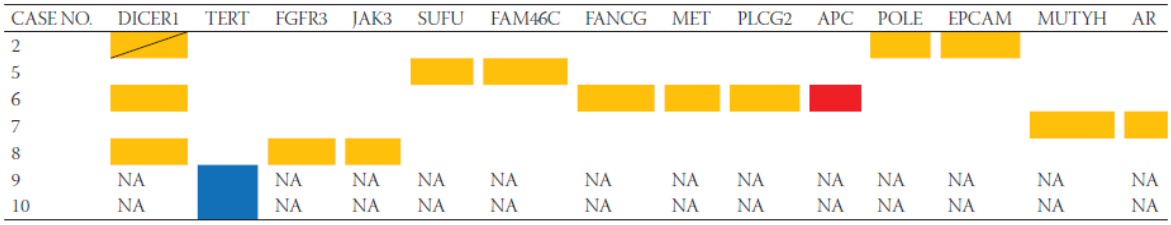

NA: not analyzible; Coding effect: missense (orange), non-sense (red), TERT (blue).

features. Both tumor types are usually located within the renal cortex, both well-circumscribed, yet non-encapsulated. In the gross section, both RO and ChRCC are predominantly brown, sometimes with a scar that is centrally located in RO. However, the central scar is not specific for RO and might be found in other renal tumors as well. Histologically, both tumors are composed of oncocytic cells, although the morphologic details and immunohistochemical features may differ. Because of these similarities, several researchers hypothesized that RO might be a potential "chromophobe adenoma" that could progress to ChRCC [16-18] in a manner similar to the adenoma-adenocarcinoma sequence in the colorectal cancer [19]. However, other authors, including the authors of this study disagree [20].

The small-cell variant of RO was first described in 2001 [10,21], although the existence of small oncocytic cells, so-called oncoblasts, was documented and discussed much earlier [22]. Several papers published afterward [11,23,24] further defined the small cell variant of RO.

ChRCC, in its classic form, is described as a solid-alveolar tumor composed of large leaf-like cells and smaller oncocytic cells. Several morphologic variants, which differed from classic morphology, were subsequently described in the literature. As the name indicates, the architecture of the adenomatoid microcystic pigmented variant comprises microcystic, cribriform areas mixed with conventional ChRCC pattern. Adenomatous structures lined by small cylindrical cells with basally located nuclei constitute a second component [4].

Multicystic ChRCC is composed either of variable-sized cysts or compressed cysts and tubules with slit-like spaces. The cellular lining is made up entirely of eosinophilic cells or a mixed population of eosinophilic and pale cells. It is likely that the two aforementioned variants represent a spectrum of one morphologic subtype in which the adenomatoid pattern progressively transforms to areas with microcystic architecture. Lipochrome pigment accumulation is constantly present in the former, whereas it was noted in <50% of cases in the latter group of tumors [8]. Within the ChRCC spectrum, ChRCC with papillary architecture is quite rare. However, it has been described in the literature [25]. Such a pattern was present focally. The cytologic features, on the other hand, followed a characteristic dual population of leaf-like and small eosinophilic cells. Foam cells were not present. Recently, series of CHRCC with prominent papillary architecture has been published [9]. The extent of papillary component in tumors ranged from 15 to 100% of the tumor volume. The cytologic characteristics were typical.

ChRCC with morphology similar to neuroendocrine tumors, namely, with trabecular/palisading/cribriform pattern was also documented. Among them were the CHRCC with true neuroendocrine differentiation, confirmed by positive staining for synaptophysin, chromogranin or CD 56 [5,7].

Tumors that showed similar architecture and cytologic features, but without positive neuroendocrine immunohistochemical staining were labeled as ChRCC with neuroendocrine-like features [7].

ChRCC with neuroendocrine differentiation and neuroendocrine-like features can be remarkably similar to the small cell variant of ChRCC. To rule out cases with true neuroendocrine differentiation, we employed three different neuroendocrine markers (synaptophysin, chromogranin, and CD56).

In the present study, the small-cell tumor population was uniform, showing mostly scant cytoplasm, arranged predominantly in solid, relatively compact areas or sheets. Only focal palisading or tubular structures were seen. Such patterns were located in transition zones between small-cell and classic ChRCC components, always comprising <5% of the small-cell component volume.

There is another parallel between the small cell oncocytoma and the small-cell variant of ChRCC. In ChRCC with an adenomatoid pattern, groups of small cells are located on the edges of adenomatoid structures or on the edges of fibrotic, scar-like foci. A similar phenomenon has been well-documented in a small cell variant of RO [11]. In classic RO, however, groups of small oncocytes are frequently found in identical location. Pseudorosettes or ribbon-like patterns were not seen in the small-cell ChRCC variant. The presence of such structures is an interesting phenomenon in the context of differential diagnosis. In a series of small-cell variants of RO [11], pseudorosettes with a PAS-positive central core were described. However, we do not believe such structures can be used as a differential diagnostic feature.

Immunohistochemical profiles of our cases were compatible with the classic variant of ChRCC, mostly showing strong, diffuse, or focal positivity for CK 7, along with diffuse or focal, weak to moderate positivity for CD117 in both tumor components. However, one case (case 9) was exceptional: The small-cell component expressed an oncocytoma-like CK7 staining pattern with diffuse, mosaic positivity in the classic part, whereas CD117 was positive solely in the classic part.

Focal weak positivity for CD56 was considered non-specific, and other neuroendocrine markers were negative. Interestingly, there was a strong positive immunohistochemical reaction for FLI1, which was present in both components in case 1. Unfortunately, the case was not suitable for molecular genetic analysis due to the low quality of DNA/RNA, but the morphology supported the diagnosis of ChRCC.

In cases with overlapping features between ChRCC, as well as cases with worrisome clinical features, association with the syndromic disease should be considered. According to clinical reports, we have no evidence of syndromic disease within our cohort. Furthermore, NGS was used to screen molecular profiles of our cases. Only five tumors were suitable for a complete NGS analysis. We were unable to document any genetic alteration linked to syndromic diseases. *FLCN*, *VHL*, and/or *SDH* gene mutations were not detected. The significance of the only pathogenic mutation of *PLCG2* gene found in our cohort remains unclear.

Renal tumors with mTOR pathway abnormalities were documented recently. Some of these newly recognized subtypes are characterized by an eosinophilic/oncocytic or chromophobe-like morphology [26]. Among them are eosinophilic solid and cystic RCC (ESC RCC), eosinophilic vacuolated tumor (EVT), and a low-grade oncocytic tumor, which can have eosinophilic/oncocytic or chromophobe-like morphology. Therefore, these tumors should be considered in the differential diagnosis of small-cell ChRCC variant. There were no morphologic features of the above-mentioned entities in our cases, and no mutations in the mTOR pathway genes were detected. However, one of our cases showed overlapping immunophenotype with EVT with positivity for CD117 and CK7 negative/focally positive.

The grading and biological behavior of ChRCC is notoriously inconsistent. Fuhrmans' grading system, classic ISUP/WHO modification of Fuhrmans' system [12], and even grading system proposed by Paner *et al.* are all practically not applicable [27,28]. Sarcomatoid transformation and/or necrosis

were the only morphologic factors significantly associated with poor prognosis in a multi-institutional study recently published by Ohashi *et al.* [29]. There was no necrosis or sarcomatoid change in any of our cases. Based on the limited available follow-up data, it is difficult to speculate about the potential impact of the presence of the small-cell tumor component on prognosis. In no case was the aggressive behavior documented. However, the follow-up period is relatively short, with a median of 48 months.

Several neoplastic entities should be considered in differential diagnosis, especially with limited material in core biopsy, where the diagnosis may be challenging compared to the more straightforward diagnostic process in resections.

In differential diagnosis, the presence of small-cell differentiation, tubular or palisading pattern, raises the question of potential neuroendocrine differentiation (either primary or metastatic).

Primary neuroendocrine tumors of the kidney are exceedingly rare. According to the WHO classification (2016), they are subdivided into two groups: (I) Well-differentiated neuroendocrine tumor (carcinoid and atypical carcinoid) and (II) poorly differentiated neuroendocrine carcinoma including small-cell and large cell variants [12]. Morphologically, carcinoids display similar features as their counterparts in other anatomical sites. Their neuroendocrine nature is confirmed by immunohistochemistry with positive staining for neuroendocrine markers.

Ewing sarcoma/peripheral neuroendocrine tumor (PNET) must be considered in cases composed of small, round, densely packed blue cells, especially on limited material and in a young patient. PNET shows features of a highly malignant neoplasm, with numerous mitotic figures and necrosis. PNET is characterized by diffuse positivity for vimentin, CD99, and FLI-1 in immunohistochemistry. In certain cases, neuroendocrine markers may be positive [30].

In none of our cases, we found mitoses. However, in case 2, PNET was a differential diagnosis on core biopsy. On a final resection specimen, 80% of the tumor was composed of a small-cell component with PNET-like morphology, solid architecture, and densely packed cells with oval, overlapping nuclei, as well as areas with typical ChRCC morphology, haphazardly present throughout the tumor mass.

Immunohistochemical examination revealed negative staining with vimentin (typical pattern characteristic for oncocytoma), whereas FLI 1 and CD99 were negative. The morphologic characteristics of cases positive for CD99 or FLI-1 were distinct from PNET, and staining was interpreted as non-specific. None of the analyzable cases showed mutation/translocation in the EWSR gene. However, cases with non-specific FLI-1 and CD99 staining were not analyzable by NGS.

Wilms tumor (WT), blastemal-rich variant, is another example of a tumor within the spectrum of small round blue cell renal tumors. Blastema-rich WT is composed of primitive cells with sticking, highly malignant morphology showing diffuse immunoreactivity for vimentin and WT1 [12]. None of our cases showed neither such morphology nor positive staining for WT1 and/or vimentin.

The tendency of urothelial carcinoma (UC) to mimic primary renal cell carcinomas, particularly in high-grade forms, is well-known. In this regard, a macroscopic examination can give many clues for differential diagnosis. In UC, renal pelvis involvement and infiltrative growth pattern with desmoplastic response are common, whereas in ChRCC, pushing border and expansile growth pattern are more common. The infiltrative growth pattern was not reported in our study. In addition, the immunohistochemical profile of our cases differed from that of typical UC.

The final situation in differential diagnosis that should be considered is that sarcomatoid differentiation within ChRCC is relatively common. Some authors suggest that sarcomatoid dedifferentiation is more prevalent in ChRCC than in any other RCC subtype [31]. The great majority of the sarcomatoid component, on the other hand, is present in the form of a high-grade, spindle-cell, mesenchymal-looking neoplastic cell population. Necrosis is common and mitotic activity is usually brisk [32].

We were not able to identify any spindling or conspicuous mitotic figures within small cell areas, as well as necrosis. Our cases also lacked the infiltrative pattern of small cells, which would be expected in sarcomatoid dedifferentiation. The architecture and cytology of small-cell component were clearly epithelial and monotonous. All of the aforementioned characteristics argue against sarcomatoid differentiation.

CONCLUSION

We herein present a group of 10 ChRCCs with a small-cell component that constitutes up to 80% of the tumor volume. Awareness of this unusual pattern and applying additional sections to find classic morphology of ChRCC, as well as excluding neuroendocrine nature by immunohistochemistry, may help resolve difficult cases.

However, a small-cell morphology does not present major diagnostic problem in resected tumors, on limited material, namely, as a core biopsy such morphology may create diagnostic challenge.

REFERENCES

[1] Thoenes W, Storkel S, Rumpelt HJ. Human chromophobe cell renal carcinoma. Virchows Archiv B Cell Pathol Incl Mol Pathol

1985;48(3):207-17.
https://doi.org/10.1007/BF02890129
[2] Thoenes W, Storkel S, Rumpelt HJ, Moll R, Baum HP, Werner S. Chromophobe cell renal carcinoma and its variants--a report on 32 cases. J Pathol 1988;155(4):277-87.
https://doi.org/10.1002/path.1711550402
[3] Michal M, Hes O, Svec A, Ludvikova M. Pigmented microcystic chromophobe cell carcinoma: A unique variant of renal cell carcinoma. Ann Diagn Pathol 1998;2(3):149-53.
https://doi.org/10.1016/s1092-9134(98)80001-4
[4] Hes O, Vanecek T, Perez-Montiel DM, Cabrero IA, Hora M, Suster S, et al. Chromophobe renal cell carcinoma with microcystic and adenomatous arrangement and pigmentation--a diagnostic pitfall. Morphological, immunohistochemical, ultrastructural and molecular genetic report of 20 cases. Virchows Arch 2005;446(4):383-93.
https://doi.org/10.1007/s00428-004-1187-x
[5] Kuroda N, Tamura M, Hes O, Michal M, Gatalica Z. Chromophobe renal cell carcinoma with neuroendocrine differentiation and sarcomatoid change. Pathol Int 2011;61(9):552-4.
https://doi.org/10.1111/j.1440-1827.2011.02689.x
[6] Kuroda N, Tanaka A, Yamaguchi T, Kasahara K, Naruse K, Yamada Y, et al. Chromophobe renal cell carcinoma, oncocytic variant: A proposal of a new variant giving a critical diagnostic pitfall in diagnosing renal oncocytic tumors. Med Mol Morphol 2013;46(1):49-55.
https://doi.org/10.1007/s00795-012-0007-7
[7] Peckova K, Martinek P, Ohe C, Kuroda N, Bulimbasic S, Mundo EC, et al. Chromophobe renal cell carcinoma with neuroendocrine and neuroendocrine-like features. Morphologic, immunohistochemical, ultrastructural, and array comparative genomic hybridization analysis of 18 cases and review of the literature. Ann Diagn Pathol 2015;19(4):261-8.
https://doi.org/10.1016/j.anndiagpath.2015.05.001
[8] Foix MP, Dunatov A, Martinek P, Mundo EC, Suster S, Sperga M, et al. Morphological, immunohistochemical, and chromosomal analysis of multicystic chromophobe renal cell carcinoma, an architecturally unusual challenging variant. Virchows Arch 2016;469(6):669-78.
https://doi.org/10.1007/s00428-016-2022-x
[9] Michalova K, Tretiakova M, Pivovarcikova K, Alaghehbandan R, Montiel DP, Ulamec M, et al. Expanding the morphologic spectrum of chromophobe renal cell carcinoma: A study of 8 cases with papillary architecture. Ann Diagn Pathol 2020;44:151448.
https://doi.org/10.1016/j.anndiagpath.2019.151448
[10] Hes O, Michal M, Boudova L, Mukensnabl P, Kinkor Z, Miculka P. Small cell variant of renal oncocytoma--a rare and misleading type of benign renal tumor. Int J Surg Pathol 2001;9(3):215-22.
https://doi.org/10.1177/106689690100900307
[11] Petersson F, Sima R, Grossmann P, Michal M, Kuroda N, Hora M, et al. Renal small cell oncocytoma with pseudorosettes A histomorphologic, immunohistochemical, and molecular genetic study of 10 cases. Hum Pathol 2011;42(11):1751-60.
https://doi.org/10.1016/j.humpath.2011.01.022
[12] Moch H, Humphrey PA, Ulbright TM, Reuter VE, editors. WHO Classification of Tumours of the Urinary System and Male Genital Organs. 4th ed. Lyon: IARC; 2016.
[13] Landrum MJ, Lee JM, Benson M, Brown GR, Chao C, Chitipiralla S, et al. ClinVar: Improving access to variant interpretations and supporting evidence. Nucleic Acids Res 2018;46(D1):D1062-D7.
https://doi.org/10.1093/nar/gkx1153
[14] Storkel S, Pannen B, Thoenes W, Steart PV, Wagner S, Drenckhahn D. Intercalated cells as a probable source for the development of renal oncocytoma. Virchows Arch B Cell Pathol Incl Mol Pathol 1988;56(3):185-9.
https://doi.org/10.1007/BF02890016
[15] Storkel S, Steart PV, Drenckhahn D, Thoenes W. The human chromophobe cell renal carcinoma: Its probable relation to intercalated cells of the collecting duct. Virchows Arch B Cell Pathol Incl Mol Pathol 1989;56(4):237-45.
https://doi.org/10.1007/BF02890022
[16] Dijkhuizen T, van den Berg E, Storkel S, de Vries B, van der Veen AY, Wilbrink M, et al. Renal oncocytoma with t(5;12;11), der(1)1;8) and add(19): "True" oncocytoma or chromophobe adenoma? Int J Cancer J Int Cancer 1997;73(4):521-4.
https://doi.org/10.1002/(sici)1097-0215(19971114)73:43.0.co;2-c
[17] Kuroda N, Toi M, Hiroi M, Enzan H. Review of chromophobe renal cell carcinoma with focus on clinical and pathobiological aspects. Histol Histopathol 2003;18(1):165-71.
https://doi.org/10.14670/HH-18.165
[18] Al-Saleem T, Balsara BR, Liu Z, Feder M, Testa JR, Wu H, et al. Renal oncocytoma with loss of chromosomes Y and 1 evolving to papillary carcinoma in connection with gain of chromosome 7. Coincidence or progression? Cancer Genet Cytogenet 2005;163(1):81-5.
https://doi.org/10.1016/j.cancergencyto.2005.05.011
[19] Delongchamps NB, Galmiche L, Eiss D, Rouach Y, Vogt B, Timsit MO, et al. Hybrid tumour "oncocytoma-chromophobe renal cell carcinoma" of the kidney: A report of seven sporadic cases. BJU Int 2009;103(10):1381-4.
https://doi.org/10.1111/j.1464-410X.2008.08263.x
[20] Brunelli M, Eble JN, Zhang S, Martignoni G, Delahunt B, Cheng L. Eosinophilic and classic chromophobe renal cell carcinomas have similar frequent losses of multiple chromosomes from among chromosomes 1, 2, 6, 10, and 17, and this pattern of genetic abnormality is not present in renal oncocytoma. Mod Pathol 2005;18(2):161-9.
https://doi.org/10.1038/modpathol.3800286
[21] Shimazaki H, Tanaka K, Aida S, Tamai S, Seguchi K, Hayakawa M. Renal oncocytoma with intracytoplasmic lumina: A case report with ultrastructural findings of "oncoblasts". Ultrastruct Pathol 2001;25(2):153-8.
https://doi.org/10.1080/019131201750222248
[22] Eble JN, Hull MT. Morphologic features of renal oncocytoma: A light and electron microscopic study. Hum Pathol 1984;15(11):1054-61.
https://doi.org/10.1016/s0046-8177(84)80249-x
[23] Magro G, Gardiman MP, Lopes MR, Michal M. Small-cell variant of renal oncocytoma with dominating solid growth pattern: A potential diagnostic pitfall. Virchows Arch 2006;448(3):379-80.
[24] Wobker SE, Williamson SR. Modern pathologic diagnosis of renal oncocytoma. J Kidney Cancer VHL 2017;4(4):1-12.
https://doi.org/10.15586/jkcvhl.2017.96
[25] Kuroda N, Iiyama T, Moriki T, Shuin T, Enzan H. Chromophobe renal cell carcinoma with focal papillary configuration, nuclear basaloid arrangement and stromal osseous metaplasia containing fatty bone marrow element. Histopathology 2005;46(6):712-3.
[26] Trpkov K, Hes O, Williamson SR, Adeniran AJ, Agaimy A, Alaghehbandan R, et al. New developments in existing WHO entities and evolving molecular concepts: The genitourinary pathology society (GUPS) update on renal neoplasia. Mod Pathol 2021;34(7):1392-24.
https://doi.org/10.1038/s41379-021-00779-w
[27] Paner GP, Amin MB, Alvarado-Cabrero I, Young AN, Stricker HJ, Moch H, et al. A novel tumor grading scheme for chromophobe renal cell carcinoma: prognostic utility and comparison with Fuhrman nuclear grade. Am J Surg Pathol 2010;34(9):1233-40.
https://doi.org/10.1097/PAS.0b013e3181e96f2a
[28] Sperga M, Martinek P, Vanecek T, Grossmann P, Bauleth K, Perez-Montiel D, et al. Chromophobe renal cell carcinoma--chromosomal aberration variability and its relation to Paner grading system: An array CGH and FISH analysis of 37 cases. Virchows Arch 2013;463(4):563-73.
https://doi.org/10.1007/s00428-013-1457-6
[29] Ohashi R, Martignoni G, Hartmann A, Calio A, Segala D, Stohr C, et al. Multi-institutional re-evaluation of prognostic factors in chromophobe renal cell carcinoma: Proposal of a novel two-tiered grading scheme. Virchows Arch 2020;476(3):409-18.
https://doi.org/10.1007/s00428-019-02710-w
[30] Antonescu C, Blay JY, Boveé J, editors. WHO Classification of Tumours: Soft Tissue and Bone Tumours. 5th ed. Lyon: IARC; 2020.
[31] Akhtar M, Kardar H, Linjawi T, McClintock J, Ali MA.

Chromophobe cell carcinoma of the kidney. A clinicopathologic study of 21 cases. Am J Surg Pathol 1995;19(11):1245-56.
[32] Brunelli M, Gobbo S, Cossu-Rocca P, Cheng L, Hes O, Delahunt B, et al. Chromosomal gains in the sarcomatoid transformation of chromophobe renal cell carcinoma. Mod Pathol 2007;20(3):303-9. https://doi.org/10.1038/modpathol.3800739

3.5 Histologic diversity in chromophobe renal cell carcinoma does not impact survival outcome: A comparative international multi-institutional study.

Predicting outcome in patients with ChRCC is difficult as it became apparent that conventionally used tool that is WHO/ISUP grading system is not reliable in this group of RCCs. This multi-institutional study was designed to assess the possible impact of morphologic variants of CHRCC on its biologic behaviour.

Cohort included 89 cases of rare ChRCC subtypes, such as adenomatoid cystic/pigmented, multicystic, neuroendocrine, papillary, small cell-like and two other rare subtypes. All cases had well documented clinical follow-up data. Additional 70 classic and eosinophilic ChRCCs were included as a control group. Variant morphology group and control group were compared by clinical and pathologic features including age, sex, tumor size, presence of tumour necrosis, and sarcomatoid differentiation. Clinical outcomes included recurrence, development of distant metastases and ChRCC related death. Results show that there were no statistically significant differences between the two groups for age at diagnosis, gender distribution, tumour size, presence of tumour necrosis, presence of sarcomatoid differentiation, and adverse outcomes. However, follow-up was slightly longer in the rare subtypes group (78.5 months) than the controls (56.1 months). In relation of tumour size, necrosis, and sarcomatoid differentiation to clinical outcome, tumour necrosis and sarcomatoid differentiation were significantly associated with poor clinical outcome in both groups (associated with metastatic disease or death). Also, tumour size was significantly increased in patients with adverse outcome in both groups.

Stage and nuclear grading are the most important prognostic factors in RCCs. However, in relation to ChRCC, WHO/ISUP nuclear grading appeared not to be applicable, as a majority of cases would be classified as high grade, predicting adverse outcome (that is in opposition to generally favourable ChRCCs outcomes). The lack of reliable prognostic factor was challenged by Paner et al. and resulted in introducing three-tiered grading scheme. Because of its given low reproducibility, this system was abandoned. Another two-grade system (based on easily reproducible features - tumour necrosis and sarcomatoid differentiation) was introduced by Ohashi et al. Even though cytologic features weren't considered, it showed to be effective in indicating ChRCCs with high risk of progression. In this study, we tried to asses and validate the aforementioned Ohashi et al. criteria on group of rare morphologic variants of ChRCC. Our findings support previous statements that both sarcomatoid differentiation and tumour necrosis were significantly associated with poor clinical outcome, and it's true for both classic/eosinophilic as well as variant pattern ChRCC. Additionally, morphologic variants seem to do not influence biologic behaviour.

Annals of Diagnostic Pathology 60 (2022) 151978

Contents lists available at ScienceDirect

Annals of Diagnostic Pathology

journal homepage: www.elsevier.com/locate/anndiagpath

Original Contribution

Histologic diversity in chromophobe renal cell carcinoma does not impact survival outcome: A comparative international multi-institutional study

Jiri Kolar [a], Andrea Feu Llaurado [b], Monika Ulamec [c], Faruk Skenderi [d], Delia Perez-Montiel [e], Isabel Alvarado-Cabrero [f], Stela Bulimbasic [g], Maris Sperga [h], Maria Tretiakova [i], Adeboye O. Osunkoya [j], Joanna Rogala [k], Eva Comperat [l], Viliam Gal [m], Ana Dunatov [n], Kristyna Pivovarcikova [k], Kvetoslava Michalova [k], Adriena Bartos Vesela [a], Maryna Slisarenko [k], Andrea Peterikova Strakova [k], Tomas Pitra [a], Milan Hora [a], Michal Michal [k], Reza Alaghehbandan [o,1], Ondrej Hes [k,*,1]

[a] Department of Urology, Charles University, Faculty of Medicine and University Hospital in Plzen, Plzen, Czech Republic
[b] Department of Pathology, Bellvitge Hospital, Barcelona, Spain
[c] Department of Pathology, Sestre milosrdnice University Hospital Center, Department of Pathology and Scientific Centre of Excellence for Reproductive and Regenerative Medicine, School of Medicine, University of Zagreb, Croatia
[d] Department of Pathology, University of Sarajevo, Faculty of Health Sciences, Sarajevo, Bosnia and Herzegovina
[e] Department of Pathology, Institute Nacional de Cancerologia, Mexico City, Mexico
[f] Department of Pathology, Centro Medico, Mexico City, Mexico
[g] Department of Pathology, University Hospital Zagreb, Croatia
[h] Department of Pathology, Stradin's University, Riga, Latvia
[i] Department of Laboratory Medicine and Pathology, University of Washington, Seattle, WA, USA
[j] Departments of Pathology and Urology, Emory University School of Medicine, Atlanta, GA, USA
[k] Department of Pathology, Charles University, Faculty of Medicine and University Hospital in Plzen, Plzen, Czech Republic
[l] Department of Pathology, University of Vienna, Vienna, Austria
[m] Department of Pathology, Alpha Medical Pathologia, Bratislava, Slovakia
[n] Department of Pathology, University of Split, Croatia
[o] Department of Pathology, Faculty of Medicine, University of British Columbia, Royal Columbian Hospital, Vancouver, BC, Canada

ARTICLE INFO

Keywords:
Kidney
Chromophobe renal cell carcinoma
Grading
Subtypes
Survival
Outcome

ABSTRACT

Predicting the clinical behavior and trajectory of chromophobe renal cell carcinoma (ChRCC) by histologic features has so far proven to be challenging. It is known that ChRCC represents a heterogeneous group of neoplasms demonstrating variable, yet distinctive morphologic and genetic profiles. In this international multi-institutional study, we aimed to assess the impact of histologic diversity in ChRCC (classic/eosinophilic versus rare subtypes) on survival outcome.

This is an international multi-institutional matched case-control study including 14 institutions, examining the impact of histologic subtypes of ChRCC on survival outcome. The study group (cases) included 89 rare subtypes of ChRCC. The control group consisted of 70 cases of ChRCC including classic and eosinophilic features, age- and tumor size-matched.

Most of the rare subtypes were adenomatoid cystic/pigmented ChRCC (66/89, 74.2%), followed by multicystic ChRCC (10/89, 11.2%), and papillary ChRCC (9/89, 10.1%). In the control group, there were 62 (88.6%) classic and 8 (11.4%) eosinophilic ChRCC. There were no statistically significant differences between the study and control groups for age at diagnosis, gender distribution, tumor size, presence of tumor necrosis, presence of sarcomatoid differentiation, and adverse outcomes. No statistically significant differences were found in clinical outcome between the rare subtypes and classic/eosinophilic groups by tumor size, necrosis, and sarcomatoid

* Corresponding author at: Department of Pathology, Charles University, Medical Faculty and Charles University Hospital Plzen, Alej Svobody 80, 304 60 Plzen, Czech Republic.
E-mail address: hes@biopticka.cz (O. Hes).
[1] Authors contributed equally.

https://doi.org/10.1016/j.anndiagpath.2022.151978

Available online 20 May 2022

differentiation. Further, no statistically significant differences were found in clinical outcome between the two groups, stratified by tumor size, necrosis, and sarcomatoid differentiation.

Our findings corroborated previous studies that both sarcomatoid differentiation and tumor necrosis were significantly associated with poor clinical outcome in classic/eosinophilic ChRCC, and this was proven to be true for ChRCC with rare histologic subtypes as well. This study suggests that rare morphologic patterns in ChRCC without other aggressive features play no role in determining the clinical behavior of the tumor.

1. Introduction

Chromophobe renal cell carcinoma (ChRCC) is the third most common renal epithelial malignancy. Predicting the clinical behavior and trajectory of ChRCC by histologic features has so far proven to be challenging. It is known that the clinical significance of conventional grading systems, such as Fuhrman nuclear grade (historical system) and the World Health Organization (WHO)/International Society of Urological Pathology (ISUP) nucleolar system, could not be demonstrated for ChRCC [1]. In contrast to clear cell RCC (CCRCC) and papillary RCC (PRCC), the WHO/ISUP grading system is not applicable to ChRCC [1,2].

Historically, evaluating risk assessment by histological grading of ChRCC has not proven successful [3-7]. One of the earlier studies conducted by Paner et al. [8] proposed a grading scheme, which ultimately did not meet clinical practice application. Subsequently, there was number of studies attempting to develop a grading system in which the clinical and prognostic behavior of ChRCC can accurately and reliably be predicted. For instance, a three-tiered grading system [8] was proposed, correlating geographic nuclear crowding and anaplasia with clinical outcome for patients with ChRCC. A subsequent study, however, found that this grading system did not provide additional prognostic information once tumor stage and sarcomatoid features were included [7]. Similarly, Ohashi et al. [3] were not able to validate the proposed three-tiered grading system or the four-tiered WHO/ISUP grading system for outcome determination in ChRCC. Instead, they proposed a two-tiered grading system, based on sarcomatoid features and necrosis, which was successful at the multivariate level. In another large study, a modified tumor grading scheme using mitotic index, cytologic eosinophilia, and architecture was not significantly associated with outcome [9]. Summarizing the current knowledge, it seems that histology alone is insufficient in predicting the behavior of ChRCC and that rather tumor size, small vessel invasion, sarcomatoid features, and microscopic necrosis affect clinical outcome in ChRCC [3-7,9,10]. It is important to note that the above proposed grading schemes/criteria are not exactly grading sensu stricto, but rather well defined adverse morphologic parameters in predicting the behavior of ChRCC.

It is known that ChRCC represents a heterogeneous group of neoplasms demonstrating variable, yet distinctive morphologic and genetic profiles. In fact, multiple studies in the last few decades have expanded our knowledge of the wide histologic spectrum of ChRCC, including adenomatoid cystic/pigmented, multicystic, neuroendocrine, small cell-like, and papillary patterns [11-20]. Nevertheless, the predictive value of ChRCC histological subtype on prognosis remains an open question.

In this international multi-institutional study, we aimed to assess the impact of histologic subtypes of ChRCC (classic/eosinophilic versus rare subtypes) on survival outcome. To the best of our knowledge, this is the first study to examine predictive value of histologic subtypes of ChRCC on prognosis.

2. Materials and methods

This is an international multi-institutional matched case-control study including 14 institutions, examining the impact of histologic diversity in ChRCC on survival outcome. Initially, 98 ChRCC with rare histologic subtypes were retrieved, of which nine cases were excluded from the study due to lack of available pertinent clinical and pathologic information.

The study group included 89 cases of rare subtypes of ChRCC such as adenomatoid cystic/pigmented (Fig. 1), multicystic (Fig. 2), neuroendocrine (Fig. 3), papillary (Fig. 4), and small cell-like (Fig. 5). It should be noted that this study included the largest series of rare subtypes of ChRCC, which were previously published by our group [11-17]. The control group consisted of 70 ChRCC including classic and eosinophilic features, age- and tumor size-matched. Additional tumors that were later added to the study were reviewed by two urologic pathologists (O. H. and R.A.) to confirm both the diagnosis and histologic subtype. The primary outcome measure of the study was to determine the impact of histologic diversity in ChRCC on clinical outcome including disease recurrence, metastasis or death.

Clinical and pathologic features including age, sex, tumor size, tumor necrosis, and sarcomatoid differentiation were obtained from clinical

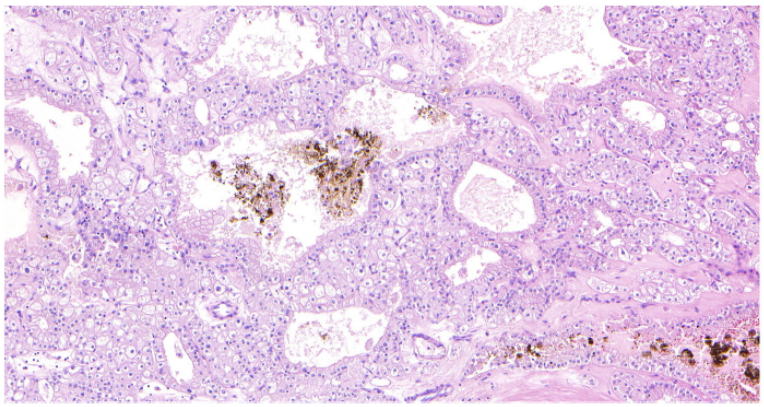

Fig. 1. Adenomatoid microcystic/pigmented ChRCC shows complex architecture with tubular and cribriform pattern and typical plant-like cells, combined with smaller eosinophilic cells.

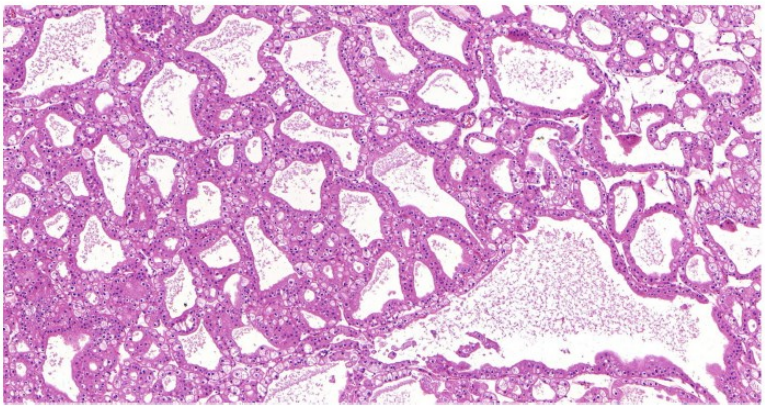

Fig. 2. Multicystic ChRCC is a cystic tumor, where cysts are lined by classic ChRCC cells.

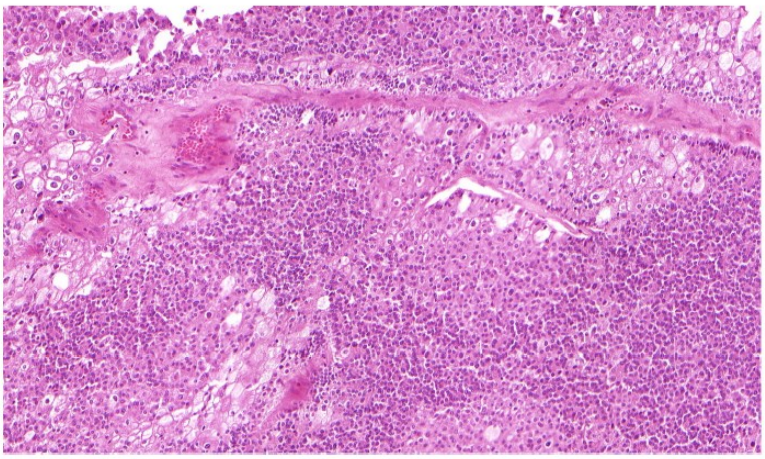

Fig. 3. ChRCC with neuroendocrine differentiation (confirmed by immunohistochemistry) is characterized by presence of features typically associated with neuroendocrine differentiation like tubular, glandular, and insular growth pattern. Formation of pseudorosettes is visible in the right side of the photo.

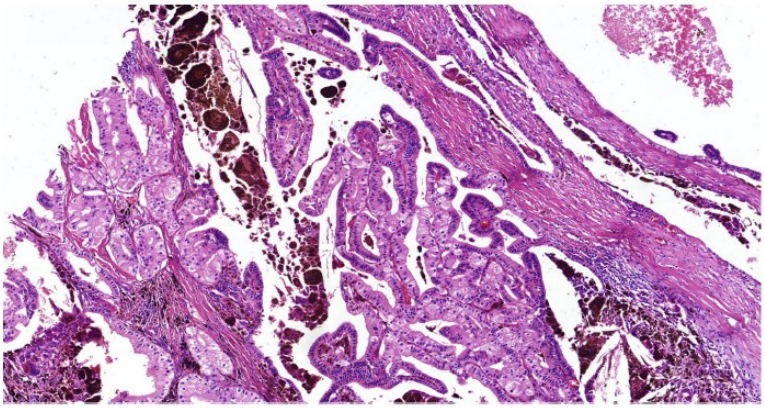

Fig. 4. Papillary ChRCC is tumor with papillary architecture, where papillae are lined by both cell types characteristic for ChRCC.

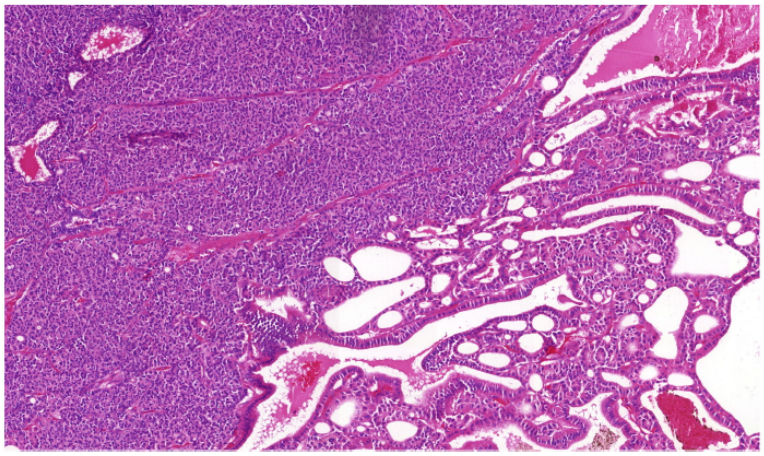

Fig. 5. ChRCC with small-like cell pattern shows a combination of classic ChRCC admixed with a small cell-like component.

Table 1
Demographic and clinical characteristics of study and control groups.

Variables	Study group[a] (n = 89)	Control group[b] (n = 70)	p-Value
Age at diagnosis (years), mean ± SD	60.5 ± 13.6	61.7 ± 12.7	0.58
Male sex, n (%)	44 (49.4%)	39 (55.7%)	0.26
Tumor size (mm), mean ± SD	58.5 ± 43.2	50.3 ± 32.5	0.19
Necrosis, n (%)	8 (9%)	3 (4.3%)	0.34
Sarcomatoid, n (%)	2 (2.2%)	3 (4.3%)	0.65
Follow-up (months), mean ± SD	78.5 ± 67.2	56.1 ± 47.2	0.019
Metastasis or death due to ChRCC	4 (4.5%)	3 (4.3%)	0.63

[a] Rare subtypes of ChRCC.
[b] Classic and eosinophilic ChRCC.

charts from each participating institution. Clinical outcomes included recurrence, development of distant metastases (defined as evidence of disease progression in non-regional lymph nodes or any organ other than the kidney) and death from ChRCC.

2.1. Statistical analysis

The values of continuous parameters were calculated as means ± standard deviation (SD). Pearson's $\chi 2$ and extended Fisher's exact tests were used for categorical variables. For comparisons between the final pathology groups, the independent samples *t*-test was used for continuous variables and the Fisher exact test was used for categorical variables.

Distant metastasis-free and cancer-specific survival rates were estimated using the Kaplan-Meier method, with the duration of follow-up calculated from surgery to distant metastases, death, or last follow-up. Associations with outcomes were evaluated using Cox proportional hazard regression models and summarized with hazard ratios (HRs) and 95% confidence intervals (CIs).

All tests were two-tailed and $p < 0.05$ was considered statistically significant. All descriptive and inferential statistical analyses were carried out using the Statistical Package for the Social Sciences (SPSS), version 19.0 (Chicago, IL, USA).

3. Results

Eighty-nine cases of rare subtypes of ChRCC (study group) and 70 classic and eosinophilic ChRCC (control group) matched for age and tumor size were included in the study. In the study group, most of the rare subtypes were adenomatoid cystic/pigmented ChRCC (66/89, 74.2%), followed by multicystic ChRCC (10/89, 11.2%), papillary ChRCC (9/89, 10.1%), neuroendocrine (1/89, 1.1%) small-like (1/89, 1.1%), and two other rare subtypes. In the control group, there were 62 (88.6%) classic and 8 (11.4%) eosinophilic ChRCC.

Table 1 presents clinicopathological characteristics of the study group and control group. There were no statistically significant differences between the two groups for age at diagnosis, gender distribution, tumor size, presence of tumor necrosis, presence of sarcomatoid differentiation, and adverse outcomes (metastatic disease or death of the disease). However, mean clinical follow-up was slightly longer in the rare subtypes group (78.5 months) than the controls (56.1 months) ($p = 0.019$).

Table 2 demonstrates relation of tumor size, necrosis, and sarcomatoid differentiation to clinical outcome in each group. In both groups, tumor necrosis and sarcomatoid differentiation were significantly associated with poor clinical outcome (metastatic disease or death of the disease). In the classic/eosinophilic group, tumor size was significantly larger among those who developed metastatic disease or died of the

Table 2
Comparing adverse clinical/histologic features (tumor size, necrosis, and sarcomatoid differentiation) according to clinical outcome in study and control groups.

Variables	Study group[a] (n = 89)		p-Value	Control group[b] (n = 70)		p-Value
	Alive (n = 85)	Metastasis or death (n = 4)		Alive (n = 67)	Metastasis or death (n = 3)	
Tumor size (mm), mean ± SD	56.8 ± 40.7	101.7 ± 86.1	0.07	46.7 ± 27.7	131.7 ± 25.6	0.02
Necrosis, n (%)	6 (7.1%)	2 (50%)	0.03	1 (1.5%)	2 (66.7%)	0.004
Sarcomatoid, n (%)	0 (0%)	2 (50%)	0.002	0 (0%)	3 (100%)	0.001

[a] Rare subtypes of ChRCC.
[b] Classic and eosinophilic ChRCC.

Table 3
Comparing adverse clinical/histologic features (tumor size, necrosis, and sarcomatoid differentiation) between study and control groups by clinical outcome.

		Study group[a] (n = 89)	Control group[b] (n = 70)	p-Value
Necrosis, n (%)	Metastasis/death (n = 4)	2 (25%)	2 (66.7%)	0.27
	Alive (n = 85)	6 (75%)	1 (33.3%)	
No necrosis, n (%)	Metastasis/death (n = 4)	2 (2.5%)	1 (1.5%)	0.57
	Alive (n = 85)	79 (97.5%)	66 (98.5%)	
Sarcomatoid, n (%)	Metastasis/death (n = 4)	2 (100%)	3 (100%)	0.31
	Alive (n = 85)	0 (0%)	0 (0%)	
No sarcomatoid, n (%)	Metastasis/death (n = 4)	2 (2.3%)	0 (0%)	0.63
	Alive (n = 85)	85 (97%)	67 (100%)	
Tumor size (mm), mean ± SD	Metastasis/death (n = 4)	102.5 ± 70.3	131.0 ± 25.7	0.19
	Alive (n = 85)	56.0 ± 38.9	46.7 ± 27.7	

[a] Rare subtypes of ChRCC.
[b] Classic and eosinophilic ChRCC.

disease (131.7 mm) than those alive (46.7 mm) (p = 0.02). Similar observation was made in the rare subtypes group (101.7 mm in metastatic disease/death vs. 56.8 mm in alive patients), but the difference was not statistically significant (p = 0.07).

Table 3 compares the study and control group, namely how the presence of adverse clinical and histologic features (tumor size, necrosis, and sarcomatoid differentiation) influence their clinical outcome. No statistically significant differences were found in clinical outcome between the two groups.

Fig. 6 presents survival plots for the study and control groups, with a log-rank test providing a p-value of 0.007 suggesting that the difference in survival between the study and control groups was statistically significant. Further, Cox proportional hazard regression models showed no significant associations between histologic subtypes and survival outcome, using tumor size, necrosis, and sarcomatoid differentiation as potential confounding variables.

4. Discussion

ChRCC is the third most common histological type among all renal neoplasms of adults, accounting for approximately 5–7% of all RCCs [21]. ChRCC is associated with more favourable outcomes in comparison to CCRCC and PRCC, with a reported 5-year survival rate of 78–100% [21]. The typical histological features of ChRCC consist of large pale and/or smaller eosinophilic tumor cells, with wrinkled nuclei and perinuclear haloes. The two main morphological subtypes of ChRCC are classic and eosinophilic. While in the classic subtype both neoplastic cell populations (large pale and smaller eosinophilic) are present in a solid alveolar growth pattern, the eosinophilic cells are the predominant cell type in the eosinophilic subtype [22].

Several aberrant histologic subtypes of ChRCC have been described over the last few decades, including adenomatoid cystic/pigmented, multicystic, neuroendocrine/neuroendocrine-like, papillary, and small cell-like [11-18]. The most common architectonical features of the adenomatoid cystic/pigmented subtype are peculiar microtubular or microcystic patterns and areas with light to dark brown pigmentation corresponding to the presence of lipochrome [12,13,18]. The multicystic subtype is considered an extreme form of the adenomatoid cystic/

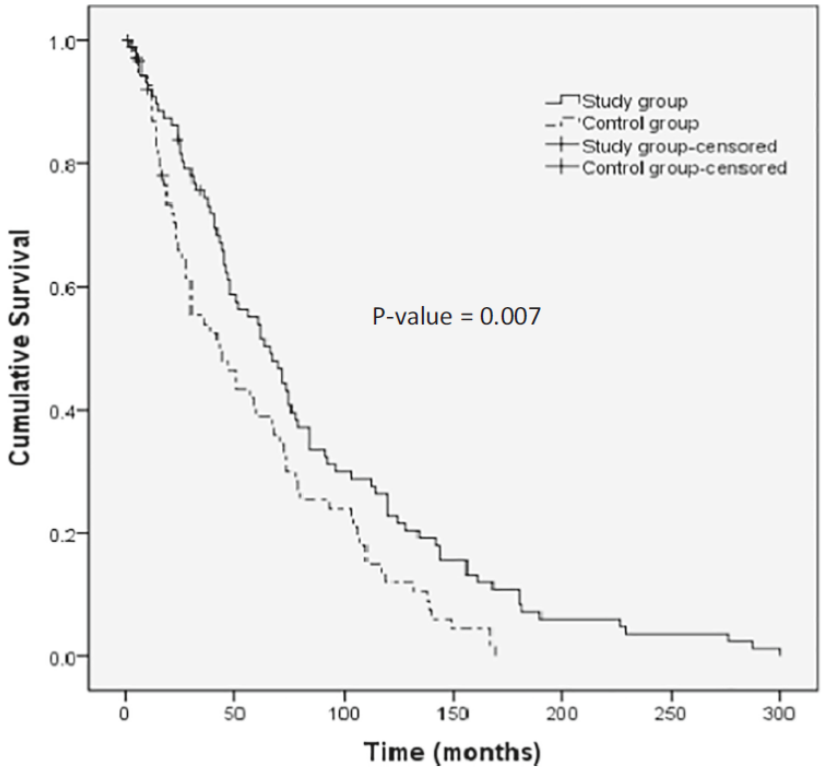

Fig. 6. Kaplan-Meier survival analysis of overall survival (OS) between study and control groups (cumulative observation).

pigmented ChRCC [17]. The neuroendocrine/neuroendocrine-like ChRCC is extremely rare and histologically is characterized by the presence of classic features of ChRCC admixed with areas morphologically consistent with neuroendocrine differentiation [11]. Papillary configuration in ChRCC is an extremely histologic feature and can represent varying percentage of tumor volume [16]. The small cell-like ChRCC has recently been described by our group [15]. It contains a variable fraction of small cells with minimal to no cytoplasm, reminiscent of small cells in renal oncocytoma (i.e. so-called oncoblast). The oncocytic subtype is characterized by tumor cells with oncocytic cytoplasm, centrally located round nuclei, and the absence of perinuclear halo. Nevertheless, the immunohistochemical characteristics and the pattern of numerical chromosomal aberrations in oncocytic ChRCC are similar to that of classic ChRCC [23].

One of the most important prognostic factors in RCC, in addition to stage, is tumor grading. Grading systems are mainly based on cytomorphological differentiation of neoplastic cells but other non-cytomorphologic elements, such as tumor necrosis, can be incorporated. The WHO recommends grading of CCRCC and PRCC using the WHO/ISUP grade, which is primarily based on nuclear features. Several grading systems have been proposed for ChRCC, however, none have proven to be clinically useful so far. Therefore, grading for ChRCC is currently not recommended by the WHO [1]. Historically, the nuclear grading by Fuhrman et al. [24] was used for grading of all RCCs. As proposed by the ISUP consensus conference in 2012, this grading system was subsequently simplified to focus only on nucleolar prominence [1]. With slight modification, the ISUP grade was later recognized by the Fourth edition of the WHO classification of genitourinary tumors in 2016 and was termed WHO/ISUP grade [25].

It is well known that in contrast to CCRCC and PRCC, the utility of Fuhrman and WHO/ISUP grading systems in predicting prognosis and clinical behavior of ChRCC is rather poor. In fact, when strictly applying the parameters of both nuclear grade systems to ChRCC, one would classify most of them as high grade, despite the majority have a favourable outcome [26]. In 2010, a three-tiered grading scheme was proposed by Paner et al. [8] which extends nuclear grading by including further parameters such as geographic nuclear crowding and objective nuclear size. However, this grading system was found to be associated with low reproducibility as a result of inter- and intra-observer variability. Furthermore, it lacked correlation with other parameters pertinent to clinical outcomes [27]. Ohashi et al. [3] recently introduced a two-tiered grading system based on the presence of sarcomatoid differentiation and tumor necrosis. In contrast to previously proposed grading systems, it showed much stronger prognostic impact and clinical outcome correlation. It effectively identified tumors at higher risk of progression. However, this grading system is not a classic and standard one as it does not include cytomorphologic factors (mostly nuclear features).

In this study, we assessed and validate prognostic criteria proposed by Ohashi et al. [3] on a large cohort of ChRCC with rare subtype histology. The spectrum of histologic diversity in subtype patterns can be divided into the following groups: 1) morphologic features (i.e., small cell-like, neuroendocrine), 2) architectural patterns (i.e., papillary, adenomatoid, microcystic, multicystic), and 3) combined morphologic and architectural patterns. Of note, the true incidence of rare patterns of ChRCC is not yet known [28].

Our findings showed that both sarcomatoid differentiation and tumor necrosis were significantly associated with poor clinical outcome in both ChRCC with rare subtype histology as well as classic/eosinophilic ChRCC groups (Table 2). Additionally, tumor size was found to be significantly associated with metastasis/death in the classic/eosinophilic ChRCC group. Similar findings were observed in the rare subtype histology group, although it was not statistically significant ($p = 0.07$). Further analysis showed that there were no statistically significant differences in clinical outcome (metastasis/death versus alive/free of disease) between the two groups, when stratified by adverse pathologic features such as sarcomatoid differentiation, tumor necrosis, and tumor size (Table 3). In other words, it showed that histologic diversity in ChRCC may not impact clinical outcome.

A Kaplan-Meier survival analysis (Fig. 6) was performed, which showed slightly better survival outcome in the rare subtype histologic group when compared with the classic/eosinophilic ChRCC group ($p = 0.007$). As the number of adverse events (metastasis/death) was very small in both groups, hence limiting the power of the model, we would caution to draw concrete conclusions. It should be noted that follow-up clinical data in control group (classic/eosinophilic ChRCC) was also significantly shorter than those in the rare subtype histologic group ($p = 0.019$). Overall, we believe that the value of statistical significant difference in Kaplan-Meier model may not directly translate into clinical significant difference in routine practice, giving the above limiting factors. Further, the Cox proportional hazard regression models were carried out and showed no significant associations between histologic subtypes and survival outcome, using tumor size, necrosis, and sarcomatoid differentiation as potential confounding variables.

It should be noted that clinical data on uncommon patterns of ChRCC are limited due to their rarity but our findings suggest that rare morphologic patterns in ChRCC play no role in determining the clinical behavior of the tumor. In fact, most rare patterns of ChRCC clinically behave in a similar fashion to that of classic/eosinophilic ChRCC. This may be due to the low incidence of aggressive histologic features such as tumor necrosis and/or sarcomatoid differentiation in ChRCC with rare patterns, which was also seen in this study.

The strengths of this study are the fact that this is the largest international multi-institutional cohort of ChRCC with rare histologic subtypes, using a matched case-control study design. The main limitation of this study was the fact that the number of adverse events (metastasis/death) in each group was very low, challenging the power of the study in using a survival analysis models.

5. Conclusion

Our findings corroborated previous studies that both sarcomatoid differentiation and tumor necrosis were significantly associated with poor clinical outcome in classic/eosinophilic ChRCC, and this was also proven to be true for ChRCC with rare histologic subtypes. It seems that rare morphologic patterns in ChRCC play no role in determining the clinical behavior of the tumor. In fact, most rare patterns of ChRCC clinically behave in a similar fashion to that of classic/eosinophilic ChRCC, which may be due to low incidence of aggressive histologic features in ChRCC with rare patterns.

Funding

The study was supported in part by the Charles University Research Fund (Cooperation Program, research area SURG), the Institutional Research Fund of University Hospital Plzen (Faculty Hospital in Plzen-FNPl 00669806).

References

[1] Delahunt B, Cheville JC, Martignoni G, Humphrey PA, Magi-Galluzzi C, McKenney J, Egevad L, Algaba F, Moch H, Grignon DJ, Montironi R, Srigley JR. Members of the IRTP. The International Society of Urological Pathology (ISUP) grading system for renal cell carcinoma and other prognostic parameters. Am J Surg Pathol 2013;37:1490–504.

[2] Delahunt B, McKenney JK, Lohse CM, Leibovich BC, Thompson RH, Boorjian SA, Cheville JC. A novel grading system for clear cell renal cell carcinoma incorporating tumor necrosis. Am J Surg Pathol 2013;37:311–22.

[3] Ohashi R, Martignoni G, Hartmann A, Calio A, Segala D, Stohr C, Wach S, Erlmeier F, Weichert W, Autenrieth M, Schraml P, Rupp NJ, Ohe C, Otsuki Y, Kawasaki T, Kobayashi H, Kobayashi K, Miyazaki T, Shibuya H, Usuda H, Umezu H, Fujishima F, Furusato B, Osakabe M, Sugai T, Kuroda N, Tsuzuki T, Nagashima Y, Ajioka Y, Moch H. Multi-institutional re-evaluation of prognostic factors in chromophobe renal cell carcinoma: proposal of a novel two-tiered grading scheme. Virchows Arch 2020;476:409–18.

[4] Volpe A, Novara G, Antonelli A, Bertini R, Billia M, Carmignani G, Cunico SC, Longo N, Martignoni G, Minervini A, Mirone V, Simonato A, Terrone C, Zattoni F, Ficarra V, Surveillance, Treatment Update on Renal Neoplasms P, Leading Urological No-Profit Foundation for Advanced Research F. Chromophobe renal cell carcinoma (RCC): oncological outcomes and prognostic factors in a large multicentre series. BJU Int. 2012;110:76–83.
[5] Lopez-Beltran A, Montironi R, Cimadamore A, Cheng L. Grading of chromophobe renal cell carcinoma: do we need It? Eur Urol 2021;79:232–3.
[6] Avulova S, Cheville JC, Lohse CM, Gupta S, Potretzke TA, Tzivian M, Thompson RH, Boorjian SA, Leibovich BC, Potretzke AM. Grading chromophobe renal cell carcinoma: evidence for a four-tiered classification incorporating coagulative tumor necrosis. Eur Urol 2021;79:225–31.
[7] Cheville JC, Lohse CM, Sukov WR, Thompson RH, Leibovich BC. Chromophobe renal cell carcinoma: the impact of tumor grade on outcome. Am J Surg Pathol 2012;36:851–6.
[8] Paner GP, Amin MB, Alvarado-Cabrero I, Young AN, Stricker HJ, Moch H, Lyles RH. A novel tumor grading scheme for chromophobe renal cell carcinoma: prognostic utility and comparison with fuhrman nuclear grade. Am J Surg Pathol 2010;34:1233–40.
[9] Przybycin CG, Cronin AM, Darvishian F, Gopalan A, Al-Ahmadie HA, Fine SW, Chen YB, Bernstein M, Russo P, Reuter VE, Tickoo SK. Chromophobe renal cell carcinoma: a clinicopathologic study of 203 tumors in 200 patients with primary resection at a single institution. Am J Surg Pathol 2011;35:962–70.
[10] Lauer SR, Zhou M, Master VA, Osunkoya AO. Chromophobe renal cell carcinoma with sarcomatoid differentiation: a clinicopathologic study of 14 cases. Anal Quant Cytopathol Histpathol. 2013;35:77–84.
[11] Peckova K, Martinek P, Ohe C, Kuroda N, Bulimbasic S, Condom Mundo E, Perez Montiel D, Lopez JI, Daum O, Rotterova P, Kokoskova B, Dubova M, Pivovarcikova K, Bauleth K, Grossmann P, Hora M, Kalusova K, Davidson W, Slouka D, Miroslav S, Buzrla P, Hynek M, Michal M, Hes O. Chromophobe renal cell carcinoma with neuroendocrine and neuroendocrine-like features. Morphologic, immunohistochemical, ultrastructural, and array comparative genomic hybridization analysis of 18 cases and review of the literature. Ann Diagn Pathol 2015;19:261–8.
[12] Michal M, Hes O, Svec A, Ludvikova M. Pigmented microcystic chromophobe cell carcinoma: a unique variant of renal cell carcinoma. Ann Diagn Pathol 1998;2:149–53.
[13] Hes O, Vanecek T, Perez-Montiel DM, Alvarado Cabrero I, Hora M, Suster S, Lamovec J, Curik R, Mandys V, Michal M. Chromophobe renal cell carcinoma with microcystic and adenomatous arrangement and pigmentation–a diagnostic pitfall. Morphological, immunohistochemical, ultrastructural and molecular genetic report of 20 cases. Virchows Arch 2005;446:383–93.
[14] Michalova K, Tretiakova M, Pivovarcikova K, Alaghehbandan R, Perez Montiel D, Ulamec M, Osunkoya A, Trpkov K, Yuan G, Grossmann P, Sperga M, Ferak I, Rogala J, Mareckova J, Pitra T, Kolar J, Michal M, Hes O. Expanding the morphologic spectrum of chromophobe renal cell carcinoma: a study of 8 cases with papillary architecture. Ann Diagn Pathol 2019;44:151448.
[15] Rogala J, Kojima F, Alaghehbandan R, Ptakova N, Bravc A, Bulimbasic S, Perez Montiel D, Slisarenko M, Ali L, Kuthi L, Pivovarcikova K, Michalova K, Bartovic B, Bartos Vesela A, Dolejsova O, Michal M, Hes O. Small cell variant of chromophobe renal cell carcinoma: clinicopathologic, and molecular-genetic analysis of 10 cases. Bosn J Basic Med Sci 2022. Online ahead of print.
[16] Michalova K, Tretiakova M, Pivovarcikova K, Alaghehbandan R, Perez Montiel D, Ulamec M, Osunkoya A, Trpkov K, Yuan G, Grossmann P, Sperga M, Ferak I, Rogala J, Mareckova J, Pitra T, Kolar J, Michal M, Hes O. Expanding the morphologic spectrum of chromophobe renal cell carcinoma: a study of 8 cases with papillary architecture. Ann Diagn Pathol 2020;44:151448.
[17] Foix MP, Dunatov A, Martinek P, Mundo EC, Suster S, Sperga M, Lopez JI, Ulamec M, Bulimbasic S, Montiel DP, Alaghehbandan R, Peckova K, Pivovarcikova K, Ondrej D, Rotterova P, Skenderi F, Prochazkova K, Dusek M, Hora M, Michal M, Hes O. Morphological, immunohistochemical, and chromosomal analysis of multicystic chromophobe renal cell carcinoma, an architecturally unusual challenging variant. Virchows Arch 2016;469:669–78.
[18] Dundr P, Pesl M, Povysil C, Tvrdik D, Pavlik I, Soukup V, Dvoracek J. Pigmented microcystic chromophobe renal cell carcinoma. Pathol Res Pract 2007;203:593–7.
[19] Kuroda N, Tamura M, Hes O, Michal M, Gatalica Z. Chromophobe renal cell carcinoma with neuroendocrine differentiation and sarcomatoid change. Pathol Int 2011;61:552–4.
[20] Parada DD, Pena KB. Chromophobe renal cell carcinoma with neuroendocrine differentiation. APMIS 2008;116:859–65.
[21] Amin MB, Amin MB, Tamboli P, Javidan J, Stricker H, Deshpande A, Menon M, de-Peralta Venturina M. Prognostic impact of histologic subtyping of adult renal epithelial neoplasms: an experience of 405 cases. Am J Surg Pathol 2002;26:281–91.
[22] Amin MB, Paner GP, Alvarado-Cabrero I, Young AN, Stricker HJ, Lyles RH, Moch H. Chromophobe renal cell carcinoma: histomorphologic characteristics and evaluation of conventional pathologic prognostic parameters in 145 cases. Am J Surg Pathol 2008;32:1822–34.
[23] Kuroda N, Tanaka A, Yamaguchi T, Kasahara K, Naruse K, Yamada Y, Hatanaka K, Shinohara N, Nagashima Y, Mikami S, Oya M, Hamashima T, Michal M, Hes O. Chromophobe renal cell carcinoma, oncocytic variant: a proposal of a new variant giving a critical diagnostic pitfall in diagnosing renal oncocytic tumors. Med Mol Morphol 2013;46:49–55.
[24] Fuhrman SA, Lasky LC, Limas C. Prognostic significance of morphologic parameters in renal cell carcinoma. Am J Surg Pathol 1982;6:655–63.
[25] Moch H, Humphrey PA, Ulbright TM, Reuter VE. WHO Classification of Tumours of the Urinary System and Male Genital Organs. Lyon, France: International Agency for Research on Cancer; 2016.
[26] Meskawi M, Sun M, Ismail S, Bianchi M, Hansen J, Tian Z, Hanna N, Trinh QD, Graefen M, Montorsi F, Perrotte P, Karakiewicz PI. Fuhrman grade [corrected] has no added value in prediction of mortality after partial or [corrected] radical nephrectomy for chromophobe renal cell carcinoma patients. Mod Pathol 2013;26:1144–9.
[27] Sperga M, Martinek P, Vanecek T, Grossmann P, Bauleth K, Perez-Montiel D, Alvarado-Cabrero I, Nevidovska K, Lietuvietis V, Hora M, Michal M, Petersson F, Kuroda N, Suster S, Branzovsky J, Hes O. Chromophobe renal cell carcinoma–chromosomal aberration variability and its relation to paner grading system: an array CGH and FISH analysis of 37 cases. Virchows Arch 2013;463:563–73.
[28] Alaghehbandan R, Williamson SR, McKenney JK, Hes O. The histologic diversity of chromophobe renal cell carcinoma with emphasis on challenges encountered in daily practice. Adv Anat Pathol 2022. Online ahead of print.

3.6 Comprehensive Review of Numerical Chromosomal Aberrations in Chromophobe Renal Cell Carcinoma Including Its Variant Morphologies.

Chromophobe renal cell carcinoma (ChRCC) is third most common renal carcinoma (RCC), accounting for 5% to 7% of all RCCs. The first genetic studies on ChRCC were conducted in the late 80', soon after its first description, and reported multiple chromosomal losses. Since then, losses of chromosomes 1, 2, 6, 10, 13, 17, and 21 have been considered a genetic hallmark of ChRCC, both for classic and eosinophilic ChRCC variant. With the development of more sophisticated molecular techniques, it became apparent that molecular background of ChRCC is more complex and heterogeneous, frequently enriched in chromosomal gains.

In this review, we briefly present genetic techniques used for the examination of chromosomal abnormalities, together with discussion on the available literature on this topic, aiming to present a comprehensive and up-to-date survey of the spectrum of chromosomal abnormalities found in classic ChRCC and its variants. Most commonly reported chromosomal losses in classic ChRCC include: 1 (71%), 10 (71%), 2 (64.3%), 17 (63.1%), 6 (59.8%),13 (50.6%), and 21 (31.5%). As for chromosomal gains, the most common are: 7 (35.2%), 19 (27.3%), 20 (27.3%), 4 (22.7%), 8 (20.5%), 9 (18.2%), and 1 (17%). Studies on eosinophilic ChRCC reveal that most common chromosomal losses are 1 (76.7%), 2 (58.1%), 17 (58.1%), 6 (53.5%), 10 (46.5%), 13 (39.5%), and 21 (37.2%). No chromosomal gains were found in eosinophilic ChRCCs. Studies on sarcomatoid ChRCCs show that most common chromosomal gains are: 3 (100%), 1 (89.5%), 2(42.1%), 10 (31.6%), 17 (31.6%), 4 (26.3%), 7 (26.3%), 8 (26.3%), 9 (26.3%), and 15 (26.3%). The most commonly reported chromosomal losses in these tumours include: 11 (30%), 2 (30%), 17 (20%), and 10 (20%), which are much less in frequency compared with classic ChRCCs. Studies of rare morphologic variants including ChRCC with pigmented microcystic adenomatoid/multicystic growth, ChRCC with neuroendocrine differentiation, ChRCC with papillary architecture, and renal oncocytoma-like variants also showed variable chromosomal numerical aberrations, including multiple losses (common), gains (less common), or chromosomal changes overlapping with renal oncocytoma. Metastatic ChRCCs appear to demonstrate overlapping genetic patterns with the primary tumours.

For years, ChRCC has been defined by multiple chromosomal losses, with most common loss of set of 7 chromosomes: 1, 2, 6, 10, 13, 17, and 21. That chromosomal instability has appeared to be much broader including loses of chromosomes 3, 5, 8, 9, 18, 21q and gains, most commonly of chromosomes 4, 7, 17, 19 and 20. Spectrum of molecular alterations in ChRCC is not limited to CNA. ChRCCs also harbour mutations of *TP53*, *PTEN* as most common, followed by deletion or hypermethylation of 9p21.3 resulting in loos CDKN2A or its expression. Less frequently identified mutations include *MTOR*, *TSC1/2*. Given the complexity of molecular genetic alterations in ChRCC, this review analyzed the existing published data, aiming to present a comprehensive up-to-date survey of the chromosomal abnormalities in classic ChRCC and its variants. The role of chromosomal

numerical aberrations as a potential tool in the differential diagnostic evaluation may be limited, potentially owing to its highly variable CNA pattern of ChRCC.

Comprehensive Review of Numerical Chromosomal Aberrations in Chromophobe Renal Cell Carcinoma Including Its Variant Morphologies

*Reza Alaghehbandan, MD, MSc, FRCPC, FCAP, FACE,** *Kiril Trpkov, MD, FRCPC,† Maria Tretiakova, MD, PhD,‡* *Ana S. Luis, MD,§ Joanna D. Rogala, MD,|| and Ondrej Hes, MD, PhD||*

Abstract: Chromophobe renal cell carcinoma (ChRCC) accounts for 5% to 7% of all renal cell carcinomas. It was thought for many years that ChRCC exhibits a hypodiploid genome. Recent studies using advanced molecular genetics techniques have shown more complex and heterogenous pattern with frequent chromosomal gains. Historically, multiple losses of chromosomes 1, 2, 6, 10, 13, 17, and 21 have been considered a genetic hallmark of ChRCC, both for classic and eosinophilic ChRCC variants. In the last 2 decades, multiple chromosomal gains in ChRCCs have also been documented, depicting a considerably broader genetic spectrum than previously thought. Studies of rare morphologic variants including ChRCC with pigmented microcystic adenomatoid/multicystic growth, ChRCC with neuroendocrine differentiation, ChRCC with papillary architecture, and renal oncocytoma-like variants also showed variable chromosomal numerical aberrations, including multiple losses (common), gains (less common), or chromosomal changes overlapping with renal oncocytoma. Although not the focus of the review, The Cancer Genome Atlas (TCGA) data in ChRCC show *TP53*, *PTEN*, and *CDKN2A* to be the most mutated genes. Given the complexity of molecular genetic alterations in ChRCC, this review analyzed the existing published data, aiming to present a comprehensive up-to-date survey of the chromosomal abnormalities in classic ChRCC and its variants. The potential role of chromosomal numerical aberrations in the differential diagnostic evaluation may be limited, potentially owing to its high variability.

Key Words: chromophobe renal cell carcinoma (ChRCC), chromosomal aberration numbers, review

(*Adv Anat Pathol* 2021;28:8–20)

Chromophobe renal cell carcinoma (ChRCC) first described in 1985 by Thoenes et al[1] accounts for 5% to 7% of all renal cell carcinomas (RCCs). ChRCC is composed of neoplastic cells with prominent cell membranes, wrinkled nuclei with perinuclear halos, and pale to eosinophilic cytoplasm. ChRCC typically presents as a sporadic tumor, but identical or similar morphologies have been also documented in a hereditary setting, such as Birt-Hogg-Dubé syndrome, known particularly for its predilection for the so-called "hybrid oncocytic/chromophobe" tumors.[2]

The most common variant of ChRCC is the "classic" one, which was initially described by Thoenes et al[1] demonstrating relatively characteristic microscopic features. Three years later (in 1988) the same group of authors described an eosinophilic variant of ChRCC[3] that shows overlapping morphologic features with benign renal oncocytoma (RO). Since then, other ChRCC subtypes/variants have been reported, such as pigmented/adenomatoid, multicystic, neuroendocrine, papillary, and sarcomatoid.[4–10]

Overall, ChRCC has a favorable prognosis with a 5-year survival rate of 78% to 100% and 10-year survival rate of 80% to 90%.[11,12] The prognosis of ChRCC is better than clear-cell RCC and is slightly better than papillary RCC. Despite its generally favorable behavior, a small subset of ChRCC presents with sarcomatoid differentiation and may progress with recurrence or metastasis in 7% and mortality in 6% of patients.[2,13] Currently, it is not recommended to grade ChRCC using the World Health Organization (WHO)/International Society of Urologic Pathologists (ISUP) grading system.[14] In 2010, Paner at al[15] proposed a grading system for ChRCC, but its correlation with the biological behavior remains to be substantiated. Most recently, in 2019, a multi-institutional study proposed a new 2-tiered "grading scheme," using necrosis and sarcomatoid differentiation that are well-documented adverse prognostic factors of ChRCC.[13]

In the early 1990s, a number of studies have shown that the stereotypical morphologic appearance of ChRCC is associated with a consistent pattern of chromosomal changes characterized by loss of specific chromosomes.[16–18] The earliest reports showed nonrandom losses in ChRCC of chromosomes 1, 2, 6, 10, 13, 17, and 21. Thus, for many years it was believed that ChRCC has a hypodiploid genome. However, more recent studies utilizing advanced molecular techniques have shown a rather more heterogenous genetic pattern with frequent co-occurring chromosomal gains and suggesting a more complex molecular genetic landscape in ChRCC.[19–21] This review analyzed the available studies on this topic aiming to present a comprehensive and up-to-date survey of the spectrum of chromosomal abnormalities found in classic ChRCC and its variants.

GENETICS METHODS DETECTING CHROMOSOMAL ABERRATIONS

First, we briefly discuss the most commonly utilized genetic methods including the traditional genetic techniques

From the *Department of Pathology, Faculty of Medicine, Royal Columbian Hospital, University of British Columbia, Vancouver, BC; †Department of Pathology and Laboratory Medicine, University of Calgary, Calgary, AB, Canada; ‡Department of Pathology, University of Washington, Seattle, WA; §Department of Pathology, Portuguese Institute of Oncology of Porto Francisco Gentil, Porto, Portugal; and ||Department of Pathology, Charles University in Prague, Faculty of Medicine and University Hospital in Plzen, Plzen, Czech Republic.
Supported by the Charles University Research Fund (project number Q39) and by the grant of Ministry of Health of the Czech Republic-Conceptual Development of Research Organization (Faculty Hospital in Plzen-FNPl 00669806).
The authors have no conflicts of interest to disclose.
Reprints: Ondrej Hes, MD, PhD, Department of Pathology, Medical Faculty and Charles University Hospital Plzen, Alej Svobody 80, Pilsen 304 60, Czech Republic (e-mail: hes@biopticka.cz).

as well as the more recent molecular technologies that have been applied for the examination of chromosomal abnormalities in ChRCC.

Classic Cytogenetics

Karyotyping or classic cytogenetic is one of the earliest traditional methods of examining chromosomal numerical aberrations, including chromosomal losses and gains. However, this technique detects only "larger" chromosomal abnormalities and the detection of "smaller" and more subtle changes may require more sophisticated techniques.

Restriction Fragment Length Polymorphism

Restriction fragment length polymorphism (RFLP) was an early tool in genome mapping and disease linkage analysis, which required larger DNA samples. This was later replaced by more inexpensive and efficient methods, some of which are discussed below.

Fluorescent In Situ hybridization

Fluorescent in situ hybridization (FISH), a hallmark of molecular cytogenetics, was first developed when classic cytogenetics and recombinant DNA technology were combined to further assist cancer cytogenetics. FISH is a rapid assay and can be utilized on any tissue (ie, fresh, frozen, formalin-fixed). It is currently used in routine practice to help solve various diagnostic questions in a targeted manner, using specific probes. It also plays a major role in assessing prognostic and therapeutic aspects of certain tumors.

Comparative Genomic Hybridization

Comparative genomic hybridization (CGH) is utilized to screen the genome for copy number alterations (CNAs) in surgical pathology. Conventional CGH was initially utilized in examining ChRCC and later its resolution was enhanced by combining it with microarray techniques, known as array comparative genomic hybridization (a-CGH).

Single-nucleotide Polymorphisms

Single-nucleotide polymorphism (SNP) genotyping array is a reliable method in detecting CNA without the need for patient-matched normal tissue. This can be carried out in paraffin-embedded tissues, which is especially important when fresh tissue for conventional cytogenetic analysis is not available.

Microsatellite Analysis

Microsatellites analysis is a sensitive method to investigate the somatic loss of heterozygosity (LOH). This technique is fast and can be applied to degrade DNA extracted from formalin-fixed tissue. In comparison to a-CGH and FISH, microsatellite analysis can detect copy number neutral LOH.

Next-generation Sequencing

a-CGH and genotyping arrays represented the standard techniques to detect genomic CNA until most recently, when high-resolution sequencing data analyses by next-generation sequencing became available.

CLASSIC CHROMOPHOBE RENAL CELL CARCINOMA

The classic variant of ChRCC was described by Thoenes et al[1] > 3 decades ago. The authors used the term "chromophobe," referring to tumors demonstrating larger cells with reticular (not clear) cytoplasm and distinct cell membranes (plant cell-like).[1] Kovacs et al[22] were the first to examine the chromosomal numerical aberrations in a case of ChRCC in 1988. They used classic cytogenetics and found losses of chromosomes 1, 2, 3, 6, 7, 9, 10, 12, 13, 17,

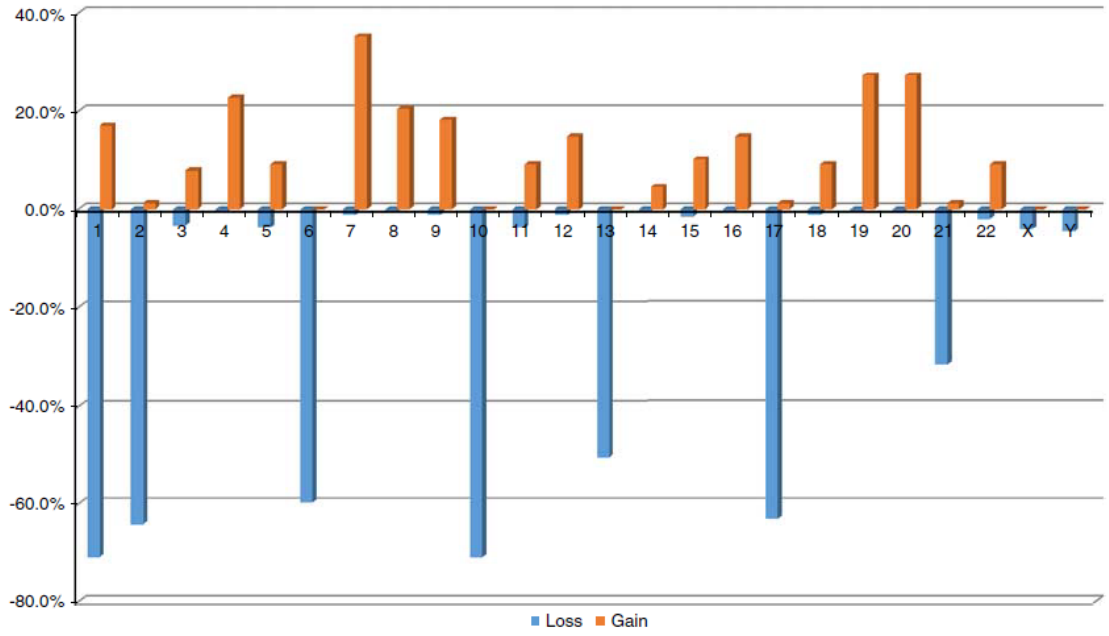

FIGURE 1. Distribution of chromosomal losses and gains in classic chromophobe renal cell carcinoma (N = 241*). *Study data from Davis et al[35] (N = 47) and Tan et al[20] (N = 15) were not included in this analysis since no detail breakdown information were available.

TABLE 1. Chromosomal Losses in Classic Chromophobe Renal Cell Carcinoma

References	Method	Cases (N)	−1	−2	−3	−4	−5	−6	−7	−8	−9	−10	−11	−12	−13	−14	−15	−16	−17	−18	−19	−20	−21	−22	−X	−Y
Kovacs et al[22]	Cytogenetics	1	100%	100%	100%			100%	100%		100%	100%		100%	100%				100%	100%			100%		
Kovacs and Kovacs[17]	Cytogenetics*	1	100%	100%				100%				100%			100%		100%		100%				100%		
Kovacs et al[23]	Restriction fragment length polymorphism	11																	55%						
Crotty et al[24]	Cytogenetics	1																								100%
van den Berg et al[25]	Cytogenetics and LOH (DNA analysis)	10																								20%
Speicher et al[18]	CGH	19	90%	84%				79%				84%			84%				68%				79%		75%	40%
Gerhaz et al[26]	Cytogenetics	1	100%	100%				100%							100%				100%	100%			100%	100%		
Shuin et al[27]	Cytogenetics	1	100%	100%			100%	100%				100%			100%		100%		100%				100%		100%	
Gunawan et al[28]	Cytogenetics	2	100%	100%				100%				100%			100%				100%							
Brunelli et al[29]	FISH	10	70%	90%				80%				60%							90%							
Brunelli et al[19]	FISH†	3	66%	66%				66%				66%							66%							
Meyer et al[30]	TMA-FISH	21	85%																							
Kim et al[31]	Virtual-karyotyping with SNP microarrays	12	100%	92%				100%				83%			83%				100%							
Vieira et al[21]	CGH and FISH on FNA samples	13						46%											46%						31%	
Brunelli et al[32]	FISH and karyotyping	11	54%	45%	18%	9%	9%	64%	18%	9%	18%	82%	18%	18%	9%	9%	18%	9%	82%	9%	9%	9%	18%	36%	18%	18%
Tan et al[20]	Single-nucleotide polymorphism (SNP) array‡	15																								
Kuroda et al[33]	FISH	1		100%								100%														
Sperga et al[34]	a-CGH and FISH	32	72%	75%			13%	53%				72%			34%				56%				31%			
Davis et al[35]	SNP array§	47																								
Kang et al[36]	CGH	8																								
Ren et al[37]	CGH and whole-exome sequencing	8																								
Ohashi et al[38]	SNP	75	93%	84%				91%				83%			76%				85%				56%			
	Total	303	71%	64%	3%	0.4%	4%	60%	1%	0.4%	1%	71%	4%	1%	51%	0.4%	2%	0.4%	63%	1%	0.4%	0.4%	32%	2%	4%	5%

*One of 3 cases was previously published[22] and the other one was not successfully karyotyped.
†The cases include both primary and metastatic chromophobe renal cell carcinomas, where the tumors showed similar copy number alteration.
‡A total of 15 cases were examined with no further breakdown details.
§A total of 47 cases were examined with no further breakdown details.
a-CGH indicates array comparative genomic hybridization; CGH, comparative genomic hybridization; FISH, fluorescent in situ hybridization; FNA, fine needle aspiration; LOH, loss of heterozygosity; SNP, single-nucleotide polymorphism; TMA, tissue microarray.

18, and 21.[22] Since the early 1990s, investigators have used other methods in addition to classic cytogenetics (ie, FISH, CGH, and SNP) to study chromosomal aberrations in ChRCC. Over the last 3 decades, there were 22 studies investigating chromosomal numerical aberrations in classic ChRCC using various methods. Herein, we discuss the findings of these studies according to the genetic methods used and compare their results. Figure 1 shows the distribution of chromosomal losses and gains in the published studies on classic ChRCC, using a weighted average of all evaluated cases in the pertinent studies. Tables 1 and 2 present detailed findings of individual studies by chromosomes and methods used.

Seven of 22 studies used the classic cytogenetic method[17,22,24–28] evaluating a total of 17 ChRCC from 1988 to 1999. These studies consistently reported losses of chromosomes 1, 2, 6, 10, 11, 13, and 17. Of the 7 studies, only 2 found chromosomal gains in classic ChRCC that included chromosomes 7, 11, 12, 16, and 19.[17,22,24–28] One study used RFLP and found a variable frequency of losses of chromosomes 3, 5, and 17.[23]

FISH was used in 5 of 22 studies (performed between 2005 and 2011) to detect chromosomal changes in 39 cases of classic ChRCC.[19,29,30,32,33] These studies also reported losses of chromosomes 1, 2, 6, 10, and 17 as the most common findings.[19,29,30,32,33] Kuroda et al[33] were the only ones using FISH to document gain of chromosome 21 in a case of aggressive ChRCC with lymph node metastasis.

There were 5 studies that used the a-CGH (performed between 1994 and 2015), to identify chromosomal aberrations in a total of 80 classic ChRCCs.[18,21,34,36,37] Similarly, the majority of these studies found losses of chromosomes 1, 2, 6, 10, 13, 17, and 21.[18,21,34,36,37] Unlike studies using classic cytogenetic and FISH methods, all CGH-based studies also consistently found chromosomal gains in classic ChRCC, most frequently involving chromosomes 3, 4, 7, 8, 9, 12, 15, 16, and 20.[18,21,34,36,37]

There were 4 SNP array-based studies examining a total of 149 classic ChRCCs from 2009 to 2019.[20,31,35,38] These studies have also consistently found losses of chromosomes 1, 2, 6, 10, 13, 17, and 21.[20,31,35,38] One of the 4 studies using the SNP array also reported gain of chromosomes 4, 7, 11, 12, 14, and 18.[38]

Overall, the above-mentioned studies show that the most common chromosomal losses in classic ChRCC are: 1 (71%), 10 (71%), 2 (64.3%), 17 (63.1%), 6 (59.8%), 13 (50.6%), and 21 (31.5%). As for chromosomal gains, the most common are: 7 (35.2%), 19 (27.3%), 20 (27.3%), 4 (22.7%), 8 (20.5%), 9 (18.2%), and 1 (17%).

In addition to the 22 studies conducted on classic ChRCC, there were 5 additional studies where the variant of ChRCC was not specified and such information could not be extracted from the published material. These studies included a total of 101 tumors evaluated between 1996 and 2010 and they used different methods, including classic cytogenetics (8 cases),[16] microsatellites analysis (2 studies: 10 and 42 cases),[39] FISH (3 cases),[40] and SNP array (2 studies: 30 and 8 cases).[41,42] Interestingly, the majority of these studies found losses of chromosomes 1, 2, 6, 10, 13, and 17, which is similar to the other reported studies on classic ChRCC; this suggests that these cases likely represented classic ChRCC. Regarding the reported chromosomal gains, Verdorfer et al[40] reported gain of chromosomes 12, 2, 5, 7, and 16 (using classic cytogenetics) and Yokomizo et al[43] found partial gain of chromosome 7q (using SNP-CGH). Tables 3 and 4 present

TABLE 2. Chromosomal Gains in Classic Chromophobe Renal Cell Carcinoma

References	Method	Cases (N)	+1	+2	+3	+4	+5	+6	+7	+8	+9	+10	+11	+12	+13	+14	+15	+16	+17	+18	+19	+20	+21	+22	+X	+Y
van den Berg et al[25]	Cytogenetics and LOH (DNA analysis)	10			30%		20%		40%	20%				40%				40%		40%	40%	40%				
Gerhaz et al[26]	Cytogenetics	1				100%	100%		100%	100%	100%		100%	100%			100%	100%			100%					
Vieira et al[21]	CGH and FISH on FNA samples	13				46%			54%	54%	46%		54%									46%				
Brunelli et al[32]	FISH and karyotyping	11		9%															9%							
Tan et al[20]	SNP array*	15																					100%			
Kuroda et al[33]	FISH	1																								
Sperga et al[34]	a-CGH and FISH	32			13%	41%	16%		59%	25%	28%			25%		13%	25%	25%		13%	59%	44%		25%		
Kang et al[36]	CGH	12																								
Ren et al[37]	CGH and whole-exome sequencing	8																								
	Total	103	17%	1%	8%	23%	9%		35%	21%	18%		9%	15%		5%	10%	15%	1%	9%	27%	27%	1%	9%		

*A total of 15 cases were examined with no further breakdown details.
a-CGH indicates array comparative genomic hybridization; CGH, comparative genomic hybridization; FISH, fluorescent in situ hybridization; FNA, fine needle aspiration; LOH, loss of heterozygosity; SNP, single-nucleotide polymorphism.

detailed findings of the individual studies by chromosomes and methods used.

Some studies interestingly also reported rare cases of classic ChRCC demonstrating diploid chromosome copy numbers.[19,30,45,46] For instance, Brunelli et al[19] reported such findings in 2 cases of ChRCC with sarcomatoid transformation, and in 1 case of ChRCC with distant metastasis; disomy of chromosomes 1, 2, 6, 10, 17 were found in the epithelial component. Meyer et al[30] also reported that 1 of 21 (5%) ChRCCs was diploid for chromosome 1.

EOSINOPHILIC CHROMOPHOBE RENAL CELL CARCINOMA

The eosinophilic variant of ChRCC was described in 1988 by Thoenes et al,[3] following the initial description of classic ChRCC in 1985. The most recent 2016 WHO renal tumor classification recognizes the eosinophilic variant of ChRCC and acknowledges the challenge to distinguish it from benign RO, but does not provide precise diagnostic criteria.

To date, there are only 4 studies that investigated chromosomal changes in eosinophilic ChRCC.[29,35,38,47]

TABLE 3. Chromosomal Losses in Chromophobe Renal Cell Carcinoma (Variant Not Stated)

References	Iqbal et al[16]	Bugert and Kovacs[39]	Bugert et al[44]	Verdorfer et al[40]	Yusenko et al[42]	Yokomizo et al[43]	
Methods	Cytogenetics	Microsatellite Analysis (LOH)	Microsatellite Analysis	Cytogenetics and FISH	High-density SNP-oligoarray	High-resolution Whole-genomic SNP and CGH	Total
# of cases	8	10	42	3	30	8	101
−1	62.5%	100%	95%		93%		90%
−1p						100%	
−1q						100%	
−2	62.5%	100%	86%		93%		86%
−2p						100%	
−2q						100%	
−3			17%		23%		14%
−4							
−5					27%		9%
−5p						12.5%	
−5q						12.5%	
−6	62.5%	100%	85%				48.5%
−6p						100%	
−6q						100%	
−7							
−8							4%
−8p						50%	
−8q						50%	
−9					40%		12%
−10	62.5%	100%	88%		93%		78%
−10p						100%	
−10q						100%	
−11							
−12				33%			1%
−13	37.5%	100%	75%		87%		68%
−13p						75%	
−13q						75%	
−14							
−15							
−16							
−17	62.5%	100%	80%		90%		82%
−17p						100%	
−17q						100%	
−18	25%				70%		25%
−18p						100%	
−18q						100%	
−19					13%		4%
−20							
−21	25%	100%	54%				34%
−21p						100%	
−21q						100%	
−22							
−X	37.5%				37%		14%
−Y	25%			33%	37%		14%

CGH indicates comparative genomic hybridization; FISH, fluorescent in situ hybridization; LOH, loss of heterozygosity; SNP, single-nucleotide polymorphism.

TABLE 4. Chromosomal Gains in Chromophobe Renal Cell Carcinoma (Variant Not Stated)

References	Verdorfer et al[40]	Yusenko et al[42]	Yokomizo et al[43]	
Methods	Cytogenetics and FISH	High-density SNP-oligoarry	High-resolution Whole-genomic SNP and CGH	Total
# of cases	3	30	8	41
+1	33%			2.4%
+2	33%			2.4%
+3	33%			2.4%
+4	66%			4.9%
+5	66%	6%		9.8%
+6	33%			2.4%
+7	66%	3%		12.2%
+7q			12.00%	
+8	33%			2.4%
+9	33%			2.4%
+10	66%	3%		7.3%
+11	66%			4.9%
+12	33%	3%		4.9%
+13	33%			2.4%
+14	66%			4.9%
+15	66%	3%		7.3%
+16	33%			2.4%
+17	66%			4.9%
+18	33%	3%		4.9%
+19	66%			4.9%
+20	66%			4.9%
+21	66%			4.9%
+22	33%			2.4%
+X				
+Y				

CGH indicates comparative genomic hybridization; FISH, fluorescent in situ hybridization; SNP, single-nucleotide polymorphism.

Brunelli et al[29] in 2005 conducted a study using FISH in 9 eosinophilic ChRCCs and found losses of chromosomes 1 (67%), 2 (56%), 6 (56%), 10 (44%), and 17 (78%), similar to the classic ChRCC, but with lower frequencies. Davis et al[35] examined the somatic genomic landscape of ChRCC using The Cancer Genome Atlas (TCGA); their study also included 19 eosinophilic ChRCCs that were evaluated by the SNP array analysis. The authors reported that only 53% (10/19) of eosinophilic ChRCCs showed the characteristic ChRCC copy number losses of chromosomes 1, 2, 6, 10, 13, and 17.[35] Interestingly, 4 of 19 eosinophilic cases exhibited diploid karyotypes and did not show any CNAs.[35]

In 2019, Ohashi et al[38] evaluated by SNP 24 eosinophilic ChRCCs in a combined Swiss/TCGA/KICH cohorts [Swiss, TCGA, and kidney chromophobe dataset (KICH)], and found losses of chromosomes 1, 2, 6, 10, 13, 17, and 21, similar to the pattern seen in classic ChRCC, but with lower frequencies of individual chromosomal losses.[38] Further, 10 of 24 (41.7%) of eosinophilic ChRCC showed absence of losses of any chromosomes [vs. 6/75 (6%) of the classic ChRCC].[38] Figure 2 shows the distribution of chromosomal losses in the above-mentioned studies and Table 5 documents detailed findings by chromosomes and methodologies used. Further, Figure 3 demonstrates comparison distribution of chromosomal losses and gains between classic and eosinophilic ChRCCs.

Most recently, a study by Liu et al[47] utilizing the a-CGH +SNP array identified 10 eosinophilic ChRCCs that showed multiple chromosomal abnormalities. The cases were identified through a review of cases considered "atypical sporadic oncocytic tumors." Four ChRCCs were hypodiploid with characteristic losses of chromosomes 1, 2, 6, 10, 11, 16, and 17. The remaining 6 cases had multiple relative chromosomal losses due to hypotetraploidy (doubled hypodiploid genomes). Detailed analysis showed that cases with 4n ploidy status had 2-copy loss of chromosomes Y, 1, 2, 6, 10, 13, and 17,

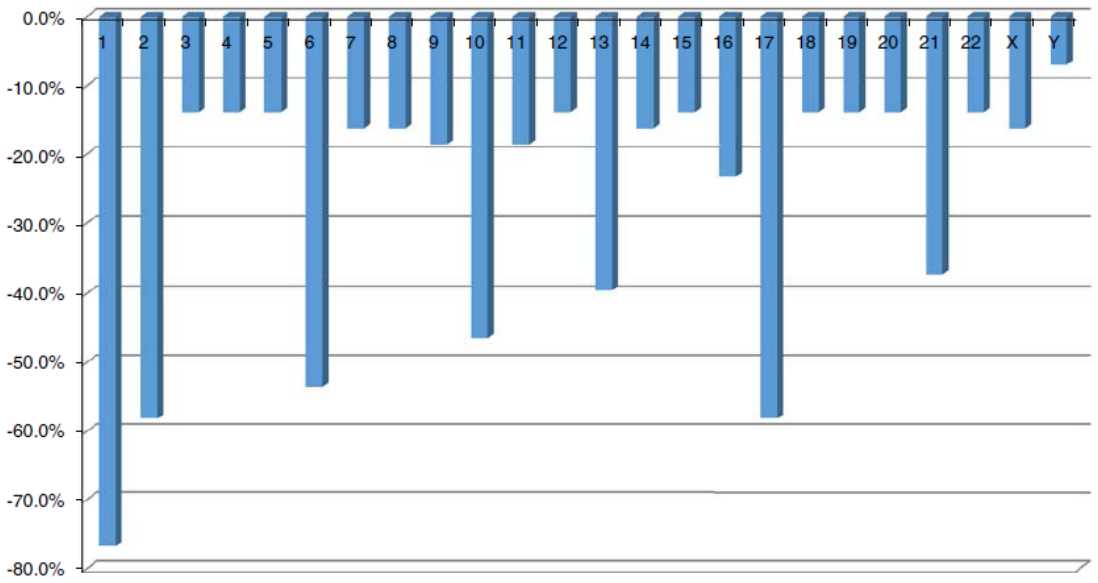

FIGURE 2. Distribution of chromosomal losses in eosinophilic chromophobe renal cell carcinoma (N = 43*). *Davis et al's[35] study data (N = 19) were not included in this analysis since no detail breakdown information were available. The authors reported loss of one copy of the entire chromosome, for most or all of chromosomes 1, 2, 6, 10, 13, and 17, seen in the majority of their cases (86%).

TABLE 5. Chromosomal Losses in Eosinophilic Chromophobe Renal Cell Carcinoma

References	Brunelli et al[29]	Davis et al[35]	Ohashi et al[38]	Liu et al[47]	
Method	FISH	SNP Array*	SNP	Cytogenomic Microarray Analysis	Total
# of cases	9	19	24	10	62
−1	67%		70.8%	100%	76.7%
−2	56%		41.7%	100%	58.1%
−3				60%	14.0%
−4				60%	14.0%
−5				60%	14.0%
−6	56%		41.7%	80%	53.5%
−7				70%	16.3%
−8				70%	16.3%
−9				80%	18.6%
−10	44%		33.3%	80%	46.5%
−11				80%	18.6%
−12				60%	14.0%
−13			45.8%	60%	39.5%
−14				70%	16.3%
−15				60%	14.0%
−16				100%	23.3%
−17	78%		45.8%	70%	58.1%
−18				60%	14.0%
−19				60%	14.0%
−20				60%	14.0%
−21			41.7%	60%	37.2%
−22				60%	14.0%
−X				70%	16.3%
−Y				30%	7.0%

*A total of 19 cases were examined with no breakdown details. The authors reported loss of one copy of the entire chromosome, for most or all of chromosomes 1, 2, 6, 10, 13, and 17, seen in the majority of their cases (86%). Further, they showed losses of chromosomes 3, 5, 8, 9, 11, 18, and 21 at significant frequencies (12% to 58%).

FISH indicates fluorescent in situ hybridization; SNP, single-nucleotide polymorphism.

consistent with typical ChRCC genetic profile, whereas chromosomes 3, 4, 7, 12, 14, 15, 16, 18, 20, and 22 frequently had 3 to 4 copies. The status of chromosomes with 2 copies and LOH indicated that one copy of these chromosomes was most likely lost initially in the diploid state (2n) before whole-genome endoduplication, while chromosomes with 2 or 3 copy numbers without LOH likely originated due to subsequent loss in the tetraploid state (4n), after the whole-genome endopduplication event.[47]

The above-mentioned studies on eosinophilic ChRCC show that most common chromosomal losses are 1 (76.7%), 2 (58.1%), 17 (58.1%), 6 (53.5%), 10 (46.5%), 13 (39.5%), and 21 (37.2%). No chromosomal gains were found in eosinophilic ChRCCs.

SARCOMATOID CHROMOPHOBE RENAL CELL CARCINOMA

Sarcomatoid differentiation in ChRCC, although rare, has been well-documented and, as in other types of RCC, carries a poor prognosis for the patient. Five studies investigated copy number changes in sarcomatoid ChRCC analyzing 20 tumors in total.[19,28,34,36,37] The methodologies used in these studies included cytogenetics (1 case), FISH (6 cases), CGH (8 cases in 2 studies, each 4 cases) and a-CGH/FISH (5 cases). Figure 4 shows the distribution of chromosomal losses and gains in these studies and Tables 6 and 7 present tables with detailed findings.

A cytogenetic-based study showed losses of chromosomes X, 1, 2, 6, 10, 13, and 17, with no chromosomal gains.[28] In contrast, Brunelli et al[19] found that the numerical chromosomal changes in sarcomatoid ChRCC are different from those found in ChRCCs with epithelial component only. They found >1 signal for most of the tested chromosomes in 4 of 6 cases, including multiple gains (polysomy) of chromosomes 1, 2, 6, 10, and 17.[19]

Kang et al[36] in a-CGH-based study examined the chromosomal changes in 4 cases of sarcomatoid ChRCC. They found gain of chromosome 3p to be significantly more frequent in these tumors compared with classic ChRCC.[36] They also found losses of 2p12-32 and 11p11-15 as additional chromosomal changes in sarcomatoid ChRCC.[36] Using a similar method (CGH), Ren et al[37] studied chromosomal aberrations in 4 sarcomatoid ChRCCs and found losses of chromosomes 1p, 2q, 21q21-22, 11p12-15, 11p11.2, 9p21, and 8p21-23. The authors also reported gains of chromosomes 3q13-21, 1q31, 9q21, 16p24/21-25, 3p24, 1q21-23, 1q11, 2p23-24, 1p13-15, and 3p21-ter.

Sperga et al[34] studied chromosomal abnormalities in 5 sarcomatoid ChRCCs and found losses of chromosome 10 and 17 and gains of chromosome 3, 4, 5, 7, 8, 9, 11, 12, 14, 15, 18, 19, 20, and 22. Similar to Brunelli et al,[19] they found concurrent chromosomal aberrations in both sarcomatoid and epithelial components in the majority of cases.[34]

Studies on sarcomatoid ChRCCs show that most common chromosomal gains are: 3 (100%), 1 (89.5%), 2 (42.1%), 10 (31.6%), 17 (31.6%), 4 (26.3%), 7 (26.3%), 8 (26.3%), 9 (26.3%), and 15 (26.3%). The most common chromosomal losses in these tumors are: 11 (30%), 2 (30%), 17 (20%), and 10 (20%), which are much less in frequency compared with classic ChRCCs.

OTHER VARIANTS OF CHROMOPHOBE RENAL CELL CARCINOMA

In addition to the well-recognized classic, eosinophilic, and sarcomatoid ChRCC, other architectural/morphologic variants such as ChRCC with pigmented microcystic adenomatoid/multicystic growth[5–7,48] (Figs. 5A–C), ChRCC with neuroendocrine differentiation[4,8,9,49,50] (Fig. 5D), ChRCC with papillary architecture[10] (Figs. 5E, F), and RO-like ChRCC variant[51] have also been described.

Adenomatoid microcystic pigmented ChRCC was first described in 1998 by Michal et al,[5] followed by a series of 20 cases in 2005[6] reported by the same group using FISH. Loss of chromosomes 1, 2, 6, 10, 13, and 21 was found in 100%, 36%, 91%, 82%, 82%, 82%, and 64% of cases, respectively. Additional series of 10 ChRCCs demonstrating a distinct multicystic growth pattern was subsequently reported,[48] with genetic features similar to those observed in the microcystic adenomatoid pigmented ChRCC. Using a-CGH in 5 cases, they found multiple losses of chromosomes 1p, 2q, 6, 13, 17, 21, and X in 2 cases, while 3 cases showed no numerical chromosomal aberrations. Most recently Gutiérrez et al[52] studied 42 cases of microcystic pigmented ChRCC using silver-enhanced in situ hybridization and found monosomy of 7 and 17 chromosomes in 1 of 36 cases and 2 of 37 cases, respectively. They also reported polysomy of chromosome 7 (in 26/36 cases) and chromosome 17 (in 4/37 cases).

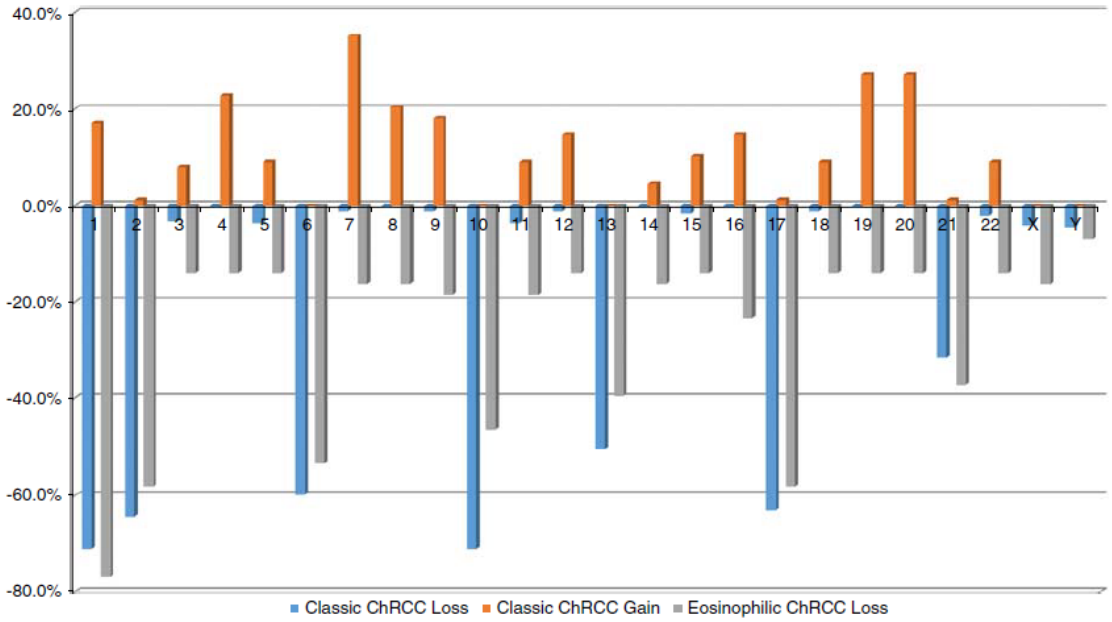

FIGURE 3. Distribution of chromosomal losses and gains in classic and eosinophilic chromophobe renal cell carcinoma (ChRCC). No chromosomal gains were reported in eosinophilic ChRCC in the literatre.

There are 2 case series and 3 case reports describing ChRCC with true neuroendocrine differentiation confirmed by immunohistochemistry and ChRCC with a neuroendocrine-like pattern (histologically similar to neuroendocrine tumors but immunohistochemically negative for neuroendocrine markers).[4,8,9,49,50] The case series by Ohe et al[49] used a-CGH in evaluating 2 ChRCC with neuroendocrine differentiation (in total they studied 3 cases, of which 1 was negative immunohistochemically for neuroendocrine markers) and they found losses of chromosomes 1, 2, 6, 10, 17, 21, and Y in both classic ChRCC and neuroendocrine areas. They also reported losses of chromosomes 1, 2, 4, 6, 9, 10, 13, 16p, 17, and 21 in both tumor components of a second case, although a loss of chromosome 5 was identified only in the neuroendocrine area. The authors

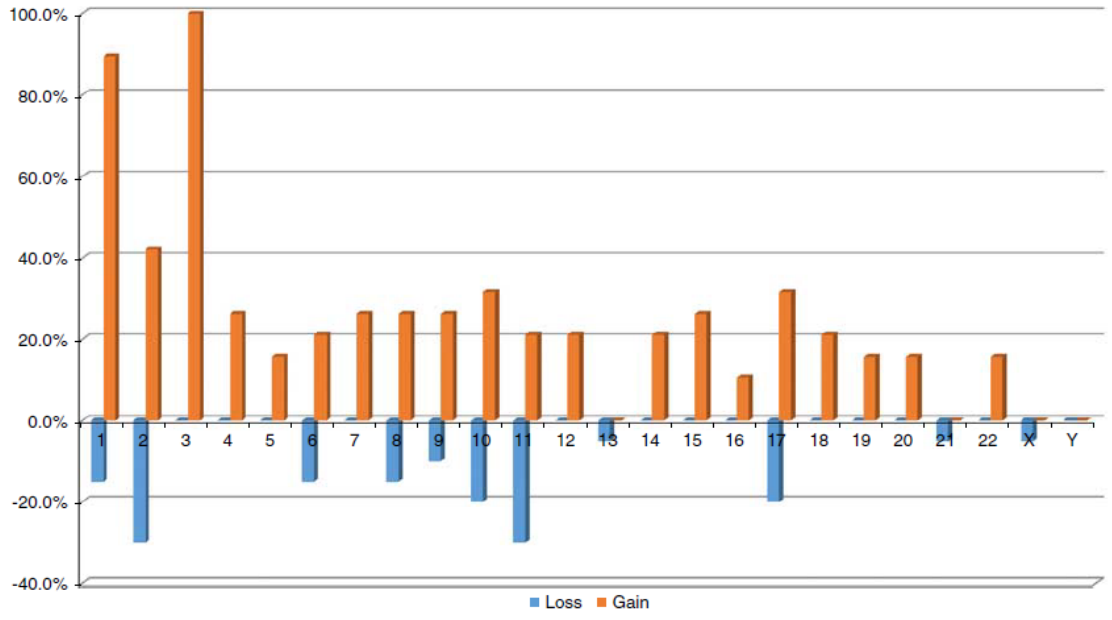

FIGURE 4. Distribution of chromosomal losses and gains in sarcomatoid chromophobe renal cell carcinoma (N = 20).

TABLE 6. Chromosomal Losses in Sarcomatoid Chromophobe Renal Cell Carcinoma

References	Gunawan et al[28]	Brunelli et al[19]	Sperga et al[34]	Ren et al[37]	Kang et al[36]	
Method	Cytogenetics	FISH	a-CGH and FISH	CGH and Whole-exome Sequencing	CGH	Total
# of cases	1	6	5	4	4	20
−1	100%	17%				15.0%
−1p				25%		
−2	100%	17%				30.0%
−2q				50%		
−2q12-32					50%	
−3						
−4						
−5						
−6	100%	33%				15.0%
−7						
−8						15.0%
−8p21-23				75%		
−9						10.0%
−9q21				50%		
−10	100%		60%			20.0%
−11						30.0%
−11p11.2				50%		
−11p11-15					50%	
−11p12-15				50%		
−12						
−13	100%					5.0%
−14						
−15						
−16						
−17	100%		60%			20.0%
−18						
−19						
−20						
−21						5.0%
−21q21-22				25%		
−22						
−X	100%					5.0%
−Y						

a-CGH indicates array comparative genomic hybridization; CGH, comparative genomic hybridization; FISH, fluorescent in situ hybridization.

found no chromosomal gains in these 2 tumors. A series of 18 unusual ChRCCs with complex architecture, including 4 with neuroendocrine differentiation and 14 with neuroendocrine-like pattern were evaluated by a-CGH and FISH methods.[4] Losses of chromosomes 1, 2, 6, and 10 were found in 3 of 4 analyzable ChRCCs with neuroendocrine differentiation, while multiple losses of chromosomes 1, 2, 6, 10, 13, 17, and 21 and gains of chromosomes 4, 11, 12, 14, 15, 16, 19, and 20 were found in 7 of 14 cases.

Kuroda et al[51] described an oncocytic variant of ChRCC reporting 5 tumors almost indistinguishable from RO. Using FISH, they found monosomy of chromosomes 7, 10, 13, and 17 in all 5 cases and loss of chromosome 21 in 4 of 5 cases.[51]

We have recently described a series of 8 ChRCC with predominant papillary architectural growth pattern.[10] Using a-CGH, 2 of 3 analyzable cases showed losses of chromosomes 1p36.33-p36.22, 9q21.11-q34.3, 1, 2, 6, 10, and 17, while the third case showed gains of chromosomes 4, 5, 7, 12, 14, 15q11.2-q25.3, 18, 19, 20, and 22.[10]

DISCUSSION

Since the introduction of ChRCC as a distinct histologic RCC entity,[1] many studies have examined the chromosomal CNA in ChRCC, using various cytogenetic and molecular methods.

Historically, multiple losses of chromosomes 1, 2, 6, 10, 13, 17, and 21 have been considered a genetic hallmark of ChRCC, both for classic and eosinophilic variants. In the early years, the pioneering investigators used classic cytogenetics, a common and available method at the time, and found that classic ChRCC is associated with multiple losses of chromosomes 1, 2, 3, 6, 7, 9, 10, 12, 13, 17, 18, and 21.[17,18,22–24,53] These findings were corroborated by studies using methods that included RFLP, CGH, microsatellite analyses, FISH, and a-CGH.[4,18,19,21,29–31,34,35,37–41,43,44,48,54,55] TCGA analysis of ChRCC confirmed the characteristic pattern of chromosomal losses of 1, 2, 6, 10, 13, and 17 in 86% of tumors, as well as documented additional losses of chromosomes 3, 5, 8, 9, 11 and 18, and 21q in 12% to 58% of tumors.[56] Of note, the analyzed tumors were mainly classic ChRCCs.

In the last 2 decades, multiple studies have also demonstrated multiple chromosomal gains in ChRCC.[4,19–21,34,36,37,40] Although this has generally been deemed an uncommon phenomenon in ChRCC, studies with larger cohorts showed a more variable genetic profile of ChRCC with multiple chromosomal losses as well as multiple gains.[4,19–21,34,36,37,40] Most frequently detected chromosomal gains were 4, 7, 15, 19, and

TABLE 6. Chromosomal Losses in Sarcomatoid Chromophobe Renal Cell Carcinoma

References	Gunawan et al[28]	Brunelli et al[19]	Sperga et al[34]	Ren et al[37]	Kang et al[36]	
Method	Cytogenetics	FISH	a-CGH and FISH	CGH and Whole-exome Sequencing	CGH	Total
# of cases	1	6	5	4	4	20
−1	100%	17%				15.0%
−1p				25%		
−2	100%	17%				30.0%
−2q				50%		
−2q12-32					50%	
−3						
−4						
−5						
−6	100%	33%				15.0%
−7						
−8						15.0%
−8p21-23				75%		
−9						10.0%
−9q21				50%		
−10	100%		60%			20.0%
−11						30.0%
−11p11.2				50%		
−11p11-15					50%	
−11p12-15				50%		
−12						
−13	100%					5.0%
−14						
−15						
−16						
−17	100%		60%			20.0%
−18						
−19						
−20						
−21						5.0%
−21q21-22				25%		
−22						
−X	100%					5.0%
−Y						

a-CGH indicates array comparative genomic hybridization; CGH, comparative genomic hybridization; FISH, fluorescent in situ hybridization.

found no chromosomal gains in these 2 tumors. A series of 18 unusual ChRCCs with complex architecture, including 4 with neuroendocrine differentiation and 14 with neuroendocrine-like pattern were evaluated by a-CGH and FISH methods.[4] Losses of chromosomes 1, 2, 6, and 10 were found in 3 of 4 analyzable ChRCCs with neuroendocrine differentiation, while multiple losses of chromosomes 1, 2, 6, 10, 13, 17, and 21 and gains of chromosomes 4, 11, 12, 14, 15, 16, 19, and 20 were found in 7 of 14 cases.

Kuroda et al[51] described an oncocytic variant of ChRCC reporting 5 tumors almost indistinguishable from RO. Using FISH, they found monosomy of chromosomes 7, 10, 13, and 17 in all 5 cases and loss of chromosome 21 in 4 of 5 cases.[51]

We have recently described a series of 8 ChRCC with predominant papillary architectural growth pattern.[10] Using a-CGH, 2 of 3 analyzable cases showed losses of chromosomes 1p36.33-p36.22, 9q21.11-q34.3, 1, 2, 6, 10, and 17, while the third case showed gains of chromosomes 4, 5, 7, 12, 14, 15q11.2-q25.3, 18, 19, 20, and 22.[10]

DISCUSSION

Since the introduction of ChRCC as a distinct histologic RCC entity,[1] many studies have examined the chromosomal CNA in ChRCC, using various cytogenetic and molecular methods.

Historically, multiple losses of chromosomes 1, 2, 6, 10, 13, 17, and 21 have been considered a genetic hallmark of ChRCC, both for classic and eosinophilic variants. In the early years, the pioneering investigators used classic cytogenetics, a common and available method at the time, and found that classic ChRCC is associated with multiple losses of chromosomes 1, 2, 3, 6, 7, 9, 10, 12, 13, 17, 18, and 21.[17,18,22–24,53] These findings were corroborated by studies using methods that included RFLP, CGH, microsatellite analyses, FISH, and a-CGH.[4,18,19,21,29–31,34,35,37–41,43,44,48,54,55] TCGA analysis of ChRCC confirmed the characteristic pattern of chromosomal losses of 1, 2, 6, 10, 13, and 17 in 86% of tumors, as well as documented additional losses of chromosomes 3, 5, 8, 9, 11 and 18, and 21q in 12% to 58% of tumors.[56] Of note, the analyzed tumors were mainly classic ChRCCs.

In the last 2 decades, multiple studies have also demonstrated multiple chromosomal gains in ChRCC.[4,19–21,34,36,37,40] Although this has generally been deemed an uncommon phenomenon in ChRCC, studies with larger cohorts showed a more variable genetic profile of ChRCC with multiple chromosomal losses as well as multiple gains.[4,19–21,34,36,37,40] Most frequently detected chromosomal gains were 4, 7, 15, 19, and

TABLE 7. Chromosomal Gains in Sarcomatoid Chromophobe Renal Cell Carcinoma

References	Brunelli et al[19]	Sperga et al[34]	Ren et al[37]	Kang et al[36]	
Method	FISH	a-CGH and FISH	CGH and Whole-exome sequencing	CGH	Total
# of cases	6	5	4	4	19
+1	83%				89.5%
+1q31			25%		
+1p13-15			100%		
+1q21-23			100%		
+1q11			75%		
+2	83%				42.1%
+2p23-24			75%		
+3		100%			100.0%
+3p				100%	
+3p21-ter			100%		
+3q13-21			75%		
+3q24			75%		
+4		100%			26.3%
+5		60%			15.8%
+5q					
+6	67%				21.1%
+7		100%			26.3%
+8		100%			26.3%
+9		80%			26.3%
+9q21			25%		
+10	100%				31.6%
+11		80%			21.1%
+11p12p15.1					
+12		80%			21.1%
+13					
+14		80%			21.1%
+15		100%			26.3%
+16					10.5%
+16p24/21-25			50%		
+17	100%				31.6%
+18		80%			21.1%
+19		60%			15.8%
+20		60%			15.8%
+21					
+22		60%			15.8%
+X					
+Y					

a-CGH indicates array comparative genomic hybridization; CGH, comparative genomic hybridization; FISH, fluorescent in situ hybridization.

20.[4,19–21,34,36,37,40] Unlike classic ChRCC, diploid chromosomal pattern was more commonly found in the eosinophilic variant. In the studies by Davis et al[35] and Ohashi et al,[38] 33% (14/43) of eosinophilic ChRCCs showed diploid status. We also recognize that some cases with diploid chromosomal pattern, suspicious for eosinophilic ChRCC, may in fact represent RO with atypical features or novel emerging entities. It is worth noting that only few studies reported diploid chromosomal copy numbers in classic ChRCC,[19,30,45,46] indicating that the landscape of molecular genetic abnormalities of ChRCC encompasses a considerably broader spectrum than previously thought. It should be noted that although both RO and ChRCC arise from the distal nephron, they do not represent a continuum of progression from benign to malignant disease. Even eosinophilic ChRCC, which share some morphologic features with RO, has a different CNA and gene expression landscape than RO.[35]

In addition to classic and eosinophilic variants, sarcomatoid differentiation in ChRCC, although uncommon, has been investigated for CNA.[19,28,34,36,37] It appears that these tumors carry multiple chromosomal gains including 1, 2, 6, 10, and 17, which are often different than the CNA seen in the epithelial component. Overall, sarcomatoid ChRCCs tend to have higher frequency of chromosomal gains, particularly in 1, 2, and 3. In contrast, these tumors appear to have lower frequency of chromosomal losses.

Studies of other rare ChRCC variants such as ChRCC with pigmented microcystic adenomatoid/multicystic growth,[5–7,48] ChRCC with neuroendocrine differentiation,[4,8,9,49,50] ChRCC with papillary architecture,[10] and RO-like ChRCC variant[51] also showed variable chromosomal numerical aberrations including multiple losses (more common) and gains (less common). CNA in metastatic ChRCCs appear to show that distant metastases demonstrate the same genetic patterns, usually chromosomal losses (monosomy), found in the primary tumors.[19]

Liu et al[47] recently discovered that ChRCC could be either hypodiploid with characteristic monosomies of chromosomes 1, 2, 6, 10, 13, and 17, or can show double hypodiploidy (4n), with relative chromosomal losses of the same set of chromosomes. This important observation of chromosomal endoduplication could explain the heterogeneity of chromosomal numeric aberrations resulting in combined losses and gains. They suggested that the phenomenon of doubled hypodiploidy, commonly observed in ChRCC, could be explained by coexisting intra-tumoral clones and/or compensatory polyploidization of the genetic imbalances, to maintain tumor viability. Additional studies comparing ChRCC with hypodiploidy and doubled hypodiploidy could help better understand their biological behavior, morphologic variation, and clinical associations.

Hybrid oncocytic/chromophobe tumors, commonly associated with Birt-Hogg-Dubé syndrome, represent a poorly understood and genetically heterogenous group of tumors that may have mixed RO and ChRCC features.[57] Recent studies have shown that these tumors cytogenetically fall between RO and ChRCC, although clustering closer to RO than to ChRCC based on RNA transcript data.[47,57] Iribe et al[58] also studied 19 tumors associated with Birt-Hogg-Dubé syndrome (12 ChRCCs, 5 hybrid oncocytic/chromophobe tumors, and 2 clear-cell RCCs) using the SNP array. The authors found 8 had balanced genomic profiles, 2 had gains in chromosome 3q, and 1 had gains in chromosomes 1q and 7.

TCGA of ChRCC showed that *TP53* and *PTEN* are the most frequently mutated genes in ChRCCs.[56,59] Loss of *CDKN2A* or its expression, by either deletion of 9p21.3 or hypermethylation, was the second most common alteration.[56,59] In addition, pathway analysis demonstrated alterations in PI3K-AKT-mTOR pathway genes, including *PTEN*, *TSC1*, *TSC2*, and *MTOR*, in ChRCCs, which would potentially result in appropriate targets for mTOR inhibitors.[38,56,59]

In summary, genomic instability, including the whole-chromosome aneuploidy, is a hallmark of human cancer, but the level of chromosomal losses and gains observed in ChRCC is remarkable. Earlier studies have shown that ChRCC characteristically demonstrates a unique pattern of chromosomal losses of 1, 2, 6, 10, 13, and 17. Subsequent studies, however, showed variable morphologies and genetic profiles with combinations of chromosomal losses and gains, suggesting that ChRCC represents a heterogenous group of neoplasms both from a morphologic and a chromosomal genetic perspective. Therefore, the role of routine evaluation of the chromosomal numerical aberrations in the differential diagnosis of ChRCC may be limited.

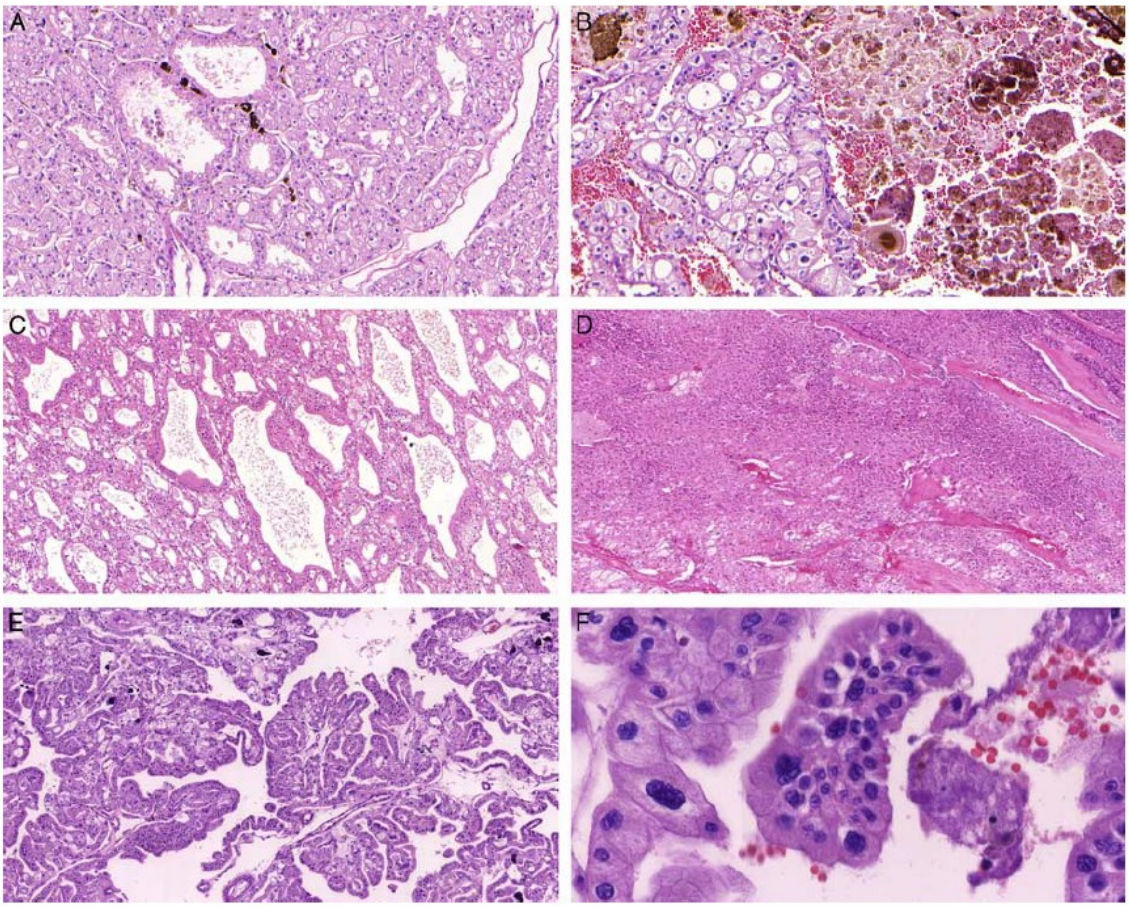

FIGURE 5. A, Adenomatoid pigmented chromophobe renal cell carcinoma (ChRCC) with complex architecture showing tubular and cribriform patterns. B, Adenomatoid pigmented ChRCC. Leaf-like cells with perinuclear clearing and voluminous deposits of lipochrome. C, Multicystic pattern in ChRCC as an unusual architectural pattern, while cytologic features are identical to classic ChRCC. D, ChRCC with neuroendocrine differentiation. Neuroendocrine differentiation must be confirmed by immunohistochemistry. E, ChRCC with papillary pattern. Rarely, ChRCC can be arranged in true papillary pattern; however, in majority of cases such structures formed only part of tumorous volume. F, ChRCC with papillary pattern in high-power view demonstrated typical raisinoid nuclei.

REFERENCES

1. Thoenes W, Storkel S, Rumpelt HJ. Human chromophobe cell renal carcinoma. *Virchows Arch B Cell Pathol Incl Mol Pathol*. 1985;48:207–217.
2. Amin MB, Paner GP, Alvarado-Cabrero I, et al. Chromophobe renal cell carcinoma: histomorphologic characteristics and evaluation of conventional pathologic prognostic parameters in 145 cases. *Am J Surg Pathol*. 2008;32:1822–1834.
3. Thoenes W, Storkel S, Rumpelt HJ, et al. Chromophobe cell renal carcinoma and its variants—a report on 32 cases. *J Pathol*. 1988;155:277–287.
4. Peckova K, Martinek P, Ohe C, et al. Chromophobe renal cell carcinoma with neuroendocrine and neuroendocrine-like features. Morphologic, immunohistochemical, ultrastructural, and array comparative genomic hybridization analysis of 18 cases and review of the literature. *Ann Diagn Pathol*. 2015;19:261–268.
5. Michal M, Hes O, Svec A, et al. Pigmented microcystic chromophobe cell carcinoma: a unique variant of renal cell carcinoma. *Ann Diagn Pathol*. 1998;2:149–153.
6. Hes O, Vanecek T, Perez-Montiel DM, et al. Chromophobe renal cell carcinoma with microcystic and adenomatous arrangement and pigmentation—a diagnostic pitfall. Morphological, immunohistochemical, ultrastructural and molecular genetic report of 20 cases. *Virchows Arch*. 2005;446:383–393.
7. Dundr P, Pesl M, Povysil C, et al. Pigmented microcystic chromophobe renal cell carcinoma. *Pathol Res Pract*. 2007;203:593–597.
8. Kuroda N, Tamura M, Hes O, et al. Chromophobe renal cell carcinoma with neuroendocrine differentiation and sarcomatoid change. *Pathol Int*. 2011;61:552–554.
9. Parada DD, Pena KB. Chromophobe renal cell carcinoma with neuroendocrine differentiation. *APMIS*. 2008;116:859–865.
10. Michalova K, Tretiakova M, Pivovarcikova K, et al. Expanding the morphologic spectrum of chromophobe renal cell carcinoma: a study of 8 cases with papillary architecture. *Ann Diagn Pathol*. 2019;44:151448.
11. Beck SD, Patel MI, Snyder ME, et al. Effect of papillary and chromophobe cell type on disease-free survival after nephrectomy for renal cell carcinoma. *Ann Surg Oncol*. 2004;11:71–77.

12. Przybycin CG, Cronin AM, Darvishian F, et al. Chromophobe renal cell carcinoma: a clinicopathologic study of 203 tumors in 200 patients with primary resection at a single institution. *Am J Surg Pathol*. 2011;35:962–970.
13. Ohashi R, Martignoni G, Hartmann A, et al. Multi-institutional re-evaluation of prognostic factors in chromophobe renal cell carcinoma: proposal of a novel two-tiered grading scheme. *Virchows Arch*. 2020;476:409–418.
14. Delahunt B, Cheville JC, Martignoni G, et al. Members of the ISUP Renal Tumor Panel. The International Society of Urological Pathology (ISUP) grading system for renal cell carcinoma and other prognostic parameters. *Am J Surg Pathol*. 2013;37:1490–1504.
15. Paner GP, Amin MB, Alvarado-Cabrero I, et al. A novel tumor grading scheme for chromophobe renal cell carcinoma: prognostic utility and comparison with Fuhrman nuclear grade. *Am J Surg Pathol*. 2010;34:1233–1240.
16. Iqbal MA, Akhtar M, Ali MA. Cytogenetic findings in renal cell carcinoma. *Hum Pathol*. 1996;27:949–954.
17. Kovacs A, Kovacs G. Low chromosome number in chromophobe renal cell carcinomas. *Genes Chromosomes Cancer*. 1992;4:267–268.
18. Speicher MR, Schoell B, du Manoir S, et al. Specific loss of chromosomes 1, 2, 6, 10, 13, 17, and 21 in chromophobe renal cell carcinomas revealed by comparative genomic hybridization. *Am J Pathol*. 1994;145:356–364.
19. Brunelli M, Gobbo S, Cossu-Rocca P, et al. Chromosomal gains in the sarcomatoid transformation of chromophobe renal cell carcinoma. *Mod Pathol*. 2007;20:303–309.
20. Tan MH, Wong CF, Tan HL, et al. Genomic expression and single-nucleotide polymorphism profiling discriminates chromophobe renal cell carcinoma and oncocytoma. *BMC Cancer*. 2010;10:196.
21. Vieira J, Henrique R, Ribeiro FR, et al. Feasibility of differential diagnosis of kidney tumors by comparative genomic hybridization of fine needle aspiration biopsies. *Genes Chromosomes Cancer*. 2010;49:935–947.
22. Kovacs G, Soudah B, Hoene E. Binucleated cells in a human renal cell carcinoma with 34 chromosomes. *Cancer Genet Cytogenet*. 1988;31:211–215.
23. Kovacs A, Storkel S, Thoenes W, et al. Mitochondrial and chromosomal DNA alterations in human chromophobe renal cell carcinomas. *J Pathol*. 1992;167:273–277.
24. Crotty TB, Lawrence KM, Moertel CA, et al. Cytogenetic analysis of six renal oncocytomas and a chromophobe cell renal carcinoma. Evidence that -Y, -1 may be a characteristic anomaly in renal oncocytomas. *Cancer Genet Cytogenet*. 1992;61:61–66.
25. van den Berg E, van der Hout AH, Oosterhuis JW, et al. Cytogenetic analysis of epithelial renal-cell tumors: relationship with a new histopathological classification. *Int J Cancer*. 1993;55:223–227.
26. Gerharz CD, Moll R, Storkel S, et al. Establishment and characterization of two divergent cell lines derived from a human chromophobe renal cell carcinoma. *Am J Pathol*. 1995;146:953–962.
27. Shuin T, Kondo K, Sakai N, et al. A case of chromophobe renal cell carcinoma associated with low chromosome number and microsatellite instability. *Cancer Genet Cytogenet*. 1996;86:69–71.
28. Gunawan B, Bergmann F, Braun S, et al. Polyploidization and losses of chromosomes 1, 2, 6, 10, 13, and 17 in three cases of chromophobe renal cell carcinomas. *Cancer Genet Cytogenet*. 1999;110:57–61.
29. Brunelli M, Eble JN, Zhang S, et al. Eosinophilic and classic chromophobe renal cell carcinomas have similar frequent losses of multiple chromosomes from among chromosomes 1, 2, 6, 10, and 17, and this pattern of genetic abnormality is not present in renal oncocytoma. *Mod Pathol*. 2005;18:161–169.
30. Meyer PN, Cao Y, Jacobson K, et al. Chromosome 1 analysis in chromophobe renal cell carcinomas with tissue microarray (TMA)-facilitated fluorescence in situ hybridization (FISH) demonstrates loss of 1p/1 which is also present in renal oncocytomas. *Diagn Mol Pathol*. 2008;17:141–144.
31. Kim HJ, Shen SS, Ayala AG, et al. Virtual-karyotyping with SNP microarrays in morphologically challenging renal cell neoplasms: a practical and useful diagnostic modality. *Am J Surg Pathol*. 2009;33:1276–1286.
32. Brunelli M, Delahunt B, Gobbo S, et al. Diagnostic usefulness of fluorescent cytogenetics in differentiating chromophobe renal cell carcinoma from renal oncocytoma: a validation study combining metaphase and interphase analyses. *Am J Clin Pathol*. 2010;133:116–126.
33. Kuroda N, Tamura M, Hes O, et al. Chromophobe renal cell carcinoma with prominent lymph node metastasis and polysomy of chromosome 21: poorly differentiated form or "presarcomatoid" form? *Med Mol Morphol*. 2011;44:168–173.
34. Sperga M, Martinek P, Vanecek T, et al. Chromophobe renal cell carcinoma—chromosomal aberration variability and its relation to Paner grading system: an array CGH and FISH analysis of 37 cases. *Virchows Arch*. 2013;463:563–573.
35. Davis CF, Ricketts CJ, Wang M, et al. The Cancer Genome Atlas Research Network. The somatic genomic landscape of chromophobe renal cell carcinoma. *Cancer Cell*. 2014;26:319–330.
36. Kang XL, Zou H, Pang LJ, et al. Chromosomal imbalances revealed in primary renal cell carcinomas by comparative genomic hybridization. *Int J Clin Exp Pathol*. 2015;8:3636–3647.
37. Ren Y, Liu K, Kang X, et al. Chromophobe renal cell carcinoma with and without sarcomatoid change: a clinicopathological, comparative genomic hybridization, and whole-exome sequencing study. *Am J Transl Res*. 2015;7:2482–2499.
38. Ohashi R, Schraml P, Angori S, et al. Classic chromophobe renal cell carcinoma incur a larger number of chromosomal losses than seen in the eosinophilic subtype. *Cancers (Basel)*. 2019;11:1492.
39. Bugert P, Kovacs G. Molecular differential diagnosis of renal cell carcinomas by microsatellite analysis. *Am J Pathol*. 1996;149:2081–2088.
40. Verdorfer I, Hobisch A, Hittmair A, et al. Cytogenetic characterization of 22 human renal cell tumors in relation to a histopathological classification. *Cancer Genet Cytogenet*. 1999;111:61–70.
41. Yusenko MV, Kovacs G. Identifying CD82 (KAI1) as a marker for human chromophobe renal cell carcinoma. *Histopathology*. 2009;55:687–695.
42. Yusenko MV, Kuiper RP, Boethe T, et al. High-resolution DNA copy number and gene expression analyses distinguish chromophobe renal cell carcinomas and renal oncocytomas. *BMC Cancer*. 2009;9:152.
43. Yokomizo A, Yamamoto K, Furuno K, et al. Histopathologic subtype-specific genomic profiles of renal cell carcinomas identified by high-resolution whole-genome single nucleotide polymorphism array analysis. *Oncol Lett*. 2010;1:1073–1078.
44. Bugert P, Gaul C, Weber K, et al. Specific genetic changes of diagnostic importance in chromophobe renal cell carcinomas. *Lab Invest*. 1997;76:203–208.
45. Renshaw AA, Henske EP, Loughlin KR, et al. Aggressive variants of chromophobe renal cell carcinoma. *Cancer*. 1996;78:1756–1761.
46. Casuscelli J, Weinhold N, Gundem G, et al. Genomic landscape and evolution of metastatic chromophobe renal cell carcinoma. *JCI Insight*. 2017;2:e92688.
47. Liu YJ, Ussakli C, Antic T, et al. Sporadic oncocytic tumors with features intermediate between oncocytoma and chromophobe renal cell carcinoma: comprehensive clinico-pathological and genomic profiling. *Hum Pathol*. 2020;104:18–29.
48. Foix MP, Dunatov A, Martinek P, et al. Morphological, immunohistochemical, and chromosomal analysis of multicystic chromophobe renal cell carcinoma, an architecturally unusual challenging variant. *Virchows Arch*. 2016;469:669–678.
49. Ohe C, Kuroda N, Matsuura K, et al. Chromophobe renal cell carcinoma with neuroendocrine differentiation/morphology: a clinicopathological and genetic study of three cases. *Hum Pathol Case Rep*. 2014;1:31–39.

50. Mokhtar GA, Al-Zahrani R. Chromophobe renal cell carcinoma of the kidney with neuroendocrine differentiation: a case report with review of literature. *Urol Ann*. 2015;7:383–386.
51. Kuroda N, Tanaka A, Yamaguchi T, et al. Chromophobe renal cell carcinoma, oncocytic variant: a proposal of a new variant giving a critical diagnostic pitfall in diagnosing renal oncocytic tumors. *Med Mol Morphol*. 2013;46:49–55.
52. Gutierrez FJQ, Panizo A, Tienza A, et al. Cytogenetic and immunohistochemical study of 42 pigmented microcystic chromophobe renal cell carcinoma (PMChRCC). *Virchows Arch*. 2018;473:209–217.
53. Akhtar M, Chantziantoniou N. Quantitative image cell analysis of cytologic smears for DNA ploidy in renal parenchymal neoplasms. *Diagn Cytopathol*. 1999;21:223–229.
54. Brunelli M, Fiorentino M, Gobbo S, et al. Many facets of chromosome 3p cytogenetic findings in clear cell renal carcinoma: the need for agreement in assessment FISH analysis to avoid diagnostic errors. *Histol Histopathol*. 2011;26:1207–1213.
55. Kato I, Iribe Y, Nagashima Y, et al. Fluorescent and chromogenic in situ hybridization of CEN17q as a potent useful diagnostic marker for Birt-Hogg-Dube syndrome-associated chromophobe renal cell carcinomas. *Hum Pathol*. 2016;52:74–82.
56. Linehan WM, Ricketts CJ. The Cancer Genome Atlas of renal cell carcinoma: findings and clinical implications. *Nat Rev Urol*. 2019;16:539–552.
57. Ruiz-Cordero R, Rao P, Li L, et al. Hybrid oncocytic/chromophobe renal tumors are molecularly distinct from oncocytoma and chromophobe renal cell carcinoma. *Mod Pathol*. 2019;32:1698–1707.
58. Iribe Y, Yao M, Tanaka R, et al. Genome-wide uniparental disomy and copy number variations in renal cell carcinomas associated with Birt-Hogg-Dube syndrome. *Am J Pathol*. 2016;186:337–346.
59. Ricketts CJ, De Cubas AA, Fan H, et al. Cancer Genome Atlas Research Network. The Cancer Genome Atlas Comprehensive molecular characterization of renal cell carcinoma. *Cell Rep*. 2018;23:3698.

3.7 Eosinophilic vacuolated tumor (EVT) of kidney demonstrates sporadic TSC/MTOR mutations: next-generation sequencing multi-institutional study of 19 cases.

Eosinophilic vacuolated tumor (EVT) of kidney is a unifying, consensus name proposed by Genitourinary Pathology Society (GUPS) for emerging entity arising from difficult to classify group of eosinophilic (oncocytic) kidney tumors. In the literature it was described under names "high-grade oncocytic renal tumor (HOT)" or "sporadic renal cell carcinoma with eosinophilic and vacuolated cytoplasm". In this multi-institutional study, we evaluated 19 EVTs, for their clinicopathological, immunohistochemical and particularly molecular features using next-generation sequencing.

All cases included in this study were sporadic and none of the patients had documented tuberous sclerosis complex. There were 8 men and 11 women, with the age range from 15 to 72 years. Pathologic stage ranged from pT1a to pT2b. Tumour size ranged from 1.5 to 11.5 cm. Follow-up data was available for 18 patients, all of them were alive and with no evidence of disease recurrence or progression during the follow-up period ranging from 12 to 198 months. All tumours were circumscribed but non-capsulated, with no necrosis and no visible macrocysts. Microscopically, tumours exhibited nested to solid growth pattern with focally present tubular architecture. On periphery of the tumour, prominent, thick-walled vessels were easily seen, as well as entrapped, non-neoplastic, small tubules. Tumours were composed of voluminous eosinophilic cells, prominent membranes with sticking, large intracytoplasmic vacuoles, round to oval nuclei, and prominent nucleoli corresponding to WHO/ISUP grade 3. Mitoses were exceptionally rare. Immunohistochemical profile was relatively consistent with positivity for Cathepsin K, CD117, CD10, and antimitochondrial antigen (MIA) in all cases, together with PAX8, AE1/AE3, and CK18. CK7 positivity was limited to scattered cells. Focal CK20 reactivity was exhibited in minority of cases. Negative staining included: vimentin, HMB45, Melan-A, and TFE3. All tumours showed retained SDHB expression. Proliferation index was less than 1%. Molecular studies in all cases revealed non-overlapping mutations of the mTOR pathway genes: *TSC1*, *TSC2*, and *MTOR*. One case with *MTOR* mutation showed a coexistent *RICTOR* missense mutation. All samples revealed low mutational rate. Microsatellite instability and copy number variations were not found in any of the 17 analyzable cases. Differential diagnosis includes mainly ambiguous group of oncocytic/eosinophilic, difficult to classify tumours, that EVT arose from. Other possible mimickers include: MiTF RCC (TFEB and TFE3), SDH-deficient RCC, and ESC RCC.

EVT represents an emerging renal entity with distinct morphology and typical genetic background with alteration of mTOR pathway. Up to date, based on limited evidence, EVT appears to follows a benign clinical course. However, future studies are necessary to confirm this conjecture.

www.nature.com/modpathol

ARTICLE

Eosinophilic vacuolated tumor (EVT) of kidney demonstrates sporadic *TSC/MTOR* mutations: next-generation sequencing multi-institutional study of 19 cases

Mihaela Farcaş[1,2], Zoran Gatalica[3], Kiril Trpkov[4,32], Jeffrey Swensen[5], Ming Zhou[6], Reza Alaghehbandan[7], Sean R. Williamson[8], Cristina Magi-Galluzzi[9], Anthony J. Gill[10,11], Maria Tretiakova[12], Jose I. Lopez[13], Delia Perez Montiel[14], Maris Sperga[15], Eva Comperat[16,17], Fadi Brimo[18], Asli Yilmaz[4], Farshid Siadat[4], Ankur Sangoi[19], Yuan Gao[20], Nikola Ptákova[21], Levente Kuthi[22], Kristyna Pivovarcikova[23], Joanna Rogala[23], Abbas Agaimy[24], Arndt Hartmann[24], Cristoph Fraune[25], Boris Rychly[26], Pavel Hurnik[27], Dušan Durcansky[28], Michael Bonert[29], Georgios Gakis[30], Michal Michal[23], Milan Hora[31] and Ondrej Hes[23,32]✉

A distinct renal tumor has recently been described as "high-grade oncocytic renal tumor" and "sporadic renal cell carcinoma with eosinophilic and vacuolated cytoplasm". The Genitourinary Pathology Society (GUPS) consensus proposed a unifying name "eosinophilic vacuolated tumor" (EVT) for this emerging entity. In this multi-institutional study, we evaluated 19 EVTs, particularly their molecular features and mutation profile, using next-generation sequencing. All cases were sporadic and none of the patients had a tuberous sclerosis complex. There were 8 men and 11 women, with a mean age of 47 years (median 50; range 15–72 years). Average tumor size was 4.3 cm (median 3.8 cm; range 1.5–11.5 cm). All patients with available follow-up data (18/19) were alive and without evidence of disease recurrence or progression during the follow-up, ranging from 12 to 198 months (mean 56.3, median 41.5 months). The tumors were well circumscribed, but lacked a well-formed capsule, had nested to solid growth, focal tubular architecture, and showed ubiquitous, large intracytoplasmic vacuoles, round to oval nuclei, and prominent nucleoli. Immunohistochemically, cathepsin K, CD117, CD10, and antimitochondrial antigen were expressed in all cases. Other positive stains included: PAX8, AE1/AE3 and CK18. CK7 was typically restricted only to rare scattered cells. Vimentin, HMB45, melan-A, and TFE3 were negative in all cases. All tumors showed retained SDHB. All cases (19/19) showed non-overlapping mutations of the mTOR pathway genes: *TSC1* (4), *TSC2* (7), and *MTOR* (8); one case with *MTOR* mutation showed a coexistent *RICTOR* missense mutation. Low mutational rates were found in all samples (ranged from 0 to 6 mutations/Mbp). Microsatellite instability and copy number variations were not found in any of the 17 analyzable cases. EVT represents an emerging renal entity that shows a characteristic and readily identifiable morphology, consistent immunohistochemical profile, indolent behavior, and mutations in either *TSC1*, *TSC2*, or *MTOR* genes.

Modern Pathology (2022) 35:344–351; https://doi.org/10.1038/s41379-021-00923-6

INTRODUCTION

Recently, two studies have described a distinct renal tumor, previously unrecognized and not listed in the 2016 WHO classification, that emerged from the group of difficult to classify eosinophilic (oncocytic) renal tumors[1,2]. This novel type of renal tumor had a readily recognizable morphology and was composed

[1]Department of Pathology, Colentina Clinical Hospital, Bucharest, Romania. [2]Onco Team Diagnostic, Bucharest, Romania. [3]Department of Pathology, Oklahoma University School of Medicine, Oklahoma, USA. [4]Department of Pathology and Laboratory Medicine, Cumming School of Medicine, University of Calgary, Calgary, Alberta, Canada. [5]Caris Life Sciences, Phoenix, AZ, USA. [6]Department of Pathology, Tufts Medical Center, Boston, MA, USA. [7]Department of Pathology, British Columbia University, Vancouver, Canada. [8]Robert J. Tomsich Pathology and Laboratory Medicine Institute, Cleveland Clinic, Cleveland, OH, USA. [9]Department of Pathology, School of Medicine, University of Alabama, Birmingham, AL, USA. [10]Cancer Diagnosis and Pathology Group, Kolling Institute of Medical Research, Royal; North Shore Hospital, St Leonards, NSW, Australia. [11]University of Sydney, Sydney NSW Australia 2006; NSW Health Pathology Department of Anatomical Pathology, Royal North Shore Hospital, St Leonards, NSW, Australia. [12]Department of Pathology, University of Washington, School of Medicine, Seattle, WA, USA. [13]Department of Pathology, Cruces University Hospital, Biocruces-Bizkaia Institute, Barakaldo, Spain. [14]Department of Pathology, Institute Nacional de Cancerologia, Mexico City, Mexico. [15]Department of Pathology, Stradin´s University, Riga, Latvia. [16]Department of Pathology, Sorbonne Université, Service d'Anatomie et Cytologie Pathologiques, Hôpital Tenon, Paris, France. [17]Department of Pathology, University of Vienna, Vienna, Austria. [18]Department of Pathology, McGill University, Montreál, QC, Canada. [19]Department of Pathology, El Camino Hospital, Mountain View, CA, USA. [20]Department of Pathology, Heath Science Centre, St. John's, NL, Canada. [21]Department of Biology and Medical Genetics, 2nd Faculty of Medicine, Charles University in Prague and Motol University Hospital, Prague, Czech Republic. [22]Department of Pathology, University of Szeged, Szeged, Hungary. [25]Department of Pathology, Charles University, Medical Faculty and Charles University Hospital Plzen, Plzen, Czech Republic. [24]Department of Pathology, University of Erlangen, Erlangen, Germany. [25]Department of Pathology, Universitätsklinikum Hamburg-Eppendorf, Hamburg, Germany. [26]Department of Pathology, Alfa Medical, Bratislava, Slovakia. [27]Department of Pathology, University Hospital Ostrava, Ostrava, Czech Republic. [28]Department of Pathology, University Hospital Nitra, Nitra, Slovakia. [29]Department of Pathology, University of Toronto, Toronto, ON, Canada. [30]Department of Urology, University of Erlangen, Erlangen, Germany. [31]Department of Urology, Charles University, Medical Faculty and Charles University Hospital Plzen, Plzen, Czech Republic. [32]These authors contributed equally: Trpkov Kiril, Hes Ondrej. ✉email: hes@biopticka.cz

Received: 5 May 2021 Revised: 27 August 2021 Accepted: 1 September 2021
Published online: 14 September 2021

of eosinophilic (oncocytic) cells with large intracytoplasmic vacuoles, atypical nuclear features with prominent nucleoli, and exhibited a relatively consistent immunohistochemical profile. The initial names proposed for this tumor were "high-grade oncocytic renal tumor (HOT)" by He et al.[1] and "sporadic renal cell carcinoma with eosinophilic and vacuolated cytoplasm" by Chen et al.[2]. All patients included in these two studies presented with non-syndromic, solitary tumors, and both studies described virtually the same tumor morphology and immunoprofile. All reported tumors had indolent behavior, although with relatively limited follow-up data. One additional case was subsequently documented in a patient with tuberous sclerosis complex (TSC)[3], in contrast to the previously reported sporadic cases. The prevalence of this type of tumor in a sporadic and syndromic setting is currently unknown.

The molecular insights into this entity have so far been limited. Chen et al. found somatic inactivating mutations of *TSC2* in 3/5 tumors tested, activating mutations of *MTOR* in 2/5 tumors tested, additionally loss of chromosome 1 in both cases showing an *MTOR* mutation, consistent with a hyperactive *MTOR* complex. He et al. also found loss of chromosome 1 (3/9), but also of chromosome 19 (4/9 cases), and loss of heterozygosity at 16p11 (3/3 cases) and 7q31 (2/3 cases) were observed. No other chromosomal gains or losses were found in both studies.

Most recently, a unifying consensus name for this entity, "eosinophilic vacuolated tumor" (EVT) has been proposed by the Genitourinary Pathology Society (GUPS)[4], to reflect the most salient morphologic features of this entity. GUPS proposed that EVT should be considered an "emerging renal entity", requiring additional work and validation.

Therefore, the aim of this study was to further characterize EVT, to evaluate and validate its molecular features and mutation profile, focusing specifically on investigating the alterations of the mTOR pathway.

MATERIAL AND METHODS

Case selection

A total of 25 cases were initially considered as possible EVT, primarily based on the morphology. Only 3 of these were previously included in the He et al. study (cases #1, #3, and #9 in the current study)[1]. However, these cases were initially not analyzed more comprehensively for molecular-genetic changes, and in the current study we provide an updated follow-up for these cases. The 22 new cases were identified and collected from the files of the University Hospital Plzen, University of Calgary, Cleveland Clinic, Institute Nacional de Cancerologia Mexico City, University of Washington, Seattle, University of Sydney, Hôpital Tenon Paris, University of Alabama at Birmingham, Stradin´s University, Riga, University of Toronto, McGill University, University of Szeged, University of Erlangen, Universitätsklinikum Hamburg-Eppendorf, Alfa Medical, Bratislava, University Hospital Ostrava, University Hospital Nitra, and Cruces University Hospital, Barakaldo. All available clinical and other data were obtained from the files of the participating institutions.

Two pathologists performed a final review of all cases (OH and KT) with a critical evaluation of the morphology, immunohistochemical profile, and molecular-genetic features. The final cohort included in the study consisted of 19 cases, based on the morphologic features, immunohistochemical profile, and molecular-genetic features. Six cases were excluded from the final cohort. One case was excluded because the DNA quality was insufficient for a complete molecular-genetic analysis, although this case fulfilled the morphologic criteria and the immunohistochemical profile for an EVT. Two patients had *FLCN* mutations, but not *TSC1*, *TSC2*, and *MTOR* mutations, despite some morphologic and immunohistochemical similarities to EVT. On further investigation, one patient had a single renal tumor (1.7 cm), skin lesions, family history of renal tumors, and a pneumothorax in the past, but was never tested genetically for Birt-Hogg-Dubé (BHD); the second patient had a single renal tumor (1.5 cm), but no history of BHD. Finally, 3 additional cases demonstrated no mutations of *TSC1*, *TSC2*, and *MTOR* when analyzed by the next-generation sequencing (NGS) panel used in this study, although they showed a morphologic similarity with EVT on the initial evaluation. No other significant molecular changes were identified in these 3 cases. Detailed information about the 6 excluded cases is provided in the Supplementary Tables 1 and 2.

Immunohistochemistry

All immunohistochemical (IHC) stains were performed at a single laboratory (University Hospital Plzen), using a Ventana Benchmark XT automated stainer (Ventana Medical System, Inc., Tucson, AZ, USA). The following primary antibodies were used: cytokeratin (polyclonal: AE1-AE3 and PCK26, Ventana, RTU), CK18 (DC 10, monoclonal, DakoCytomation, Carpinteria CA, 1: 100), CK7 (OV-TL12/30, monoclonal, DakoCytomation, 1:200), cytokeratin 20 (M7019, monoclonal; Dako; 1:100), racemase/AMACR (P504S, monoclonal; Zeta, Sierra Madre, CA; 1:50), vimentin (V9, monoclonal; Cell Marque, Rocklin, CA; RTU), Ki-67 (monoclonal, MIB-1, 1:400, Dako), TFE3 (monoclonal, MRQ-37, RTU, Ventana Medical System, Inc.), c-kit (CD117, polyclonal, DakoCytomation, 1:300), CD10 (Sp67, monoclonal, Ventana, RTU), anti-melanosome (HMB45, monoclonal, DakoCytomation, 1:200), Melan A (A103, monoclonal, Ventana, RTU), PAX 8 (MRQ-50, monodonal, CellMarque, Rocklin, CA, RTU), antimitochondrial antibody (113-1, monoclonal, Biogenex, San Ramon, CA, 1:500), SDHB (polyclonal, Sigma Aldrich, St. Luis, MO, 1:50), cathepsin K (3F9, monoclonal, Abcam, Cambridge, UK, 1:400). Primary antibodies were visualized using a supersensitive streptavidin-biotin-peroxidase complex (BioGenex). Internal biotin was blocked using the standard protocol for the Ventana Benchmark XT automated stainer (hydrogen peroxide based). Appropriate positive and negative controls were used. IHC result were interpreted as follows: (−) if 0% of neoplastic cells were positive; (+/−) <10% of cells positive); (+) 10–25% of cells positive; (++) >25–50% of cells positive; (+++); >50–75% of cells positive; and (++++) >75–100% of cells positive.

Next-generation sequencing

The tumor DNA samples were profiled using massively parallel sequencing of exons from 592 genes (SureSelect XT, Agilent, Santa Clara, CA and the NextSeq instrument, Illumina, San Diego, CA), as previously described[5]. The tumor mutational burden (TMB) was assessed by calculating the number of nonsynonymous missense mutations, excluding common germline variants, in one megabase of DNA. TMB was considered high if ≥11 mutations/megabase (muts/Mb) were detected[6] Microsatellite instability (MSI) was calculated from the NGS data by direct analysis of short tandem repeat tracts in the target regions of sequenced genes. The count only included alterations that resulted in increases or decreases in the number of repeats; high microsatellite instability (MSI-H) was defined as ≥46 altered microsatellite loci. This threshold was established by comparing NGS results with PCR-based microsatellite fragment analysis results in ~2100 samples[7].

RESULTS

Clinicopathologic and immunohistochemistry results

Clinicopathologic data and immunohistochemistry results are summarized in Table 1. There were 8 men and 11 women (M:F = 1:1.4), with a mean patient age of 47 years (median 50; range 15–72 years). Average tumor size was 4.3 cm (median 3.8; range 1.5–11.5 cm). Pathologic stage pT1a was found in 12/18 cases, 5/18 were pT1b, and 1/18 was pT2b (tumor size and stage information was not available for case #19). All patients (18/19) with available follow-up data were alive and without evidence of disease (recurrence or progression) during the follow-up, ranging from 12 to 198 months (mean 56.3, median 41.5 months).

Grossly, all tumors were circumscribed and solid, lacked a well-formed capsule, macrocysts, and necrosis. The cut surface was gray, tan-mahogany or dark brown (Fig. 1). On microscopy, the common architectural patterns included solid, compact acinar, nested, or broad trabecular, as well as focal tubular or tubulocystic architecture. Prominent thick-walled vessels were typically present at the periphery and small non-neoplastic tubules were often entrapped at the periphery. The neoplastic cells had prominent membranes and voluminous eosinophilic cytoplasm, usually non-homogeneous, with variable granularity, typically condensed toward the cell periphery, reminiscent of chromophobe RCC (ChrRCC). Importantly, the cells had ubiquitous and large intracytoplasmic vacuoles and round to oval nuclei, with more

Table 1. Clinicopathologic features, follow-up, and immunohistochemical findings in patients with eosinophilic vacuolated tumor (EVT).

Patient	Age (years)	Gender	Size (cm)	Follow-up (months)[a]	CD117	CK7	CK20	Cathepsin K	CD10	MIA	AMACR	Vimentin
1	37	F	3.1	52	++	+/−	−	++++	++++	++++	+++	−
2	52	M	4.1	36	++	+/−	−	+++	+++	++++	−	−
3	59	F	1.5	162	++++	+/−	+/−	++++	++++	++++	+++	−
4	63	F	2.5	198	+++	+/−	NA	+	+++	++++	+	−
5	68	F	4.5	48	+++	+/−	−	++++	+++	++++	−	−
6	31	F	3.5	31	++++	+/−	−	+++	++++	+++	−	−
7	25	M	3.8	75	++++	+/−	−	++	++++	++++	+++	−
8	72	M	3.5	144	+	+/−	−	++++	++	++++	++	−
9	54	M	2.6	50	+++	+/−	−	++	+++	++++	++	−
10	59	F	4.0	18	+++	−	−	+	++	+	+	−
11	50	M	5.5	12	+++	+/−	−	+++	+++	+	+	−
12	15	M	11.5	19	+++	+/−	−	+	+++	+	+	−
13	69	F	4.0	47	+	−	+	+++	++++	++++	++	−
14	27	F	3.0	58	+++	+/−	+	++++	+++	++++	++++	−
15	36	F	4.0	NA	+	−	+	+++	++++	+++	++	−
16	61	F	5.0	15	+/−	+	+	+++	++++	++++	+++	−
17	42	M	7.0	18	+/−	−	−	+++	NA	++++	+	−
18	64	M	2.5	16	++	−	−	+++	++++	+	++	−
19	44	F	NA	15	++	+	+	++++	+++	+	+	−

NA not available, *CK* cytokeratin, *MIA* antimitochondrial antigen, *AMACR* Alpha Methylacyl-CoA Racemase.
[a]All patients with available follow-up were alive and without evidence of disease (recurrence or progression) during the follow-up. Immunohistochemistry: (+/−) <10% of cells positive); (+) 10–25% of cells positive; (++) >25–50% of cells positive; (+++); >50–75% of cells positive; (++++) >75–100% of cells positive; (−) negative.

granular to coarse chromatin, and prominent nucleoli (corresponding to WHO/ISUP grade 3), although often even larger inclusion-like nucleoli were found in virtually all cases. Mitoses were an exceptionally rare finding.

On immunohistochemistry, cathepsin K was expressed in all cases, as well as CD117 (in some cases, both were focal) (Fig. 2). All tumors were also positive for CD10 and antimitochondrial antigen (MIA). Other positive stains (not listed in Table 1) included PAX8, AE1/AE3, and cytokeratin (CK) 18; SDHB were retained in all cases, exhibiting strong and diffuse reactivity. AMACR was also variably positive in the majority of cases (16/19). CK7 was typically very focal and limited, restricted to scattered positive cells, usually not exceeding 10% of neoplastic cells overall. Focal CK20 reactivity was also noted in 6/18 evaluated tumors, typically limited and very focal. All tumors were completely negative for vimentin. Other negative stains (not listed in Table 1) included HMB45, Melan-A, and TFE3. Ki67 reactivity was very low in most of the cases (<1%), typically with 0–3 positive cells/high-power field.

Molecular results

Molecular-genetic findings are summarized in Table 2 and Fig. 3. All 19 analyzed cases showed non-overlapping mTOR pathway mutations in either *TSC1*, *TSC2*, or *MTOR* genes. Four cases showed exclusive pathogenic *TSC1* gene mutations. *TSC2* gene mutations were identified in 7 cases. Single pathogenic (or likely pathogenic) *MTOR* gene mutations were identified in 8 cases; one of these showed a coexistent *RICTOR* missense mutation (case #7). Low mutational rates were found in all samples, ranging from 0 to 6 mutations/Mbp. Microsatellite instability and copy number variations were not found in any of the 17 analyzable cases. Of note, two cases (#3 and #9) that lacked copy number variations in the current study, were also analyzed in the previous study by He et al. and showed −19p and −1, +19p, respectively (shown as cases #2 and #12)[1]. The differences in the results for these two cases likely stem from the methodological differences in the techniques used. While He et al. used CGH microarray analysis, which is comprehensive genome-wide screen for copy gains and losses, in the current study we only screened for isolated gene amplifications (at least six copies) involving a specific gene panel, which allows for a less detailed chromosomal analysis.

DISCUSSION

This study represents the largest molecular evaluation series of EVT reported to-date, assembled through a multi-institutional collaboration. Importantly, we confirmed non-overlapping mTOR pathway genes mutations in all studied cases, which further confirms and validates the molecular profile of EVT[2]. All EVT cases included in this series showed mutually exclusive alterations of *TSC1* (4/19), *TSC2* (7/19), or *MTOR* (8/19) genes. Although only single inactivating *TSC1* and *TSC2* gene mutations were detected in some samples, two different mutations were found in other cases (e.g., case #1, #3, #4, #14, #15, and #19); it is presumed that the samples with only one detected mutation had biallelic inactivation either due to synonymous mutations or LOH. This discrepancy can be explained by the limitations of the methodology used, which does not capture the intronic or promoter regions of the gene, including the LOH or epigenetic changes. We can only speculate on the significance of the concomitant *MTOR*/*RICTOR* alterations observed in one tumor (case #7) and their role as possible co-oncogenic drivers, as postulated recently in non-small cell lung cancer[8]. Nevertheless, the consistent molecular profile observed in this study, in addition to the characteristic morphology and immunoprofile, further support the notion that EVT truly represents a distinct renal entity. Of note, none of the 19 patients showed clinical features or other findings (for example renal angiomyolipomas) typically associated with TSC, indicating the sporadic nature of the studied tumors. Lastly, all patients with renal EVTs were alive and without evidence of disease recurrence or progression during the follow-up, which further supports the initial observations that this likely represents an indolent tumor type.

In 2018, He et al. presented a study that included a multi-institutional series of 14 cases, and proposed that this renal tumor potentially represents a distinct entity; some of the authors of the current study also participated in that study[1]. He et al. initially

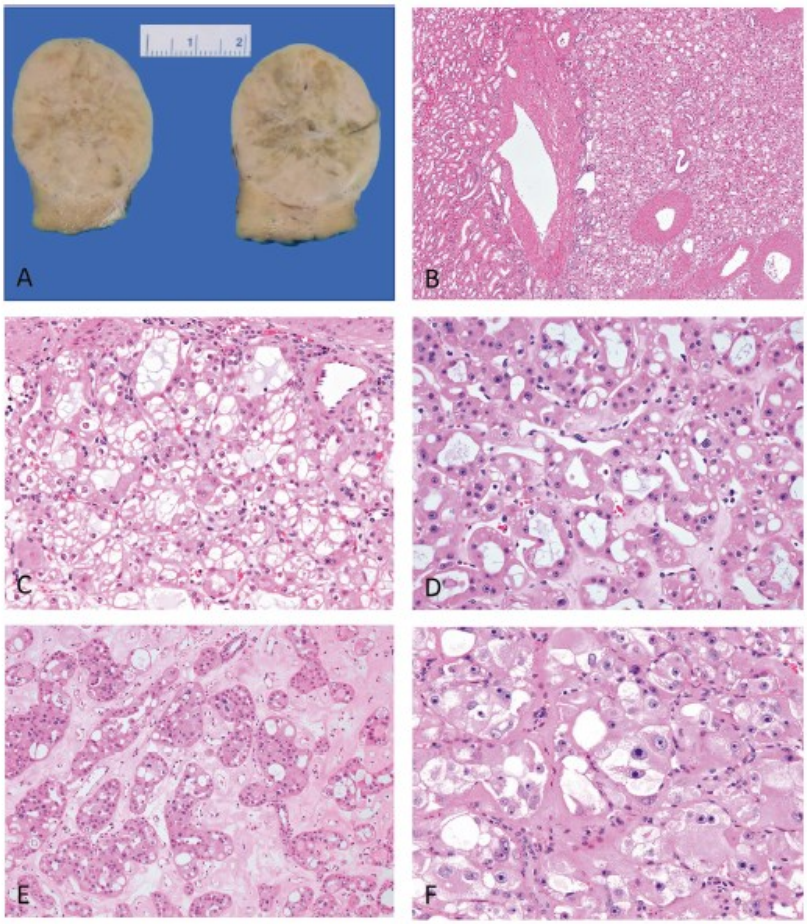

Fig. 1 Eosinophilic vacuolated tumor (EVT) - gross and morphologic features. A EVT is a grossly a circumscribed and solid tumor, and lacks a well-formed capsule, macrocysts, and necrosis. The cut surface can be gray (as shown), tan-mahogany or dark brown. **B** On microscopy, they often show solid growth, and large thick-walled vessels are typically found at the periphery, with entrapped non-neoplastic tubules. **C** The neoplastic cells have large intracytoplasmic vacuoles. **D**, **E** Other growth patterns include tubular and nested, often set in stromal areas in the background. **F** The neoplastic cells, in addition to large vacuoles, have voluminous eosinophilic cytoplasm, round to oval nuclei, and often very prominent nucleoli, that focally may appear as inclusions.

designated this type of tumor as "high-grade oncocytic tumor" (HOT)[1]. 9/14 cases of the initial study were analyzed by aCGH, although a more extensive molecular-genetic analysis was not performed. Subsequently, in 2019, Chen et al. reported a single-institution series of 7 cases, designated "sporadic renal cell carcinomas with eosinophilic and vacuolated cytoplasm", demonstrating virtually identical clinicopathologic and histomorphologic features[2]. In 5/7 cases, in which they performed molecular analysis, 3 had a *TSC2* inactivating mutations (2 with independent *TSC2* mutations). The other 2 analyzed cases harbored a *MTOR c.7280T>G, p.(L2427R)* mutation. In the current study, we found that *MTOR* mutations were slightly more frequent than the *TSC2* ones (8 and 7 cases, respectively); in addition, we also found 4 cases with *TSC1* mutations. Both cases with *MTOR* activating mutations in the study by Chen et al.[2] also had a loss of chromosome 1, as shown initially by He et al.[1]. The presence of hyperactive mTORC1 signaling was supported by the diffuse immunohistochemical staining for p-S6 and p-4EBP1[2].

Similar to the current series, all patients in the two initial studies presented with solitary, tan-yellow to brown tumors, and had no prior history of syndromic associations, including TSC[1,2]. All initially reported tumors were stage pT1a or pT1b, with identical mean size of 3.4 cm, ranging from 1.5 to 7 cm[1,2]. Regarding the immunoprofile, the evaluated cases in these two series were Cathepsin K positive (negative in only 1 case); 9/14 cases in the series by He et al. also had CD117 expression, while CK7 was either negative or only focally positive in both studies[1,2]. CD10 expression was documented in 12/13 cases in the He et al. study (not performed by Chen et al.)[1]. The remaining immunoprofile documented in the He et al. study essentially mirrored the findings of the current study. Examples of EVT (HOT) were also studied by electron microscopy and demonstrated numerous intracytoplasmic mitochondria resembling the findings in renal oncocytoma[9]. In the study by He et al., 10 patients with available follow-up were without disease progression after a mean follow-up of 28 months (range 1–112 months)[1]. Similarly, Chen et al. also

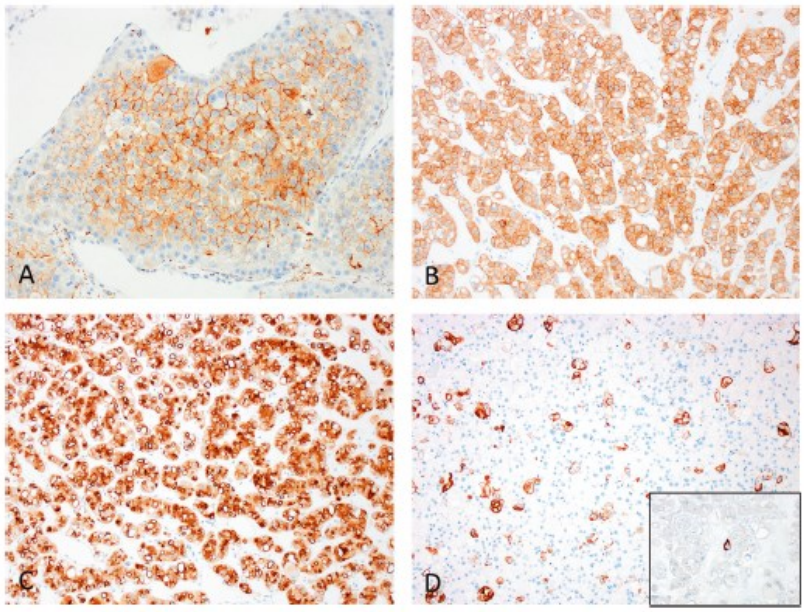

Fig. 2 Eosinophilic vacuolated tumor (EVT) – immunohistochemistry. A On immunohistochemistry, cathepsin K was expressed in all cases. Of note, in some cases we have also noted a focal membranous (or submembranous) pattern, in addition to the cytoplasmic one, that was more common. **B** Reactivity for CD117 was also found in all cases (in some cases, both cathepsin K and CD117 were focal). **C** All tumors were also positive for CD10. **D** CK7 was typically very focal and found in only scattered cells; in some cases, only very rare CK7 positive cells were present (inset).

Table 2. Molecular-genetic findings: mutations in *TSC1*, *TSC2*, *MTOR*, and *RICTOR*, copy number variation in tested genes.

Case	TSC1	TSC2	MTOR	RICTOR	CNV
1[a]	c.1997+1G>T; c.2278A>T	w.t.	w.t	n/a	None
2	c.2374C>T	w.t.	w.t.	w.t.	None
3[a]	n/a	c.5161-1G>T; c.1373_1393del21	n/a	n/a	None
4	n/a	c.1801_1802delinsT; c.911G>A	n/a	n/a	None
5	n/a	c.784delA	n/a	n/a	None
6	n/a	w.t.	c.7280T>G	n/a	None
7	w.t.	w.t.	c.7257_7259delinsTGT	c.910C>A	n/a
8	w.t.	w.t.	c.7280T>A	w.t.	None
9[a]	w.t.	w.t.	c.5930C>A	w.t.	None
10	w.t.	w.t.	c.7280T>C	w.t.	None
11	c.2299C>T	w.t.	w.t.	w.t.	None
12	w.t.	w.t.	c.7280T>G	w.t.	None
13	w.t.	w.t.	c.4343_4363del	w.t.	None
14	c.1548_1550delinsTC; c.736A>G	w.t.	w.t.	w.t.	None
15	w.t.	c.953_959del; c.4650_4651del	w.t.	w.t.	None
16	w.t.	c.2384del	w.t.	w.t.	None
17	w.t.	w.t.	c.7280T>A	w.t.	None
18	w.t.	c.5227C>T	w.t.	w.t.	None
19	w.t.	c.4803dup; c.5238_5255del	w.t.	w.t.	None

w.t. wild type, *n/a* not analyzable/available.
[a]Published in Virchows Archives 2018.

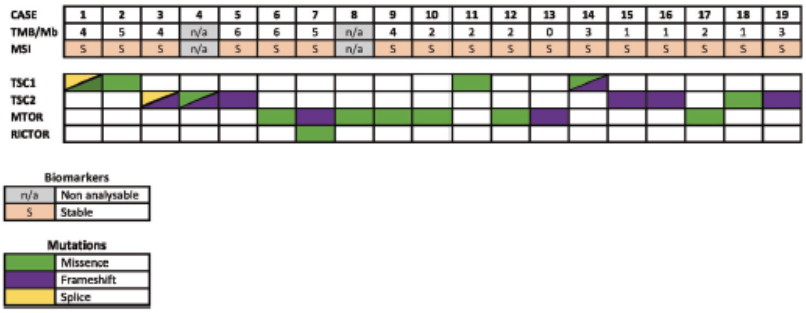

Fig. 3 Eosinophilic vacuolated tumor (EVT) – molecular findings. All 19 analyzed cases showed non-overlapping mTOR pathway substitution mutations in either *TSC1*, *TSC2*, or *MTOR* genes. In some cases, combinations of splice-missense, splice-frameshift, frameshift-missense, or dual frameshift mutations were found. The mutation details are shown in Table 2.

reported an indolent behavior in all 5 patients with available median follow-up of 12 months (range 10–128 months)[2].

One female patient with EVT (designated as "HOT") was subsequently reported in a TSC patient[3]. However, this patient had a known history of TSC and also had multiple small angiomyolipomas and one small renal cell carcinoma with fibromyomatous (angioleiomyomatous) stroma, adjacent to the EVT[3], as typically seen in TSC patients[10]. In our opinion, similar or virtually identical tumors to EVT, according to our assessment of the available illustrations and provided data, have also been included in some recent studies, albeit designated with different names. For example, such tumors with similar morphology harboring *TSC* mutations have been included in a series of "eosinophilic renal tumors"[11]. Further, some examples illustrated in the study by Palsgrove et al. (listed as cases #6 and #7) may also represent EVT, rather than eosinophilic solid and cystic renal cell carcinoma (ESC RCC), as proposed by the authors[12]. Taking into account that several studies used different terminology to describe essentially the same renal tumor type, the Genitourinary Pathology Society (GUPS) consensus group has recently proposed a new unifying name "eosinophilic vacuolated tumor" (EVT) for this entity[4]. The proposed name reflects the typical morphologic features ("eosinophilic and vacuolated"), and avoids the "high-grade" descriptive characterization used initially; the term "tumor" instead of "carcinoma" was preferred, given that all reported cases so far had indolent behavior[4].

In our view, the most important differential diagnostic category for EVT are those tumors that are difficult to classify and exhibit 'borderline' or overlapping features between oncocytoma and ChrRCC, which can be found either in syndromic or sporadic setting[10,13–17]. Such eosinophilic (oncocytic) tumors with overlapping morphologies pose a common diagnostic dilemma and do not fit into any of the currently recognized renal tumor categories in the WHO classification[13,18]. In brief, the typical EVT morphology is beyond the morphologic spectrum of renal oncocytoma, despite the IHC similarities that include reactivity for CD117, accompanied by focal CK7 expression, typically restricted to scattered cells or cell clusters. Although the "plant cell-like" pattern of classic ChrRCC can superficially resemble EVT, ChrRCC lacks marked cytoplasmic vacuoles, "atypical" nuclear features with very prominent nucleoli, and exhibits irregular ("raisinoid") nuclei, not seen in EVT. Although both oncocytoma and ChrRCC demonstrate CD117 reactivity, they are negative for cathepsin K, as seen in EVT. Of note, ChrRCC also typically shows diffuse CK7 reactivity, unlike EVT.

The recent GUPS update on the novel developments in existing renal tumors proposed the term "*oncocytic renal neoplasm of low malignant potential, not further classified*", when referring to solitary and sporadic, difficult to classify 'borderline' tumors with overlapping features between oncocytoma and ChrRCC.[19]. Hereditary cases, that are typically multifocal and bilateral, should exclusively be named *"hybrid oncocytic tumors"*. Such cases with "hybrid" morphology in the setting of BHD syndrome are often characterized by scattered clusters and individual cells with clear cytoplasm, exhibiting a "checkerboard" mosaic pattern. Indeed, we found a significant morphologic and immunoprofile overlap between EVT and two similar tumors that had *FLCN* mutation. These tumors were initially considered as possible EVTs, but were excluded from the final cohort because both lacked *TSC/MTOR* mutations and showed instead *FLCN* mutations (Fig. 4A, B). One of these patients likely had an inherited BHD syndrome, and one likely had a new somatic mutation, without the BHD stigmata. These two cases demonstrated similar morphology to EVT, despite some subtle differences, such as a mosaic-type pattern and absence of prominent nucleoli (i.e., high-grade nuclear features) and they also had immunohistochemical similarities with EVT (see Supplementary Tables 1 and 2). From a practical standpoint, we would consider those cases with documented *FLCN* mutations (and absent *TSC/MTOR* mutations) as "*hybrid oncocytic tumors*". For the sake of the study clarity, we also excluded 4 additional cases: one case because it had low DNA quality that did not allow to perform all genetic studies, and 3 cases that had similar morphology and immunohistochemical profile (CD117, CD10, cathepsin K, and MIA positive) to EVT, but had no identifiable mutations of *TSC1*, *TSC2*, and *MTOR* (Fig. 4C, D). It is possible that these cases may have had undetected *TSC/MTOR* mutations when analyzed by the NGS panel applied in this study; however, they also lacked other identifiable mutations. Such cases are currently best considered *"renal oncocytic neoplasms, not otherwise specified"*. If signing out such cases in practice, one may add *"with EVT-like features"*.

Other, less common renal tumors that can potentially mimic EVT include MiTF RCC (TFEB and TFE3), SDH-deficient RCC, and ESC RCC, another novel renal entity and their distinguishing features have been covered in several recent reviews[4,9,18,20]. Regarding the similarities with ESC RCC, EVT indeed shares molecular similarities that include the presence of *TSC2* and *TSC1* mutations and activation of the mTOR pathway; additionally, rare examples of both entities have been found in TSC patients. EVT can be distinguished from ESC RCC primarily on morphology, as it typically lacks a macrocystic gross component (typically found in ESC RCC), has large cytoplasmic vacuoles (not usually seen in ESC RCC), and generally lacks the coarse cytoplasmic granularity seen in ESC RCC (such granularity can however rarely be found in some EVTs). There are also IHC differences between EVT and ESC RCC. EVT typically exhibits CD117+/vimentin−/CK20− profile (though rare cases may show focal CK20+ cells), which is different from the typical ESC RCC immunoprofile CD117−/vimentin+/CK20+[4].

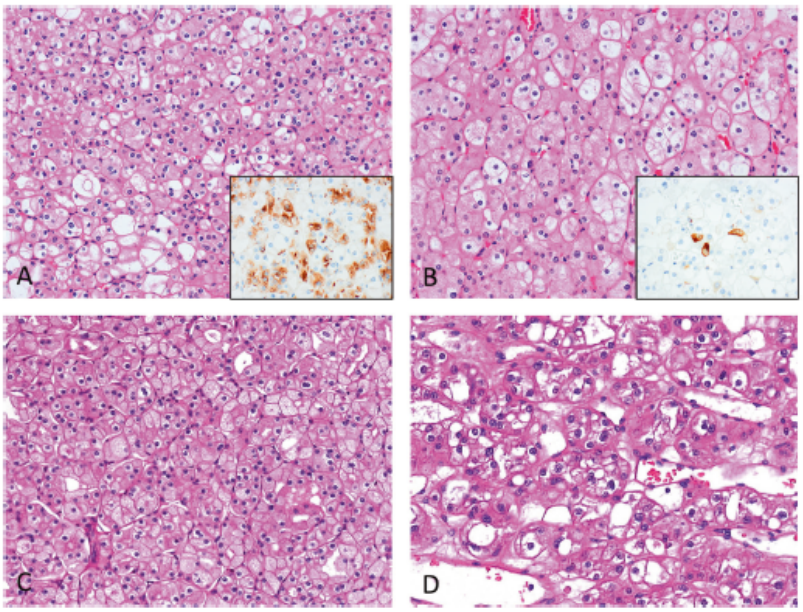

Fig. 4 Examples of cases excluded from the study that showed similarities with eosinophilic vacuolated tumor (EVT). Two cases with *FLCN* mutations are illustrated in **A** and **B**. These two cases had similar morphology to EVT, despite some subtle differences, including a more mosaic-type growth and absence of prominent nucleoli. One of these patients (**A**) likely had a true BHD syndrome, and one (**B**) had a new mutation, without the BHD stigmata. Both cases lacked *TSC/MTOR* mutations. They also showed immunohistochemical similarities with EVT, including cathepsin K reactivity, either more diffuse (**A** – inset), or focal (**B** – inset). Both cases were also positive for CD117 and for CK7 (both > 30%) (not shown). Two additional cases that had no identifiable mutations of *TSC1*, *TSC2*, and *MTOR*, but with very similar morphology to EVT are illustrated in **C** and **D**. It is possible that these cases may have had undetected *TSC/MTOR* mutations, but they also lacked other identifiable mutations.

Cathepsin K is also positive in the majority of ESC RCC and in EVT. In EVT, the positivity is either diffuse (most of the cases) or focal; in some cases, we have also noticed a focal membranous pattern (possibly a submembranous condensation), in addition to the more common cytoplasmic one. In ESC RCC, the positivity for cathepsin K is often patchy, cytoplasmic, with rare cases showing either diffuse reactivity or, very rarely, complete absence of staining[4,12,21].

TSC/MTOR mutations appear to be more commonly found in some other novel renal entities, for example RCC with fibromyomatous stroma[9,12,18,22–25]. However, such mTOR pathway mutations have also been found in AML (or PEComas), and in some common renal tumors, such as metastatic clear cell RCC or papillary RCC[26–29], acquired cystic disease associated (ACD) RCC[25], and in rare examples of "unclassified aggressive RCCs"[30]. It appears that the tumors with *TSC/MTOR* mutations represent a diverse group of renal neoplasms showing variable morphologies and immunoprofiles, and different biologic behaviors. Thus, the introduction of a potential concept of "TSC-associated renal tumor family", although appealing, is currently unjustifiable, based on the available evidence, and requires further study[4].

In summary, EVT is an emerging low-grade renal entity that can be either diagnosed or suspected on morphology, and shows a relatively uniform immunohistochemical profile. We confirmed in this study that EVT is consistently associated with mTOR pathway abnormalities, including non-overlapping mutations in *MTOR*, *TSC2*, and *TSC1*. All reported cases so far, including the ones from this study, exhibited an indolent behavior. The findings from our study strongly support the conclusion that EVT should be recognized as a distinct and novel renal entity.

DATA AVAILABILITY

All data are shown in the article.

REFERENCES

1. He, H. et al. "High-grade oncocytic renal tumor": morphologic, immunohistochemical, and molecular genetic study of 14 cases. *Virchows Arch* **473**, 725–738 (2018).
2. Chen, Y. B. et al. Somatic mutations of TSC2 or MTOR characterize a morphologically distinct subset of sporadic renal cell carcinoma with eosinophilic and vacuolated cytoplasm. *Am. J. Surg. Pathol.* **43**, 121–131 (2019).
3. Trpkov, K. et al. High-grade oncocytic tumour (HOT) of kidney in a patient with tuberous sclerosis complex. *Histopathology* **75**, 440–442 (2019).
4. Trpkov, K. et al. Novel, emerging and provisional renal entities: The Genitourinary Pathology Society (GUPS) update on renal neoplasia. *Mod. Pathol.* **34**, 1167–1184 (2021).
5. Gatalica, Z., Xiu, J., Swensen, J. & Vranic, S. Comprehensive analysis of cancers of unknown primary for the biomarkers of response to immune checkpoint blockade therapy. *Eur. J. Cancer* **94**, 179–186 (2018).
6. Samstein, R. M. et al. Tumor mutational load predicts survival after immunotherapy across multiple cancer types. *Nat. Genet* **51**, 202–206 (2019).
7. Vanderwalde, A., Spetzler, D., Xiao, N., Gatalica, Z. & Marshall, J. Microsatellite instability status determined by next-generation sequencing and compared with PD-L1 and tumor mutational burden in 11,348 patients. *Cancer Med.* **7**, 746–756 (2018).
8. Ruder, D. et al. Concomitant targeting of the mTOR/MAPK pathways: novel therapeutic strategy in subsets of RICTOR/KRAS-altered non-small cell lung cancer. *Oncotarget* **9**, 33995–34008 (2018).
9. Siadat, F. & Trpkov, K. ESC, ALK, HOT and LOT: Three letter acronyms of emerging renal entities knocking on the door of the WHO Classification. *Cancers* **12**, 1 (2020).
10. Guo, J. et al. Tuberous sclerosis-associated renal cell carcinoma: a clinicopathologic study of 57 separate carcinomas in 18 patients. *Am. J. Surg. Pathol.* **38**, 1457–1467 (2014).

11. Tjota, M. et al. Eosinophilic renal cell tumors with a TSC and MTOR gene mutations are morphologically and immunohistochemically heterogenous: clinicopathologic and molecular study. *Am. J. Surg. Pathol.* **44**, 943–954 (2020).
12. Palsgrove, D. N. et al. Eosinophilic solid and cystic (ESC) renal cell carcinomas harbor TSC mutations: Molecular analysis supports an expanding clinicopathologic spectrum. *Am. J. Surg. Pathol.* **42**, 1166–1181 (2018).
13. Williamson, S. R. et al. Diagnostic criteria for oncocytic renal neoplasms: a survey of urologic pathologists. *Hum. Pathol.* **63**, 149–156 (2017).
14. Petersson, F. et al. Sporadic hybrid oncocytic/chromophobe tumor of the kidney: a clinicopathologic, histomorphologic, immunohistochemical, ultrastructural, and molecular cytogenetic study of 14 cases. *Virchows Arch* **456**, 355–365 (2010).
15. Delongchamps, N. B. et al. Hybrid tumour 'oncocytoma-chromophobe renal cell carcinoma' of the kidney: a report of seven sporadic cases. *BJU Int.* **103**, 1381–1384 (2009).
16. Mai, K. T., Dhamanaskar, P., Belanger, E. & Stinson, W. A. Hybrid chromophobe renal cell neoplasm. *Pathol. Res. Pr.* **201**, 385–389 (2005).
17. Hes, O., Petersson, F., Kuroda, N., Hora, M. & Michal, M. Renal hybrid oncocytic/chromophobe tumors - a review. *Histol. Histopathol.* **28**, 1257–1264 (2013).
18. Trpkov, K. & Hes, O. New and emerging renal entities: a perspective post-WHO 2016 classification. *Histopathology* **74**, 31–59 (2019).
19. Trpkov, K. et al. New developments in existing WHO entities and evolving molecular concepts: the Genitourinary Pathology Society (GUPS) update on renal neoplasia. *Mod. Pathol.* **34**, 1392–1424 (2021).
20. Alaghehbandan, R., Perez Montiel, D., Luis, A. S. & Hes, O. Molecular genetics of renal cell tumors: a practical diagnostic approach. *Cancers* **12**, 1 (2019).
21. Tretiakova, M. S. Eosinophilic solid and cystic renal cell carcinoma mimicking epithelioid angiomyolipoma: series of 4 primary tumors and 2 metastases. *Hum. Pathol.* **80**, 65–75 (2018).
22. Trpkov, K. et al. Eosinophilic, solid, and cystic renal cell carcinoma: Clinicopathologic study of 16 unique, sporadic neoplasms occurring in women. *Am. J. Surg. Pathol.* **40**, 60–71 (2016).
23. Trpkov, K. et al. Eosinophilic solid and cystic renal cell carcinoma (ESC RCC): Further morphologic and molecular characterization of ESC RCC as a distinct entity. *Am. J. Surg. Pathol.* **41**, 1299–1308 (2017).
24. Parilla, M. et al. Are sporadic eosinophilic solid and cystic renal cell carcinomas characterized by somatic tuberous sclerosis gene mutations? *Am. J. Surg. Pathol.* **42**, 911–917 (2018).
25. Shah, R. B. et al. "Renal cell carcinoma with leiomyomatous stroma" harbor somatic mutations of TSC1, TSC2, MTOR, and/or ELOC (TCEB1): Clinicopathologic and molecular characterization of 18 sporadic tumors supports a distinct entity. *Am. J. Surg. Pathol.* **44**, 571–581 (2020).
26. Schultz, L. et al. Immunoexpression status and prognostic value of mTOR and hypoxia-induced pathway members in primary and metastatic clear cell renal cell carcinomas. *Am. J. Surg. Pathol.* **35**, 1549–1556 (2011).
27. Kwiatkowski, D. J. et al. Mutations in TSC1, TSC2, and MTOR are associated with response to rapalogs in patients with metastatic renal cell carcinoma. *Clin. Cancer Res.* **22**, 2445–2452 (2016).
28. Roldan-Romero, J. M. et al. Molecular characterization of chromophobe renal cell carcinoma reveals mTOR pathway alterations in patients with poor outcome. *Mod. Pathol.* **33**, 2580–2590 (2020).
29. Chaux, A. et al. Dysregulation of the mammalian target of rapamycin pathway in chromophobe renal cell carcinomas. *Hum. Pathol.* **44**, 2323–2330 (2013).
30. Chen, Y. B. et al. Molecular analysis of aggressive renal cell carcinoma with unclassified histology reveals distinct subsets. *Nat. Commun.* **7**, 13131 (2016).

AUTHOR CONTRIBUTIONS

M.F.: drafted paper, evaluated results; G.Z., J.S., P.N.: performed genetic analyses; Z.M., A.R., W.S.R., M.-G.C., G.A., T.M., M.M.: helped with design and interpretation of results; L.J.I., P.-M.D., S.M., C.E., B.F., Y.A., S.F., S.A., G.Y., K.L., P.K., R.J., A.A., H.A., F.C., R.B., H.M., D.D., B.M.: provided cases with full details, G.G., M.H.: evaluated clinical information, T.K. and O.H.: coordinated whole study, edited draft and constructed discussion.

FUNDING INFORMATION

This study was supported by the Charles University Research Fund (project number Q39) and by the grant of Ministry of Health of the Czech republic-Conceptual Development of Research Organization (Faculty Hospital in Plzen- FNPl 00669806).

COMPETING INTERESTS

The authors declare no competing interests.

ETHICS APPROVAL

The study was performed in accordance with the Declaration of Helsinki. Ethic committee approval was not required by Charles University and University Hospital Plzen.

ADDITIONAL INFORMATION

Supplementary information The online version contains supplementary material available at https://doi.org/10.1038/s41379-021-00923-6.

Correspondence and requests for materials should be addressed to Ondrej Hes.

Reprints and permission information is available at http://www.nature.com/reprints

Publisher's note Springer Nature remains neutral with regard to jurisdictional claims in published maps and institutional affiliations.

4 Conclusion

The classification of renal neoplasms is a dynamic and changing area of pathology, particularly in recent years. New light in understanding of this field of human pathology were given by widely employed molecular studies, exploring well established entities, as well as provisional ones. There are other factors stimulating the development in a group of renal neoplasms by constant attempts of authors to remove renal tumours from "unclassified" category. Current findings in renal neoplasm field were fully summarized in consensus works by The Genitourinary Pathology Society (GUPS) (3, 4) and in the 5th edition of WHO classification (2). The dissertation presented here discusses author´s seven articles describing new developments of well-established entitles (PRCC and ChRCC) together with an emerging entity from "other oncocytic category" - recently described as EVT.

Papillary renal cell carcinoma used to be traditionally subdivided into type 1 and type 2 (35, 36). Such subtyping is no longer recommended, as it became apparent that papillary architecture may also be a part of molecularly defined TFE3-rearranged RCC or FH deficient RCC. Clear cell papillary renal cell tumour and CCRCC may also exhibit papillary architecture (focal or extensive) (8) . In addition, the spectrum of PRCCs is much wider than initially proposed - small series of distinct subtypes of PRCC which do not fit into the type 1 and type 2 categories have been described in the literature (37). Molecular pathology findings partially pushed and helped to put an end to the era of this division of PRCC (38). *MET* gene mutations and polysomies of chromosomes 7 and 17 and loss of the Y chromosome had been considered "iconic" for PRCC (33). With new insights, it became evident that spectrum of molecular alterations in PRCCs is much wider, and there is no single molecular alteration absolutely typical for PRCC (37). In addition, recent evidence shows that WHO/ISUP grade and tumour architecture are better predictors of biological outcome than classical subtyping (11). Awareness of PRCCs morphologic spectrum, low threshold to apply immunohistochemical stains (as FH / TFE3) and usage of molecular tools are crucial to eliminate/diagnose molecularly defined carcinomas with papillary features (TFE3-rearranged RCC or FH deficient RCC) and with confidence sign out renal carcinoma with papillary architecture as PRCC in every day practice.

Oncocytic PRCC was included in 4th WHO edition as a possible "type 3" of PRCC and was defined as PRCC with voluminous, finely granular, evenly distributed eosinophilic cytoplasm and oncocytoma-like nuclei (usually with low nuclear grade). The nuclei should be typically single-layered and linearly aligned (33). Interestingly, the majority of cases from initial studies/cohorts describing OPRCC (39, 40) would not fulfill the WHO 2016 diagnostic criteria of OPRCC. This oncocytic "subtype" of PRCC during 6 years from the 2016 "blue book" edition has undergone many changes. The so-called PRCC with reverse polarity/papillary renal cell tumour with reverse polarity (described in recent publications (15, 41)) shows similarities with "oncocytic PRCC" defined by WHO 2016. This tumor is composed of oncocytic cells with papillary and tubulopapillary growing pattern and exhibits typically low grade nuclei aligned away from basement membrane (single-layered).

Immunoprofile of PRCC with reverse polarity /papillary renal cell tumour with reverse polarity is characteristic and relatively constant (with GATA3, CK7 positivity and vimentin negativity). Presence of *KRAS* mutation is molecular signature in majority of cases (16). It became evident that tumours grouped under umbrella term „OPRCC" form a heterogeneous group with broad morphologic spectrum, with no distinct immunoprofile, no consistent molecular-genetic background, and not well established biological behavior (42). Papillary RCC with reverse polarity/renal cell tumour with reverse polarity is probably only small part of this "oncocytic PRCC" group. As a result, "OPRCC" is no longer mentioned in recent 5th WHO edition as separate subtype of PRCC (2), and "OPRCC" may only serve as descriptive term for tumours with papillary architecture and oncocytic cells (42). Instead, PRCC with reverse polarity/papillary renal cell tumour with reverse polarity gained a formal position among listed there morphologic variants of PRCC (2).

Group of oncocytic/eosinophilic renal tumours has been discussed very actively in recent years. Classic oncocytic/eosinophilic entities (such as RO and ChRCC) were enriched in rare morphologic subtypes/variants and new insights in their molecular-genetic background. There are some changes in nomenclature of tumours in this "oncocytic/eosinophilic renal tumours" group. It was clarified that tumours with overlapping features between RO and ChRCC developing in hereditary setting should be designated as hybrid oncocytic tumour (typically patients with multiple bilateral eosinophilic tumours) (3). Solitary oncocytic/eosinophilic tumours morphologically in the grey zone between RO and ChRCC evolving in sporadic setting fall into "oncocytic renal neoplasm of low malignant potential, not further classified" category (3). The designation "oncocytic renal neoplasm of low malignant potential, NOS" is more clinical management category rather than definitive and separate tumour entity. Unfortunately, it still remains group of oncocytic/eosinophilic tumours difficult to classify.

New developments revealed that two lesions may potentially arise from "oncocytic/eosinophilic renal tumours" group - low grade oncocytic tumor (LOT) and eosinophilic vacuolated tumor (EVT). LOT is defined by its CK7 diffuse positivity and CD117 (24-26) negativity, compact growth with nests of low-grade, monotonous cells with frequent abrupt transition to area with loose stroma and elongated neoplastic cells on this background. Recent studies showed that morphologic spectrum may be much broader including tumours with RO-like morphology (43). EVT exhibits nests of cells frequently set in loose stroma. Low magnification reveals cells with voluminous, eosinophilic cytoplasm, striking intracytoplasmatic vacuoles and nuclei with high grade morphology and prominent nucleoli. Immunoprofile is less constant, with most frequent positivity for CD117, CD10, and Cathepsin K. CK7 is negative or restricted to rare scattered cells. Both tumours exhibit mutations of mTOR pathway genes (*TSC1*, *TSC2*, *MTOR*) (27-30), and both may occur in sporadic setting, however they may be rarely found in patients with tuberous sclerosis complex (27, 28). Up to date, limited available data indicate benign behaviour of these tumours, future works are required to validate this findings (44). Mutations in the *TSC1* or *TSC2* are also molecular signature of eosinophilic solid and cystic RCC (ESC RCC) -

emerging entity in 4th WHO edition (33), newly regular entity with formal position in current 5th WHO "blue book" (2) (thanks to the evidence obtained in last 6 years).

Molecular technics are becoming an integral part of routine histologic examination and an "engine" for new developments. However, it has to be mentioned, that increasing number of newly described entities with distinctive morphologies share similar molecular alterations. This common genetic background in many morphologically different entities raise the question if instead of multiplicating new entities, we shouldn't cluster that tumours under one diagnostic category – the question of whether we should use the approach of the so-called splitters or lumpers. Especially if available data shows their indolent behaviour (44). We believe, this question will be answered in the future with more available evidences.

Multiplicity of newly described entities cannot obscure the fact, that classic renal tumours (namely CCRCC, PRCC, ChRCC and RO) account for more than 90% of renal neoplasms (45). Morphology still remains critical for every day routine practice. Moreover, up to date knowledge of molecular landscape of renal tumours is not well translated to treatment options. Molecular signature of RCC may gain clinical importance and justification in the light of developing targeted therapies. Additionally, the possibility of syndromic associations emphasizes proper recognition of molecularly defined RCCs as patients and their families require genetic consulting.

5 References

1. Kovacs G, Akhtar M, Beckwith BJ, Bugert P, Cooper CS, Delahunt B, et al. The Heidelberg classification of renal cell tumours. J Pathol. 1997;183(2):131-3.
2. Board. WCoTE. Urinary and male genital tumours. (WHO classification of tumours series, 5th ed.; vol. 8). Lyon (France):: International Agency for Research on Cancer; 2022.
3. Trpkov K, Hes O, Williamson SR, Adeniran AJ, Agaimy A, Alaghehbandan R, et al. New developments in existing WHO entities and evolving molecular concepts: The Genitourinary Pathology Society (GUPS) update on renal neoplasia. Mod Pathol. 2021;34(7):1392-424.
4. Trpkov K, Williamson SR, Gill AJ, Adeniran AJ, Agaimy A, Alaghehbandan R, et al. Novel, emerging and provisional renal entities: The Genitourinary Pathology Society (GUPS) update on renal neoplasia. Mod Pathol. 2021;34(6):1167-84.
5. Srigley JR, Delahunt B, Eble JN, Egevad L, Epstein JI, Grignon D, et al. The International Society of Urological Pathology (ISUP) Vancouver Classification of Renal Neoplasia. Am J Surg Pathol. 2013;37(10):1469-89.
6. Kojima F, Bulimbasic S, Alaghehbandan R, Martinek P, Vanecek T, Michalova K, et al. Clear cell renal cell carcinoma with Paneth-like cells: Clinicopathologic, morphologic, immunohistochemical, ultrastructural, and molecular analysis of 13 cases. Ann Diagn Pathol. 2019;41:96-101.
7. Williamson SR, Kum JB, Goheen MP, Cheng L, Grignon DJ, Idrees MT. Clear cell renal cell carcinoma with a syncytial-type multinucleated giant tumor cell component: implications for differential diagnosis. Hum Pathol. 2014;45(4):735-44.
8. Alaghehbandan R, Ulamec M, Martinek P, Pivovarcikova K, Michalova K, Skenderi F, et al. Papillary pattern in clear cell renal cell carcinoma: Clinicopathologic, morphologic, immunohistochemical and molecular genetic analysis of 23 cases. Ann Diagn Pathol. 2019;38:80-6.
9. Williamson SR, Halat S, Eble JN, Grignon DJ, Lopez-Beltran A, Montironi R, et al. Multilocular cystic renal cell carcinoma: similarities and differences in immunoprofile compared with clear cell renal cell carcinoma. Am J Surg Pathol. 2012;36(10):1425-33.
10. Gonzalez ML, Alaghehbandan R, Pivovarcikova K, Michalova K, Rogala J, Martinek P, et al. Reactivity of CK7 across the spectrum of renal cell carcinomas with clear cells. Histopathology. 2019;74(4):608-17.
11. Yang C, Shuch B, Kluger H, Humphrey PA, Adeniran AJ. High WHO/ISUP Grade and Unfavorable Architecture, Rather Than Typing of Papillary Renal Cell Carcinoma, May Be Associated With Worse Prognosis. Am J Surg Pathol. 2020;44(5):582-93.
12. Ulamec M, Skenderi F, Trpkov K, Kruslin B, Vranic S, Bulimbasic S, et al. Solid papillary renal cell carcinoma: clinicopathologic, morphologic, and immunohistochemical analysis of 10 cases and review of the literature. Ann Diagn Pathol. 2016;23:51-7.
13. Skenderi F, Ulamec M, Vanecek T, Martinek P, Alaghehbandan R, Foix MP, et al. Warthin-like papillary renal cell carcinoma: Clinicopathologic, morphologic, immunohistochemical and molecular genetic analysis of 11 cases. Ann Diagn Pathol. 2017;27:48-56.
14. Trpkov K, Athanazio D, Magi-Galluzzi C, Yilmaz H, Clouston D, Agaimy A, et al. Biphasic papillary renal cell carcinoma is a rare morphological variant with frequent multifocality: a study of 28 cases. Histopathology. 2018;72(5):777-85.
15. Al-Obaidy KI, Eble JN, Cheng L, Williamson SR, Sakr WA, Gupta N, et al. Papillary Renal Neoplasm With Reverse Polarity: A Morphologic, Immunohistochemical, and Molecular Study. Am J Surg Pathol. 2019;43(8):1099-111.
16. Al-Obaidy KI, Saleeb RM, Trpkov K, Williamson SR, Sangoi AR, Nassiri M, et al. Recurrent KRAS mutations are early events in the development of papillary renal neoplasm with reverse polarity. Mod Pathol. 2022;35(9):1279-86.

17. Hes O, Michal M, Kuroda N, Martignoni G, Brunelli M, Lu Y, et al. Vimentin reactivity in renal oncocytoma: immunohistochemical study of 234 cases. Arch Pathol Lab Med. 2007;131(12):1782-8.
18. Liu YJ, Ussakli C, Antic T, Liu Y, Wu Y, True L, et al. Sporadic oncocytic tumors with features intermediate between oncocytoma and chromophobe renal cell carcinoma: comprehensive clinicopathological and genomic profiling. Hum Pathol. 2020;104:18-29.
19. Foix MP, Dunatov A, Martinek P, Mundo EC, Suster S, Sperga M, et al. Morphological, immunohistochemical, and chromosomal analysis of multicystic chromophobe renal cell carcinoma, an architecturally unusual challenging variant. Virchows Arch. 2016;469(6):669-78.
20. Hes O, Vanecek T, Perez-Montiel DM, Alvarado Cabrero I, Hora M, Suster S, et al. Chromophobe renal cell carcinoma with microcystic and adenomatous arrangement and pigmentation--a diagnostic pitfall. Morphological, immunohistochemical, ultrastructural and molecular genetic report of 20 cases. Virchows Arch. 2005;446(4):383-93.
21. Michalova K, Tretiakova M, Pivovarcikova K, Alaghehbandan R, Perez Montiel D, Ulamec M, et al. Expanding the morphologic spectrum of chromophobe renal cell carcinoma: A study of 8 cases with papillary architecture. Ann Diagn Pathol. 2020;44:151448.
22. Peckova K, Martinek P, Ohe C, Kuroda N, Bulimbasic S, Condom Mundo E, et al. Chromophobe renal cell carcinoma with neuroendocrine and neuroendocrine-like features. Morphologic, immunohistochemical, ultrastructural, and array comparative genomic hybridization analysis of 18 cases and review of the literature. Ann Diagn Pathol. 2015;19(4):261-8.
23. Rogala J, Kojima F, Alaghehbandan R, Ptakova N, Bravc A, Bulimbasic S, et al. Small cell variant of chromophobe renal cell carcinoma: Clinicopathologic and molecular-genetic analysis of 10 cases. Bosn J Basic Med Sci. 2022;22(4):531-9.
24. Trpkov K, Williamson SR, Gao Y, Martinek P, Cheng L, Sangoi AR, et al. Low-grade oncocytic tumour of kidney (CD117-negative, cytokeratin 7-positive): a distinct entity? Histopathology. 2019;75(2):174-84.
25. Mansoor M, Siadat F, Trpkov K. Low-grade oncocytic tumor (LOT) - a new renal entity ready for a prime time: An updated review. Histol Histopathol. 2022;37(5):405-13.
26. Guo Q, Liu N, Wang F, Guo Y, Yang B, Cao Z, et al. Characterization of a distinct low-grade oncocytic renal tumor (CD117-negative and cytokeratin 7-positive) based on a tertiary oncology center experience: the new evidence from China. Virchows Arch. 2021;478(3):449-58.
27. Pivovarcikova K, Alaghehbandan R, Vanecek T, Ohashi R, Pitra T, Hes O. TSC/mTOR Pathway Mutation Associated Eosinophilic/Oncocytic Renal Neoplasms: A Heterogeneous Group of Tumors with Distinct Morphology, Immunohistochemical Profile, and Similar Genetic Background. Biomedicines. 2022;10(2).
28. Lerma LA, Schade GR, Tretiakova MS. Co-existence of ESC-RCC, EVT, and LOT as synchronous and metachronous tumors in six patients with multifocal neoplasia but without clinical features of tuberous sclerosis complex. Human Pathology. 2021;116:1-11.
29. Samaratunga H, Egevad L, Thunders M, Iczskowski KA, van der Kwast T, Kristiansen G, et al. LOT and HOT … or not. The proliferation of clinically insignificant and poorly characterised types of renal neoplasia. Pathology. 2022;54(7):842-7.
30. Williamson SR, Hes O, Trpkov K, Aggarwal A, Satapathy A, Mishra S, et al. Low-grade oncocytic tumour of the kidney is characterised by genetic alterations of TSC1, TSC2, MTOR or PIK3CA and consistent GATA3 positivity. Histopathology. 2023;82(2):296-304.
31. Williamson S. Clear cell papillary renal cell carcinoma: an update after 15 years. Pathology. 2020;53.
32. Hes O, Compérat EM, Rioux-Leclercq N. Clear cell papillary renal cell carcinoma, renal angiomyoadenomatous tumor, and renal cell carcinoma with leiomyomatous stroma relationship of 3 types of renal tumors: a review. Annals of Diagnostic Pathology. 2016;21:59-64.
33. Moch HHP UT, Reuter V. The WHO classification of tumours of the urinary system and male genital organs. Lyon, France: IARC Press; 2016.

34. Kuroda N, Trpkov K, Gao Y, Tretiakova M, Liu YJ, Ulamec M, et al. ALK rearranged renal cell carcinoma (ALK-RCC): a multi-institutional study of twelve cases with identification of novel partner genes CLIP1, KIF5B and KIAA1217. Mod Pathol. 2020;33(12):2564-79.
35. Delahunt B, Eble JN. Papillary renal cell carcinoma: a clinicopathologic and immunohistochemical study of 105 tumors. Mod Pathol. 1997;10(6):537-44.
36. Delahunt B, Eble JN, McCredie MR, Bethwaite PB, Stewart JH, Bilous AM. Morphologic typing of papillary renal cell carcinoma: comparison of growth kinetics and patient survival in 66 cases. Hum Pathol. 2001;32(6):590-5.
37. Pitra T, Pivovarcikova K, Alaghehbandan R, Hes O. Chromosomal numerical aberration pattern in papillary renal cell carcinoma: Review article. Ann Diagn Pathol. 2019;40:189-99.
38. Saleeb RM, Brimo F, Farag M, Rompré-Brodeur A, Rotondo F, Beharry V, et al. Toward Biological Subtyping of Papillary Renal Cell Carcinoma With Clinical Implications Through Histologic, Immunohistochemical, and Molecular Analysis. Am J Surg Pathol. 2017;41(12):1618-29.
39. Lefèvre M, Couturier J, Sibony M, Bazille C, Boyer K, Callard P, et al. Adult papillary renal tumor with oncocytic cells: clinicopathologic, immunohistochemical, and cytogenetic features of 10 cases. Am J Surg Pathol. 2005;29(12):1576-81.
40. Hes O, Brunelli M, Michal M, Cossu Rocca P, Hora M, Chilosi M, et al. Oncocytic papillary renal cell carcinoma: a clinicopathologic, immunohistochemical, ultrastructural, and interphase cytogenetic study of 12 cases. Annals of Diagnostic Pathology. 2006;10(3):133-9.
41. Al-Obaidy KI, Saleeb RM, Trpkov K, Williamson SR, Sangoi AR, Nassiri M, et al. Recurrent KRAS mutations are early events in the development of papillary renal neoplasm with reverse polarity. Modern Pathology. 2022;35(9):1279-86.
42. Pivovarcikova K, Grossmann P, Hajkova V, Alaghehbandan R, Pitra T, Perez Montiel D, et al. Renal cell carcinomas with tubulopapillary architecture and oncocytic cells: Molecular analysis of 39 difficult tumors to classify. Ann Diagn Pathol. 2021;52:151734.
43. Mohanty SK, Satapathy A, Aggarwal A, Mishra SK, Sampat NY, Sharma S, et al. Oncocytic renal neoplasms with diffuse keratin 7 immunohistochemistry harbor frequent alterations in the mammalian target of rapamycin pathway. Modern Pathology. 2022;35(3):361-75.
44. Hes O, Trpkov K. Do we need an updated classification of oncocytic renal tumors? Modern Pathology. 2022;35(9):1140-50.
45. Akgul M, Williamson SR. Immunohistochemistry for the diagnosis of renal epithelial neoplasms. Semin Diagn Pathol. 2022;39(1):1-16.

6 Publications

6.1 Publications of the author, which are the basis of the dissertation

1. Kolar J, Llaurado AF, Ulamec M, Skenderi F, Perez-Montiel D, Alvarado-Cabrero I, Bulimbasic S, Sperga M, Tretiakova M, Osunkoya AO, **Rogala J**, Comperat E, Gal V, Dunatov A, Pivovarcikova K, Michalova K, Vesela AB, Slisarenko M, Strakova AP, Pitra T, Hora M, Michal M, Alaghehbandan R, Hes O. Histologic diversity in chromophobe renal cell carcinoma does not impact survival outcome: A comparative international multi-institutional study. Ann Diagn Pathol. 2022 May 20;60:151978. IF not available

2. **Rogala J**, Kojima F, Alaghehbandan R, Ptakova N, Bravc A, Bulimbasic S, Perez Montiel D, Slisarenko M, Ali L, Kuthi L, Pivovarcikova K, Michalova K, Bartovic B, Bartos Vesela A, Dolejsova O, Michal M, Hes O. Small cell variant of chromophobe renal cell carcinoma: Clinicopathologic and molecular-genetic analysis of 10 cases. Bosn J Basic Med Sci. 2022 Jul 29;22(4):531-539. IF 3.76

3. Farcaş M, Gatalica Z, Trpkov K, Swensen J, Zhou M, Alaghehbandan R, Williamson SR, Magi-Galluzzi C, Gill AJ, Tretiakova M, Lopez JI, Montiel DP, Sperga M, Comperat E, Brimo F, Yilmaz A, Siadat F, Sangoi A, Gao Y, Ptákova N, Kuthi L, Pivovarcikova K, **Rogala J**, Agaimy A, Hartmann A, Fraune C, Rychly B, Hurnik P, Durcansky D, Bonert M, Gakis G, Michal M, Hora M, Hes O. Eosinophilic vacuolated tumor (EVT) of kidney demonstrates sporadic TSC/MTOR mutations: next-generation sequencing multi-institutional study of 19 cases. Mod Pathol. 2022 Mar;35(3):344-351. IF 8.209

4. Pivovarcikova K, Grossmann P, Hajkova V, Alaghehbandan R, Pitra T, Perez Montiel D, Sperga M, **Rogala J**, Slisarenko M, Bartos Vesela A, Svajdler P, Michalova K, Rotterova P, Hora M, Michal M, Hes O. Renal cell carcinomas with tubulopapillary architecture and oncocytic cells: Molecular analysis of 39 difficult tumors to classify. Ann Diagn Pathol. 2021 Jun;52:151734. IF 2.134

5. Alaghehbandan R, Trpkov K, Tretiakova M, Luis AS, **Rogala JD**, Hes O. Comprehensive Review of Numerical Chromosomal Aberrations in Chromophobe Renal Cell Carcinoma Including Its Variant Morphologies. Adv Anat Pathol. 2021 Jan;28(1):8-20. IF 4.571

6. Michalova K, Tretiakova M, Pivovarcikova K, Alaghehbandan R, Perez Montiel D, Ulamec M, Osunkoya A, Trpkov K, Yuan G, Grossmann P, Sperga M, Ferak I, **Rogala J**, Mareckova J, Pitra T, Kolar J, Michal M, Hes O. Expanding the morphologic spectrum of chromophobe renal cell carcinoma: A study of 8 cases with papillary architecture. Ann Diagn Pathol. 2020 Feb;44:151448. IF 2.09

7. **Rogala J**, Kojima F, Alaghehbandan R, Agaimy A, Martinek P, Ondic O, Ulamec M, Sperga M, Michalova K, Pivovarcikova K, Pitra T, Hora M, Ferak I, Marečková J, Michal M, Hes O. Papillary renal cell carcinoma with prominent spindle cell stroma -

tumor mimicking mixed epithelial and stromal tumor of the kidney: Clinicopathologic, morphologic, immunohistochemical and molecular genetic analysis of 6 cases. Ann Diagn Pathol. 2020 Feb;44:151441. IF 2.090

6.2 Other author's publications related to the topic of dissertation thesis

1. Williamson SR, Hes O, Trpkov K, Aggarwal A, Satapathy A, Mishra S, Sharma S, Sangoi A, Cheng L, Akgul M, Idrees M, Levin A, Sadasivan S, San Miguel Fraile P, **Rogala J**, Comperat E, Berney DM, Bulimbasic S, McKenney JK, Jha S, Sampat NY, Mohanty SK. Low-grade oncocytic tumour of the kidney is characterised by genetic alterations of TSC1, TSC2, MTOR or PIK3CA and consistent GATA3 positivity. Histopathology. 2023 Jan;82(2):296-304. IF 7.778

2. Alaghehbandan R, Limani R, Ali L, **Rogala J**, Vanecek T, Steiner P, Hajkova V, Kuthi L, Slisarenko M, Michalova K, Pivovarcikova K, Hora M, Pitra T, Michal M, Hes O. Clear cell renal cell carcinoma with prominent microvascular hyperplasia: Morphologic, immunohistochemical and molecular-genetic analysis of 7 sporadic cases. Ann Diagn Pathol. 2022 Feb;56:151871. Not available

3. Prochazkova K, Ptakova N, Alaghehbandan R, Williamson SR, Vaněček T, Vodicka J, Treska V, **Rogala J**, Pivovarcikova K, Michalova K, Slisarenko M, Hora M, Michal M, Hes O. Mutation Profile Variability in the Primary Tumor and Multiple Pulmonary Metastases of Clear Cell Renal Cell Carcinoma. A Review of the Literature and Analysis of Four Metastatic Cases. Cancers (Basel). 2021 Nov 24;13(23):5906. IF 6.575

4. Marek-Bukowiec K, Ratajczyk K, **Rogala J**, Kosiński M, Kowal P, Witkiewicz W. An oncogenic, somatic mutation of PIK3CA identified in 2 primary malignancies: clear cell renal cell carcinoma and prostate adenocarcinoma in the same patient. Pol Arch Intern Med. 2021 Jan 29;131(1):93-95. IF 5.218

5. Pitra T, Pivovarcikova K, Alaghehbandan R, Compérat EM, Hora M, **Rogala J**, Slisarenko M, Michal M, Hes O. Utility of NKX3.1 immunohistochemistry in the differential diagnosis of seminal vesicles versus prostatic tissue in needle biopsy. Ann Diagn Pathol. 2020 Dec;49:151644. IF 2.090

6. Pires-Luis AS, Martinek P, Alaghehbandan R, Trpkov K, Comperat EM, Perez Montiel DM, Bulimbasic S, Lobo J, Henrique R, Vanecek T, Pivovarcikova K, Michalova K, Pitra T, Hora M, Marques A, Lopes JM, **Rogala J**, Mareckova J, Michal M, Hes O. Molecular Genetic Features of Primary Nonurachal Enteric-type Adenocarcinoma, Urachal Adenocarcinoma, Mucinous Adenocarcinoma, and Intestinal Metaplasia/Adenoma: Review of the Literature and Next-generation Sequencing Study. Adv Anat Pathol. 2020 Sep;27(5):303-310. IF 3.875

7. Kojima F, Bulimbasic S, Alaghehbandan R, Martinek P, Vanecek T, Michalova K, Pivovarcikova K, Michal M, Hora M, Murata SI, Sugawara E, **Rogala J**, Limani R, Hes O. Clear cell renal cell carcinoma with Paneth-like cells: Clinicopathologic, morphologic, immunohistochemical, ultrastructural, and molecular analysis of 13 cases. Ann Diagn Pathol. 2019 Aug;41:96-101. IF 1.877

8. Trpkov K, Williamson SR, Gao Y, Martinek P, Cheng L, Sangoi AR, Yilmaz A, Wang C, San Miguel Fraile P, Perez Montiel DM, Bulimbasić S, **Rogala J**, Hes O. Low-grade oncocytic tumour of kidney (CD117-negative, cytokeratin 7-positive): a distinct entity? Histopathology. 2019 Aug;75(2):174-184. IF 3.626

9. Pivovarcikova K, Agaimy A, Martinek P, Alaghehbandan R, Perez-Montiel D, Alvarado-Cabrero I, **Rogala J**, Kuroda N, Rychly B, Gasparov S, Michalova K, Michal M, Hora M, Pitra T, Tuckova I, Laciok S, Mareckova J, Hes O. Primary renal well-differentiated neuroendocrine tumour (carcinoid): next-generation sequencing study of 11 cases. Histopathology. 2019 Jul;75(1):104-117. IF 3.626

10. Pivovarcikova K, Martinek P, Grossmann P, Trpkov K, Alaghehbandan R, Magi-Galluzzi C, Pane Foix M, Condom Mundo E, Berney D, Gill A, Rychly B, Michalova K, **Rogala J**, Pitra T, Micsik T, Polivka J, Hora M, Tanas Isikci O, Skalova S, Mareckova J, Michal M, Hes O. Fumarate hydratase deficient renal cell carcinoma: Chromosomal numerical aberration analysis of 12 cases. Ann Diagn Pathol. 2019 Apr;39:63-68. IF 1.877

11. Gonzalez ML, Alaghehbandan R, Pivovarcikova K, Michalova K, **Rogala J**, Martinek P, Foix MP, Mundo EC, Comperat E, Ulamec M, Hora M, Michal M, Hes O. Reactivity of CK7 across the spectrum of renal cell carcinomas with clear cells. Histopathology. 2019 Mar;74(4):608-617. IF 3.626

12. Rotterova P, Martinek P, Alaghehbandan R, Prochazkova K, Damjanov I, **Rogala J**, Suster S, Perez-Montiel D, Alvarado-Cabrero I, Sperga M, Svajdler M, Michalova K, Pivovarcikova K, Daum O, Hora M, Dusek M, Ondic O, Stehlikova A, Michal M, Hes O. High-grade renal cell carcinoma with emperipolesis: Clinicopathological, immunohistochemical and molecular-genetic analysis of 14 cases.Histol Histopathol. 2018 Mar;33(3):277-287. IF 1.777

13. Ratajczyk K, Czekaj A, **Rogala J**, Kowal P. Adult Wilms tumor with inferior vena cava thrombus and distal deep vein thrombosis - a case report and literature review. World J Surg Oncol. 2018 Feb 23;16(1):38. IF 2.768

6.3 Presentations on scientific conferences

Kidney tumor friends, 14-16.10.2021, Plzen, Czech Republic
Presentation: Papillary renal cell carcinoma with prominent spindle cell stroma - tumor mimicking mixed epithelial and stromal tumor of the kidney: Clinicopathologic, morphologic, immunohistochemical and molecular genetic analysis of 6 cases.

Updates in GU pathology, 13-14.12.2019, Warsaw, Poland
Presentation: Diagnostic traps in urinary bladder pathology.

31st European Congress of Pathology, 7-11.09.2019, Nice, France
Presentation: Papillary renal cell carcinoma with prominent spindle cell stroma - tumor mimicking mixed epithelial and stromal tumor of the kidney: Clinicopathologic, morphologic, immunohistochemical and molecular genetic analysis of 6 cases.

Salzburg Cleveland Clinic Seminar in Pathology, 16-22.06.2019, Salzburg, Austria
Case presentation: Unusual sclerotic tumor of the kidney.

Polish Society of Pathology regional meeting, 15.06.2018, Wroclaw, Poland
Presentation: Cribriform lesions in prostate.